AN ALKALIC VOLCANIC SUITE OF THE LABRADOR TROUGH, LABRADOR

by

© JAMES LLEWELYN EVANS, B.Sc. (HONS.)

A Thesis

submitted in partial fulfillment of the
requirements for the degree of
MASTER OF SCIENCE

DEPARTMENT OF GEOLOGY
MEMORIAL UNIVERSITY OF NEWFOUNDLAND
JANUARY, 1980

ST. JOHN'S NEWFOUNDLAND

ABSTRACT

The Nimish Subgroup igneous suite is a linear belt of volcanic and plutonic rocks in the Dyke Lake area of the southern Labrador Trough.

The volcanics are interbedded with the sediments of the Wishart and Sokoman Formations of the Aphebian aged, Knob Lake Group. The Sokoman Formation forms a time stratigraphic horizon that separates the lower Petitsikapau Lake Formation from the upper Astray Lake Formation of the Nimish Subgroup. The occurrence of these volcanics within the Knob Lake Group is unique relative to Labrador Trough stratigraphy, as elsewhere the Knob Lake Group is a dominantly sedimentary succession and volcanics are restricted to the younger Doublet Group.

Stratigraphic relationships between the Nimish Subgroup and the Sokoman Formation indicate contemporaneous volcanic, clastic and chemical sedimentary activity. The internal stratigraphy of the Sokoman Formation exhibits a three-fold subdivision that is broadly correlatable with similar subdivisions in the Schefferville "main ore zone", 30 miles to the northwest. A detailed facies and paleogeographic model relating the volcanic activity to iron formation deposition in the Dyke Lake area is presented.

The rocks of the Dyke Lake area have been affected by lower greenschist facies metamorphism during the Hudsonian orogenic event, circa 1735 my. Geochemical evidence indicates that the igneous rocks of the Nimish Subgroup have been metasomatized with large degrees of mobility in Na_2O, K_2O, CaO, MgO, SiO_2, FeO and Fe_2O_3 suspected. The "immobile trace elements", Ti, Zr, Nb, Y and Ga imply that the Nimish lavas are a mildly alkaline suite that has an alkali basalt-trachyandesite-comendite differentiation scheme.

The rare earth element, REE, geochemistry of the Nimish Subgroup is supportive of the alkaline nature of the volcanics and has been used to model the fractional crystallization petrogenesis involved in the two volcanic cycles. The geological, geochemical and geophysical evidence indicates that the Nimish Subgroup lavas are possibly a rift facies, alkaline suite related to the tensional tectonic regime that preceeded the extrusion of voluminous tholeiitic lavas of the Doublet Group.

TABLE OF CONTENTS

PAGE

ABSTRACT ii

TABLE OF CONTENTS iv

LIST OF TABLES ix

LIST OF FIGURES xi

CHAPTER I

INTRODUCTION

1.1 Location and Access 1

1.2 Previous Work 1

1.3 Present Investigation 2

1.4 Physiography and Glaciation 3

1.5 Statement of Problem 4

1.6 Acknowledgements 6

CHAPTER II

GENERAL GEOLOGY

2.1 Introduction 8

2.2 Stratigraphy 12

2.2.1 Attikamagen Formation 12

2.2.2 Denault Formation 14

2.2.3 Fleming Formation 17

2.2.4 Wishart Formation 18

2.2.5 Nimish Subgroup 21

2.2.5.1 Nomenclature 21

2.2.5.2 Distribution and Thickness . . 22

2.2.5.3 Lithology and Petrography . . . 23

2.2.5.4 Intrusive Rocks 28

2.2.6 Sokoman Formation 29

2.2.6.1 Nomenclature 29

2.2.6.2 Distribution and Thickness . . 31

2.2.6.3 Lithofacies and Petrography . . 33

2.2.7 Menihek Formation 39

CHAPTER III

STRATIGRAPHY OF THE SOKOMAN FORMATION

3.1 Internal Subdivision of the Sokoman Formation . 41

3.2 Stratigraphy and Paleofacies Environments of the Sokoman Formation 44

3.2.1 The Lower Iron Formation 44

3.2.2 The Middle Iron Formation 48

3.2.3 The Upper Iron Formation 50

CHAPTER IV

STRUCTURAL GEOLOGY

4.1 Structural Geology 53

CHAPTER V

PETROCHEMISTRY OF THE NIMISH SUBGROUP

5.1 Introduction 57

5.2 Theoretical Geochemical Effects of Low Grade Metamorphism 58

5.3 Metamorphism of the Nimish Subgroup 63

5.4 Igneous Geochemistry of the Nimish Subgroup . . 74

5.4.1 Introduction 74

5.4.2 Major Element Geochemistry 75

5.4.2.1 Harker Diagrams 75

5.4.2.2 $Na_2O + K_2O$ versus SiO_2 Diagram 80

5.4.2.3 AFM Diagrams 82

5.4.3 Trace Element Geochemistry 84

5.4.4 Discussion of Petrologic Classification 90

CHAPTER VI

IGNEOUS PETROGENESIS OF THE NIMISH SUBGROUP

6.1 Introduction 95

6.2 Rare Earth Element Geochemistry of the Petitsikapau Lake Formation 96

6.2.1 Geochemical Subdivision of the Petitsikapau Lake Formation 96

6.2.2 Rare Earth Element Abundances of the Petitsikapau Lake Formation 100

6.2.3 Rare Earth Element Petrogenetic Relations in the Petitsikapau Lake Formation . . . 104

6.3 Rare Earth Element Geochemistry of the Astray Lake Formation 111

6.3.1 Geochemical Subdivision of the Astray Lake Formation 111

6.3.2 Rare Earth Element Abundances of the Astray Lake Formation 116

6.3.3 Rare Earth Element Petrogenetic Relations in the Astray Lake Formation 121

6.4 Rare Earth Element Geochemistry of the Intrusive Rocks of the Nimish Subgroup 126

6.5 Rare Earth Element Modelling of the Nimish Subgroup 130

6.5.1 Introduction 130

6.5.2 Rare Earth Element Modelling of JS - 464 of the Point Lake Pluton . . . 136

6.5.3 Rare Earth Element Modelling of JS - 033 and JS - 505 of the Astray Lake Formation 141

6.5.4 Rare Earth Element Modelling of the Average Acidic Analyses of the Astray Lake Formation 149

6.6 Discussion 153

CHAPTER VII

TECTONIC AFFINITIES OF THE NIMISH SUBGROUP

7.1 Discussion 162

CHAPTER VIII

ECONOMIC GEOLOGY

8.1 Discussion 176

CHAPTER IX

CONCLUSIONS

9.1 Discussion 179

BIBLIOGRAPHY 182

APPENDIX A 204

APPENDIX B 216

APPENDIX C 237

APPENDIX D 259

APPENDIX E 289

APPENDIX F 308

LIST OF TABLES

		PAGE
Table 1:	Stratigraphic column for the Dyke Lake area	10
Table 2:	Major element mobility during low grade metamorphism	61
Table 3:	Means, standard deviations and correlation matrix for the mafic members of the Petitsikapau Lake Formation	68
Table 4:	K/Rb and Rb/Sr ratios for the Nimish Subgroup, Little Aden Suite and standard average basalts	72
Table 5:	Average compositions of the petrogenetic subdivisions of the Nimish Subgroup . .	97
Table 6:	Rare earth element concentrations of selected volcanic rocks of the Nimish Subgroup	101
Table 7:	Rare earth element concentrations of selected intrusive rocks of the Nimish Subgroup	127
Table 8:	Modelled and actual trace element abundances of JS - 464 of the Point Lake Pluton	140
Table 9:	Modelled and actual trace element abundances in sample JS - 033 of the Astray Lake Formation.	140
Table 10:	Modelled and actual trace element abundances in sample JS - 505 of the Astray Lake Formation	148
Table 11:	Modelled and actual trace element abundances in the average acidic lava of the Astray Lake Formation	148

Table 12: Comparison of trace element data for the Nimish Subgroup with other Proterozoic and modern basalt sequences 172

Table 13: Precision and accuracy for the fused pellet - XRF method - major elements . . 209

Table 14: Relative accuracies of the fused pellet and pressed pellet XRF methods 210

Table 15: Precision and accuracy of the pressed pellet - XRF method - trace elements . . 213

LIST OF FIGURES

		PAGE
Fig. 1 :	1:50,000 geological map of the Dyke Lake area (in pocket)	
Fig. 1a:	Structural cross-sections AB and CD of fig. 1 (in pocket)	
Fig. 2 :	Composite stratigraphic sections of the Sokoman Formation of the Dyke Lake area (in pocket)	
Fig. 3 :	Eh - pH diagram for the Fe-C-O-H system, from Zajac (1974)	43
Fig. 4 :	Schematic stratigraphy of the Sokoman Formation	49
Fig. 5 :	The "Spilite Diagram" (Hughes, 1973) for the Doublet Group and Hematite Lake volcanics	65
Fig. 6 :	The "Spilite Diagram" (Hughes, 1973) for the Nimish Subgroup	65
Fig. 7 :	Na_2O versus K_2O diagram for the Nimish Subgroup	65
Fig. 8 :	Major element Harker diagrams for the Nimish Subgroup	76
Fig. 9 :	$Na_2O + K_2O$ versus SiO_2 diagram for the Nimish Subgroup	81
Fig. 10:	$Na_2O + K_2O$ versus SiO_2 diagram for the Doublet Group and Hematite Lake volcanics	81
Fig. 11:	AFM diagrams for the Nimish Subgroup . .	83
Fig. 12:	$(Zr/TiO_2) \times 10^4$ versus SiO_2 diagram for the Nimish Subgroup	86

Fig. 13: Nb/Y versus SiO_2 diagram for the Nimish Subgroup 86

Fig. 14: Nb/Y versus $(Zr/TiO_2) \times 10^4$ diagram for the Nimish Subgroup 87

Fig. 15: Ga versus $(Zr/TiO_2) \times 10^4$ diagram for the Nimish Subgroup 87

Fig. 16: Whole rock rare earth element patterns for the Petitsikapau Lake Formation . . 102

Fig. 17: Ce/Sm versus Sm diagram for the Nimish Subgroup 106

Fig. 18: Sm/Er versus Sm diagram for the Nimish Subgroup 107

Fig. 19: Whole rock rare earth element patterns for the Astray Lake Formation 117

Fig. 20: Whole rock rare earth element patterns for selected intrusive rocks of the Nimish Subgroup 128

Fig. 21: REE modelling of JS - 464, Point Lake Pluton, Best fit pattern from all possible sources 138

Fig. 22: REE modelling of sample JS - 033 of the Astray Lake Formation from the associated normal basic lavas 144

Fig. 23: REE modelling of sample JS - 505 of the Astray Lake Formation from the associated normal basic lavas 146

Fig. 24: REE modelling of the acidic lavas, Astray Lake Formation, Best fit pattern from all possible sources . . . 151

Fig. 25: Ti/100 - Zr - Y·3 diagram (Pearce and Cann, 1973) for the Nimish Subgroup . . 170

CHAPTER I

INTRODUCTION

1.1 - Location and Access:

The Dyke Lake - Astray Lake area is located in the Labrador Trough, 60 miles southeast of Schefferville, between latitudes 54° 15' and 54° 45' N and longitudes 66° 00' W and 66° 30' W. The area is accessible by an unpaved road from Schefferville to Astray Lake then by boat along the Astray - Dyke Lake system. The lakes are open to float plane and canoe from mid-July to October but spring flooding makes landing difficult in places. Access within the area is quite good as the area is surrounded by lakes with many deep bays indenting the larger peninsulas.

1.2 - Previous Work:

The first systematic mapping of the area was by Fahrig (1949) of the Iron Ore Company of Canada (I.O.C.) who carried out one inch to one half mile mapping over the whole area. His stratigraphic scheme was a southerly extension of the geology of the Knob Lake (later named Schefferville) mining district and included recognition of the Nimish Volcanics, a suite of mafic to intermediate lavas and tuffs interbedded with sedimentary rocks in what was termed the Nimish Group.

This work was followed by more detailed, 1" - 1000', I.O.C. mapping projects (Stevenson, 1952; Meliherscik, 1952; Kavanagh, 1952; Perrault, 1952; Usher, 1953) which covered the whole Dyke Lake - Astray Lake area.

In conjunction with the mapping of Usher (1953), Sauvé (1953) completed an M.Sc. thesis on the sedimentological features of the Nimish volcanic and sedimentary rocks of the Dyke Lake - Astray Lake Peninsula. The Dyke Lake area was also discussed briefly by Zajac (1974).

1.3 - Present Investigation:

This thesis embodies the results of eleven weeks field work during the summer of 1977 followed by petrologic and geochemical investigations through the summer of 1978. The work is a continuation of the project done with the Newfoundland Department of Mines and Energy of which the preliminary results are published in Evans (1978). This work was expanded by obtaining rare earth element analyses of a selected suite of samples and using these data as a base for petrogenetic investigations.

Mapping was conducted on 1:50,000 scale with specific emphasis being placed on the internal stratigraphy of the Nimish volcanics and their relations to the interbedded lenses of iron formation. Numerous sections of iron formation were

measured to develop an internal stratigraphy for the iron formation and a paleogeographic model for the area.

Laboratory work included petrographic studies of the various rock types and whole-rock chemical analyses of the volcanic and associated intrusive rock suites. Major and trace element data on the various facies of iron formation were collected to test for any intermixing between the cherty iron formation and volcanic detritus.

1.4 - Physiography and Glaciation:

The physiography is controlled by the underlying bedrock which, as in other areas of the Trough, has a prominent northwest-southeast structural grain. The volcanics are responsible for the main relief and form long curvilinear ridges with a maximum relief of 200 m above lake level. Other lithotypes form the gently sloping inland areas. In the extreme western part of the area, north of Marble Lake, fig. 1, the ridges are formed by the Fleming Chert Breccia. Faults modify this topography producing some very steep cliffs notably west of Point Lake and east of Roger Lake. There is about 15 percent bedrock exposure on average but the Attikamagen, Denault, Wishart and Menihek Formations are very poorly exposed with less than 5 percent exposure in most places.

Much evidence exists to show that the Dyke Lake region was strongly affected by glaciation. Hilltops have been scraped clean and littered with numerous large glacial erratics. Glacial striae are found both at the shoreline and on the hilltops implying an ice thickness of at least 200 m. Stoss-side smoothing and polishing and lee side plucking have produced small-scale roche moutonées. Eskers up to 3 km long with a relief of 70 m can be discerned on air photographs south of Esker Lake. With the exception of the hilltops the whole area has been covered by morainal deposits.

Two periods of glaciation are recognized within the area. The first and most prominent glaciation followed the structural grain of the area with the ice moving from the northwest to the southeast, while a later recessive event shows a mean strike of northeast. This later event is only recognized by glacial striae and stoss-side smoothing in the northern part of the area (Usher, 1953).

1.5 - Statement of Problem:

The occurrence of the mafic to intermediate volcanics of the Nimish Subgroup within the quartzite-iron formation sedimentary succession of the Knob Lake Group is unique within the Labrador Trough (Dimroth et al., 1970). Elsewhere in the Trough volcanic rocks are almost solely ultrabasic to basic in

composition and are associated with thick shale and intrusive gabbro sequences. The different sedimentary and geochemical associations of the two main occurrences of volcanic rocks in the Labrador Trough imply that different tectonic-petrogenetic factors controlled these two cycles of volcanism. Geochemical data on the volcanics of the Doublet Group are presented in Baragar (1960) and Dimroth et al. (1970).

Further study of the Dyke Lake area in the form of this thesis was undertaken with five main goals:

(1) To produce a map outlining the general stratigraphy of the area and how the Nimish volcanics locally disrupt the otherwise continuous stratigraphy of the Labrador Trough.

(2) To look at detailed facies relationships within the iron formation.

(3) To test for any possible genetic links between the volcanics and the cherty iron formation.

(4) To obtain geochemical data on the Nimish volcanics in order to assess their petrologic affinities and internal petrogenetic relationships.

(5) To compare the geochemical results with the available data of the Doublet Group.

1.6 - Acknowledgements:

The initial eight months of thesis work was supervised and financially supported by the Mineral Development Division of the Newfoundland Department of Mines and Energy. The work was done in coordination with the general mapping program of the Labrador Trough under the Newfoundland Mineral Development Agreement with the Federal Departments of Mines and Energy and Regional Economic Expansion. The author is extremely grateful for the opportunity to coordinate this graduate work with the Newfoundland Department of Mines and Energy.

Miss Joan Burry provided capable assistance throughout the field season while Mr. Doug Dunka also helped during the first week. Field support services were coordinated by Mr. W. Tuttle and supplied by Laurentian Air Services of Schefferville, Quebec. Thin sections were provided by Messrs. F. Thornhill, G. Ford and L. Warford, while Mr. D. Press and Mrs. G. Andrews cooperated to produce the chemical analyses summarized in this report. Mr. J. Vahtra assisted in X-Ray mineral identification work.

Preliminary manuscripts were typed by Ms. D. Peavy, C. Gullage, D. Downey, C. Neary, P. Evans and L. Murphy while the final draft was prepared by C. Trussler.

Figures 1 - 15 were drafted by Messrs. K. Byrne, W. Howell, G. Martin and Ms. K. Stienhauser, while figures 16 - 25 were prepared by Mr. B. Hiscock.

Field discussions with Drs. I.S. Zajac, W.R. Smyth, B.J. Fryer and R.J. Wardle were quite useful in formulating my ideas. The field work was supervised by Dr. R.J. Wardle, who along with Drs. W.R. Smith, D.G. Bailey and R.V. Gibbons read initial drafts of the manuscript. The thesis work was supervised by Dr. B.J. Fryer to whom the author is grateful for his patience, time in discussions and financial assistance.

CHAPTER II

GENERAL GEOLOGY

II.1 - Introduction:

The map area lies about 30 miles southeast of Schefferville in the centre of the Labrador Trough. The area is underlain by a supracrustal sequence of the Aphebian age Circum-Ungava geosyncline (Dimroth et al., 1970). The stratigraphy of this area is unique within the Labrador Trough in that volcanics occur within the Knob Lake Group as well as the Doublet Group.

The volcanics occur in a large lens-like body that extends southeast of Schefferville for about 125 km and covers an area of 400 km^2. These mafic to intermediate volcanic extrusive and hypabyssal rocks occur interbedded with the Wishart and Sokoman Formations with possible tuffaceous equivalents occurring as early as the Attikamagen Formation.

Since the Nimish volcanics are found to occur at several stratigraphic horizons within the Knob Lake Group it is no longer possible with the rules of the American Commission on Stratigraphic Nomenclature (1970) to continue the use of the term Nimish Group (Usher, 1953; Sauve, 1953), or Nimish Formation (Melihercsik, 1952). Those volcanics which overlie the Sokoman Formation (largely restricted to the western part

of the area) are now termed the Astray Lake Formation, fig. 1; while those which underlie the Sokoman but overlie the Wishart Formation (restricted to the eastern part of the area) are now termed the Petitsikapau Lake Formation. The two volcanic formations and associated intrusive rocks are collectively termed the Nimish Subgroup.

The oldest exposed rocks in the area, Table 1, are the thinly bedded grey siltstones and shales of the Attikamagen Formation. The base of this unit is not exposed but it is probably conformably underlain by the sandstones, conglomerates and arkoses of the Seward Formation (Wardle, 1976). Conformably overlying, and in part possibly a facies equivalent to the Attikamagen Formation, are the finely laminated dolomites and dolomite breccias of the Denault Formation.

North of Marble Lake the Denault Formation is disconformably overlain by the Fleming Chert Breccia while elsewhere in the area it grades conformably into the Wishart Formation. Contacts between the Wishart and Fleming Formation north of Marble Lake are gradational. The Wishart Formation represents a transgressive sequence of basal siltstones, sandstones and quartzites with an upper siltstone member which thickens markedly to the southeast.

The Wishart is conformably overlain by the Sokoman cherty iron formation in the central part of the area while north of

TABLE 1

TABLE OF FORMATIONS

ERA	FORMATION AND THICKNESS (METRES)	LITHOLOGY
APHEBIAN	Menihek Formation (1,000+)	Gray to black siltstones and shales; minor argillite.
	CONFORMABLE CONTACT	
	Astray Lake Formation (0-700)	Mainly aphyric basic and intermediate lavas; minor tuffs, agglomerates and sandstones.
	GRADATIONAL CONTACT	
	Sokoman Formation (20-150)	Oxide, silicate, carbonate and clastic facies of Superior-type cherty iron formation.
	GRADATIONAL CONTACT	
	Petitsikapau Lake Formation (0-1,000)	Mainly aphyric basic and ultrabasic lavas; minor tuffs, agglomerates and porphyritic lavas.
	CONFORMABLE CONTACT	
	Wishart Formation (100-700)	Orthoquartzite, feldspathic sandstone and siltstone.
	GRADATIONAL CONTACT	
	Fleming Formation (0-130)	Massive chert breccia; minor chert rich sandstone.
	DISCONFORMABLE CONTACT	
	Denault Formation (0-500)	Laminated dolomite and silty dolomite, dolomite breccia; minor siltstone and shale.
	GRADATIONAL CONTACT	
	Attikamagen Formation (1,000+)	Gray siltstones, shales, and slates; minor tuffs and sandy beds.

Marble Lake and in the eastern part of the area it is overlain by volcanic and sedimentary rocks of the Petitsikapau Lake Formation. Interbedding of Wishart lithologies with small lenses of intermediate volcanic rocks occurs east of Dyke Lake and Fawley Lake and on the peninsula at the south end of Dyke Lake.

The Sokoman Formation is interbedded with, and conformably overlies, the Petitsikapau Lake Formation in the eastern part of the area and occurs below the Astray Lake Formation volcanic rocks in the central part of the area. Structural and sedimentological relations between the Sokoman, Astray and Petitsikapau Lake formations indicate contemporaneous volcanic activity with both clastic and chemical sedimentation. The Astray Lake and Sokoman Formations are conformably overlain by the gray silstones and shales of the Menihek Formation, the top of which is not recognized in the study area. A series of pre-tectonic dioritic to gabbroic sills and sheets, have intruded the rocks of this area.

The area was deformed in the Hudsonian orogenic event, circa 1,735 m.y. (Stockwell, 1964) which produced a series of upright to slightly overturned open folds separated by numerous high angle reverse faults. The area can be divided primarily into three main structural/stratigraphic blocks with boundaries along faults running the length of Dyke and Astray Lakes.

These faults separate an area in the east where the volcanics (Petitsikapau Lake Formation) occur predominantly below the iron formation, from an area in the centre where the volcanics (Astray Lake Formation) occur primarily above the iron formation. The western most fault block has very few volcanic rocks exposed. The deformation was accompanied by prograde lower greenschist grade metamorphism and the inhomogeneous development of chloritic and micaceous penetrative fabrics.

II.2 - Stratigraphy:

II.2.1 - Attikamagen Formation:

In the Dyke Lake - Astray Lake area the Attikamagen outcrops sporadically with best exposures occurring north of Marble Lake. The thickness of the unit is unknown as the base is not exposed, but an estimate of 300 to 700 m was given for the Knob Lake area (Zajac, 1974) while in the Andre Lake area it varies from 375 to 1700 m (Wardle, 1976).

Typically the Attikamagen Formation is a laminated to thinly bedded, gray to black fissile shale or siltstone with minor argillaceous beds. Beds and lenses of silty dolomite are present north of Marble Lake while graded bedding and the presence of minor amounts of volcanic detritus suggest a tuffaceous component to the shales at the south end of Dyke Lake. Up to 15 percent fine sand-size angular fragments of

quartz and feldspar are present in some beds associated with a matrix of altered silicates, chlorite, clay minerals and opaques. Thin carbonaceous laminae occur sporadically along bedding planes. The cement is usually a very fine grained quartz but dolomite is present north of Marble Lake. In the areas where the Attikamagen Formation are highly sheared, a poorly developed penetrative cleavage of muscovite and chlorite is visible.

The Attikamagen Formation conformably overlies the Upper Seward Formation (Wardle, 1976) and passes gradationally into the Denault Formation dolomites in the west.

The fine laminations, lack of major cross-bedding, and interbedding with minor quartzite and dolomite beds imply a near shore, low energy environment of deposition for these rocks. The juxtaposition of carbonaceous shales and carbonate rocks in the upper Attikamagen Formation implies large changes in the Eh/pH conditions of the sedimentary basin possibly resulting from local relief in a restricted depositional basin. Such a paleogeography could promote lens-like accumulations of carbonates with fine scale interbedding at the margins, as seen locally in the Dyke Lake area.

II.2.2 - Denault Formation:

The best exposure of the Denault Formation is along the long peninsula separating Astray and Marble Lakes. Typically the Denault Formation is extremely variable in thickness, ranging from 200 m to 1,000 m over a 35-mile stretch in the Knob Lake area (Zajac, 1974). A complete section of the Denault is missing in the Dyke Lake area, but it is at least 500 m thick across the Astray Lake - Marble Lake Peninsula.

The formation consists of interbedded, finely laminated, variably clean, silty and cherty dolomites. An upper member of gray siltstones and shales very similar to the Attikamagen Formation is present above the carbonates west of Fawley Lake. These sedimentary rocks are provisionally included in the Denault Formation but correlations with the work of Wardle and Doherty (1977) may show them to be members of the Dolly Formation as described by Harrison et al. (1972). Typically the carbonates are gray on fresh surface but weather to a deep orange color. Low angle planar crossbeds and fine scale sedimentary slumping structures are preserved in some localities.

Outcrops on the Astray Lake - Marble Lake Peninsula have spectacular beds of coarse dolomite breccias interbedded with finely laminated dolomites. These breccias contain rectangular

blocks of massive to laminated silty dolomite up to 1 m across. The blocks are aligned with long axes parallel to bedding planes and are set in a cherty dolomitic matrix. No sedimentary structures such as graded bedding or crossbeds were noted within these breccia units.

A common feature, unique to the Denault Formation, is a well developed system of rectangular fractures. This fracture pattern exists on scales up to 3 metres and occurs both within and cutting across fragments in the dolomite breccia. Little or no movement occurred along these fractures and they are commonly filled with veins of gray to black chert and quartz.

In thin section the Denault Formation shows irregular subplanar bedding defined by concentration of clay minerals along bedding planes. Angular silt size detrital quartz makes up to 15 percent of some silty beds while trace amounts of detrital mica occur near the contact with the Attikamagen Formation north of Marble Lake. The dolomite forms a mosaic of anhedral to subhedral rhombs up 30 mm in size. Some beds show development of orbicular shaped pure dolomite lenses about 3 mm across, aligned parallel to bedding.

Contact relationships of the Denault Formation with other formations are variable. The base of the Denault is a gradational contact with the Attikamagen Formation while the upper contact varies from a disconformable relation with the

Fleming Formation north of Marble Lake to a presumed gradational contact with the overlying Wishart Formation on the east short of Dyke Lake. The Denault seems to be missing in the southern part of the Dyke Lake - Astray Lake peninsula where the Attikamagen Formation appears to be directly overlain by the Wishart Formation. Alternatively the lower section of the Wishart Formation in this area could be the upper siltstone member of the Denault Formation, or Dolly Formation as recognized by Wardle and Doherty (1977).

In all aspects the Denault Formation resembles an evaporitic, lagoonal type dolomite formed by diagenetic alteration of calcerous muds. The close association of fine shales and silty dolomites, the possibly storm generated intraformational dolomite breccias and the rectangular fracture pattern within the dolomite clasts (typical of shrinkage cracks in an evaporitic environment) are common sedimentological features of restricted shoreline basins in a tropical environment (Wilson, 1975). Algal structures, which are often associated with modern tropical lagoonal environments, were not recognized in the Dyke Lake area but have been noted within the Denault Formation of adjacent areas (Harrison et al., 1972; Donaldson, 1966).

II.2.3 - Fleming Formation:

Regionally the distribution of the Fleming Formation is restricted to areas underlain by the Denault Formation (Dufresne, 1952). In the Dyke Lake area the Fleming Formation is restricted to the westernmost fault block where it immediately overlies the Denault dolomites. Exposure of the Fleming Formation is very irregular as it outcrops in large lens-like bodies with intervening areas not exposed. The Fleming Formation varies from 0 to 130 m in the Dyke Lake area.

The unit consists almost entirely of chert breccia. Thin beds of cherty quartzite are interbedded with the massive breccia on the islands in Marble Lake. The breccia contains angular fragments of laminated to massive, multicolored chert up to 0.5 m across, set in a fine grained, recrystallized, quartzose matrix. No sedimentary structures or regional grain size variations were recognized in the area. In thin section, fragments of well rounded, occasionally fractured, spherical quartz grains up to 5 cm in size, comprise up to 20 percent of the clast population. Traces of cryptocrystalline, carbonaceous opaque material define the chert laminations. Minor chlorite and opaques were recognized within the matrix.

Generally it is accepted that the Fleming Formation is an intraformational conglomerate with variable contact relations

(Zajac, 1974). Considering its coarse grained character and the abrupt lithologic change, the Fleming Formation probably disconformably overlies the Denault Formation. Harrison (1952) maintained that a band of slate 1-4 feet thick separates the two formations in the Knob Lake area but this has not been recognized in the Dyke Lake area.

Contact relations with the overlying Wishart Formation are also complex. In the Dyke Lake area the interbedding of thin quartzite beds and massive chert breccia and the chert cement in the lower units of the Wishart Formation implies a gradational, conformable contact. Conversely, immediately northwest of the Dyke Lake area the chert breccia becomes much thicker and outcrops very close to the Sokoman Formation (Usher, 1953) implying that the Fleming Formation may be in part a facies equivalent of the Wishart Formation.

II.2.4 - Wishart Formation:

The Wishart Formation forms the most continuous unit in the area and is used as a marker horizon for structural and stratigraphic interpretations. In the Dyke Lake area, the unit is variable in thickness and ranges from 0 - 100 m in the northwest to 500 - 700 m in the southeastern section of the map area. Best exposures of the Wishart Formation are in fault blocks on Astray Hill at the southern end of the Dyke Lake -

Astray Lake Peninsula and on the peninsula at the south end of Dyke Lake.

The dominant lithology of the Wishart Formation is a light gray, massive to well bedded, medium to coarse grained quartzite with 5 - 10 percent argillaceous material. From northeast to southwest the rocks generally become thicker bedded, more poorly sorted and more feldspathic in composition and interbedded lavas and sills become more prevalent. Towards the top of the formation interbeds of gray siltstone become more abundant.

A lean, gray, massive chert horizon of about 3 m thickness lies at the top of the Wishart Formation south of Charlie Lake. This chert member was also recognized in the Schefferville area (Harrison et al., 1972).

Sedimentary structures of the Wishart Formation in the Dyke Lake area are restricted to occasional occurrences of low angle, herring bone cross-bedding.

Petrographically, the Wishart lithologies consist chiefly of quartz fragments with alkali feldspar and composite chert grains rarely making up more than 15 percent of the rock. The development of strained, undulose extinction, subgrain boundaries and dislocations is quite common. Despite their quartz-rich composition, the detritus is angular to subrounded and poorly sorted, even in orthoquartzite examples. In the feldspathic

wackes and interbeds of siltstones and shales, the silt size matrix constitutes up to 30 percent of the rock. This silty material is occasionally recrystallized to a muscovite, stilpnomelane, chlorite and opaque assemblage which defines a fissility usually parallel to bedding.

Locally the Wishart Formation exhibits clouding of quartz grains, a porous texture and thin films of hematite coating vugs and grain boundaries. This is attributed to weathering processes resulting from subaerial exposure during a period of Cretaceous block faulting (Harrison et al., 1972).

Contact relations with the Wishart Formation and adjacent formations are not well exposed in the Dyke Lake area. The interbedding of chert breccia and chert cemented quartzite on the islands of Marble Lake implies a gradational basal contact. Regionally, however, the base of the Wishart Formation is transgressive since it overlies the Attikamagen Formation in the centre of the Trough and oversteps the Fleming and Denault Formations, with local interbedding of Wishart and Denault (Harrison, 1952; Baragar, 1967), to unconformably overlie the Archean at the western margin of the Trough. The contact is usually marked by a conglomerate horizon in the Knob Lake area (Zajac, 1974).

The upper contact of the Wishart Formation is marked by a lean chert and basal units of the iron formation in the west

and by thick volcanic flows of the Petitsikapau Lake Formation in the east giving conformable to paraconformable contacts. Elsewhere in this area of the Trough, the top of the Wishart is marked by a well developed quartz pebble conglomerate possibly reflecting near shore deposition during a short lived regression in the area (Zajac, 1974).

The Wishart Formation in the Dyke Lake area shows features indicative of a littoral to sublittoral depositional environment. Sedimentation was essentially continuous with the near shore conglomerates and related disconformities of the Schefferville area being replaced in the Dyke Lake area by finer grained sedimentation and gradational contacts.

II.2.5 - Nimish Subgroup:

II.2.5.1 - Nomenclature:

The Nimish volcanics were first recognized by Fahrig (1949) who used the term to name the volcanic rocks interbedded with the Knob Lake Group sediments in the Astray Lake - Birch Lake area. Succeeding workers used the term "Nimish" in varying contexts. Melihercsik (1952) assigned the volcanics formational status, Usher (1953) and Sauvé (1953) used the term Nimish Group, while Kavanagh (1952), Perrault (1952) and Stevenson (1952) used the term Nimish volcanics to describe the lithotype, not assigning them any formal stratigraphic status.

Work in the 1977 field season has shown the need for recognition and further subdivision of the Nimish volcanics into an upper and lower formation based on stratigraphic, petrologic and geochemical data. The author proposed the term Petitsikapau Lake Formation for those volcanics that occur below and interbedded with the lower Sokoman Formation, fig. 1, while Astray Lake Formation was proposed for those volcanics and associated sediments that occur above and interbedded with the upper Sokoman Formation (Evans, 1978). The term Nimish Subgroup includes the Petitsikapau Lake and Astray Lake Formations as well as the gabbroic intrusive rocks associated with the volcanics.

II.2.5.2 - Distribution and Thickness:

The two volcanic formations are dominated by basalts which occur throughout the area. The areas west of Point Lake and on Jasper Mountain (the hill immediately east of Roger Lake, fig. 1) represent two centres of volcanic activity for the Petitsikapau Lake and Astray Lake Formations respectively and are distinguished by porphyritic intermediate to acidic volcanic and tuffaceous rocks. A maximum thickness of 1,000 m is suggested for the Petitsikapau Lake Formation and 700 m for the Astray Lake Formation, but thicknesses are difficult to estimate because of inconsistencies in the volcanic stratigraphy

and the numerous folds and faults that repeat the section.

Considering the general lithologic similarities of the Petitsikapau Lake and Astray Lake Formations, the lithologic descriptions will be combined with any features unique to either formation noted in the text.

II.2.5.3 - Lithology and Petrography:

Massive to amygdaloidal, intermediate to mafic aphyric volcanic rocks make up 65 - 75 percent of the two formations. These rocks are massive to slightly vesicular in outcrop with some examples showing a concentric veining pattern of up to .50 m in diameter. Vein minerals are chlorite, hematite, quartz and epidote which along with calcite and potash feldspar are the dominant minerals infilling vesicles. The origin of this veining is somewhat enigmatic. Usher (1952) described it as liesegang banding resulting from weathering processes in arid environments but the presence of the green-schist grade metamorphic mineral epidote in some examples would seem to indicate a hydrothermal origin.

Pillow lavas up to 1 m across with 10 cm chloritic rims are only well preserved in the north end of the Dyke Lake - Petitsikapau Lake Peninsula but are recognized sporadically throughout the area. These lavas always have finer scale concentric veining within the pillows. Thin lenticular beds

of volcanogenic sandstones are interbedded with the pillow lavas.

In thin section the lavas are invariably altered to lower greenschist facies assemblages of calcite, chlorite, albite, epidote, opaques and minor quartz. Adularian potash feldspar is seen locally as a replacement mineral after plagioclase and as a vein mineral. This combined with the high and erratically distributed K_2O values of the volcanics, Section V.3, indicates some form of potash metasomatism. The opaque minerals are dominantly magnetite with secondary hematite occurring locally. Magnetite occurs as anhedral masses and small subhedral microphenocrysts implying high level crystal fractionation of iron oxides along with secondary metasomatic opaque formation. No primary ferromagnesian phases or pseudomorphs were recognized in thin section. Groundmass albite laths are locally aligned in flow textures and surrounded by a chloritic mesostasis. An aphyric intersertal to pilotaxitic texture is the most common igneous texture preserved in these rocks.

Porphyritic lavas are generally restricted to the Petitsikapau Lake Formation where they make up about 20 percent of the exposed lavas. Porphyritic lavas are only found in small amounts in the Astray Lake Formation east of Roger Lake.

The porphyritic lavas are very homogenous and individual flows can be traced for 2 - 3 km along strike. Small scale concentric veining is developed locally but no large scale pillow lavas were recognized within the porphyritic flows.

The dominant phenocryst phase is altered euhedral to subhedral crystals of plagioclase up to 5 cm long. The plagioclase is usually partially replaced by albite, adularia, carbonate and lesser amounts of muscovite and epidote. These minerals often occur in simple and twinned plagioclase pseudomorph aggregates forming coarse glomerophenocrysts. Relict zoning is sometimes preserved through the alteration. Subhedral phenocrysts of augitic clinopyroxene up to 1 cm long were found in two sections. The pyroxenes are relatively fresh with only thin chloritic rims. Magnetite occurs as an abundant microphenocryst phase similar to the aphyric lavas. Groundmass mineralogy and textures are also similar to the aphyric lavas giving porphyritic to glomeroporphyritic, intersertal to pilotaxitic textures.

Acid volcanic rocks are restricted to two localities, immediately east of Point Lake and west of Roger Lake, where they make up about 5 percent by volume of the Petitsikapau Lake and Astray Lake Formations. In these localities the lavas occur at the top of a thick mafic volcanic pile. The geographic

restriction of the silica rich volanics, their associations with coarse angular sediments and their stratigraphic relationships with the mafic volcanics imply that these areas are volcanic centres associated with the Petitsikapau Lake and Astray Lake Formation volcanic cycles.

The acidic rocks are massive in outcrop and of limited aerial extent. Flow alignment of feldspar phenocrysts is developed locally. The rocks vary petrographically from dacites to coarse feldspar phyric trachytes, rhyodacites and rhyolites. They are typically porphyritic with small euhedral phenocrysts of orthoclase and albite set in a groundmass of aligned albite laths. Phenocrysts are often corroded and partially replaced by carbonate or potash feldspar. Quartz and adularia veins are quite common making the primary nature of the potash feldspar phenocrysts somewhat dubious. Euhedral microphenocrysts of magnetite are present in some examples. Chlorite, quartz and clay minerals make up the mesostasis. A porphyritic trachytic to pilotaxitic texture is common in these rocks.

Tuffaceous and volcanic-sedimentary rocks of the Petitsikapau Lake and Astray Lake Formations may be divided into coarse conglomerates and agglomerates which are spatially associated with the acidic volcanics, and finer grained tuffaceous and agglomeritic rocks which occur more distally.

A crude qualitative concentric zonation pattern of clast size within the fragmental rocks is developed around centres west of Point Lake and east of Roger Lake.

On Jasper Mountain, east of Roger Lake, there is a series of coarse agglomerates and conglomerates interbedded with acidic volcanics and tuffaceous sandstones. The dominant clast lithologies represented are red microcrystalline jasper, fine grained red rhyolite, rhyolite porphyry, aphyric mafic volcanics and minor amounts of oxide facies iron formation and gray Wishart Formation sandstones. The fragments are up to 0.75 m across and are subangular to well rounded. Generally they are very poorly sorted boulder conglomerates but some of the finer grained sandstones are moderately well sorted. The matrix of the agglomerates is very similar to that of the associated sandstones, consisting of angular sand size particles of quartz, feldspar, chert, and mafic and acidic volcanics.

Sedimentary structures are rare as the conglomeratic beds exhibit massive bedding up to 2 m thick, and in places a clast supported texture. Poorly developed, small scale trough cross-beds and graded bedding are preserved in the finer grained sandstones.

The very coarse, immature nature of the sedimentary structures within the conglomerate units and the association with acidic volcanics imply that these fragmental rocks are

part of an alluvial fan, or coarse river deposit, formed around the subaerially exposed volcanic centre responsible for the interbeds of acidic volcanics.

The tuffaceous rocks found in the surrounding areas contain only 5 - 15 percent clastic material. The most common lithotype is red jasper with lesser amounts of rhyolite, basalt, quartz and feldspar. No recrystallization has occurred along the clast boundaries. The gravel-sized clasts are usually well rounded, moderately well sorted and occur in continuous horizons either at the top or bottom of flows. Poorly developed graded bedding was the only sedimentary structure recognized.

II.2.5.4 - Intrusive Rocks:

The intrusive rocks of the Dyke Lake area were originally included in the Montagnais intrusive suite by Stevenson (1952), Perrault (1952) and Usher (1953) who used the term to describe all the pretectonic sills intruded into the Kaniapiskau Supergroup in the Dyke Lake area. In this report the intrusives are included as part of the Nimish Subgroup, since it is later demonstrated that they are chemically similar to, and therefore probably cogenetic with, the Petitsikapau Lake and Astray Lake Formations. Best exposures are southeast of Hughes Lake and at the north end of Marble Lake.

The intrusive rocks consist of a suite of massive, medium to coarse grained rocks that range from dioritic to gabbroic composition. The suite is very homogenous with only small variations in color index noted. In thin section the intrusives show a mineralogy of clinopyroxene, plagioclase and skeletal magnetite with accessory apatite, chlorite and occasional orthoclase, quartz and micropegmatite. The sill to the west of Point Lake has a more alkalic composition and locally contains 15 - 20 percent modal potash feldspar and cumulus apatite. Textures are quite variable with phenocrysts of clinopyroxene, plagioclase, magnetite and occasional potash feldspar and apatite occurring sporadically in a groundmass of ophitic to subophitic intergrowths of clinopyroxene and plagioclose. The feldspars are partially altered to albite and adularia and the groundmass is largely recrystalized to chlorite and opaques. The phenocrysts of opaques and clinopyroxenes remain relatively fresh.

II.2.6 - Sokoman Formation:

II.2.6.1 - Nomenclature:

The Sokoman Formation is a cherty Precambrian iron formation of the Superior type (Gross, 1965). It is the most important economic formation within the Labrador Trough and is mined for iron ore in the Schefferville area.

Early subdivisions of the stratigraphy of the Knob Lake region (Harrison, 1952; Dufresne, 1952) recognized two formations between the top of the Wishart Formation and bottom of the Menihek Formation. The term Ruth Formation was applied to all the black ferruginous siltstones and shales overlying the Wishart quartzites while the Sokoman Formation included all the cherty iron formation units between the Ruth and Menihek Formations.

In the main ore zone of the Schefferville area, the Ruth Formation included parts of the Lower Sokoman Formation, which when highly altered is indistinguishable from the Ruth siltstones. This situation has been further complicated by the work of Zajac (1974) who showed that the Ruth Formation of the main ore zone is stratigraphically equivalent to the lowermost silicate-carbonate facies of the Sokoman Formation in the Stakit Lake and other areas. On the basis of these stratigraphic inconsistencies, and petrologic evidence which implies a similar diagenetic history of iron enrichment for the Ruth and Sokoman Formations, Zajac proposed that the Ruth Formation be included as a member of the Sokoman Formation.

In the Dyke Lake area, the Ruth Formation is very thin or absent and is only exposed in three isolated areas making it a minor component of the stratigraphy and not worthy of formational status. The writer has therefore followed Zajac

(1974) and included the Ruth Formation as a basal member of the Sokoman Formation. The Sokoman Formation can be divided into Lower, Middle and Upper Iron Formation units based on the variable mineralogy and sedimentary structures present. These divisions are believed to be equivalent to the similar subdivision proposed by G.S. Card for I.O.C. workers of the Schefferville area (Harrison, 1972). The common abbreviations for the facies and the lithologic types are given in fig. 2.

II.2.6.2 - Distribution and Thickness:

The Sokoman Iron Formation is poorly exposed throughout the Dyke Lake area with best exposures occurring west of Tee Lake and Evans Lake and south of Charlie Lake.

In the eastern Dyke Lake - Petitsikapau Lake Peninsula, the Petitsikapau Lake Formation underlies and is interbedded with the Lower Iron Formation while in the western Dyke Lake - Astray Lake Peninusla, the Petitsikapau Lake Formation is largely missing and the volcanics of the Astray Lake Formation overlie the iron formation. Relative to these periods of volcanism, the iron formation forms a continuous time-stratigraphic horizon that has a continuous internal stratigraphy. A facies of iron formation rich in clastic detritus, termed magnetic graywacke by the I.O.C. geologists, is similarly recognized in the Dyke Lake area. The magnetite

graywackes occur as separate homogeneous units stratigraphically equivalent to the main body of the iron formation, as on the western shore of Petitsikapau Lake, or as lenticular interbeds within the volcanic pile as in the Tee Lake and Icombe Lake areas, (fig. 2).

Considering the lack of outcrop and degree of interbedding with the volcanics, accurate thicknesses of the iron formation are very difficult to establish. Figure 2 gives the composite stratigraphic sections for 14 different localities and shows how the iron formation and its stratigraphic subdivisions vary in distribution and thickness throughout the Dyke Lake area. Thicknesses quoted in this diagram are approximate as contacts are often unexposed, sections often incomplete and thicknesses of facies of the Iron Formation within each locality variable, all making the diagram somewhat schematic.

Despite these problems minimum thicknesses for the iron formation can be estimated, varying from 20 m at Eileen Lake (section XII, Figure 2) to 150 m at Pierres Point (section V). The Iron Formation might be 500 m thick on the large peninsula at the north end of Dyke Lake (section I) where outcrops of steeply dipping magnetite graywacke outcrop on each side of the easternmost peninsula. No outcrops are available inland to confirm their continuity.

II.2.6.3 - Lithofacies and Petrography:

The sedimentological and petrologic features of the iron formation are best described by taking each facies in turn. In this section "primary" will be used for all textures resulting from the deposition of the sediment, while "secondary" and "secondary diagenetic" will be reserved for all features related to post-sedimentation, pre-metamorphic processes.

The basal unit of the iron formation in the Dyke Lake area is comprised of black ferruginous siltstones and shales (old Ruth Formation) which outcrop at the base of sections south of Charlie Lake (section VI, Figure 2), north of section III and on the peninsula at the south end of Dyke Lake. These rocks are very poorly exposed and often highly fractured; consequently any large scale primary sedimentary structures are obscured. In thin section they are finely laminated with 1 - 2 mm beds defined by traces of carbonaceous material.

The rock is comprised of 50 - 60 percent angular to subrounded, silt size quartz, plagioclase and potash feldspar fragments set in an opaque clay size matrix. In places this matrix has recrystallized to a stilpnomelane-muscovite-chlorite assemblage forming a strong primary fissility subparallel to bedding. In exposures at the south end of Dyke Lake and northeast of Section III, the rock contains euhedral, 3 mm

sized crystals of pyrite distributed along bedding planes. This unit is distinguished from the other two siltstone and shale members of the Knob Lake Group by the presence of potash feldspar and the abundance of carbonaceous material.

The silicate-carbonate facies is best exposed in Sections I and X. It shows well developed subplanar bedding of 1 - 2 cm thickness with beds defined by variations in the carbonate and silicate mineral proportions. Rocks poor in carbonate are usually poorly bedded and commonly exhibit an irregular conchoidal fracture.

The primary mineralogy of this facies is highly variable. The most common primary assemblage found is siderite, greenalite, magnetite and chert with minor amounts of minnesotaite. In assemblages void or low in carbonate, minnesotaite becomes the dominant silicate phase, almost to the exclusion of greenalite and carbonate. It is also associated with an increased magnetite content.

In this facies siderite occurs as subhedral rhombs and composite mosaics, up to 100 nm across, intergrown with anhedral microcrystalline chert. Greenalite is present as pleochroic, subhedral, tabular crystals of 50 nm size when in its primary state and as large irregular felted masses when replacing other silicates or oxides. Minnesotaite is usually present as bundles of radiating acicular crystals. These crystals are

usually spread randomly throughout a bed or clustered in a crude spherical pattern reflecting a relict granular texture. Secondary diagenetic magnetite occurs as a series of subhedral, 50 nm crystals aligned roughly parallel to bedding or in crystal aggregates forming a relict granular texture similar to minnesotaite. This "fish net" texture, typical of minnesotaite and magnetite, represents diagenetic remobilization of iron and recrystallization of primary Fe-Si gels (French, 1973). Occasional large anhedral crystals of magnetite are probably the result of diagenetic or secondary replacement of iron carbonates.

The grain size and texture of the recrystallized quartz varies from mosaics of cryptocrystalline rounded blebs to homogeneous angular crystals up to 100 nm across. The large quartz grains are associated with relict granular and oolitic horizons. Gross (1961) suggested that these sand-like horizons would have had a higher interstitial water content than the thinly layered non-granular types, which would promote diffusion and recrystallization to form larger grains.

A unique silicate-carbonate facies has been noted in many sections. In this rock type all the primary iron silicates are pseudomorphically replaced by stilpnomelane while the carbonates are replaced by iron oxides. The pseudomorphic textures indicate that this mineral assemblage probably

developed in the diagenetic environment. The geochemistry of this facies, as discussed in Evans (1978), indicates that the primary SCIF was diluted by volcanic ash and subsequently recrystallized. Iron formation facies of this type are called Volcanic - SCIF facies.

The carbonate iron formation, best exposed in Sections V and XIII, typically forms thick subplanar beds with lean chert interbeds 3 - 7 cm thick. Finer laminations are discernable in thin section. The primary mineralogy is siderite and chert with minor amounts of magnetite and iron silicates. Variations in the percentage of siderite and chert define the bedding with siderite occurring as interlocking subhedral crystals up to 100 nm long surrounded by anhedral intergrowths of recrystallized quartz. Primary oxides and silicates rarely make more than 5 percent of the rock. Alteration and leaching effects are similar to those noted for the silicate-carbonate facies.

The oxide facies of the iron formation is the most variable rock type. It can display very regular, well developed planar bedding or high energy sedimentary structures such as coarse, high-angle trough cross beds, graded beds and intraformational conglomerates. Granular and oolitic textures are also common but are often obscured by diagenetic processes which tend to remove the iron from the oolitic layers and recrystallize the

chert. In thin section oxide facies rocks consist almost entirely of chert, magnetite and hematite. Magnetite usually forms as anhedral aggregates crudely aligned along bedding planes or as relict granules similar to the textures in the oxides and silicates of the silicate-carbonate facies. Hematite, when in its primary state, forms very fine grained crystals in bedded nodular horizons or in detrital jasper phases such as oolites, granules and intraclasts. In these cases it is usually disseminated throughout the granule or clast and has undergone little or no remobilization.

The impure clastic facies of the iron formation, magnetite graywacke, is primarily restricted to the northeast section of the Dyke Lake area with smaller occurrences also found in Sections VI and VII. This facies is quite variable in grain size, sedimentary structures and its relation to the surrounding rock type.

Along the western shore of Petitsikapau Lake and in Sections I and II, it occurs as a homogeneous sedimentary succession possibly up to 500 m thick bounded by the Petitsikapau Lake Formation volcanics at the bottom and the Menihek Formation at the top. In contrast the unit also occurs as lenticular beds interbedded within these volcanics (Sections VI, VII and VIII). These intravolcanic units range from 20 - 50 m long and up to 25 m wide and pinch out laterally. The

magnetite graywackes are in conformable contact with the associated volcanics and were probably deposited in small sedimentary basins or ponds within the volcanic pile.

In outcrop, the graywackes commonly show graded bedding, low angle planar cross bedding, rip up clasts and a rhythmic alteration of medium to coarse graywacke and pebble conglomerate with thin laminae of magnetic gray chert. Load casts, ball and pillow structures and soft sediment deformation features are common in some of the finer grained samples. The characteristic sedimentary structures, the preservation of chert laminae within conglomeratic units and the interbedding with submarine pillow lavas imply that these rocks result from down slope movement of unconsolidated sediment deposited in isolated structural and stratigraphic pools along slopes and on the basin floor. These deposits could possibly be likened to turbidites with the typical sedimentary structures, alternation of coarse and fine sediments and the thin chert-oxide laminae classed as equivalent to the pelagic unit that is sometimes preserved at the top of classical turbidite sequences.

In thin section, this unit is rich in detrital volcanic material, quartz, feldspar, jasper, magnetite and occasional fragments of iron formation. Grain sizes and proportions of these phases are highly variable. Most of the fragments are

subrounded and fresh in appearance and have probably undergone previous sedimentary reworking. Mafic volcanic fragments are invariably altered to chlorite, albite and opaques with minor amphibole and epidote. Sauvé (1953) recognized ilmenite and titanium-rich magnetite within these graywackes implying that the volcanics as well as the iron formation were sources for the detrital opaques. Diagenetic structures and matrix mineralogy of the magnetite graywackes are variable but generally similar to the different facies of the cherty iron formation.

II.2.7 - Menihek Formation:

The best exposure of the Menihek Formation is at Pierres Point (Section V, Figure 2) with smaller outcrops being found in the syncline north of Evans Lake and along the west shore of Petitsikapau Lake. A complete section of Menihek Formation is nowhere exposed in the Labrador Trough, but a minimum of 330 m was measured at Pierres Point (Usher, 1953). In the core of the Petitsikapau syncline (Wardle and Doherty, 1977) the Menihek Formation has a minimum thickness of approximately 1,000 m.

The Menihek Formation consists of a monotonous series of well bedded gray to black siltstones and shales with minor argillaceous and graywacke beds. The rock is composed of

angular to acicular fragments of quartz and plagioclase feldspar surrounded by a dense intergrowth of chlorite, sericite and opaques. Minor amounts of carbonaceous material are present in the darker shales (Harrison, 1952). The rock is also pyritiferous in exposures north of Evans Lake. A well developed fracture cleavage occurs sporadically throughout the area.

Contact relations with the underlying Sokoman Formation at Pierres Point are conformable but the presence of subaerial volcanics, pyroclastics, and conglomerates above the Sokoman Formation on the Dyke Lake - Astray Lake Peninsula indicates a possible local disconformity.

The Menihek Formation, as the uppermost member of the Knob Lake Group, represents a return to a quiet, deeper water environment of deposition similar to that of the Attikamagen Formation.

CHAPTER III

STRATIGRAPHY OF THE SOKOMAN FORMATION

III.1 - Internal Subdivision of the Sokoman Formation:

In the Schefferville ore zone the boundary between the Lower and Middle iron formation, LIF - MIF, is marked by a transition from a lower silicate-carbonate facies, SCIF, to a jasper bearing oxide facies, JMIF (Schwellnus, 1957). In the Dyke Lake area however, this JMIF marker horizon is usually separated from the SCIF lithology by a jasper-free, oxide facies unit, ChMIF (Sections VI, VII, VIII, X), fig. 2. In these cases the boundary was put at the top of the last SCIF horizon, marking the major mineralogical and Eh-pH change in the sedimentary environment.

Recent petrographic studies of unmetamorphosed iron formations (Klien, 1973) have proposed that the presence or absence of jasper does not really reflect variations in the depositional environment but rather a different diagenetic history for the sediment. Thus the ChMIF unit found on top of the SCIF in the Dyke Lake area could be stratigraphically equivalent to the JMIF of the Knob Lake area. Alternatively, this difference may be a result of the bathymetry of the basin, with the presence of jasper reflecting a more oxidizing,

turbulent, near shore environment (James, 1954). Figure 3, taken from Zajac (1974), gives the generalized Eh-pH diagram for the Fe-C-O-H system. Jasper in the form of disseminated hematite, is favoured by acidic to neutral, relatively oxidizing solutions, while magnetite, siderite and the iron silicates are thermodynmically more stable in more basic, reducing waters. These chemical relations may reflect bathymetric conditions with oxidizing, neutral waters found in turbulent, near shore areas and basic, reducing waters in deeper water areas where circulation is more restricted. This latter argument is supported by the fact that where the SCIF - JMIF transition is developed (Sections II, V and XIII) the area is geographically close to, and directly correlateable with the Schefferville area stratigraphy (II and V), or is associated with an inferred paleohigh which implies a near shore depositional environment (Zajac, 1974).

Similarly, the boundary between the Middle and Upper Iron Formation, UIF, is not directly comparable between the Knob Lake and Dyke Lake areas. In the Knob Lake area the boundary is taken as the last occurrence of jasper rich beds, representing a transition from a JMIF facies to a CIF facies (Schwellnus, 1957). In the Dyke Lake area the Upper Iron Formation is poorly represented as it is usually either unexposed (Section III, XI, XII) or its place is taken by

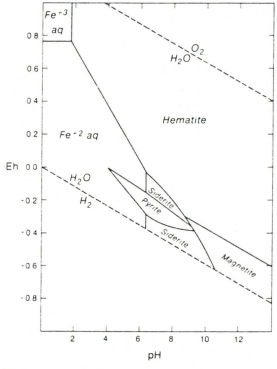

Figure 3a: Stability relations of hematite, magnetite, siderite and pyrite in water at 25°C. Total dissolved sulphur = 10 – 6 M/L. Total dissolved carbonate = 10 M/L. After Zajac (1974, p. 32).

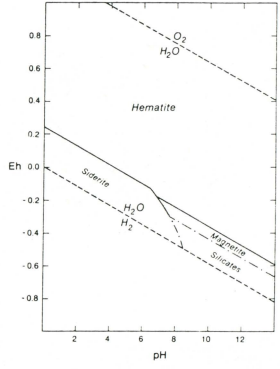

Figure 3b: Stability relations of hematite, magnetite, siderite and hypothetical iron silicates with different $Fe^{+2} - Fe^{+3}$ ratios in water 25°C. Total dissolved carbonate = 10 M/L. Only fields of solids are shown. After Zajac (1974, p. 32).

volcanic flows and interbedded sediments (Sections II, V, VI, VII, VIII, X). In localities where chemical sediments in the Upper Iron Formation are developed, Sections I, IV, V, XIII, XIV, the MIF - UIF transition is marked by a change to a CIF and SCIF lithology, similar to that found in the Schefferville area. The MIF - UIF boundary is therefore put at the top of the last oxide facies unit.

The similarities and differences between the general stratigraphy of the Schefferville and Dyke Lake areas serve to indicate that they were both part of the same sedimentary basin, undergoing the same regional fluctuations in Eh-pH conditions of basin water but that they both possess specific features, peculiar to certain areas, which reflect the temporal variations in volcanism and paleogeography of the Schefferville - Dyke Lake sedimentary basin.

III.2 - Stratigraphy and Paleofacies Environments of the Sokoman Formation:

III.2.1 - The Lower Iron Formation:

The stratigraphy of the Iron Formation in the Dyke Lake area is best analyzed by dividing the area into eastern, western and central zones with zone boundaries running along the lengths of Dyke and Astray Lakes (Figs. 1 and 2). Relative to Figure 2, Sections I, II, III, IV, IX, XIII and XIV belong

to the eastern zone, Sections VI, VII, VIII, X, XI and XII to the central zone and V to the western zone. These zones are distinguishable both on the basis of their regional stratigraphic relationships to the volcanics and the internal stratigraphy of the iron formation. They are separated by major high angle reverse faults.

Immediately preceeding the deposition of the iron formation, the Schefferville - Dyke Lake sedimentary basin was probably part of the large epicontinental sea that surrounded the Ungava Craton (Dimroth et al., 1970). The preceeding transgression of the Wishart Formation had eroded the Archean Craton down sufficiently to preclude any significant clastic input during the deposition of the iron formation. Similarly, slopes within the basin must have been very shallow. The eastern part of the Dyke Lake basin was also affected by submarine and subaerial volcanism of the Petitsikapau Lake Formation. The structures of the volcanics indicate that they formed a large submarine volcanic pile that covered the whole of the Dyke Lake - Petitsikapau Lake peninsula. At least one subaerial volcanic centre was present west of Point Lake. This inferred paleo-topography had a strong control on the facies distribution during LIF deposition.

The Lower Iron Formation of the eastern zone is characterized by a thin JMIF facies iron formation west of

Point Lake, Section (XIV), which grades northward into a sequence of interbedded SCIF - CHMIF at Evans Lake (XIII). This trend, which apparently represents increasing water depth, continues to the north with the Tee Lake (IX) and Dale Lake sections (IV), showing an interbedding of submarine mafic pillow lavas and magnetite graywackes. The northern extremity of this zone (sections I and II) reflects a return to chemical sedimentation with the deposition of SCIF lithologies similar to those of the Schefferville area.

These facies variations are readily explained when related to the associated volcanics. Directly below the iron formation in the southern regions (Sections XIII and XIV) is a series of intermediate to acidic volcanics and associated tuffaceous and conglomeratic rocks. The sedimentological and petrological evidence is compatible with a model of a subaerially exposed volcanic centre around which the final products of a Petitsikapau Lake Formation volcanic cycle were erupted. This model of a volcanic island within the sedimentary basin provides, a paleo-high for the development of slope controlled Eh-pH gradients from north to south, a source for the abundant volcanic detritus within the magnetite graywackes and also the required slope instability to account for the possible mass flow features in the magnetite graywackes. The northernmost sections (I and II) were probably unaffected

by these mass flow deposits and hence reflect the general chemical sedimentary nature of the LIF outside of the Dyke Lake area.

The section at Charlie Lake, (VII), typifies the probable sedimentary succession of the Lower Iron Formation in the central zone. In this section the Wishart Formation is overlain successively by lean chert, black ferruginous siltstones, lean chert and SCIF lithologies. The lean chert that lies at the top of the Wishart Formation has been recognized elsewhere in the Trough (Zajac, 1974; Klein, 1976) and marks the beginning of large scale, homogenous, chemical sedimentation within the sedimentary basin of the Labrador Trough.

The Lower Iron Formation of the central zone probably represents a broad platformal basin of little relief that was a southern extension of the Schefferville basin.

Chemical sedimentation prevailed in the western zone during the Lower Iron Formation with the section at Pierres Point (V) showing CIF at the base grading up into a thin SCIF unit. This basal CIF unit is also present to the northwest of Pierres Point where it is the dominant facies of Zajac's member 1 in areas east of the Stakit Lake paleohigh (Zajac, 1974).

In summary the stratigraphy of the Lower Iron Formation in the Dyke Lake area depicts a series of subaerial volcanic islands in the southeast with a sedimentary basin in the north

and west which maintains relatively low relief throughout the area of the central and western zones, as shown schematically in Figure 4a.

III.3.2 - The Middle Iron Formation:

The Middle Iron Formation in the Dyke Lake area shows a change to oxide facies chemical sedimentation throughout the area except in the northeast where clastic magnetite graywackes and minor volcanics prevailed (Sections I and II). This change is also seen in the Schefferville (Schwellnus, 1957; Zajac, 1974) and Andre Lake areas (Dufresne, 1950; Wardle, 1976) implying a basin-wide change in Eh-pH conditions. Zajac (1974) has demonstrated that this change to oxide facies mineralogy in the Schefferville area is strongly related to the development of sedimentological features characteristic of high energy, near shore conditions. This is also the case in the Andre Lake (Wardle, 1976) and Dyke Lake areas where cross-bedding, intra-formational jaspilite conglomerates and oolites are common. The associated mineralogical and sedimentological variations are best explained by an overall lowering of the sea level or regression, exposing more land area to turbulent, more oxidizing waters.

The LIF - MIF transition proceeded differently in the various zones of the Dyke Lake basin. In the eastern zone,

SCHEMATIC STRATIGRAPHY OF SOKOMAN FORMATION

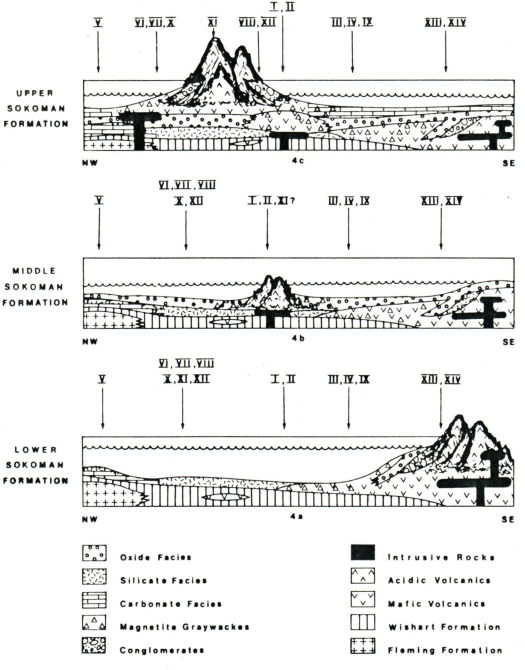

Figure 4

the northern and central areas underwent mixed cherty oxide facies and magnetite greywacke sedimentation. The volume of the latter increases to the north where Sections I and II are dominated by magnetite greywackes and minor mafic volcanics of the Astray Lake Formation. With the overall lowering of the water level these volcanics were probably subaerially exposed and contributed to the greywackes associated with them, fig. 4b.

In the central zone the change to Middle Iron Formation deposition shows a transition zone of interbedded CHMIF and SCIF units throughout the zone. This mineralogical association possibly reflects the deeper water conditions that were similarly prevalent during Lower Iron Formation deposition in the central zone. The upper units of the Middle Iron Formation in the central zone are more typical of the general regression, showing turbulent, near shore JMIF facies deposition.

III.2.3 - The Upper Iron Formation:

The Upper Iron Formation, UIF, in the Dyke Lake - Knob Lake basin shows a general reversion back to more reducing conditions indicated by the CIF and SCIF facies present in the eastern and western zones. The basin-wide change in the Eh-pH conditions accompanied by the development of quiet water sedimentary structures is interpreted as a large scale transgression and deepening of the basin waters.

In the central zone this transition is replaced by an abrupt change to a volcanic - graywacke stratigraphy, typical of the LIF of the eastern zone. This shift in the centre of volcanism to the Jasper Mountain - Charlie Lake area (Sections VI and XI) becomes the dominant paleogeographic feature controlling the internal stratigraphy of the iron formation.

The UIF of the eastern zone is marked by CIF facies in the south (Sections IV, XIII and XIV) and a mixture of CIF and clastic magnetite graywackes in the north (Sections I and II). The presence of deep water, SCIF facies at the top of Section XIV implies that by the time of UIF deposition the volcanic island in the Point Lake area had been eroded below wave base and was not contributing clastic detritus to the sedimentary basin. Therefore, the graywackes of the northern sector of the zone must have come from another source, either the volcanic islands that were developing to the southwest in the central zone, or from some other unexposed volcanic centre.

Figure 4c represents the paleogeographic interpretation of the UIF stratigraphy in the Dyke Lake area. The figure represents a conical-shaped depositional basin with a ring of laterally graded, coarse to fine clastic sediments located around the volcanic centre of Jasper Mountain. Farther away from this subaerially exposed island the areas were generally deeper and devoid of clastic input which resulted in CIF and

SCIF deposition. This model correlates well with Zajac (1974) who showed that the southern section of UIF in the Knob Lake Basin is dominated by clastic facies of iron formation, while those further away from the volcanic centres retained CIF and SCIF facies chemical sedimentation.

The contact of the Iron Formation with the overlying Menihek Formation is not exposed in the Dyke Lake area. The carbonaceous and locally pyritiferous mineralogy of the Menihek Formation indicates continued restricted circulation within a closed sedimentary basin, but the lack of chert and iron rich horizons implies a substantial change in the chemistry of the basin waters.

CHAPTER IV

STRUCTURAL GEOLOGY

The structural geology of the Dyke Lake - Astray Lake area is dominated by a series of northeast trending, high angled reverse faults and tight to open, upright to slightly overturned folds formed during the Hudsonian orogenic event (circa - 1735 m.y. Stockwell, 1964).

Faults are marked by steep topographic depressions and by disruption of stratigraphic lineaments that are easily recognized on air photographs. The major faults of the area, which run along the lengths of Dyke and Astray Lakes, separate the western central and eastern blocks described in previous sections. Each of the structural zones contains numerous minor faults, but these do not appear to have seriously disrupted the stratigraphy. Since the Dyke Lake and Astray Lake faults juxtapose zones of contrasting stratigraphy it is likely that considerable amounts of section have been removed along their length.

In the cross sections A - B and C - D (Fig. 1a) the faults are shown as high angle reverse faults that sole out at depth in the Attikamagen and to a lesser extent, Menihek Formations. The middle formations of the Knob Lake Group appear

to have behaved as passive structural masses that were moved along shear planes located in the less competent shales of the Attikamagen and Menihek Formations. This style of deformation was also described by Harrison et al. (1972) whose detailed work in the Schefferville area proved the existence of many major décollements within the shale members of the Knob Lake Group.

Definite structural evidence of Cretaceous block faulting, which was instrumental in the formation of ore grade material in the Schefferville area, is lacking in the Dyke Lake area, but numerous sections of the iron formation do show Cretaceous age leaching effects similar to those in the Schefferville ore zone.

Fold axes in the Dyke Lake - Astray Lake area parallel the NE-NNE trend of the thrust faults and are probably pre- and synkinematic with respect to faulting. The style of folding is one of long, sinuous, upright to slightly overturned, tight to open anticlines and synclines that are usually complicated by reverse faults along fold axes and fold limbs. Dips of strata vary from 40° to vertical in the central and eastern zones, while the western zone shows more gentle dips consistently around 45°. Perhaps the presence of a thick volcanic mass acting as a large competent structural body in the central and eastern zones prevented the development of the regular fold

pattern that is typical of other areas in the Trough and caused the tight upright folding and closely spaced thrusting noted. The apparent deflection of the fold axes north of Evans Lake on the Dyke Lake - Petitsikapau Lake Peninsula is probably secondary and related to a sinistral strike-slip component in the faults north of Evans Lake.

As described in Chapter III metamorphic recrystallization and replacement reactions associated with this Hudsonian metamorphic event produced sub- to lower greenschist facies mineral assemblages in all formations. This facies of metamorphism is consistent with the general distribution of metamorphic isograds within the Labrador Trough which ranges from essentially unmetamorphosed sediments on the western margin to garnet bearing amphibolite grade assemblages at the eastern margin of the Trough (Dimroth et al., 1970; Zajac, 1974; Wardle, 1976; Wardle and Doherty, 1977). Further discussion on the degree of geochemical mobility associated with the metamorphism and the relation of the regional metamorphic event to more localized metamorphic/metasomatic processes possibly associated with the Nimish volcanic activity is presented in Chapter V.

Metamorphic realignment of minerals during the Hudsonian orogenic event is very poorly developed in the Dyke Lake area and seems to be largely controlled by local structures. In

the Wishart Formation quartz grains have retained their randomly distributed undulose extinction angles and the dolomite crystals of the Denault Formation similarly show no evidence of realignment of deformation. Evidence of metamorphism within the Sokoman Formation is nonexistent or is masked by diagenetic reactions, while very weak S1 chloritic fabrics are found near some small shear zones within the volcanics.

The best evidence of mineral alignment is found in the Attikamagen or Denault Formation siltstones found at the south end of Dyke Lake. In these rocks chlorite and muscovite form a S1 fabric oriented parallel to bedding in highly sheared outcrops. The fabrics are vertical to slightly overturned to the east implying slight overturning of the folds to the west. These fabrics are not found in unsheared outcrops of the Attikamagen Formation and, similar to the chloritic fabrics of the Nimish Subgroup, seem to be more closely related to local shear zones than a regional metamorphic pressure gradient.

No metamorphic recrystallization is present within the Menihek Formation. Outcrops in the northeastern sector of the area show evidence of brittle fracturing while those exposed elsewhere show little or no effect from the orogenic event.

CHAPTER V

PETROCHEMISTRY OF THE NIMISH SUBGROUP

V.1 - Introduction:

The volcanic rocks of the Nimish Subgroup have been shown to be stratigraphically divisible into two major volcanic cycles warranting subdivision into the Petitsikapau Lake and Astray Lake Formations (Evans, 1978). The main purpose of this thesis is to use the whole rock chemical data of the two formations to check for similarities and differences between the two formations and to determine possible geochemical affinities of the volcanic suite (Appendix B). A limited number of the samples were analyzed for the rare earth elements (Table 7 and 20), and a series of models were derived from these data to test fractional crystallization relationships between the rock types and to provide geochemical evidence in support of the proposed subdivision of the Nimish volcanics.

The ensuing discussion offers a brief review of current work on the geochemical effects of submarine hydrothermal alteration, followed by a discussion of the effect of such alteration on the Nimish Subgroup. The standard means of presenting major element data are reviewed and some of the more recently developed petrologic discrimination diagrams based on

the relatively immobile trace elements are used to provide a general geochemical classification for the Nimish Subgroups. This classification is discussed in relation to the petrography of the samples and the geochemical classification based on major element chemistry.

V.2 - Theoretical Geochemical Effects of Low Grade Metamorphism:

Since all the volcanic rocks of the Dyke Lake area have undergone sub- to lower greenschist facies metamorphism some knowledge of the effects of this metamorphism on the bulk chemistry of the volcanics is needed before discussing the igneous geochemistry.

Numerous studies have been carried out on the effects of low grade metamorphism on the geochemistry of mafic igneous rocks (Hart, 1970; Thompsen et al., 1970; Cann, 1969, 1970; Smith and Smith, 1976; Hajash and Scott, 1976; Wood et al., 1976; Condie et al., 1977; Floyd, 1977). The alteration processes have also been simulated in the laboratory through the hydrothermal experiments of Hajash (1975) and Bischoff and Dickson (1975). These studies have resulted in a series of somewhat contradictory conclusions which are related to variations in the experimental method and the conditions of metamorphism studied. Integration of these results leads to

recognition of a threshold of significant alteration for each element which is a complex function of temperature, pressure, brine chemistry, original rock composition, gaseous pressures, etc.

Miyashiro et al. (1969) demonstrated the applicability of this concept by showing the change in behaviour of the Fe^{+3}/Fe^{+2} ratio from sub- to lower greenschist facies metamorphism of submarine mafic volcanics. The dependence of Cu and Ni mobility on the temperature and duration of the hydrothermal experiments of Hajash (1975) also recognizes the complex nature of geochemical mobility. Laboratory work on ore solution geochemistry has produced quite elaborate models noting the effects of the various geochemical parameters that control ore mineral transport (Krauskopf, 1967). The natural environment is much more complex than can be experimentally modelled, so generalizations about the degree of mobility of any element must be considered relative to other elements or other conditions; in this sense ideas on metasomatic alteration are highly subjective.

Aside from the chemical factors, certain physical parameters also control the mobility of elements during low grades of metamorphism. Coish (1976) and Spooner (1977) have shown that many metamorphic facies assemblages may be present in obducted ophiolite suites which were presumably affected by only one

period of alteration. Frey et al. (1974) have pointed out that the glassy and crystalline portions of basaltic lavas respond differently to low temperature alteration. Similarly, Hajash and Scott (1976) have stressed the large temperature and brine composition variations present in the alteration environment associated with the formation of pillow lavas. These range from the very high temperature deuteric alteration connected with the trapped volcanic fluids to sub-greenschist temperature alteration related to secondary halmyrolysis.

The combination of all the physical and chemical factors possibly involved in obscuring primary lava chemistry in the metamorphic/metasomatic environment along with the chemical changes that occur upon subaerial exposure reduce the effect of alteration studies on igneous petrology and petrogenesis to one of generalizations and assumptions. The general consensus on the mobility of the major elements during average submarine alternation, as compiled from the aforementioned documents, is summarized in Table 2. The subaerial weathering data are taken from Wedepohl (1974).

The behaviour of trace elements for the most part follows that of the major elements for which they show affinities during normal igneous processes. Specific studies on the behaviour of trace elements (Cann, 1969, 1970; Frey et al., 1974; Wood et al., 1976; Condie et al., 1977) have led to the recognition

TABLE 2

MOBILITY OF THE MAJOR ELEMENT OXIDES DURING LOW GRADE METAMORPHISM

SUBMARINE WEATHERING

VERY MOBILE:	$+H_2O$, $+Fe^{+3}/Fe^{+2}$, $+K_2O$, $-CaO$, $-MgO$
MOBILE:	$-Na_2O$, $-SiO_2$
SLIGHTLY IMMOBILE:	+ Fe
IMMOBILE:	TiO_2, Al_2O_3, P_2O_5

SUBAERIAL WEATHERING

VERY MOBILE:	$-CaO$, $-Na_2O$, $-MgO$, $-K_2O$, $+H_2O$
MOBILE:	$-SiO_2$, $-P_2O_5$
IMMOBILE:	Fe, Al_2O_3, TiO_2

GREENSCHIST GRADE METAMORPHISM

VERY MOBILE:	$-CaO$, $+H_2O$
MOBILE:	$+Na_2O$, $+SiO_2$, $+MgO$, $+FeO$, $-K_2O$, $-Al_2O_3$
IMMOBILE:	TiO_2, Fe^{+3}/Fe^{+2}, P_2O_5

* NOTE: '+' refers to a net addition of that compound while '-' refers to a net loss during the period of geochemical mobility.

of a group of trace elements which are relatively insensitive to most hydrothermal alteration processes. These "relatively immobile elements" (Cann, 1969) are generally the heavy, highly charged, transition ions. The relatively incompatible nature of these elements is also especially useful as they serve as good discriminating factors between altered tholeiitic and alkalic basalts. The list of generally accepted immobile elements has grown since the original use of Ti, Zr, Nb and Y by Cann (1970) notably with the addition of Hf and Sc (Frey et al., 1974), Ta (Wood et al., 1976), P_2O_5 (Floyd and Winchester, 1975) and Ga and Ce (Winchester and Floyd, 1977).

The compatible transition elements such as Ni, Cr, Co and V have been shown to be immobile in some studies (Frey et al., 1974; Condie et al., 1976) and also have been used in magma type discrimination diagrams (Bloxam and Lewis, 1973) but the experimental work of Hajash (1975) indicates that they are susceptible to high temperature alteration. In addition, their susceptibility to slight variations in the degree of fractionation distort distributions on a discriminant diagram if the stratigraphic control is not perfect.

The susceptibility of the rare earth elements, REE, to secondary hydrothermal alteration was originally discussed by Frey et al. (1974), who showed that the REE as a whole were only slightly affected by submarine alteration processes.

Generally there was a tendency for a slight increase in the light rare earths, LREE, La-Nd, and a decrease in the heavy rare earths, HREE, Er-Yb. This would have the effect of increasing the La/Yb and steepening the REE pattern, making the rock seem more alkalic.

This conclusion was similarly reached by Wood et al. (1976), Condie et al. (1977) and Floyd (1977) but in general the degree of variation caused by this process is considered small and the use of the REE as a magma type discriminant in altered rocks is generally accepted (Herrmann, 1972).

V.3 - Metamorphism of the Nimish Subgroup:

As discussed in Chapter II.2.5.3 the mineralogy of the Nimish volcanics implies that a sub- to lower greenschist facies metamorphism has affected these rocks. The development of large chloritic rims on the pillow lavas and the general restriction of quartz and epidote as vein and amygdaloidal minerals to pillow lavas implies that the recognized grade of metamorphism occurred at or near the time of extrusion of the volcanic rocks. Later regional metamorphic effects on the volcanic rocks appear to be minor as the compressive forces only produce small non-penetrative shear zones with localized mineral alignment. The presence of low grade metamorphism in mafic volcanic rocks that formed in submarine basins implies the Nimish volcanics

have been affected by a submarine hydrothermal event similar to that documented in submarine volcanic centres of today. In this aspect the general conclusions reached in Section V.2 and Table 2 would probably apply to the geochemistry of the Nimish volcanics.

Figures 5 and 6, from Hughes (1973) give an indication of the degree of alteration the Nimish Subgroup has undergone. The area between the two curves represents the bounds of all recognized primary igneous compositions, with analyses outside these boundaries considered altered. The Petitsikapau Lake and Astray Lake Formations, and associated intrusive rocks, or Nimish Subgroup, as they will be referred to when no distinction is made on the diagram discussed, show a strong shift towards potash enrichment with about 25 percent plotting outside the igneous spectrum. In contrast the Doublet group shows a shift towards soda enrichment; behavior more typical of spilitization. The potash enrichment of the Nimish Complex is mineralogically represented by the partial replacement of plagioclase by muscovite and potash feldspar and the minor vein and amygdaloidal occurrences of quartz and adularia. Potash enrichment is significant as it implies metasomatism under conditions quite unlike those associated with normal spilitization where soda enrichment is the norm.

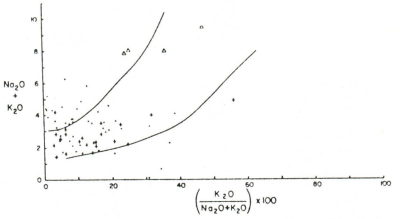

Figure 5: 'Spilite diagram', Hughes (1973), for the Doublet Group and Lac Musset Volcanics.
+ = Doublet Group, Baragar (1960)
• = Doublet Group, Dimroth et al. (1970)
Δ = Lac Mussett Volcanics, Dimroth et al. (1970)

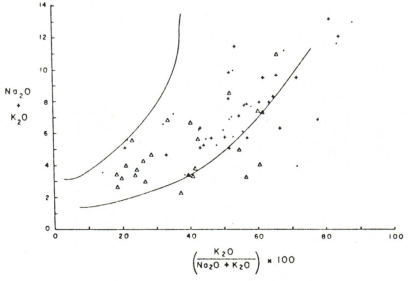

Figure 6: 'Spilite diagram', Hughes (1973), for the Nimish Subgroup.
• – Petitsikapau Lake Formation
+ – Astray Lake Formation
Δ – Intrusive rocks

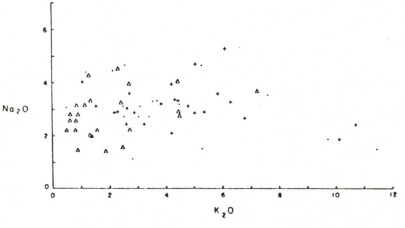

Figure 7: Na_2O versus K_2O diagram for the Nimish Subgroup
Symbols the same as Figure 6.

The lack of a strong negative correlation between Na_2O and K_2O, (fig. 7), discounts Na - K substitution as a means of generating the high K_2O content of the Nimish Subgroup lavas. Possibly these high values have resulted from the net addition of K as a replacement for Ca in feldspar sites.

Experimental and theoretical work by Hemley (1959) and Helgeson (1964, 1969) have shown that metasomatic alteration in the feldspar system is controlled by the ionic ratios, K^+/Na^+, K^+/Ca^{++} and Na^+/Ca^{++} in the metasomatic fluid, and to a lesser extent by temperature, with a high temperature causing a greater degree of potash fixation. Considering the low grade mineral assemblages of the Nimish volcanics, high K^+/Na^+ and K^+/Ca^{++} in a metasomatic fluid altering the volcanics at normal spilitic temperatures (200 - 300°C) would seem to be the best explanation for the observed alteration.

This unusual fluid composition may be the result of an increased K^+/Na^+ ratio in the brines of the volcanic - sedimentary basin caused by the deposition of Na - Fe - Si gels in the formation of the contemporaneous iron formation (Eugster and Jones, 1968; Eugster, 1969; Eugster and Chou, 1973; French, 1973). Alternatively this potash enrichment could be explained by fluid migration through the K_2O rich shales of the Attikamagen Formation or through a high K_2O/Na_2O in the original magma and/or late-stage volcanic fluids.

Potash metasomatism is not a widespread phenomenon and has only been documented in a few places. Vallance (1960) in an historical review of the mineralogy of spilitic rocks noted that DeRoever (1942) described a suite of alkali basalts from the Permian of Timor in which all of the primary feldspar had been replaced by an adularian feldspar forming a rock he termed "poenlite". Vallance also described occurances from the Rhine Valley and Yellowstone National Park in the U.S.A. where potassic alteration of feldspars was noted but not on the scale of DeRoever's description. More recently Gunn and Roobol (1976) has described a few samples from the lesser Antilles island arc of the Caribbean which show potash enrichment. The exact nature and origin of the alteration for the above suites is unknown, but like the Nimish area it must be a function of the fluid chemistry and temperature of the metasomatic environment.

The effect of this potash metasomatism on the major and trace element contents is analyzed through the use of correlation coefficients, as presented for the mafic members of the Petitsikapau Lake Formation in Table 3. This limited population was chosen in an effort to isolate an homogenous group of samples which are geographically and stratigraphically distinct, and have presumably undergone a similar primary petrogenetic history but varying degrees of secondary alteration.

TABLE 3

MEANS, STANDARD DEVIATIONS AND CORRELATION MATRIX FOR THE MAFIC MAMBERS OF THE PETITSIKAPAU LAKE FORMATION *

	FE2O3	TIO2	P2O5	SIO2	CAO	K2O	MGO	AL2O3	FEO	NA2O	LOI	MNO	ZR	SR	RB	ZN	CU	BA	NB	GA	PB	NI	CR	V	Y
X	6.09	2.24	0.23	45.34	5.24	2.84	5.87	14.33	9.11	2.96	3.95	0.22	189.	523.	54.	117.	50.	1346.	28.	21.	3.	53.	38.	259.	31.
SD	1.67	0.53	0.16	3.78	1.43	1.81	2.54	1.24	1.45	0.77	0.49	0.04	49.	2233.	5	25.9	22.6	33.0	723.3	7.3	2.5	3.9	50.2	47.4	54.7	5.5

CORRELATION MATRIX CALCULATION FOR 21 SETS OF DATA

	FE2O3	TIO2	P2O5	SIO2	CAO	K2O	MGO	AL2O3	FEO	NA2O	LOI	MNO	ZR	SR	RB	ZN	CU	BA	NB	GA	PB	NI	CR	V	Y
VBLI	2	3	4	5	6	7	8	9	10	11	12	13	14	15	16	17	18	19	20	21	22	23	24	25	
1	0-260	-21	-478	125	-454	133	-357	-55	29	263	837	-217	230	-309	785	259	19	-244	177	75	-177	-264	254	-65	
2	0	0	168	137	-265	74	-133	-5	-173	442	-273	-174	641	-204	21	-139	-245	53	469	475	-59	-262	147	512	477
3	0	0	0	594	-416	557	-599	372	-751	-56	-594	-126	972	-98	653	242	-22	395	885	-32	642	-426	-112	-263	375
4	0	0	0	0	-375	-926	-896	611	-846	141	-814	-849	724	-16	817	-328	-647	626	576	-130	405	-427	-314	-459	535
5	0	0	0	0	0	-551	740	-756	223	-419	356	413	-594	169	-643	-27	674	-462	-592	-141	-173	594	515	227	-134
6	0	0	0	0	0	0	-873	592	-355	-196	-492	-626	693	-169	959	-203	-606	638	707	-210	327	-412	-350	-557	449
7	0	0	0	0	0	0	0	-738	492	-100	557	476	-643	24	-883	142	675	-526	-626	173	-257	639	524	521	-433
8	0	0	0	0	0	0	0	0	-281	343	-374	-567	433	-36	559	-163	-566	337	249	-8	70	-574	-531	-353	132
9	0	0	0	0	0	0	0	0	0	-274	772	67	-643	-170	-436	-76	393	-422	-519	-113	-537	337	169	56	-926
10	0	0	0	0	0	0	0	0	0	0	-335	-51	177	16	-130	-146	-131	-62	115	421	-61	-347	-75	372	154
11	0	0	0	0	0	0	0	0	0	0	0	230	-556	57	-535	135	469	-496	-497	-176	-569	334	181	7	-334
12	0	0	0	0	0	0	0	0	0	0	0	0	-453	65	-522	697	512	-120	-379	210	62	31	-25	477	-152
13	0	0	0	0	0	0	0	0	0	0	0	0	0	58	669	41	-686	416	837	-8	467	-502	-263	-315	304
14	0	0	0	0	0	0	0	0	0	0	0	0	0	0	-92	25	-395	339	-16	-692	194	-96	-181	-347	-163
15	0	0	0	0	0	0	0	0	0	0	0	0	0	0	0	-156	-578	714	724	-251	373	-413	-324	-551	415
16	0	0	0	0	0	0	0	0	0	0	0	0	0	0	0	0	3	-30	-174	266	163	-233	-241	191	159
17	0	0	0	0	0	0	0	0	0	0	0	0	0	0	0	0	0	-499	-597	30	-224	490	331	421	-342
18	0	0	0	0	0	0	0	0	0	0	0	0	0	0	0	0	0	0	540	-142	343	-594	-571	-366	334
19	0	0	0	0	0	0	0	0	0	0	0	0	0	0	0	0	0	0	0	31	461	-395	-151	-242	701
20	0	0	0	0	0	0	0	0	0	0	0	0	0	0	0	0	0	0	0	0	-81	12	247	757	73
21	0	0	0	0	0	0	0	0	0	0	0	0	0	0	0	0	0	0	0	0	0	-274	-326	-107	338
22	0	0	0	0	0	0	0	0	0	0	0	0	0	0	0	0	0	0	0	0	0	0	574	125	-482
23	0	0	0	0	0	0	0	0	0	0	0	0	0	0	0	0	0	0	0	0	0	0	0	336	-274
24	0	0	0	0	0	0	0	0	0	0	0	0	0	0	0	0	0	0	0	0	0	0	0	0	-40

* Note: All correlation coefficients are quoted on a scale of -1,000 to +1,000. Correlations of an oxide or element to itself are set at zero instead of +1,000 for clarity.

Through this restriction all recognized correlations should either be a result of the spilitization process or slight variations in phenocryst concentrations as documented in the petrography section.

Geochemical evidence for normal spilitization reactions is seen in the positive correlation of FeO and MgO with LOI and the complementary negative correlation of SiO_2 with LOI. The compatible trace elements Ni, Cr and V all show low correlations with LOI implying that, in contrast to MgO, these trace elements were not affected by the alteration and that the maximum temperature of the alteration is consistent with the lower greenschist mineral assemblages present (Hajash, 1975). The divergence of MgO and FeO with the compatible trace elements during this alteration is supported by the relatively low positive correlation between these groups of elements and indicates that MgO and FeO were mobile during the alteration.

The relations among the alkali and alkali earth metals are also presented in figures 6 and 7. The strong negative correlation of K, Rb and Ba with Ca is consistent with the noted plagioclase alteration and their similar susceptibility to hydrothermal processes as well as normal plagioclase fractionation within these lavas. Sr shows a low correlation with Ca and therefore could have been mobile during alteration as Sr and Ca should be strongly positively correlated if due to plagioclase fractionation.

The interrelationships of the relatively immobile elements P, Zr, Nb and Y are all positive and show high correlations ranging from +682 to +844. As a group these elements show a high positive correlation with SiO_2, a high negative correlation with MgO and show little or no correlation with LOI which implies that they remained relatively immobile. The correlation of these elements with TiO_2 are very low and presumably reflect erratic amounts of magnetite phenocrysts given the assumption that TiO_2 is immobile during low grade metamorphism (Table 3).

These results are consistent with the findings of Cann (1969, 1970), Thompsen et al. (1970) and Wood et al. (1976). Therefore it is likely that the distribution of these relatively immobile elements reflect the pre-metamorphic geochemistry and that the alteration had little effect.

Views on the use of alkali trace element ratios as petrogenetic indicators and their susceptibility to secondary alteration is varied (Hart, 1969; Jakes and White, 1970; Hart, 1970). Hart (1969) has shown that there is a decrease in K/Rb as K_2O increases in most altered basic volcanics except in glass rich spilites where K/Rb decreases as K_2O decreases. The former trend he equates with greater Rb fixation during low temperature alteration while the latter is explained by the high Rb concentration in the easily leached

volcanic glass. These views differ from those of Jakes and White (1970) who argue that there is no change in the K/Rb ratio until amphibolite grade metamorphism despite a compilation of K/Rb ratios from various calc-alk aline suites in the South Pacific which showed a range from 300 - 600.

Table 4 gives a comparison of the average K/Rb and Rb/Sr ratios of the mafic members of the volcanic formations and the least altered samples of the Petitsikapau Lake Formation (Sample #JS-133, Js-57, Js-517, JB-57), and Astray Lake Formation (Sample #JS-205, JB-79, JS-15). The large standard deviations of Rb/Sr and K/Rb ratios within the groups of samples noted confirms the mobility of these elements. Although the deviations cast some doubt on this approach the increase in the average K/Rb and Rb/Sr from the unaltered samples to the total suite for each formation is consistent with distinct additions of K and to a lesser extent Rb. This trend of increasing K/Rb ratio with metamorphism is contradictory to the general trends of greenschist grade metamorphism which usually involve a lowering of the K/Rb ratio due to greater Rb fixation at lower temperatures. This may be due to a peculiar fluid composition abnormally rich in K. The higher Rb/Sr ratio in the altered and unaltered samples of the Astray Lake Formation relative to the Petitsikapau Lake Formation reflects the lack of Sr rich, plagioclase porphyritic lavas in the Astray Lake Formation.

TABLE 4

K/Rb AND Rb/Sr RATIOS FOR THE BASALTIC MEMBERS OF THE NIMISH SUBGROUP, LITTLE ADEN SUITE AND STANDARD AVERAGE BASALTS

	K/Rb	Rb/Sr
TOTAL PETITSIKAPAU LAKE FORMATION	410 (70)	0.119 (.110)
UNALTERED PETITSIKAPAU LAKE FORMATION	365 (99)	0.073 (0.036)
TOTAL ASTRAY LAKE FORMATION	424 (111)	0.190 (.134)
UNALTERED ASTRAY LAKE FORMATION	414 (121)	0.091 (.027)
PERALKALINE LITTLE ADEN SUITE	311	0.097
OCEANIC ALKALIC BASALT	418	0.040
OCEANIC ISLAND THOLEIITIC BASALT	1000	0.025
CALC - ALKALINE BASALT	340	0.030

* Data from Engel et al., (1967), Cox et al., (1970), Jakes and White, (1970), and Appendix B. Numbers in brackets are standard deviations.

In conclusion there seems to be ample evidence for significant mass transfer of K_2O, CaO, MgO, FeO and Fe_2O_3 causing important changes in the chemical composition of the Nimish Subgroup lavas. The classical methods of petrogenesis, as discussed by Green and Ringwood (1967) and O'Hara (1968) would be of little use in discussing the petrogenesis of the Nimish Subgroup given this conclusion. Therefore, I have attempted a petrologic classification based upon the recognized immobile trace elements and have treated the petrogenesis solely through the use of rare earth elements.

Due to the limited number of samples analyzed for REE and the desire to only analyze the least altered samples available, it was impossible to test the degree of geochemical mobility that has affected these elements. Given the general geochemical similarity of the REE with incompatible elements such as Zr and Y, which have been shown to be immobile in the Nimish Subgroup, and the studies in the literature which support the relative insensitivity of the REE to secondary hydrothermal alteration (Frey et al., 1974; Wood et al., 1976), it was presumed that the REE concentrations reflect the original pre-alteration concentrations. As such, geochemical data for Ti, Zr, Y, Nb and the REE are used with much more certainty than the major elements throughout the thesis.

V.4 - Igneous Geochemistry of the Nimish Subgroup:

V.4.1 - Introduction:

Discussion of the geochemistry of the Nimish Subgroup will be divided into four main sections. Initially the major elements will be reviewed using a few standard diagrams to provide a background for comparison of the trace element data. A subdivision of the analyses will then be based upon the relatively immobile trace element abundances and the rare earth element data will be discussed in relation to these groupings. Finally the rare earth data will be used to place some limits upon the possible petrogenetic relations between the proposed lava types.

With regards to the preceding discussion on the secondary alteration of the Nimish volcanics the author realizes that the distributions of the major elements may be altered and that generalizations made upon this data are questionable. As a result the discussion will be brief and the diagrams will be presented mainly for reference.

Raw geochemical data is given in Appendix B with representative averages presented in Table 5.

V.4.2 - Major Element Geochemistry:

V.4.2.1 - Harker Diagrams:

The major element oxides are plotted against SiO_2 in Figure 8. A feature common to all the diagrams is the lack of many intermediate volcanics (52 percent $< SiO_2 <$ 66 percent) in the Petitsikapau Lake Formation. Similarly a lack of acidic volcanics ($SiO_2 >$ 66 percent) could be postulated for the Astray Lake Volcanics, as the four analyses plotted (JS-500, 501, 502, 503) represent agglomeratic (rhyolite) clasts. This deficiency in intermediate and acidic volcanic rocks is possibly due to normal igneous volume relationships, however this lack of differentiation seems to be common throughout the Labrador Trough where only two or three localities of acid or intermediate volcanics have been found (Dimroth, 1970).

The distribution of the major elements in Figure 8 reflects predictable igneous inter-element associations. The roughly parallel trends of MgO, FeO and Fe_2O_3 is very similar to a variation diagram scheme originally documented in Iceland (Carmichael, 1964). Carmichael concluded that the similarity of these patterns was a result of a high fO_2 in the melt which favoured the coprecipitation of magnetite with the ferromagnesian phases. In the Dyke Lake area this high fO_2 could be due to an original high magmatic fO_2 increased through differentiation or interaction of the magma chamber with seawater or connate waters.

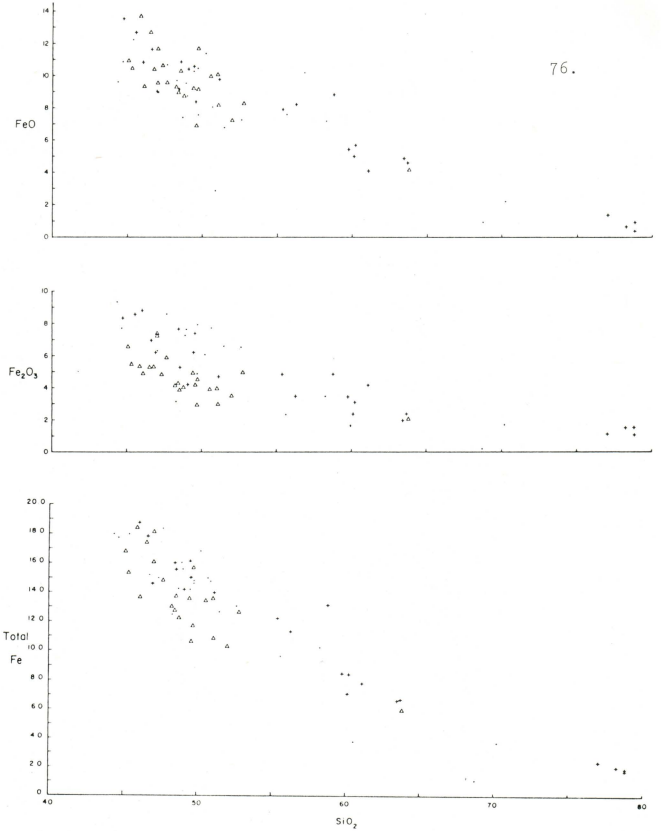

Figure 8a: Variation diagram for the major oxides FeO, Fe_2O_3 and total Fe for the Nimish Subgroup.

• – Petitsikapau Lake Formation
+ – Astray Lake Formation
△ – Intrusive rocks

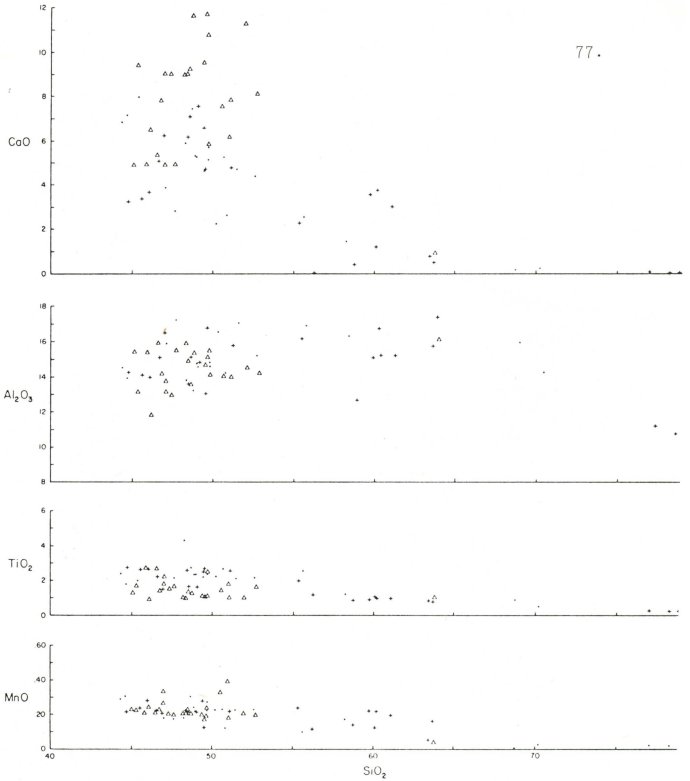

Figure 8b: Variation diagram for the major oxides CaO, Al_2O_3, TiO_2, MnO in the Nimish Subgroup.

• – Petitsikapau Lake Formation

+ – Astray Lake Formation

△ – Intrusive rocks

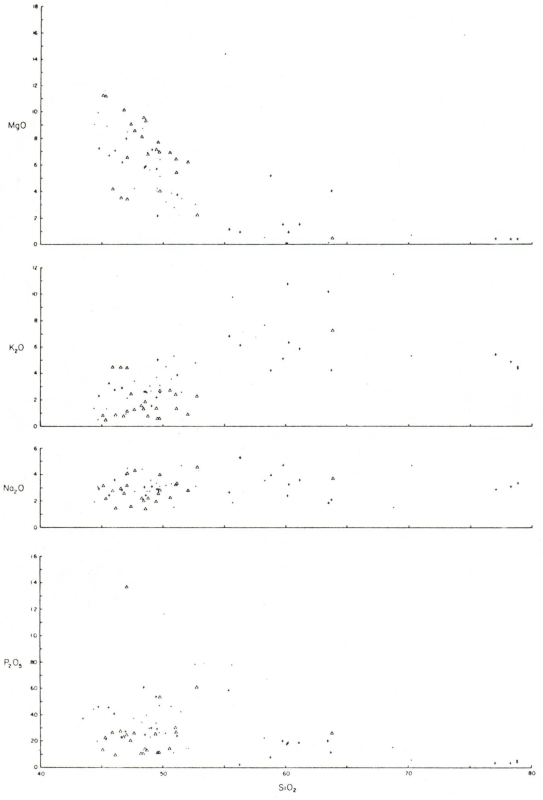

Figure 8c: Variation diagram for the major oxides MgO, K_2O, Na_2O, P_2O_5, in the Nimish Subgroup.

• – Petitsikapau Lake Formation
+ – Astray Lake Formation
△ – Intrusive rocks

The large degree of scatter on the CaO v. SiO_2 variation diagram could be attributed to secondary mobility of CaO and clinopyroxene accumulation in the gabbros. The distribution in the Al_2O_3 v. SiO_2 diagram represents variable percentages of plagioclase phenocrysts in the Nimish Subgroup mafic and intermediate lavas. The sharp depletion of Al_2O_3 in the acidic rocks of the Astray Lake Formation serves to distinguish them from the equivalent acidic rocks of the Petitsikapau Lake Formation.

Although not readily apparent in Figure 8 there seems to be a variation in the fractionation behaviour of Al_2O_3 between the two volcanic cycles. In general Al_2O_3 builds up to a peak of 16 - 17 percent at about 48 - 52 percent SiO_2 and then undergoes gradual depletion in the Petitsikapau Lake Formation, while in the Astray Lake Formation Al_2O_3 reaches its maximum at 60 percent SiO_2, and then drops off suddenly. This variation in the Al_2O_3 distribution is readily documented in the petrography of the two formations, as the mafic lavas of the Petitsikapau Lake Formation are commonly plagioclase porphyritic while those of the Astray Lake Formation are aphyric.

The depletion of TiO_2, represented by titaniferous magnetite microphenocrysts, continues from the basaltic rocks through the intermediate and acidic members of the suite. TiO_2 is distinctly lower in the intrusive rocks possibly resulting

from variations in fO_2 during crystallization of the intrusives and the resultant effect on magnetite stability.

MnO shows only slight variations marked by a preference for incorporation into the abundant pyroxene of the intrusive rocks and an overall depletion with fractionation.

K_2O exhibits an expected highly scattered linear increase with SiO_2 until the acidic rocks, while the distribution of Na_2O vs. SiO_2 reflects the low correlation coefficient of these two elements, (Table 3). Comparison of the Na_2O and K_2O Harker diagrams with Figures 6 + 7 confirms that potassium was the dominant mobile element during metasomatism.

P_2O_5 shows a very erratic distribution, presumably caused by an overall high P_2O_5 content associated with sporadic intersection of the apatite stability field during differentiation. The high P_2O_5 content of plutonic sample JS-048, 1.30 percent, reflects the cumulus apatite in this sample.

V.4.2.2 - Na_2O + K_2O Versus SiO_2 Diagram:

Figures 9 + 10 give the Na_2O+K_2O vs. SiO_2 diagrams for the igneous rocks of the Doublet Group and Nimish Subgroup respectively. The boundary lines, as defined by Kuno (1966), classify the Doublet Group as a transitional tholeiitic to high alumina basaltic suite, while the Nimish Subgroup plots as a strongly alkalic suite. In unaltered rocks this diagram

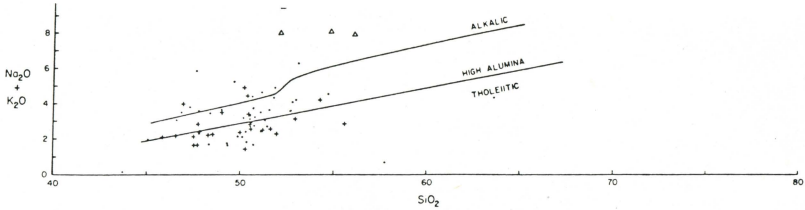

Figure 9: Total alkalis versus silica diagram for the Doublet Group and Lac Musset Volcanics.
+ = Doublet Group, Baragar (1960)
• = Doublet Group, Dimroth et al. (1970)
△ = Lac Mussett Volcanics, Dimroth et al. (1970)

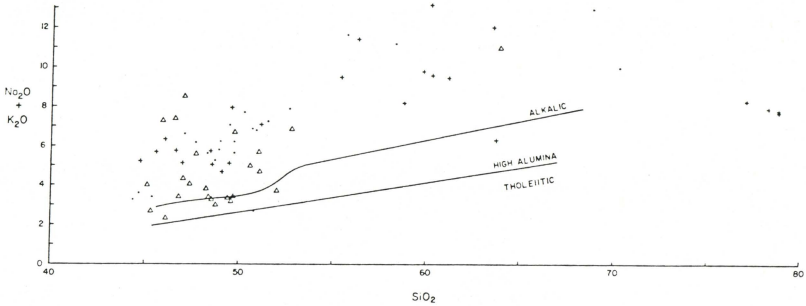

Figure 10: Total alkalis versus silica diagram for the Nimish Subgroup.
• – Petitsikapau Lake Formation
+ – Astray Lake Formation
△ – Intrusive Rocks

is a very sensitive indicator of the degree of alkalinity of a volcanic suite, but in consideration of the metasomatism documented in Section V.3 this conclusion is doubtful based on this diagram alone.

The trachyandesite samples collected from the volcanics within the Seward Formation north of Schefferville (Dimroth et al., 1970) are seemingly only mildly spilitized, Figure 5, and hence their alkalic tendencies in Figure 9 might truly be indicative of their primary geochemistry.

V.4.2.3 - AFM Diagrams:

Figure 11 compares the chemical trends of the Petitsikapau Lake and Astray Lake Formations and associated intrusive rocks with some well documented suites on AFM diagrams. The Little Aden suite comes from the southern Arabian Peninsula between the Red Sea and the Indian Ocean, where it is associated with initial stages of rifting of the Red Sea (Cox et al., 1970). The oceanic island tholeiite trend is taken from Thingmuli, Iceland (Carmichael, 1964) while the calc-alkaline trend comes from the Cascades suite, as summarized by Carmichael et al. (1974).

The distribution of the two volcanic cycles and intrusive rocks on the AFM diagram are superficially similar, and when plotted together form a coherent, well-defined variation trend.

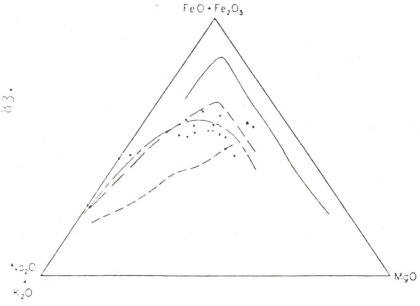

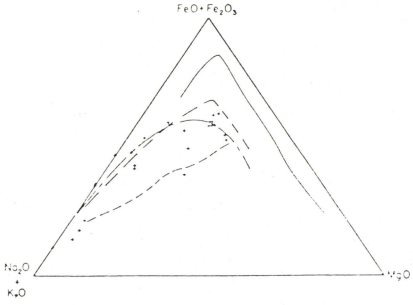

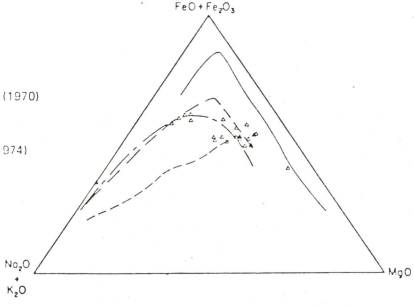

Figure 11: AFM diagrams for the Nimish Subgroup.

X – Petitsikapau Lake Formation, + – Astray Lake Formation,

Δ – Intrusive rocks.

———————— – Doublet Group, Baragar (1960), Dimroth et al. (1970)

——— ——— – Thingmuli trend, Iceland, Carmichael (1964)

— ——— — – Little Aden trend, Africa, Cox et al. (1970)

— — — — — – Cascade calc-alkaline trend, Carmichael et al. (1974)

As expected, the intrusive rocks plot closer to the MgO - FeO join while the mafic members of the extrusive cycles plot more in the centre of the diagram. The relative lack of intermediate rocks in the Petitsikapau Lake Formation relative to the Astray Lake Formation is also displayed here.

As a whole the rocks of the Nimish Subgroup plot on a trend roughly similar to the oceanic island tholeiite suite of Carmichael (1964) or the Little Aden suite as described by Cox et al. (1970). Petrogenetic affinities of the Nimish Subgroup to either of these igneous rock series are not possible to establish from this diagram.

The strong iron-enrichment trend of the Doublet Group is typical of a tholeiitic trend, and according to Dimroth (1971) the Doublet Group shows a close similarity to modern ocean floor tholeiites.

V.4.3 - Trace Element Geochemistry:

In this section the trace element geochemistry of the Nimish volcanics will be only superficially treated in an attempt to generate a classification scheme from which the discussion of the petrogenetic relations of the Nimish Subgroup may be related. In this study it was found that a recent set of diagrams devised by Winchester and Floyd (1977) provided an internally consistent petrologic nomenclature.

Figures 12 - 15 are the set of diagrams devised to discriminate between different magma series on the basis of the fractionation of immobile trace elements (Winchester and Floyd, 1977). They are not meant to imply tectonic settings or mode of origin of the suites but are designed to give an indication of various differentiation trends relative to some well documented, unaltered volcanic suites. The application of these diagrams to the Nimish volcanics seems justified as the classification suggested is internally consistent and generally compatible with those of previous diagrams. No significant differences were noted among the Petitsikapau Lake and Astray Lake Formations or associated intrusive rocks in these diagrams.

Despite some degree of scatter the general differentiation trend shown in Figures 12 - 15 is alkali basalt - trachyandesite - comendite/pantellerite. This classification is similar for all four diagrams with inconsistencies only occuring in the separation of alkali and sub-alkali basalts in Figure 15, andesites and trachyandesites in Figure 12, and rhyolite from the comendite/pantellerite field in figures 12 + 13.

In consideration of the large degree of generalization and subjective interpretation that went into the preparation of these diagrams, the boundaries presented in Figures 12 - 15 should be considered as fields of transition rather than sharp

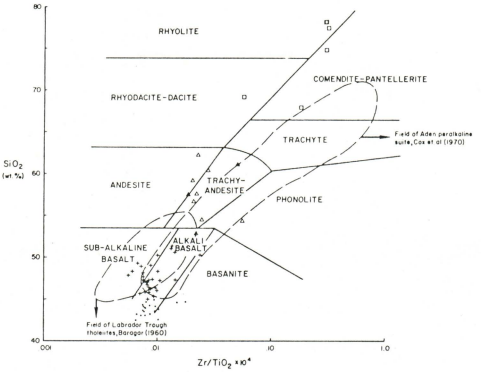

Figure 12 $Zr/TiO_2 \times 10^4$ versus SiO_2 diagram for the Nimish Subgroup (undivided). Symbols and fields as on figure 14.

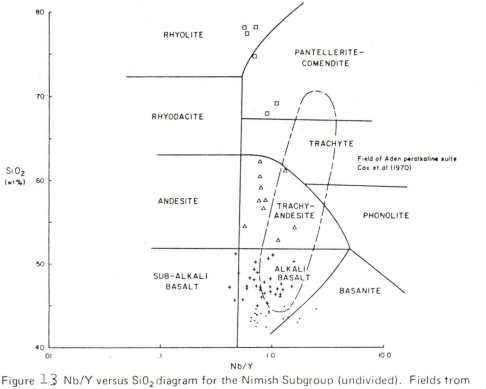

Figure 13 Nb/Y versus SiO_2 diagram for the Nimish Subgroup (undivided). Fields from Winchester and Floyd (1977).

- • – Ultrabasic
- + – Basic
- △ – Intermediate
- □ – Acidic

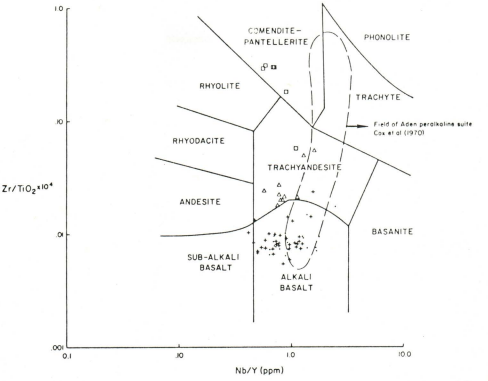

Figure 14 Nb/Y versus $Zr/TiO_2 \times 10^4$ diagram for the Nimish Subgroup (undivided). Symbols and fields as on figure 14.

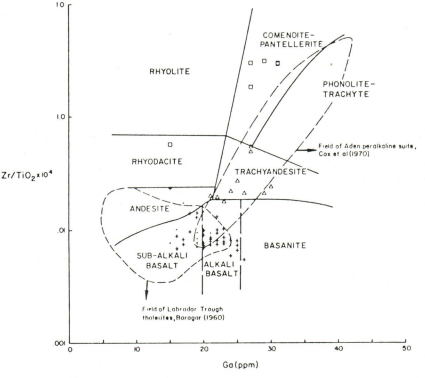

Figure 15: Ga versus $Zr/TiO_2 \times 10^4$ diagram for the Nimish Subgroup (undivided). Symbols and fields as on figure 14.

lines and as such the accuracy inherent in this system is suspect. The author realizes the limitations involved with this sort of classification system and uses it only as a base from which to discuss the application of standard major element classification schemes to the Nimish Subgroup. The author believes that the general tendency for the Nimish Subgroup samples to cluster within only three petrologic fields in any one diagram, and the internal consistency of this classification within the group of diagrams supports the use of this form of classification despite its limitations. Furthermore the consistency of classification implied by these diagrams is much greater than that noted for other classification schemes, Section V.4.4, and as such if any further discussion is to follow, this classification must be taken as the basis for comparison. REE data presented in Sections VI.2.2 and VI.3.2 support the general classification presented here.

Classification of the more silicic differentiates of the Nimish Subgroup is less precise than the mafic members because the trace element concentrations and ratios depend strongly on what accessory phases are crystallizing; e.g. crystallization of apatite strongly depletes Y and raises the Nb/Y ratio in the melt. Similarly, changes in fO_2 through normal differentiation or interaction with seawater and groundwater affects the precipitation of oxides and hence TiO_2 contents.

The argument against the use of the Zr/TiO_2 ratio as a discriminant parameter in the Nimish Subgroup on the grounds of fluid/magma interactions does not seem justified because if significant seawater or groundwater interaction occurred it should affect the basic as well as acidic members. Given the mafic volcanic's relatively greater degree of alteration (see Section VI.3.2) and the submarine volcanic structures noted in these rocks, this type of interaction should produce wide variations in the Zr/TiO_2 of the mafic members which is not seen in Figure 12. Similarly, following the period of water introduction, further fractionation in a high pH_2O environment would produce higher Zr but lower TiO_2 contents because the TiO_2 would be effectively depleted by the preceding fractionation step. These factors should produce a positive correlation of Zr/TiO_2 with SiO_2 as an index of differentiation. This does not seem to be the case as there is an essentially vertical trend in the 40 - 50 percent SiO_2 range before the trend towards positively correlated higher Zr/TiO_2 ratios develops. The general shape of a vertically oriented "tail" on this diagram was also noted in all unaltered suites published by Floyd and Winchester (1977). Therefore opaques in the basaltic members of the Nimish Subgroup are probably the result of high initial TiO_2 and total Fe in a relatively oxidized magma rather than interaction with seawater or groundwater.

In Figures 12 - 15 the Nimish Subgroup is compared to the available data for the Little Aden suite (Cox et al., 1970) and the Doublet Group of the Labrador Trough (Baragar, 1960). These comparisons serve to distinguish the dominantly tholeiitic trends of the Doublet Group from the mildly alkaline trends of the Nimish Subgroup and strengthen the comparison of the Nimish Subgroup with the Little Aden suite.

V.4.4 - Discussion of the Petrologic Classification:

The use of the petrologic names given in Figures 12 - 15 for the volcanic rocks of the Nimish Subgroup do not strictly comply with the rules of petrologic classification of igneous rocks as described by Carmichael et al. (1974), and Irvine and Baragar (1972). Perhaps this is to be expected considering the way numerous rock types were grouped together under the common headings as presented in Figures 12 - 15 (Winchester and Floyd, 1977). For example the grouping of alkali basalts includes the following igneous rock types as described in the literature: olivine basalt, alkali olivine basalt, trachybasalt, hawaiite and mugearite.

According to Carmichael et al. (1972) the basalt family, which is distinguished by having a silica range of 45 - 52 percent, a calcic plagioclase with An $>$ 50 and by the presence of augite with or without olivine, is petrographically divided

into two main groups using such features as the phenocryst and groundmass phases, and slight textural variations. Geochemically they are distinguished primarily on the presence of hypersthene in the CIPW norm (Carmichael et al., 1974) along with the alkali metal and incompatible trace element concentrations. The hypersthene normative, or subalkaline group of basalts, may be further divided into tholeiitic and high-alumina basalts, the latter being non-porphyritic basalts having greater than 17 percent Al_2O_3. Irvine and Baragar (1972) base their division of alkaline and sub-alkaline basalts on the total alkalis versus silica diagram, projections within the basalt tetrahedron and the use of the ternary plot Ol-Cpx-Opx (Chayes, 1966).

The alteration of the Nimish volcanics makes use of all of these classification parameters except the Al_2O_3 distinction inapplicable. The feldspars have been partially replaced by adularia and albite leaving an average of only 30 percent molecular proportion of anorthite in the mafic rocks (Appendix B). Olivine or olivine pseudomorphs have not been recognized and fresh clinopyroxene as a phenocryst or groundmass phase is very rare.

Plots of the recalculated normative proportions show a very large scatter of values straddling the critical plane of basaltic undersaturation. Most samples of both formations are both

olivine and orthopyroxene normative and are metaluminous with about equal proportions of (Ca+Na+K) and Al. A similar straddling of the alkaline-subalkaline boundary, but with a greater degree of scatter, was noted for the Ol-Opx-Cpx diagram of Chayes (1966), (not shown).

Most of the mafic rocks are metaluminous but JB-29 of the Petitsikapau Lake Formation and JS-193 of the Astray Lake Formation have the extreme peraluminous character with 2.83 and 2.07 wt. percent of corundum in the norm. Although the suite is generally high in Al_2O_3, no non-porphyritic rocks of basaltic composition in the Nimish Subgroup have Al_2O_3 contents greater than 17 percent and hence show no affinity with the high Al_2O_3 basalt family.

In conclusion on the basis of major elements alone the basic rocks of the Nimish Subgroup are metaluminous, olivine-hypersthene normative basalts, a conclusion that is in contradiction to that reached on the trace element diagrams, Figures 12 - 15. The more sub-alkaline character predicted by the major element chemistry could be the result of silica and alkali metal addition during the alteration of the feldspar for which there is petrographic and geochemical evidence. Similarly MgO and FeO mobility may have strongly affected these results.

The petrologic classification of the intermediate rocks is much more vague and the general trachyandesite grouping of Floyd and Winchester (1977) includes all trachyandesites, latites and benmoreites described from the literature. Irvine and Baragar (1972) use a system based upon the nature of the associated basaltic parent, normative plagioclase composition and normative color index to classify intermediate lavas. All of these parameters are inapplicable to the altered Nimish lavas. Carmichael et al. (1974) distinguish andesites from trachyandesites on textural evidence and the presence of quartz or nepheline in the norm recalculations. The alkali and alumina chemistry of the pyroxene and amphibole phases is also taken as an indicator of the degree of alkalinity.

The majority of the intermediate analyses of the Nimish Subgroup are quartz normative although sample JS-208 does have 1.41 percent normative nepheline. The rocks are equally split between peraluminous and metaluminous character with JS-208 of the Astray Lake Formation having a high of 2.83 percent normative corundum. The peraluminous character of some mafic and intermediate lavas is not unexpected considering the nature of the metasomatic alteration in which the plagioclase fledspar to alkali feldspar transition would release excess alumina which would not be readily transported out of the system.

The division between the comendite/pantellerite association and the dacite-rhyolite association is based on the relative abundance of alkalis and alumina, with the comendites and pantellerites having a peralkaline chemistry by definition. Petrographically this results in aegirine augites and alkali amphiboles as phenocrysts in pantellerites while comendites are the associated leucocratic varieties. The rhyolitic rocks of the Nimish Subgroup approach the dividing line with cation proportions of (Na+K)/Al consistently over .90 and normative corundum below 1.0 percent in all samples except JS-111 where it is 1.07 percent. According to the classification schemes of Macdonald and Bailey (1973) and Macdonald (1975a) all the acidic analyses of the Nimish Subgroup consistently plot as comendites despite their (Na+K)/Al ratios. This inferred peralkaline chemistry is strongly supported by the REE chemistry of these samples as discussed in Section VI.3.2.

These analyses again stress the transitional alkaline - subalkaline chemistry of the Nimish volcanic suite as is demonstrated by the whole rock chemistry of the more mafic members in the various trace element diagrams, Figures 12 - 15.

CHAPTER VI

IGNEOUS PETROGENESIS OF THE NIMISH SUBGROUP

VI.1 - Introduction:

Detailed petrogenetic discussion of the Nimish Subgroup is limited by the degree and nature of the secondary alteration, sample distribution, analytical errors and uncertainty as to whether all the volcanic rocks of a given formation are directly related through the same fractionation process. As a result the present treatment of this subject is highly generalized and contains many subjective assumptions, but the author does believe that this discussion demonstrates a number of possible igneous interrelationships that could have been involved in the petrogenesis of these volcanics. As with all modelling exercises the demonstration of a possible genetic process does not identify the "true" or even necessarily the most probable process in consideration of the large number of variables involved. The author recognizes these limitations and only attempts the modelling as a means for tentatively linking the more geochemically extreme members of the two volcanic formations.

Following from the previous discussion the rocks will be divided into chemical subdivisions based on SiO_2 content.

Variations in major and trace element chemistry within these groups will be discussed and a number of representative samples will be identified. The REE chemistry of these samples will be discussed and,following a brief description of the REE modelling process, the feasibility of a number of key petrogenetic transitions will be demonstrated.

VI.2 - Rare Earth Element Geochemistry of the Petitsikapau Lake Formation:

VI.2.1 - Geochemical Subdivision of the Petitsikapau Lake Formation:

As discussed previously there is a disparate number of basic and slightly ultrabasic lavas in the Petitsikapau Lake Formation. Aside from obvious inconsistencies, such as in Na_2O and K_2O contents, the average composition for this group of rocks, Table 5, resembles an olivine-hypersthene normative basalt with moderately high TiO_2, P_2O_5 and Zr. The average values for these latter elements are well above any of the representative ocean floor, continental or volcanic arc type tholeiitic basalts compiled by Carmichael et al. (1974). They do however compare rather favourably with some of the alkalic oceanic island and continental alkali basalt suites compiled in that study. Most notable are the Canary Islands (Ibarrola, 1969) and the previously mentioned Little Aden suite

TABLE 5

AVERAGE ABUNDANCES FOR THE PETROLOGIC SUBDIVISIONS OF THE NIMISH SUBGROUP+

	PETITSIKAPAU LAKE FORMATION					ASTRAY LAKE FORMATION		
	AVERAGE BASIC LAVAS	INTERMEDIATE LAVA - JS-104	ACIDIC LAVAS JS-111	ACIDIC LAVAS JS-098	PLUTONIC ROCK JS-464*	AVERAGE BASIC LAVA	AVERAGE INTER-MEDIATE LAVA	AVERAGE ACIDIC LAVA
SiO_2	46.84 - (2.78)	54.46	69.17	67.90	61.26	45.98 - (1.68)	57.54 - (2.58)	77.21
TiO_2	2.24 - (0.53)	1.13	0.88	0.51	1.02	2.23 - (0.47)	0.96 - (0.11)	0.29
Al_2O_3	14.33 - (1.24)	15.34	16.11	13.88	15.57	14.29 - (1.40)	15.41 - (1.08)	10.75
Fe_2O_3	6.06 - (1.67)	3.25	0.20	1.65	2.01	6.76 - (1.65)	2.96 - (0.77)	1.30
FeO	9.11 - (1.45)	6.70	0.92	2.12	3.99	10.35 - (1.66)	5.29 - (1.29)	0.82
MnO	0.22 - (0.04)	0.16	0.10	0.03	0.04	0.20 - (0.04)	0.15 - (0.07)	0.01
MgO	6.87 - (2.54)	0.50	0.00	0.70	0.48	5.38 - (1.61)	0.79 - (0.66)	0.41
CaO	5.24 - (1.63)	1.37	0.19	0.24	0.89	4.97 - (1.75)	1.98 - (1.51)	0.05
Na_2O	2.96 - (0.77)	3.32	1.51	4.51	3.59	2.70 - (0.28)	3.37 - (1.22)	3.15
K_2O	2.84 - (1.81)	7.14	11.52	5.12	6.95	2.77 - (1.02)	7.05 - (2.32)	4.68
P_2O_5	0.35 - (0.16)	0.21	0.15	0.05	0.25	0.39 - (0.13)	0.16 - (0.04)	0.04
LOI	3.96 - (0.49)	2.99	0.72	1.05	1.77	4.33 - (0.73)	2.15 - (0.38)	0.41
Zr	189 - (49)	276	502	927	510	173 - (33)	233 - (32)	866
Sr	523 - (233)	76	39	788	72	381 - (189)	183 - (132)	20
Rb	54 - (26)	152	205	135	163	57 - (27)	94 - (35)	178
Zn	117 - (23)	193	23	40	77	121 - (22)	101 - (9)	40
Cu	50 - (30)	21	8	11	9	32 - (9)	19 - (4)	9
Ba	1346 - (733)	948	1133	658	789	1161 - (373)	1382 - (489)	190
Nb	28 - (7)	30	46	114	66	24 - (7)	29 - (12)	95
Ga	21 - (3)	30	15	27	27	23 - (2)	24 - (3)	29
Pb	3 - (4)	11	4	13	0	4 - (4)	4 - (3)	7
Ni	50 - (50)	7	4	10	7	30 - (20)	10 - (3)	13
Cr	38 - (47)	4	8	9	0	22 - (15)	11 - (3)	4
V	258 - (85)	28	21	20	40	271 - (111)	68 - (13)	15
Y	31 - (7)	53	42	127	51	31 - (6)	34 - (4)	151

* Sample taken from the Point Lake pluton, Appendix B.
\+ Bracketed numbers indicate standard deviations.

(Cox et al., 1970). The close similarity of the Nimish mafic lavas with the basalts of Canary Islands among the wide ranging geochemistry seen in volcanic oceanic islands is very interesting because both suites contain highly alkaline rhyolites as the predominant acidic fractionation product.

Standard deviations of these averages show a significant degree of spread within this group. Closer examination of the individual analyses (Appendix B) shows that the deviation is largely a result of the presence of a number of distinct subgroups. Specifically the samples JB - 57, JS - 181, JS - 57 and JS - 133 form a coherent group that is uniformly depleted in TiO_2, P_2O_5 and Zr and enriched in MgO, Ni and Cr. Similarly the samples JS - 517 and JS - 46 are significantly higher than the general basaltic average in P_2O_5 and Zr and have complementary lower MgO, Ni and Cr. Averages taken on the remaining 14 basic lavas alone only marginally differ from the figures in Table 5 but the standard deviations drop by an average of 35% signifying that these centrally distributed 14 lavas form a coherent subgroup.

A total of four samples were chosen to give a representative cross section of the mafic lavas for REE analysis (JB - 57, JS - 41, JB - 24, JS - 62). The first of these is a member of the relatively depleted subgroup and was chosen as a representative sample because it is petrographically relatively unaltered and

has low Na_2O and K_2O contents, which are taken to indicate a minimum of secondary alteration (Section V.3). The other three samples are all relatively unaltered members of the middle subgroup or the normal basic lavas. Unfortunately REE data for the enriched mafic lavas are unavailable due to analytical problems.

In going from the mafic to intermediate members of the Petitsikapau Lake Formation there is a predictable increase in incompatible elements and decrease in compatible elements which continues into the acidic members. The small number of samples available from these more fractionated rock types is indicative of their percentage exposure and as such they have been taken to be representative of the acidic and intermediate members of this formation.

The major element chemistry of the acidic sample JS - 111 is strikingly different from the other acidic sample JS - 098. The very high K_2O content is representative of the high percentage of potash feldspar phenocrysts. The REE data for this sample should be treated in recognition of this factor as it does not represent a true liquid composition and is possibly uniformly depleted in the REE by up to 35% based on estimated phenocryst/matrix percentages.

The three non-mafic members of the Petitsikapau Lake Formation (JS - 104, JS - 111, JS - 098) were all analyzed for

REE so this total of seven samples gives the best possible representation of the volcanic rocks within the Petitsikapau Lake Formation.

Petrographic descriptions of these representative samples are given in Appendix F.

VI.2.2 - Rare Earth Element Abundances of the Petitsikapau Lake Formation:

The rare earth element concentrations of the seven representative samples of the Petitsikapau Lake Formation are listed in Table 6 and are plotted normalized to the chondritic abundances of Haskin et al. (1968) in fig. 16. The precision and accuracy of these analyses are discussed in Appendix A.

The first feature apparent from the REE patterns is the consistent steeply inclined nature of the patterns. This trend of a linear decrease in abundance with increased atomic number of the rare earths is typical of alkalic rocks of all tectonic settings (Frey, 1969; Herrmann, 1974; Floyd, 1977) and is consistent with the tentative conclusion of an alkalic chemistry for the Nimish volcanics based upon the major and trace elements. These general patterns could be also typical of a non-alkaline volcanic rock that has undergone significant fractionation of minerals compatible with the MREE and HREE such as hornblende or garnet, but the high overall REE concentrations in the mafic members of this formation discounts this possibility.

Table 6

RARE EARTH ELEMENT CONCENTRATIONS OF SELECTED VOLCANIC ROCKS*

	La	Ce	Pr	Nd	Sm	Eu	Gd	Dy	Er	Yb	Lu
Pritsikapau Lake Formation:											
Depleted Basic Lavas:											
JB - 057	40.38	71.43	7.48	37.44	8.12	2.19	6.47	4.57	1.67	-	-
Normal Basic Lavas:											
JS - 041	54.69	102.46	10.60	50.82	10.39	3.35	7.84	5.43	2.12	-	-
JS - 062	49.33	99.41	11.20	52.96	11.06	3.45	8.40	5.64	2.52	-	-
JB - 024	48.02	100.40	11.77	51.41	11.61	3.86	9.15	7.76	3.15	-	-
Intermediate Lavas:											
JS - 104	82.84	153.34	15.50	69.71	13.36	4.01	9.76	7.59	3.81	-	-
Acidic Lavas:											
JS - 111	74.71	153.06	17.65	75.22	14.93	3.35	10.99	8.85	4.62	3.55	-
JS - 098	597.07	1086.70	104.18	385.69	72.21	12.59	49.71	36.81	14.09	-	-
Astray Lake Formation:											
Depleted Basic Lavas:											
JB - 079	24.50	47.61	5.10	25.09	5.40	1.38	4.17	3.21	1.34	-	-
Normal Basic Lavas:											
JS - 015	40.51	82.59	9.74	42.53	8.88	2.74	7.29	5.76	2.81	2.49	0.32
JS - 193	43.60	92.10	11.08	50.00	10.41	3.71	8.66	6.55	2.93	2.32	0.42
Depleted Intermediate Lavas:											
JS - 033	50.43	93.90	9.59	42.22	8.30	2.80	6.41	4.94	2.29	-	-
Normal Intermediate Lavas:											
JS - 505	49.73	102.65	12.28	48.51	9.79	2.53	8.40	7.83	4.13	3.88	0.60
Enriched Intermediate Lavas:											
JS - 204	91.10	268.59	18.27	75.56	15.15	5.39	11.96	8.91	3.51	-	-
Acidic Lavas:											
JS - 502	157.60	300.22	29.67	118.23	23.31	2.62	19.90	21.04	13.56	9.39	0.40
JS - 503	153.40	276.29	28.50	113.64	22.58	2.28	20.40	21.48	14.97	11.80	1.10
Chondrite Normalizing Values:+	0.33	0.88	0.112	0.60	0.181	0.069	0.349	0.31	0.20	0.20	0.034

* All data in ppm.

\+ Chondritic values from Haskin et al., (1968).

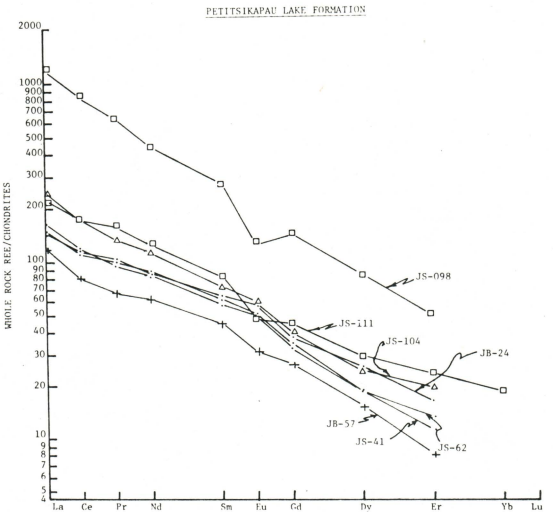

Fig. 16: Whole rock REE Patterns of Petitsikapau Lake Formation

+ - Depleted Basic Volcanics
. - Normal Basic Volcanics
△ - Intermediate Volcanics
□ - Acidic Volcanics

The basic geochemical subdivision of the Petitsikapau Lake Formation is supported by variations in the rare earth element patterns. The depleted basic volcanics, as represented by sample JB - 57, show a steeply inclined distribution ranging from 120x chondrites for La to 8x chondrites for Er with a slight negative Eu anomaly. JB - 57, as with most other analyses of the Petitsikapau Lake Formation, shows a slight La "kick" or distinct break in the pattern at Ce, implying relatively high values for La. This problem was found in most all of the analyses and was inherent in the experimental procedure at the time of analysis (Eby, 1972; B.J. Fryer, pers. comm.).

The normal basic lavas form a very coherent group except for a slight divergence for the heavy rare earth elements Dy and Er. La concentrations range from 146 to 166x chondrites, a spread of 13 percent, while Er varies from 11x for JS - 041 to 16x for JB - 024 giving a spread of 37 percent. All the normal basic lavas exhibit a slight positive Eu anomaly.

The rare earth pattern of the intermediate sample, JS - 104, is distinguished from the normal basic lavas by having higher LREE (La=251x chondrites) but similar MREE abundances. The heavier REE also appear enriched. This is consistent with larger bulk Kd values for the middle REE than either the LREE or HREE in the phases that fractionated to form this lava. JR - 104 exhibits a slight positive Eu anomaly.

The relatively depleted acidic sample, JS - 111, shows a pattern very similar to that of JS - 104 except that it is 10 - 30 percent higher in all the REE except for La, Ce and Eu. This sample has a distinct negative Eu anomaly with a calculated Eu/Eu* = .778 (Philpotts, 1972). The enriched acidic sample, JS - 098, is distinctive by virtue of its very high overall abundances and relatively large Eu anomaly, Eu/Eu* = .610.

The large difference in the REE chemistry of the two acidic samples complements the large variations in Zr, Nb and Y (Appendix B). These differences are consistent with the previously described "phenocryst volume/incompatible trace element concentration" relationships, and a greater degree of fractionation in JS - 098.

VI.2.3 - Rare Earth Element Petrogenetic Relations in the Petitsikapau Lake Formation:

Since the REE patterns for the recognized sub-divisions for the Petitsikapau Lake Formation differ, specific features of these patterns can provide petrogenetic restraints on possible parent - daughter relationships. One way to pinpoint the role of specific minerals in petrogenetic relations is to observe how certain REE ratios change with differentiation as each mineral will fractionate between any two REE to a different degree. An example of this approach is given in fig. 17 and 18.

In fig. 17 the Ce/Sm ratios are plotted against the Sm abundances. Similar parameters with a Sm/Er ratio are used in fig. 18. The different mineral vectors point in the direction that the REE composition of the melt would go if the representative mineral was removed from the system. The reciprocal vector would represent accumulation of these phases. The different lengths of the vectors are meant to imply the relative effect of the different minerals. For clinopyroxene, orthopyroxene, olivine, plagioclase and magnetite the length represents the result that would occur if 50 percent fractionation of that mineral occurred. The value for apatite is calculated for 1 percent fractionation while that for zircon in fig. 17 is for 5 percent. The large decrease in the Sm/Er ratio caused by even 5 percent fractionation of zircon is too large to show on this scale and the vector is only meant to imply direction in fig. 18. The dashed lines BKD are calculated on the basis of taking a fractionating assemblage of 40 percent olivine, 30 percent clinopyroxene and 30 percent plagioclase which is mixed with apatite in the ratio of 150:1 and fractionated to 50 percent volume reduction. The strong effect of apatite on plots of this type is illustrated by this calculation.

These diagrams should not be interpreted by looking for general trends formed by the Petitsikapau Lake or Astray Lake Formations, but more specifically as a series of imaginary

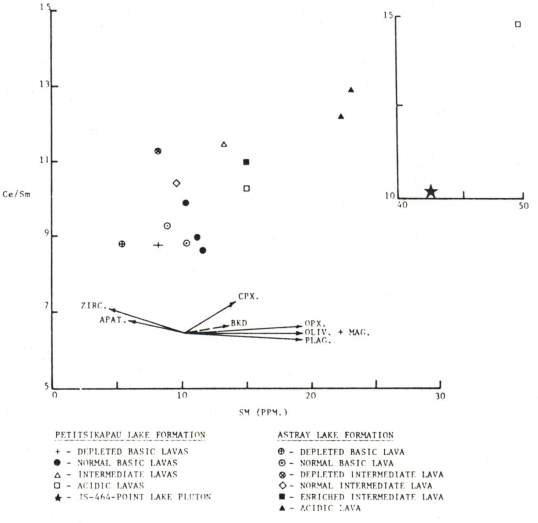

Fig. 17: Ce/Sm vs. Sm diagram for representative samples of the Nimish Subgroup

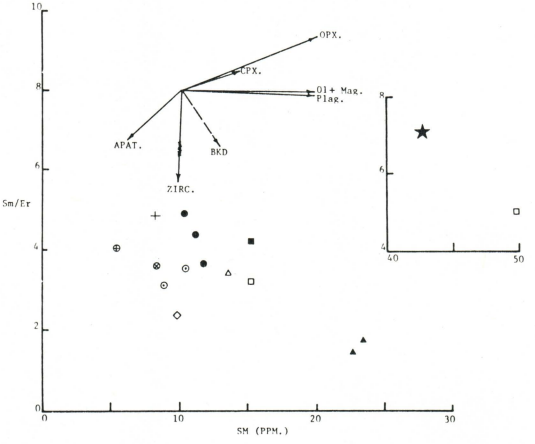

Fig. 18: Sm/Er vs. SM diagram for representative samples of the Nimish Subgroup.

vectors between any two data points which indicate the fractionating or accumulating mineral assemblage that could have been involved in the derivation of one sample from another.

The analytical precision implied by this diagram is deceptive as all data points should have $\pm$ 10% error bars both horizontally and vertically. Addition of this precision data would seriously reduce the clarity of the diagram so all discussion of petrogenetic implications generated by these diagrams should be interpreted in relation to this analytical error.

By using this approach the validity of the proposed stratigraphic subdivision of the Nimish Subgroup can be tested. Similarly by isolating particularly distinct inferred parent - daughter relationships, more detailed trace element modelling calculations can offer insight into the specific nature of the fractional crystallization process responsible for the petrogenesis of the Nimish Subgroup.

Derivation of the normal basic lavas from the relatively depleted basic lava subgroup is possible with the fractionation of ferromagnesian minerals from the latter, fig. 17, but would seem to require some apatite removal in fig. 18. This inferred apatite fractionation is inconsistent with the sharp increase in P_2O_5 that is noted between these rock types (Appendix B). The discrepancy in the two figures is not significant in

consideration of the implied error bars and hence the derivation of the normal basic lavas from the depleted basic lavas is consistent with a ferromagnesian mineral fractionation assemblage that does not include apatite.

The plot of the intermediate sample JS - 104 relative to the distribution of the normal basic lavas demonstrates the necessity of apatite crystallization in the formation of the former from the latter as the increase in Ce/Sm is higher than is possible by clinopyroxene alone, fig. 17. The decrease in Sm/Er also exceeds the capabilities of plagioclase. The inferred fractionating mineral assemblage for this transition is ol+cpx+plag$\pm$opx+mag+apat, with clinopyroxene probably as the dominant ferromagnesian phase.

The derivation of the relatively depleted acidic sample, JS - 111, must have followed much the same pattern as the intermediate sample of the Petitsikapau Lake Formation with a slightly higher degree of fractionation. The fractionating mineral assemblage would be the same as that for JS - 104 except that clinopyroxene would seem to be of less importance.

The hypothetical derivation of both the intermediate and depleted acidic sample from an average normal basic lava by ferromagnesian minerals fractionation is consistent with the drop in FeO, MgO and CaO, Table 5. The especially large drop in TiO_2 (60%), P_2O_5 (45%), and V (90%) signify the onset of

magnetite and apatite fractionation that was not present in the derivation of the normal basic lavas from the depleted basic rock type.

The derivation of the depleted acidic sample JS - 111 from the intermediate sample is only marginally possible in recognition of experimental error, fig. 17 and 18. This transition is considered unlikely because the transition calls for an actual decrease in the La content while Zr increases by 100%. No known mineral or combination of minerals is capable of doing this. Therefore the normal basic lavas are considered the most probable source rock for JS - 111.

The possible parent to the subvolcanic plutonic rock which is very closely associated with the acidic rocks of the Petitsikapau Lake Formation, JS - 464, (fig. 1; Table 7), can not be discerned from these diagrams as the average normal basic lava, intermediate or relatively depleted acidic samples are all capable of producing this composition with slight variations in the proportions of olivine, clinopyroxene, plagioclase and apatite in the fractionating assemblage. Similarly major and trace element data offer few constraints. Decision on the probable parent to JS - 464 will rest on the best fit models as derived from each of the proposed source rocks (Section VI.5.2).

The enriched acidic sample JS - 098 could be derived from JS - 464 by 80 - 90% fractionation of a clinopyroxene + plagioclase + apatite $\pm$ olivine + magnetite assemblage. Apatite and/or zircon would have to be very prominent in this fractionation step in consideration of the steep extrapolated derivation line, fig. 18.

Note that it would be impossible to derive the enriched acidic sample from the depleted basic, normal basic, intermediate or depleted acidic samples as in all cases apatite would have to be a very minor phase in the fractionating component. This is inconsistent with the large drop in P_2O_5 noted for all these cases, Table 5; so the closely associated pluton was considered the most probable source rock for JS - 098.

VI.3 - Rare Earth Element Geochemistry of the Astray Lake Formation:

VI.3.1 - Geochemical Subdivision of the Astray Lake Formation:

Comparison of the composition of the average basic lava for the Astray Lake Formation with that of the Petitsikapau Lake Formation, Table 5, reveals no significant differences, so the discussion on the general geochemical affinities of the average composition of the basaltic members of the Petitsikapau Lake Formation presented in Section VI.2.1 applies.

The close similarity in the geochemical distributions within the basic members of the two volcanic formations is consistent with their similar geologic setting, general petrography and period of formation. The two volcanic formations are possible examples of separate cycles of volcanism that are generally related to the same larger scale, geotectonic event, but which fractionated under slightly different pressure - temperature conditions.

A closer look at the standard deviations presented for the Astray Lake Formation in Table 5 reveals further similarities with the Petitsikapau Lake Formation. As with the younger volcanic cycle, a more depleted basic subgroup (JS - 31, JB - 79) is identifiable by having roughtly 40% less TiO_2, P_2O_5, Nb, Y and Zr and 25% more MgO and CaO. No significant analyses complementary to the enriched basic rocks of the Petitsikapau Lake Formation were noted.

As a means of obtaining a good distribution of representative samples for REE analyses, JB - 79 was chosen from the depleted basic subgroup and JS - 15 and JS - 193 from the more centrally distributed normal basic subgroup. These samples were chosen from within the respective subgroup on the basis of petrographic evidence on alteration and low Na_2O/K_2O ratios. Petrographic descriptions of these representative samples are given in Appendix F.

In going from the mafic to intermediate and acidic members of the Astray Lake Formation the close similarity with the Petitsikapau Lake Formation is lost. An initial divergence lies in the percentage exposure of the acidic rocks in the two formations. Only three individual samples were collected from the Petitsikapau Lake Formation while the intermediate and acidic averages for the Astray Lake Formation are derived from six samples taken from relatively well exposed outcrop areas.

Geochemically the average intermediate analysis of the Astray Lake Formation is similar to the intermediate sample of the Petitsikapau Lake Formation, JS - 104, for all elements except P_2O_5, Zr and Y in which the average intermediate analysis of the Astray Lake Formation is significantly depleted. The true meaning of this comparison is hard to determine considering the stratigraphic control available, but it is interesting that no rock similar to JS - 104 was found in the well exposed section on Jasper Mountain which could indicate a divergence in the fractionation pattern of the two formations during their respective stages of "trachyandesite" formation, figs. 12 - 15.

More evidence for this divergence is present within the acidic members of the two formations. Petrographically the acidic members of the Astray Lake Formation are red, generally

aphyric very fine grained to glassy alkali rhyolites while the complementary rocks in the Petitsikapau Lake Formation are rich in feldspar and quartz phenocrysts set in a more granular roughly flow banded matrix. The chemistry of the two groups of acidic rocks also reflects a profound difference. As mentioned previously the four samples from the Astray Lake Formation are very similar. These volcanic rocks are characterized by high SiO_2, total alkalis, Zr, Nb, Y and REE and low alumina making modal Na_2O + K_2O almost equal to modal Al_2O_3. The two acidic samples of the Petitsikapau Lake Formation differ in having higher TiO_2 and Al_2O_3 and significantly lower SiO_2. The magnitude of these geochemical differences, Table 5, supports the contention that the two formations represent two separate cycles of volcanism.

The consistency in the acidic rock analyses of the Astray Lake Formation should be noted with only Y, Rb and Ba showing any significant variation (Appendix B). The low Rb and high Ba of sample JS - 502 is primarily due to the presence of about 15% modal potash feldspar phenocrysts that is not present in the other three acidic samples. The reason for the differences in Y values is unknown.

The strong preference of potash feldspar for a high Ba/Rb is shown by the average rhyolite Kd values of 6.12 for Ba as compared to 0.34 for Rb (Appendix E). This relationship

also holds for the acidic rocks of the Petitsikapau Lake Formation in that the K - feldspar phyric sample JS - 111 is richer in Rb and Ba than the Na - feldspar phyric JS - 098 which is richer in Sr (Appendix B). The preservation of these apparent primary alkali trace element abundances provides evidence to support the observation that in general the acidic rocks of the Nimish Subgroup escaped the large scale metasomatism that so strongly altered the basic and intermediate rocks.

In order to get a representative sampling of the intermediate and acidic members of the Astray Lake Formation for REE analyses, three intermediate samples (JS - 033, JS - 505, JS - 204) and two acidic samples (JS - 502, JS - 503) were chosen. All these samples are of typical rock types found in the formation and were specifically chosen because of their relatively unaltered petrography and major element chemistry. Sample JS - 204 was chosen because of its unique chemistry within the intermediate lavas, having high Zr and Nb with relatively low P_2O_5.

Petrographic descriptions of these rock types are given in Appendix F.

VI.3.2 - Rare Earth Element Abundances of the Astray Lake Formation:

The rare earth element concentrations of the eight representative samples of the Astray Lake Formation are listed in Table 6 and plotted normalized to the average chondritic values of Haskin et al. (1968) in fig. 19.

Similar to the Petitsikapau Lake Formation, the depleted basic lava, JB - 79, is conspicuous by its low overall abundances, slight negative Eu anomaly and steeply inclined pattern. The pattern of this sample is almost identical to that of the depleted basic lava of the Petitsikapau Lake Formation with approximately 20 - 30% lower abundances (La = 74x chondrites).

The REE patterns for the two normal basic lavas are sub-parallel throughout the REE. The largest difference occurs at Eu where JS - 193 has a slight positive Eu anomaly and an abundance of 54x chondrites, and JS - 15 has no Eu anomaly and a 40x chondrite concentration. The normal basic lavas show a distinct flattening of the steeply inclined patterns in the region of the HREE Dy, Er, Yb and Lu.

Relative to the depleted basic lavas the intermediate sample JS - 033 is slightly richer in La (153x chondrites) but markedly depleted in the HREE (Dy = 11x chondrites). As such it is generally classified as a depleted intermediate lava.

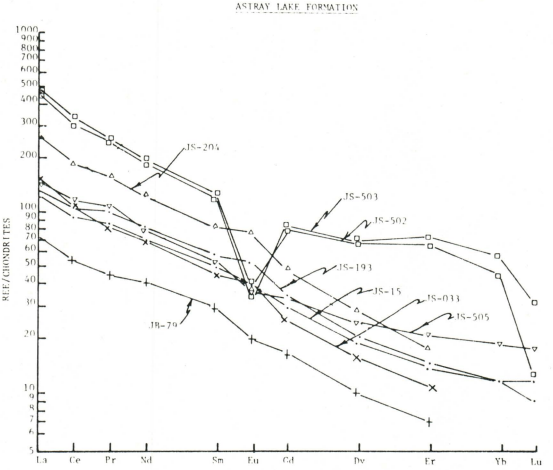

Fig.19: WHOLE ROCK REE PATTERNS OF THE ASTRY LAKE FORMATION

+ - DEPLETED BASIC VOLCANICS
. - NORMAL BASIC VOLCANICS
X - DEPLETED INTERMEDIATE VOLCANICS
▽ - NORMAL INTERMEDIATE VOLCANICS
△ - ENRICHED INTERMEDIATE VOLCANICS
□ - ACIDIC VOLCANICS

This sample shows a much steeper REE pattern than the normal basic lavas with a small positive Eu anomaly, Eu/Eu* = 1.14, and a slightly concave up pattern for the LREE. No levelling off is present in the HREE abundances. The REE pattern of this sample relative to the normal basic group, having higher LREE and lower concentrations of the MREE and HREE, poses strict limitations on the genesis of this intermediate sample from the normal basic rocks (Section VI.5.3).

The normal intermediate sample JS - 505 has a similar La content (151x chondrites) but is significantly enriched in all other REE relative to JS - 033. The LREE abundances are the same as the average normal basic lava but the HREE are markedly enriched showing a similar levelling off pattern. This sample has a negative Eu anomaly, Eu/Eu* = 0.84.

The relatively enriched intermediate sample, JS - 204, shows a pattern more similar to the straight, steeply inclined pattern of JS - 033 than to JS - 505 but with greater overall abundances (La = 279x chondrites). This Ca rich, feldspar - phyric sample has a large positive Eu anomaly, Eu/Eu* = 1.28.

It should be noted that the general increase in REE abundances from JS - 033 through JS - 505 and JS - 204, is complemented by a similar increase in the Zr, Nb and Y contents (Appendix B). This supports the earlier assumption that the REE remained relatively immobile during secondary processes

as was documented for Zr, Nb and Y (Section V.3). These internally consistent geochemical variations and the different petrography for the three samples (Appendix F) are the basis for the general subdivision of the intermediate lavas of the Astray Lake Formation into depleted, normal and enriched intermediate subgroups.

The REE patterns for the two analyzed acidic samples of the Astray Lake Formation are remarkably similar as are their major and trace elements. The LREE have a slight concave-up pattern and a high La value of 478x chondrites. The HREE show a pronounced levelling off and develop a small concave-up pattern centred at Dy before turning strongly convex downwards at Yb. Both samples have large negative Eu anomalies, with the aphyric sample JS - 503 having a slightly greater anomaly, $Eu/EU^* = .32$, as compared to .36 for the slightly potash feldspar phyric JS - 502.

The rare earth patterns of these acidic samples are very significant because they are identical to the low Fe, transitional comendites/pantellerites of the type area of pantellerites, the volcanic island of Pantellaria in the Channel of Sicily, Mediterranean Sea (Villari, 1975). The analyses given by Villari have the same concave-up pattern for the LREE, steep negative Eu anomaly and concave down pattern for the HREE, also showing a marked point of inflection

at Yb. The HREE patterns for the associated mafic volcanic rocks of Pantellaria are very similar to the mafic and intermediate samples of the Nimish Subgroup. The uniqueness of these REE patterns offers strong support to the tentative classification of the Nimish Subgroup as an alkaline volcanic suite.

Comparison of the REE patterns of the representative samples for the Petitsikapau Lake and Astray Lake Formations show distinct similarities and differences generally supporting previous discussions based on major and trace element chemistry. More specifically the two relatively depleted basic samples show almost identical patterns with minor differences in their absolute abundances. Similarly the normal basic lavas of the two formations are very consistent within their own formational subgroup and generally similar to each other.

Within the intermediate and acidic members there is more divergence as is expected from major and trace element data. The intermediate sample of the Petitsikapau Lake Formation, JS - 104, looks very similar to the relatively enriched intermediate sample of the Astray Lake Formation, JS - 204. The other two intermediate analyses show no direct counterparts within the Petitsikapau Lake Formation but the distinct HREE flattened pattern of JS - 505 implies close petrogenetic affinities with the similar tendency seen in the acidic samples

of the Astray Lake Formation. The REE pattern of these alkali rhyolites is similarly not directly comparable with the straight, steeply inclined patterns found for the acidic Petitsikapau Lake Formation volcanics. The uniqueness of their REE pattern poses distinct limitations on their possible mode of genesis (Section VI.5.3).

VI.3.3 - Rare Earth Element Petrogenetic Relations of the Astray Lake Formation:

The petrogenetic relations of the Astray Lake Formation were treated in the same manner as the Petitsikapau Lake Formation. Fig. 17 and 18 give the positions of the representative analyses on the Ce/Sm vs. Sm and Sm/Er vs. Sm diagrams.

The parent-daughter relations between the depleted basic and normal basic lavas are consistent with about 30 percent fractionation of an olivine gabbro assemblage. The somewhat high Sm value for the depleted basic rock JB - 79, fig. 19, gives an anomalously low Ce/Sm and high Sm/Er which may imply a significant proportion of augite, fig. 17, and apatite, fig. 18, in the fractionating assemblage. Application of the $\pm$ 10 percent error bars for both the depleted basic and normal basic lavas would discount the significance of this hypothesis (Appendix A).

The plot of the relatively depleted intermediate lava JS - 033 to the average normal basic lava in fig. 17 reflects the dominant role that apatite played in that fractionation step. This is consistent with the sharp drop in P_2O_5 noted between these two rock types. Similarly the large drop in TiO_2 signifies the onset of magnetite crystallization. Both of these petrogenetic implications are similar to those documented for the Petitsikapau Lake Formation. The apparent discrepancy between the normal basic lavas indicated in fig. 18 is insignificant in consideration of the $\pm$ 10% error bars for each data point (Appendix A).

Alternatively the depleted intermediate lavas of the Astray Lake Formation are plagioclase prophyritic (up to 20% modal phenocrysts) and as such there would be a component equivalent to the mirror image of the plagioclase vector involved in diluting the REE abundances. This would have little effect on the Ce/Sm ration, fig. 17, but could partially account for the actual decrease in the Sm and Sm/Er relative to the normal basic lavas, fig. 18.

Similarly another factor that could be involved in this discrepancy is the REE pattern of the normal basic lavas themselves, in which the levelling off of the HREE gives a higher Sm/Er ratio than if the pattern remained linear. This levelling off tendency is also developed in the normal

intermediate lava JS - 505. Modelling calculations relating a HREE enriched sample to a sample with a linear pattern proved to be very difficult in obtaining a good fit and indicate close genetic relations between volcanics with similar HREE patterns.

The extrapolated fractionation line between the average normal basic lava and JS - 505 is marginally shorter than a similar line to JS - 033, fig. 17, implying smaller degrees of fractionation in the former case.

Figure 18 negates the formation of JS - 033 from JS - 505 while fig. 17 shows that the derivation of JS - 505 from JS - 033 is improbable but possible within the limits of experimental error. The improbable nature of this latter transition is also supported by the major element data. Firstly JS - 033 contains lower TiO_2 and Cr relative to JS - 505, while Ni, MgO, CaO and V are only marginally higher. Although the data are only for a single sample and perhaps not statistically significant, it would take a very precise combination of olivine, augite and magnetite in the fractionating mineralogy to generate a set of bulk Kds which could produce the required trends.

Secondly the percentage of increase in the incompatible elements is also inconsistent with JS - 033 as a source for JS - 505. Nb and Y increase by 29% and 12% respectively

whereas Zr increases by only 9%, and this is over an interval where a certain amount of apatite fractionation must occur in order to decrease the P_2O_5. This relationship seems unlikely as apatite fractionating would strongly deplete Nb and Y, but have little effect on Zr (Appendix E). If this is the case a small amount of zircon must also have fractionated which seems unlikely because no zircon was found in this section and zircon crystals are not normally recognized in basic to intermediate lavas with only 200 ppm. Zr (Williams et al., 1954). The combination of these factors makes it most likely that the normal basic lavas are the source rock for both JS - 033 and JS - 505.

A more detailed discussion of the REE modelling implications of this transition is left to Section VI.5.3.

The relatively enriched incompatible trace element concentrations and unique REE pattern of the enriched intermediate sample of the Astray Lake Formation, JS - 204, implies that it was formed under different circumstances than those for the other intermediate samples. The effects of a higher degree of fractionation and a smaller amount of apatite in the cumulus mineralogy is readily displayed in figs. 17 and 18. No generalizations regarding possible plagioclase/olivine + clinopyroxene ratios in the cumulus phases can be made from these figures, but the derivation of these rocks from some

form of normal basic lava through fractional crystallization is not a difficult transition with respect to the REE patterns and modelling calculations; as such it will not be discussed further.

Relatively little information is available from fig. 17 or 18 as to the possible parent to the acidic members of the Astray Lake Formation. Fig. 18 supports the tentative conclusion that the enriched intermediate samples could not have been the source rock for the acidic samples because such a step would call for close to 1 percent modal cumulus apatite which is inconsistent with the slight drop in average P_2O_5 values of the two groups (Table 5). Among the other three possible choices (normal basic lavas, JS - 033 and JS - 505), the second would seem to be the least probable relative to fig. 18 as it calls for a moderate amount of apatite fractionation which would conflict with the P_2O_5 values. A higher silicate/apatite cumulate ratio is needed for the normal intermediate samples as a source rock relative to the normal basic lavas; an implication which is consistent with the major and trace element data.

A conclusion on the most probable source rocks for the acidic members of the Astray Lake Formation will be left to the REE modelling section, VI.5.4.

VI.4 - Rare Earth Element Geochemistry of the Intrusive Rocks of the Nimish Subgroup:

The REE abundances of six intrusive rocks of the Nimish Subgroup are listed in Table 7 and plotted normalized to chondritic values in fig. 20. The analyses are grouped according to the different plutons of the area (Appendix B), the locations of which may be inferred from fig. 1.

The most striking factor in the REE patterns of the intrusive rocks is their close similarity with the associated volcanic rocks. The slopes displayed by these samples are comparable with the volcanics and the absolute abundances are within the range of the extrusive rocks. No intrusive samples show any levelling off in the HREE as noticed in some of the volcanic samples. Little or no Eu anomalies are developed in these patterns. The only well displayed difference between the intrusive and extrusive is the tendency for the intrusive rocks to have a slight concave down pattern. This is probably indicative of the abundant clinopyroxene in these samples, the Kds of which mimic this curved pattern.

The close similarity of the REE abundances of the intrusive and extrusive igneous rocks of the Dyke Lake area supports the conclusion, based on major and trace element data, that they are genetically related. The similarity of the patterns also implies that the intrusive rocks are not the cumulate

Table 7

RARE EARTH ELEMENT CONCENTRATIONS OF SELECTED INTRUSIVE ROCKS*

	La	Ce	Pr	Nd	Sm	Eu	Gd	Dy	Er	Yb	Lu
Point Lake Pluton:											
JS - 095	94.88	169.78	18.31	79.48	18.89	5.22	15.03	10.13	3.54	2.42	-
JS - 464	220.18	422.98	45.66	206.04	42.37	9.75	33.92	21.39	5.90		
Evans Lake Pluton:											
JS - 221	29.11	61.54	6.58	32.83	7.71	2.27	6.14	4.42	1.01	-	-
JS - 260	39.48	81.13	8.72	39.19	7.81	2.31	6.08	3.83	1.01	-	-
Eilleen Lake Pluton:											
JS - 292	60.98	115.08	11.04	51.36	10.04	2.80	7.03	4.45	1.00	-	-
Tyra Lake Pluton:											
JS - 162	106.48	203.33	21.35	88.89	17.35	4.41	13.80	9.75	3.81	-	-
Chondrite Normalizing Values:+	0.33	0.88	0.112	0.60	0.181	0.069	0.249	0.31	0.20	0.20	0.034

* All data listed in ppm.

\+ Chondritic values from Haskin et al., (1968).

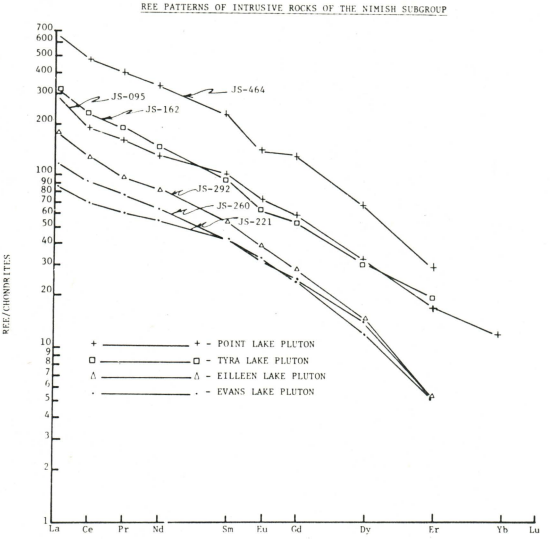

Fig.20: REE PATTERNS OF SELECTED INTRUSIVE ROCKS OF THE NIMISH SUBGROUP.

chambers for the various fractionation steps as modelled in Sections VI.5.2 to VI.5.4, but are more probably intrusive equivalents to the volcanic rocks that did not reach the surface. This implies that the main fractionation/accumulation chambers of the aforementioned petrogenetic steps are concealed at depth and not represented by the exposed intrusive bodies; as is supported by the lack of cumulus textures in the gabbroic bodies.

Only moderate amounts of internal fractionation within individual plutonic bodies are implied by the trace element and REE data. The Point Lake Pluton is an exception to this conclusion as it shows wide ranges in REE, Zr, Nb, Y and P_2O_5. This large range is partly due to the inclusion of sample JS - 464 which is not connected to that main body of the pluton and shows the most extreme incompatible element concentrations. The P_2O_5 and Zr abundances of JS - 095 and JS - 048, both of the Point Lake Pluton, however confirms some degree of internal fractionation (Appendix B).

Due to the somewhat inconclusive stratigraphic-structural relations and small but significant degrees of fractionation within the plutonic bodies of the Nimish Subgroup, no attempt was made to coordinate them into any modelling scheme except to show that their REE patterns are similar to the extrusive rocks and hence could be derived by similar processes.

VI.5 - Rare Earth Element Modelling of the Nimish Subgroup:

VI.5.1 - Introduction:

The use of the REE in studies of igneous petrogenesis has been made quantitative by the determination of a series of mineral-liquid distribution coefficients for each element (Schnetzler and Philpotts, 1968; Nagasawa and Schnetzler, 1971; Shimizu and Kushiro, 1974). The distribution coefficients are defined by the following equation:

$$Kd^i_x = \frac{C^i_x}{C^i_{liq}}$$

where: C^i_x = Concentration of element i in mineral phase x.

C^i_{liq} = Concentration of element i in the coexisting liquid.

Kd^i_x = Distribution coefficient of element i between phase x and coexisting liquid.

which describes the behaviour of an element in any crystal-liquid system during fractional crystallization or partial melting processes. The Kd values were originally determined by separating phenocryst and groundmass phases and analyzing each for their trace amounts of REE (Schnetzler and Philpotts, 1968). As more studies are published it becomes evident that the Kd values in any situation depends upon the temperature, pressure, fO_2, and the nature of the coexisting phases, but that measured Kd values of similar rock types are comparable.

In general the REE behave as a coherent group during most petrologic processes and show a regular internal fractionation. The systematic and predictable nature of the REE behaviour along with their resistance to secondary alteration makes them quite useful in modelling the petrogenesis of altered volcanic rocks.

The petrogenesis of the Nimish volcanics has been approached using these assumptions. The REE abundances of relatively unaltered samples from the recognized subdivisions of the Nimish volcanics are taken to be representative of those groups and are mathematically modelled to test the proposed parent-daughter relationships. In this section only the key petrogenetic transitions, as identified through figs. 17 and 18 and associated discussions, will be modelled. Specifically these exercises will include: (1) determining the most probable source rock for JS - 464 among the various rock types of the Petitsikapau Lake Formation, (2) demonstrating the possibility of deriving the intermediate rocks JS - 033 and JS - 505 from the normal basic lavas of the Astray Lake Formation, and (3) testing the possibility that the peculiar REE patterns of the alkali rhyolites for the Astray Lake Formation could be formed through fractional crystallization of the associated volcanics.

The results of these modelling calculations were obtained through the operation of the computer program STEM (System for Trace Element Modelling), developed by the author and presented in documented form in Appendix C. Discussion of the logic of the program, origin of the modelling equations and user oriented features are given in Appendix D while the Kd values used are tabulated in Appendix E. The set of Kd values used for each case of modelling are those most consistent with the rock types modelled and are presented in the following discussion. All calculations were done with the assumption that only the surface of the phenocryst phases was in equilibrium with the coexistent liquid. This was done in consideration of the abundance of zoned phenocrysts present which support surface equilibrium conditions and the assumption that the Nimish Subgroup underwent high - level, low pressure fractionation (Arth, 1976).

Previous discussions indicated that the intrusive rocks of the Nimish Subgroup are not cumulate in nature and that any cumulate rocks associated with the formation of the extrusive rocks are not exposed in the Dyke Lake area. In general this would imply that fractionation occurred deep in the crust and that crystal - liquid Kd values representing a total equilibrium situation should be used (Arth, 1976). This conclusion is untenable both on the nature of the phenocrysts

present and the fact that a maximum of 3 - 5 km of supracrustal rocks are exposed in the area. As there is no evidence for a significant erosional break between the Wishart Formation and the Nimish Subgroup - Sokoman Formation complex, this thickness implies a 1 - 2 Kb minimum pressure range for fractionation of the Nimish Subgroup. As no concrete geologic evidence supports the contention that the fractionation occurred much below the 3 - 5 Km depth and the petrologic data supporting high level fractionation, I have assumed that any relevant fractionation probably occurred within a 5 - 15 Km (2 - 5 Kb) range. As such this is generally classified as high level fractionation (O'Hara, 1965, 1968) which justifies the use of surface equilibrium Kd values (Arth, 1976).

The abundances of the minerals used for the model source materials deviate somewhat from the average normative proportions listed in Appendix B. This was found necessary because the CIPW norms calculated with the substantially altered major element chemistry are quite unrealistic in some cases and are generally unworkable in the modelling equations. The major problems are in the normative K - feldspar, plagioclase and diopside abundances. Predictably K - feldspar was anomounously high which tended to deplete the Al_2O_3 in the first step of the CIPW calculations which in turn results in a low abundance of normative anorthite. This effect is compounded

by the overall loss of CaO during the alteration. Similarly following the steps of CIPW calculations most of the CaO is used to balance the excess of Al_2O_3 in anorthite and very little is left for the formation of diopside. In the mafic members this also tends to give a complementary over-abundance of olivine and/or orthopyroxene.

As a result the normative compositions were adjusted to compensate for these problems by increasing the diopside and anorthite components and decreasing the potash feldspar, olivine and orthopyroxene proportions to give more realistic normative compositions for these slightly alkalic volcanic rocks. For ease of calculation any orthopryoxene in the norm was disregarded and roughly, equally divided between diopside and olivine. This latter generalization produces only minor, symmetrical changes in the modelled REE patterns with the estimated error in accuracy overshadowed by the range in percentage fractionation used in the modelling diagrams.

The author believes that these somewhat arbitrary adjustments do not discount the underlying validity of this approach. Given that the REE are relatively immobile and as a group they portray a mildly alkaline volcanic suite it is reasonable to start with a generalized alkali basalt normative composition. Furthermore slight variations in

the composition of the starting material produces only minor effects on modelled REE abundances and the adjustments only become significant in the extreme case where one mineral phase is almost totally used up. With the very low proportions of diopside in the normative recalculations the loss of this phase was a constant restraint on modelling calculations. Some form of adjustment was necessary in order to even generally discuss the inferred petrogenetic relationships through REE modelling. Given the exotic and very divergent nature of some of the REE patterns of the Nimish Subgroup it was thought that investigation into the possibility of cogenesis of these lavas was necessary to support the previously discussed recognition of two separate volcanic formations. Only through these generalizations is this line of inquiry possible.

The modal abundances in the cumulate fractions are consistent with the major and trace element chemistry of these adjusted norms and are adjusted within these inferred limitations to produce a best fitting pattern.

The trace elements Cr, Ni, Ti, Y, Nb, Zr and V were also modelled through the computer program. The Kd values for these minerals have not been as well studied as the REE but the sample calculations given produce reasonable results and serve as a good check on the assumptions used for the fractionating assemblage.

The ranges of fractionation used in the modelling exercises were estimated from the relative Zr contents of the source and daughter rocks assuming that Zr is "perfectly incompatible".

VI.5.2 - Rare Earth Element Modelling of JS - 464 of the Point Lake Pluton:

Generally no specific limiting factors could be placed upon the possible source rock or fractionating assemblage that was involved in the production of the plutonic rock JS - 464, but the normal basic lavas, the intermediate lava, JS - 104, and the acidic lava, JS - 111, are all possible source rocks.

With any one of these parent minerals the fractionating assemblage should consist predominantly of plagioclase + potash feldspar $\pm$ diopside and magnetite. From fig. 17 clinopyroxene would seem to be a more prominent phenocryst phase with a normal basic source rock than with JS - 104 or JS - 111. Similarly apatite should be expected to play a very small role in any of the models tested. The use of zircon in the source and cumulate mineralogies was introduced to give more accurate modelled Zr values while the very small amounts used produce only very small effects on the modelled REE abundances.

These petrogenetic inferences are included in the various starting assemblages, cumulus mineralogy and percentage fractionation data used in the generation of the three best-fitting modelled curves, fig. 21. The input data used to generate these curves are presented below.

Normal Basic Lavas: - 82.5% fractionation, Average basaltic Kd values

	Oliv.	Aug.	Plag.	Apat.	Zirc.	Kfeld.	Mag.
Source	10.00	30.00	40.00	1.00	0.20	6.80	12.00
Cumulates	11.70	35.00	47.00	0.20	0.10	2.00	4.00

Intermediate Lavas: - 75% fractionation, Average dacitic Kd values

	Oliv.	Aug.	Plag.	Apat.	Zirc.	Kfeld.	Mag.
Source	0.0	14.50	55.00	0.30	0.20	22.00	8.00
Cumulates	0.0	9.00	68.00	0.10	0.10	20.00	2.80

Acidic Lava, JS - 111: - 65% fractionation, Average Rhyolitic Kd values

	Aug.	Plag.	Apat.	Zirc.	Kfeld.	Mag.	Qtz.
Source	2.00	25.00	0.30	0.50	50.00	2.20	20.00
Cumulates	2.75	27.00	0.0	0.25	68.00	2.00	0.0

Obviously the most probable source rock type for JS - 464 is the normal basic lavas in which the modelled REE abundances are within 20 percent of the measured abundances in all cases, fig. 21. The very large Eu anomaly produced by the fractionation of JS - 104 or JS - 111 reflects the improbability of these source rocks. The strong modelled depletion for Eu

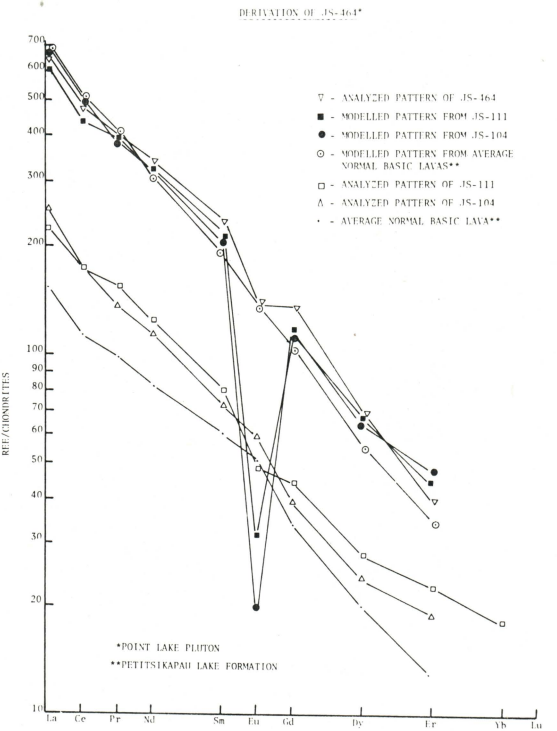

Fig. 21: REE MODELLING OF #JS-464, POINT LAKE PLUTON. BEST FIT PATTERNS FROM ALL POSSIBLE SOURCES.

could be partially a result of inappropriate feldspar-Eu Kd values, as they are a function of fO_2 (B.J. Fryer, pers. comm.), but the range of deviation seems too great. Alternatively this anomaly could result from Eu mobility during secondary alteration (Sun and Hanson, 1978), but previous discussions on the relatively unaltered K, Rb and Ba contents and the fresh petrography of the acidic samples of both formations probably discounts this possibility.

The lack of an Eu anomaly in the modelled normal basic pattern is the only significant divergence from the actual pattern of JS - 464 in this source rock case. Aside from inappropriate feldspar - Eu Kd values, this anomaly could be explained by the positive Eu anomaly of the average normal basic lava whose Eu value is somewhat artificially high due to the presence of 10-15% plagioclase phenocrysts characteristically rich in Eu. Slightly less clinopryoxene in the cumulate phases and/or the source rock for the normal basic model might have produced a tighter modelled fit for the MREE and HREE but the large degree of fractionation restricted the proportions of fractionating phases.

The modelled trace element abundances for the normal basic case, Table 8, are fairly consistent with this crystallizing assemblage. Modelled Nb and Y are quite high because of the low abundance of cumulus apatite. This low value

TABLE 8

TRACE ELEMENT ABUNDANCES IN JS - 464 OF THE POINT LAKE PLUTON

	ACTUAL	MODELLED	% DIFFERENCE
Cr	0	0	-
Ni	7	1	- 86%
Ti	1.02	0.73	- 28%
Y	51	75	+ 47%
Nb	66	84	+ 27%
Zr	510	476	- 7%
V	40	3	- 93%

* Calculated at 82.5% fractionation.

TABLE 9

TRACE ELEMENT ABUNDANCES OF THE DEPLETED INTERMEDIATE LAVAS OF THE ASTRAY LAKE FORMATION

	ACTUAL	MODELLED	% DIFFERENCE
Cr	10	1	- 90%
Ni	12	3	- 75%
Ti	0.92	1.13	+ 23%
Y	31	29	- 6%
Nb	25	22	- 12%
Zr	209	233	+ 11%
V	75	41	- 45%

* Calculated at 15% fractionation.

was used because if more apatite was subtracted a significantly higher degree of fractionation is needed to approach the REE pattern of JS - 464, which would imply a higher amount of zircon fractionation. Detailed mineralogical studies have not revealed significant amounts of zircon crystals in the acidic or intermediate volcanics of the Nimish Subgroup (T. Krogh, pers. comm.) and hence it seems that the stability volume of zircon was never achieved. Therefore calling for extensive zircon fractionation is unreasonable. As it stands, the normal basic model calls for .10 percent zircon fractionation. Without this added loss of zircon the modelled abundance of Zr would be 871 ppm.

VI.5.3 - Rare Earth Element Modelling of JS - 033 and JS - 505 of the Astray Lake Formation:

The discussion in Section VI.3.3 showed that the derivation of JS - 033 and JS - 505 from an average normal basic lava of the Astray Lake Formation were very critical petrogenetic steps. Figure 17 showed the important role that apatite played in this transition while the sharp decrease in TiO_2, V and Cr indicates the presence of magnetite fractionation (Appendix B). The larger change in the Ce/Sm ratio coupled with a smaller increase in Zr for JS - 033 (fig. 17; Appendix B), implies that a slightly smaller percentage of fractionation

was involved in the formation of JS - 033 than JS - 505 from the normal basic lavas of the Astray Lake Formation. Similarly apatite, which is the controlling mineral with respect to the Ce/Sm ratio, must have been a more important phase in the formation of JS - 033.

Some generalizations can also be made on the clinopyroxene/plagioclase ratio in the fractionating assemblage for these two cases. The REE chemistry, figs. 17 and 18, implies that clinopyroxene is a more important phase in the formation of JS - 033 than JS - 505 as it would complement the increase in Ce/Sm and decrease in Sm/Er caused by apatite fractionation, helping to explain the large changes in these ratios noted with an inferred derivation from a normal basic source rock.

These geochemical/petrogenetic inferences are supported by the petrography of JS - 033 and JS - 505 (Appendix F). JS - 033 is a plagioclase porphyritic intermediate lava with occasional flow alignment textures. The relative densities of plagioclase and typical basaltic liquids precludes the settling out of these plagioclase phenocrysts so it is possible that these phenocrysts could have been carried up with the fractionated liquid that formed sample JS - 033. As such, loss of plagioclase through fractionation in the formation of JS - 033 would be minimal and a high clinopyroxene/plagioclase ratio in the cumulus phases relative to JS - 505 would be expected.

Conversely JS - 505 is a potash feldspar - phyric intermediate rock that lies immediately above JS - 033, fig. 1. The absence of plagioclase feldspar phenocrysts in this sample is significant in its possible implication that plagioclase feldspar had totally fractionated out of the system during the petrogenesis of this sample. A high plagioclase/clinopyroxene ratio in the fractionating assemblage for JS - 505 was used to account for these observations.

These general limitations are incorporated into the modelling input data as summarized in figs. 22 and 23.

Accurate modelling of JS - 033 was extremely difficult as apatite totally dominated the bulk Kd calculations for the LREE and MREE. As a result when the MREE bulk Kd values are made high enough to produce the required depletion over the small percentage of fractionation, the Kd values for La and Ce approach 1 and hence little LREE enrichment was possible. This results in low modelled La and Ce abundances, fig. 22.

A similar problem was experienced in the HREE where the chemically measured depletion was more than that allowed by apatite modelling alone. In this case large amounts of cumulus clinopyroxene were added in an effort to decrease the modelled abundances of HREE and as called for in the previous discussion. The results indicate that it was not enough in that Dy and Er are still modelled too high. A small amount

DERIVATION OF DEPLETED INTERMEDIATE LAVAS*

	OLIV.	AUG.	PLAG.	APAT.	ZIRC.	KFELD.	MAG.
SOURCE	10.00	32.00	40.00	1.00	0.20	6.80	10.00
CUMULATES	20.00	56.00	10.00	2.50	0.0	0.0	11.50

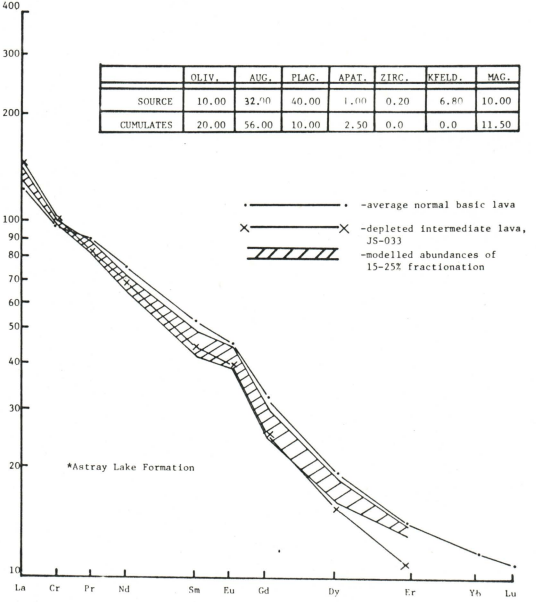

Fig22 : REE MODELLING OF DEPLETED INTERMEDIATE LAVAS FROM THE NORMAL BASIC LAVAS, ASTRAY LAKE FORMATION.

of zircon fractionation would produce a closer fit for the HREE but this was considered improbable with the low Zr contents of the two rock types. The reason for this modelling discrepancy could be due to inaccurate apatite Kds or to possible anomalously high Dy, Er, Yd and Lu abundances in the normal basic lavas resulting from their peculiar HREE levelling off pattern. Further discussion of the variation in HREE patterns is left to Section VI.6.

The other modelled trace element abundances, Table 9, agree very closely in all cases except Cr. This relatively close correspondence is surprising considering the amount of apatite and magnetite fractionated and their strong control on the listed trace elements (Appendix E).

The best fit model for the generation of the normal intermediate lava, JS - 505, from the normal basic lavas is presented in fig. 23. The fit is fairly good for the LREE and MREE but is low for the HREE. These low abundances persist despite the HREE levelling pattern for the normal basic lavas, and the low clinopyroxene/plagioclase ratio in the fractionating phase. This serves to emphasize the larger degree of HREE enrichment displayed by the normal intermediate sample relative to the normal basic lavas. These HREE enrichments are in turn superceded by the acidic rocks of the same Astray Lake Formation.

DERIVATION OF NORMAL INTERMEDIATE LAVAS*

	OLIV.	AUG.	PLAG.	APAT.	ZIRC.	KFELD.	MAG.
Source	10.00	32.00	40.00	1.00	0.20	6.80	10.00
Cumulates	34.00	10.00	43.00	1.00	0.0	0.0	12.00

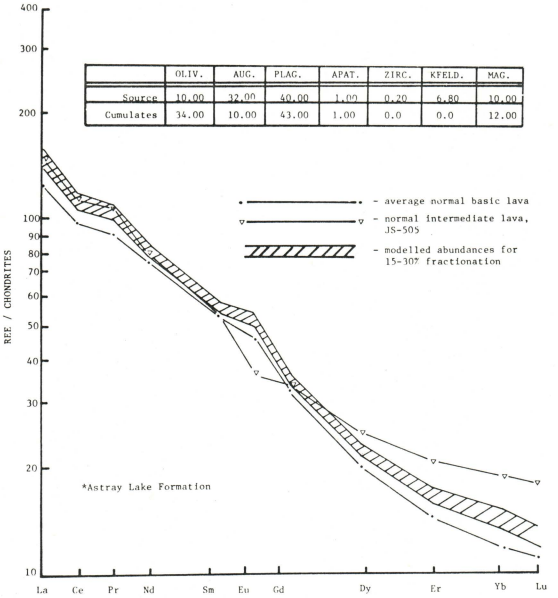

Fig. 23: REE MODELLING OF NORMAL INTERMEDIATE LAVAS FROM THE NORMAL BASIC LAVAS, ASTRAY LAKE FORMATION.

The inability to successfully model this transition could be due to a number of factors: appropriateness of the apatite Kd values, experimental error, problems in generalizations of source and associated cumulate normative compositions and possible secondary mobility of the REE. The consistency of the HREE enrichment amongst these samples and their close association around the volcanic centre of the Jasper Mountain area also adds the possibility that the HREE are controlled by complexing processes within volcanic gas phases associated with the final stages of fractionation. Further discussion of this aspect is left to Section VI.6.

Small variations in the extreme clinopyroxene/plagioclase ratio of the cumulate phases chosen for this step could be easily accommodated with only minor changes in the modelled pattern. A large amount of plagioclase cumulates was modelled because it is consistent with the previous discussion on feldspar mineralogy and produces the closest approximation to the HREE abundances of the normal intermediate samples that is possible by derivation from the normal basic lavas. Choice of any other source material would deviate even more in the HREE because it is only the normal basic lavas that approximate the HREE enriched pattern of the normal intermediate lavas.

The modelled trace element abundances for this transition, Table 10, are all very consistent except for Ni and Cr which

TABLE 10

TRACE ELEMENT ABUNDANCES OF THE NORMAL INTERMEDIATE LAVAS OF THE ASTRAY LAKE FORMATION

	ACTUAL	MODELLED	% DIFFERENCE
Cr	10	1	- 90%
Ni	9	2	- 78%
Ti	0.98	1.19	+ 21%
Y	35	36	+ 3%
Nb	32	27	- 16%
Zr	228	243	+ 7%
V	61	43	- 30%

* Calculated at 20% fractionation.

TABLE 11

TRACE ELEMENT ABUNDANCES OF THE ACIDIC LAVAS OF THE ASTRAY LAKE FORMATION

	ACTUAL	MODELLED	% DIFFERENCE
Cr	13	1	- 92%
Ni	4	2	- 50%
Ti	0.29	0.63	+ 117%
Y	151	105	- 30%
Nb	95	93	- 2%
Zr	866	764	- 12%
V	15	2	- 87%

* Calculated at 75% fractionation.

are reasonable considering the aforementioned arguments on the precision of these elements. The close modelled abundances displayed by Nb and Y in this step and Table 9, both of which involved substantial apatite, supports the assumption that these elements roughly follow Dy in their geochemical behaviour (Appendix D).

VI.5.4 - Rare Earth Element Modelling of the Average Acidic Analyses of the Astray Lake Formation:

Little can be said about possible source rocks for the acidic samples of the Astray Lake Formation except that it was not the enriched intermediate sample JS - 104 or the depleted basic lava JB - 79, figs. 17 and 18. In this case a similar approach to that used to determine the probable source for JS - 464 was followed. The best fitting curves for each possible source are plotted together for comparison in fig. 24. The source and cumulate mineralogy, and percentage of fractionation used in each case is listed below.

Due to the high percentages of fractionation involved in all cases the proportions in the cumulate mineralogy were determined by estimating the mineral proportions that would leave a residual composition that approximates the normative composition of the acidic rocks (i.e. half quartz and half alkali feldspar with minor iron oxides). Small amounts of

apatite fractionation are included to comply with the drop in P_2O_5 contents noted in all cases. As noted in the summary table of input data, different Kd value sets are used for the intermediate and basaltic source rocks.

Normal Basic Lavas: - 80% fractionation, Average Basaltic Kds

	Oliv.	Aug.	Plag.	Apat.	Zirc.	Kfeld.	Mag.
Source	10.00	32.00	40.00	1.00	0.20	6.80	10.00
Cumulates	11.00	33.00	44.00	0.55	0.0	6.00	5.45

Depleted Intermediate Lavas: - 80% fractionation, Average Dacitic Kds

	Aug.	Plag.	Apat.	Zirc.	Kfeld.	Mag.	Qtz.
Source	10.00	50.00	0.20	0.30	25.00	4.50	10.00
Cumulates	11.00	55.00	0.22	0.0	27.50	4.00	2.28

Normal Intermediate Lavas: - 75% fractionation, Average Dacitic Kds

	Aug.	Plag.	Apat.	Zirc.	Kfeld.	Mag.	Qtz.
Source	5.00	49.00	0.20	0.20	29.60	6.00	10.00
Cumulates	6.00	54.00	0.25	0.0	30.00	3.50	6.25

From fig. 24 it seems that the best source rock for the acidic lavas is the intermediate sample JS - 505 as it is the only one that approximates the HREE enrichment of the acidic lavas. The difference at Lu could be analytical error (Appendix A). The contrasting modelled HREE patterns produced from a source with a linear distribution of HREE (JS - 033) relative to one with a moderately enriched HREE pattern

DERIVATION OF ACIDIC LAVAS*

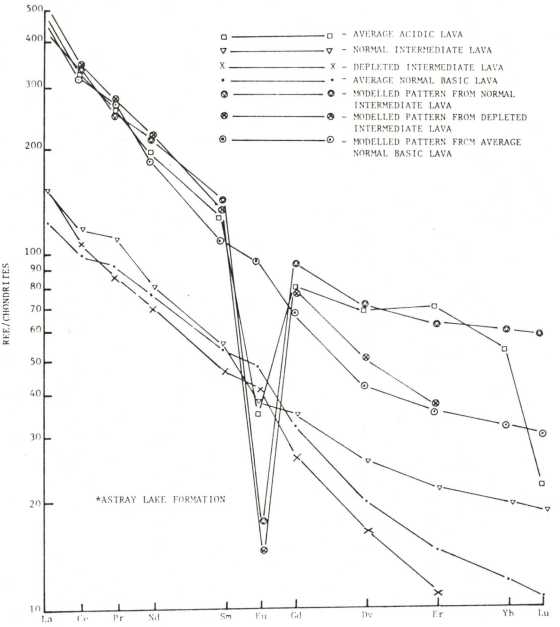

FIG. 24: REE MODELLING OF ACIDIC LAVAS, ASTRAY LAKE FORMATION. BEST FIT PATTERN FOR ALL POSSIBLE SOURCES.

(normal basic lavas) is well displayed in this figure. The lack of any negative Eu anomaly in the modelled normal basic pattern would be partially compensated for by the use of dacitic Kds in the higher levels of fractionation, if this were possible within the computer program.

The petrogenetic relationship of the acidic lavas with the normal intermediate lavas rather than the normal basic lavas, which seem to be the parent for the other types, is not unexpected considering their close association in the field. In this sense JS - 505 might represent the products of some form of high level fractionation chamber formed in a similar fashion to that envisaged for the plutonic rock JS - 464 which is associated with the Petitsikapau Lake Formation.

The other modelled trace element abundances for the normal intermediate source rock are listed in Table 11. The fit is not close for TiO_2, Y or Zr but at these high levels of fractionation slight variations in the percentage of crystallization have large effects on the trace element abundances. For example with only 5 percent further fractionation the Y value rises to 124 ppm, Zr to 928 ppm and TiO_2 drops to 0.59 percent, which more closely approximate the measured average abundances.

The demonstration that this petrogenetic transition is possible lends support to the argument that fractional

crystallization was responsible for the formation of the alkali rhyolites and similarly consolidates the argument that all the volcanic rocks of the Nimish Subgroup could be cogenetic and as such are probably related to the same large scale, tetonic event.

VI.6 - Discussion

The preceeding discussions have attempted to explain the petrogenesis of the Petitsikapau Lake and Astray Lake volcanic cycles by means of a fractional crystallization model. Although there are shortcomings in a few of the proposed cases the pattern implied is fairly consistent and compatible with the geological and geochemical evidence available.

The detailed geochemical and experimental studies on the petrogenesis of the transitional alkali basalt-peralkaline rhyolite suite are not wholly consistent with this interpretation. Macdonald (1975b) in a review of the role of fractional crystallization in the formation of peralkaline, silica saturated volcanic rocks stressed the inconsistencies of the fractional crystallization model with the observed silica gap (lack of a proportionate amount of intermediate rocks), and the inability of experimental work to explain their formation.

Chayes (1963) was the first to recognize the scarcity of published analyses in the $53\% < SiO_2 < 57\%$ range among

oceanic island volcanic suites. He interpreted this as strong evidence against the basalt-trachyte series forming by conventional means of fractional crystallization in which more evolved rocks should occur in progressively smaller percentages. This view has been challenged by Macdonald (1963) and Baker (1968) who argued that this apparent gap was mainly due to personal sampling bias and/or level of erosion, and conducted statistical sampling surveys to prove it. Similarly Bryan (1964) has pointed out that some layered intrusions have pronounced silica gaps and hence the silica distribution may be a function of the mechanics of crystallization.

Baker (1975) and Macdonald (1975) in reviews of the peralkaline suites of oceanic and continental areas have concluded that this silica gap is indeed real and perhaps has some petrogenetic/tectonic significance as discussed in Chapter VII. Aside from the volcanic islands of Socorro (Bryan, 1964) and Gran Canaria (Baker, 1975) the only place where a bimodal distribution of SiO_2 is well developed is in continental rift areas such as the East African Rift. A fractional crystallization model is often very difficult to apply to these suites and alternative hypotheses should be considered (Macdonald et al., 1970).

The disproportionately large volume of salic magmas relative to mafic members in certain areas of the East African Rift Valley prompted Bailey and Schairer (1966) to suggest that the alkali-rich acidic rocks formed from partial melting in the deep crust or upper mantle. Wright (1966, 1969) found ultrabasic nodules in some phonolites and trachytes from New Zealand and Nigeria which he interpreted as indicating a direct mantle origin for these rocks.

The volumetric proportions of acidic rocks in the Nimish Subgroup is impossible to estimate because of the unknown factors of the amount of erosion and level of exposure. Therefore it is unrealistic to discount a fractional crystallization model for the Nimish Subgroup by the presence or absence of a silica gap. Similarly the close geographical association of the various rock types and the plausibility of the implied petrogenetic relationships discussed previously support a fractional crystallization model.

The experimental petrology of peralkaline rocks has been historically treated relative to the Q - Ne - Ks residua system (Hamilton and MacKenzie, 1965) in which fractionation of an alkali feldspar from trachytic liquid drives the composition away from albite - orthoclase thermal divide. A slight deficiency or excess in SiO_2 and/or Na + K + Ca relative to Al will produce a silica saturated or under-

saturated, peralkaline or peraluminous melt upon further fractionation. Bailey (1975) has shown that the quartz-feldspar cotectic of the Q - Ne - Ks system is equivalent to all comendite and some pantellerite compositions but the plots of the high Fe pantellerites are highly distorted in this projection. Generally these extreme pantelleric compositions conform to the natural eutectic of the Na_2O-Al_2O_3-Fe_2O_3-SiO_2 system (Bailey and Schairer, 1966; Macdonald, 1974) and in this sense cannot be explained by feldspar fractionation alone.

Ferrara and Treuil (1975) have proposed that the fractionation towards a pantellerite or comendite composition is controlled by the fO_2 of crystallization, with a low fO_2 favouring feldspar fractionation leading to a comenditic composition while a high fO_2 favours the iron rich pantellerites. Villari (1975) found volcanological evidence to support this view in the mixed high and low Fe pantellerite suite of the Island of Pantellaria. Martin (1975) has shown that the mixing of anhydrous trachyandesites with a gaseous steam phase will cause extraction of a silicic, high Fe^{+3}, Na, K and low Al liquid very similar to common pantellerites. Bailey (1975) also stressed the possible importance of alkali rich gaseous activity in the formation of peralkaline rocks noting (1) the high F, Cl and CO_2 contents of peralkaline rhyolites, (2) the

abundance of alkaline volcanic exhalations and springs, (3) the alkali losses during devitrification indicating that the alkalis are only lightly absorbed on crystalline and glass phases, and (4) the fenitic metasomatism often associated with alkaline volcanic centres.

As the acidic rocks of the Nimish Subgroup approach comenditic composition (Macdonald, 1975) the theoretical formation of these lavas is consistent with the abundance of feldspar fractionation used in fig. 23, although contamination by means of gaseous activity should not be ruled out.

The petrogenetic modelling of the Nimish Subgroup is generally consistent with the fractionation models proposed from the major element data of similar transitional basalt - alkali rhyolite suites that do not have prominent silica gaps such as the Little Aden suite (Cox et al., 1970) and the Boina centre (Barberi et al., 1975) also of the Afar region. In each of the above suites an assemblage of olivine plus subordinate clinopyroxene and plagioclase fractionated to form the ferro-basalts from the primary alkali olivine basalts. Similar to the Nimish Subgroup, TiO_2 and P_2O_5 abundances build up until the formation of the intermediate lavas while alkali feldspar phenocrysts mark the transition to the peralkaline acidic rocks. Barberi et al. (1975) stress the sympathetic variation between total Fe, Fe^{+2}/Fe^{+3}, and Eu, noting signi-

ficant breaks in the fractionation pattern at the onset of magnetite and apatite fractionation. This was similarly noted in the Nimish Subgroup. These general comparisons support the classification of the Nimish Subgroup as an alkaline volcanic suite. The possible tectonic implications of these petrogenetic similarities are discussed in Chapter VII.

Attempts have been made to model the major element abundances in the proposed fractionation steps through the use of petrochemical subtraction equations and estimated compositions of phenocryst phases. The results of these calculations proved to be consistent with the general trends but highly erratic in individual cases. Generally the proposed major element fractionation models produced intermediate rocks from basic rocks and acidic rocks from intermediate rocks, etc., but the fine points such as the $CaO-Na_2O-K_2O$ and $MgO-FeO$ abundances and ratios were very inaccurate. The reasons for these discrepancies may be due to a number of factors such as the alteration that has effected the samples, the simplification of the mineral proportions used in the modelling, the unknown composition of the phenocryst phases and the insensitivity of petrochemical subtraction equations to slight changes in the fractionation assemblage such as zoning in phenocrysts, which is common in alkalic suites. The author believes that this discrepancy

is not too serious as the Nimish Subgroup has experienced substantial alteration of most major elements and the models proposed give reasonable results for the trace elements and, except for a few cases, produce overlapping REE patterns.

The main problem with the REE modelling is in the fractionation within the Astray Lake Formation, figs. 22 and 23, in which an overlapping modelled field was not obtained, or extreme cumulate compositions were necessary to obtain the overlap. The discrepancies invariably occurred in the HREE, Dy - Yb, in which some samples show a distinct levelling off, (normal basic, normal intermediate and acidic lavas), while others maintain a steeply inclined pattern, (depleted basic, depleted intermediate and enriched intermediate lavas). The uniqueness of the two sets of patterns might imply that there are two separate magma series represented in the Astray Lake Formation but the close field association of the two series, (most notably the depleted and normal intermediate lavas), makes this seem unlikely. A certain amount of zircon fractionation would help in the REE modelling of certain petrogenetic relations such as in fig. 23, but this also seems unlikely considering the low Zr contents of both the parent and daughter rock types and the lack of any petrographic evidence supporting this assumption.

The other possible explanation for these discrepancies is that the REE abundances of the HREE enriched lavas have been increased by some form of HREE complexing process.

The original documentation of this process comes from Fryer and Edgar (1977) who showed that the relatively enriched HREE abundances of eudialyte bearing peralkaline rocks is primarily contained in the mineral eudialyte and that this mineral showed varying REE patterns between intrusive complexes. The differences in the eudialyte mineral Σ Ce/ΣY ratios were interpreted as a function of the importance and duration of REE complexing at that particular stage of fractionation, with the beginning of eudialyte fractionation probably representing the point at which the REE complexes begin to break down. Bowden and Whitley (1974) noticed a similar form of HREE enrichment associated with the late stage albitization of some peralkaline granites. Experimental work recognizing the stability of HREE complexes in the presence of halogens and CO_2 as volatile constituents has been documented by Bandurkin (1961).

If this HREE pattern complexing process was operative during the fractionation of the Nimish Subgroup certain geochemical traces of the activity should remain. The HREE enriched patterns of the normal intermediate and acidic lavas of the Astray Lake Formation and the difficulty of modelling

their REE patterns may indicate some form of extraneous factor of this sort.

In conclusion it can be said that notwithstanding a few minor discrepancies, volcanic rocks of the Nimish Subgroup do form a distinct geochemical suite which displays a recognizable fractionation pattern that can be modelled with REE data using a few reasonable generalizations and assumptions. The models proposed obviously do not possess any degree of geochemical rigidity in terms of producing a comprehensive study of the interrelationships designed to explicitly define the fractionation relationships. Rather they serve to demonstrate the petrogenetic possibilities within this suite, and in doing so, offer support for their recognition as two separate volcanic formations generally related to the Aphebian tectonic event responsible for the formation of the Nimish Subgroup.

CHAPTER VII

TECTONIC AFFINITIES OF THE NIMISH SUBGROUP

The tectonic affinities of any Proterozoic volcanic suite is a highly speculative topic considering the small number of studies done on such areas and the uncertainty in the nature of tectonic processes during this period. Similarly the geology of the Aphebian Era, or earliest Proterozoic period, 2400 my - 1735 my, is unique within the global stratigraphic record and hence cannot be compared to modern day tectonic environments. The worldwide distribution of extremely large, Aphebian age, sedimentary basins which consistently show a dolomite + quartzite + iron formation type stratigraphy, such as the Labrador Trough, reflect a tectonic and atmospheric environment that has not been repeated in the history of the earth. Therefore the significance of the Nimish volcanics relative to this globally correlated stratigraphy becomes even more enigmatic because the nature of the dominant geologic processes of this era are poorly understood themselves.

With reference to this background the tectonic affinities of the Nimish Subgroup will be discussed relative to other Aphebian sedimentary basins, volcanic suites of Labrador of a

similar age and to modern day tectonic/volcanic associations that are comparable to the geochemistry of the Nimish volcanics.

Large scale deposits of Aphebian age cherty iron formation are found in the Hammersley Basin of Western Australia, the Transvaal System of South Africa, the Aminikie and Marquette Supergroups of the Great Lakes region of North America, the Minas Gerais Basin of Brazil and the Labrador Trough of Quebec and Labrador. With some reservations these sedimentary basins resemble each other in age, basin size, chemistry, mineralogy, volcanic and clastic associations and the general temporal restriction of the iron formation to certain horizons in the stratagraphic succession (Trendall, 1968). The main differences lie in the stratigraphic sequence, thicknesses and thickness variations, sedimentary structures and the abundance of diagenetic riebeckite. Unfortunately the most important factor of these iron formation basins relative to this study, that of the volcanic and clastic associations, is perhaps the least studied of the above.

In review papers by Trendall (1968), Van Dorr (1973), Bayley and James (1973) and Beukes (1973) the occurrence of volcanic rocks in iron formation-bearing, Aphebian-aged sedimentary basins is highly variable. In the Hammersley Basin abundant mafic volcanic rocks are found in the lower Fortescue

and upper Wyloo Groups with only minor amounts of questionable tuffaceous material in the iron bearing Hammersley Group (Trendall, 1968). Volcanics within the iron formation strata of the Transvaal Supergroup are restricted to one thin volcanic unit, the Ongeluk Lavas, which can be traced over most of the Transvaal Basin although a few mafic volcanics are found in the underlying Wolkberg Group. Intermediate and acidic lavas are quite commonly found associated with the small banded iron formation members of the older Witwatersraand Supergroup (Beukes, 1973). The volcanological associations of the Brazilian iron formations are not well understood but they are believed to be largely restricted to the uppermost Sobara Formation of the Minas Series (Van Dorr, 1973).

Pillowed volcanic rocks, predominantly of mafic composition, are restricted to the upper Baraga Group of the Marquette Range Supergroup of the Wisconsin and Michigan area of the northern United States (Bayley and James, 1973). The volcanics are missing from the correlative rocks in the Aminikie Group of Minnesota and western Ontario. Small discontinuous units of banded iron formation are also found throughout the numerous Middle Precambrian inliers of the Rocky Mountain Belt in the western United States. The Yavapai Series of central Arizona is especially significant amongst these as it is a dominantly volcanic sequence made up of flows and volcanic breccias

ranging in composition from basalt to rhyolite. Interbedded sediments consist of thin, lens shaped, beds of jasper bearing, cherty iron formation that contain variable amounts of volcanic detritus; similar to the magnetite greywacke facies stratigraphy of the Dyke Lake area. The average composition of this facies of the cherty iron formation is similarly rich in MnO and Al_2O_3 reflecting contemporaneous volcanic activity (Bayley and James, 1973).

The author was unable to find any geochemical data on the aforementioned volcanic suites so direct comparison with the Nimish volcanics is impossible. Therefore the only comparative geochemistry discussed is with the other volcanic members of the Labrador Trough and with Cenozoic volcanic suites which geochemically resemble the Nimish Subgroup.

The petrochemistry of the Nimish volcanics is generally consistent with a transitional, alkali olivine basalt - trachyandesite - comendite differentiation scheme. Macdonald (1975) and Baker (1975) in reviews of the geological occurrences of igneous suites which form peralkaline acidic volcanics recognized six major tectonic associations. The most prominent of these is in continental areas of epeirogenic uplift and rifting (the Oslo Graben, Rhine Graben, Mediterranean region, East African Rift Valley). Other recognized continental tectonic settings of acidic peralkaline volcanism are: (1)

during late stages of tectonic activity often marked by large scale normal faulting and graben formation (the Gardar Province of southwest Greenland), (Upton, 1974) and the White Mountain magma series of the New England Appalachians (Foland et al., 1971; Rodgers, 1970), (2) in isolated igneous centres of volcanic regimes dominated by subduction induced, calc-alkaline volcanism (Mayor Island, New Zealand), (Ewart et al., 1968a) and (3) in linear belts associated with the back arc areas of subduction zones (the alkaline province of Japan), (Kuno, 1966); Basin and Range Province of the southwest United States (Noble and Parker, 1975).

Baker (1975) noted two further geological associations of peralkaline volcanism in the oceanic environment: (4) as islands near the crestal zone of oceanic rises (Easter, Ascension and Bouvet Islands) and (5) as islands arising from extensive submarine plateaus (Gran Canaria, Kerguelen and the Azores Islands).

Baker recognized that the majority of oceanic peralkaline volcanics were comenditic in composition with only the islands of Socorro and Gran Canaria possessing flows of pantelleric chemistry. He also found a general correlation between the alkalinity of the basaltic parent and the degree of peralkalinity of the acidic derivative. A significant silica gap is also related to the alkali basalt - pantellerite association, and

as such, is only developed in the Socorro and Gran Canaria suites. These petrochemical associations have no direct tectonic explanations as Gran Canaria is built upon a large submarine plateau while Socorro is located near the crest of the East Pacific Rise. The correlation of dominantly pantellerite volcanism, relatively more alkalic mafic volcanics and a significant silica gap is also recognized in the continental environments (Macdonald, 1975).

Continental peralkaline volcanism differs from the oceanic varieties in that the continental suites are associated with other magma series while the oceanic suites are not. Generally the occurrences of comendite and/or peralkaline volcanism found near rift zones of continental regions are associated with ultra - potassic alkalic magmatism. This differs from the calc-alkaline volcanic associates of the dominantly comenditic volcanism found in the latter three continental tectonic associations as identified previously.

In general there seems to be two general geological associations of the transitional/alkali basalt to peralkaline rhyolite differentiation scheme:

(1) A dominantly comenditic acidic volcanism associated with transitional basalts, mugearites and trachytes that show no silica gap and are found in oceanic islands or continental regions active during

orogenic or post - orogenic periods dominanted by calc-alkaline volcanism.

(2) A comenditic and/or pantelleritic, bimodal suite associated with alkalic to ultrapotassic basalts predominantly found in continental areas of epeirogenic uplift and rifting or as an isolated, geochemically similar, volcanic suite found in some oceanic islands.

The tectonic setting of the Nimish Subgroup during the period of volcanism was probably of a continental nature covered by a shallow epicontinental sea which reflects the surrounding "miogeosynclinal" sediments and the general scarcity of pillow lavas (Dimroth, 1968, 1970a; Dimroth et al., 1970). The basaltic pillow lava - shale - gabbro assemblage of the Doublet Group offers a distinct contrast with the Nimish Subgroup and the Knob Lake Group in general. The Doublet Group has been generally interpreted to represent the predominantly volcanic infilling of a large linear basin that paralelled the Knob Lake sedimentary basin throughout the length of the Labrador Trough (Dimroth, 1970a, 1971; Dimroth et al., 1970).

The geophysical work of Kearey (1977) and Thomas and Gibb (1975) on the northern Labrador Trough and Cape Smith Fold Bets also supports a continental tectonic setting for the

"miogeosynclinal" facies of the Labrador Trough. The geophysical models developed by these authors calls for a distinct thickening of the continental crust on the "inland" or "miogeosynclinal" side of the Labrador Trough and a marked depression of the mantle - crust boundary underneath the Doublet Group. These crustal geophysical models are generally consistent with geological features of the "miogeosynclinal" and "eugeosynclinal" division of the Labrador Trough proposed by Dimroth (1968, 1970a, 1971) and Dimroth et al., (1970).

The lack of any calc - alkaline volcanics in the vicinity of this continental setting is a factor in favour of the Nimish Subgroup being related to the second association of acidic peralkaline volcanics as identified previously. Similarly the presence of such alkalic volcanic suites as the Hematite Lake trachyandesites and the ultra - potassic lamprophyre suite of the Labrador Trough (Dimroth, 1970b; Dressler, 1975), both of which are possibly Aphebian aged, gives temporal volcanic associates more typical of the second petrologic - tectonic grouping.

These highly generalized petrologic - tectonic associations are quite interesting in consideration of the tectonic setting classification presented in fig. 25 (Pearce and Cann, 1973). In this plot the mafic members of the Nimish Subgroup show

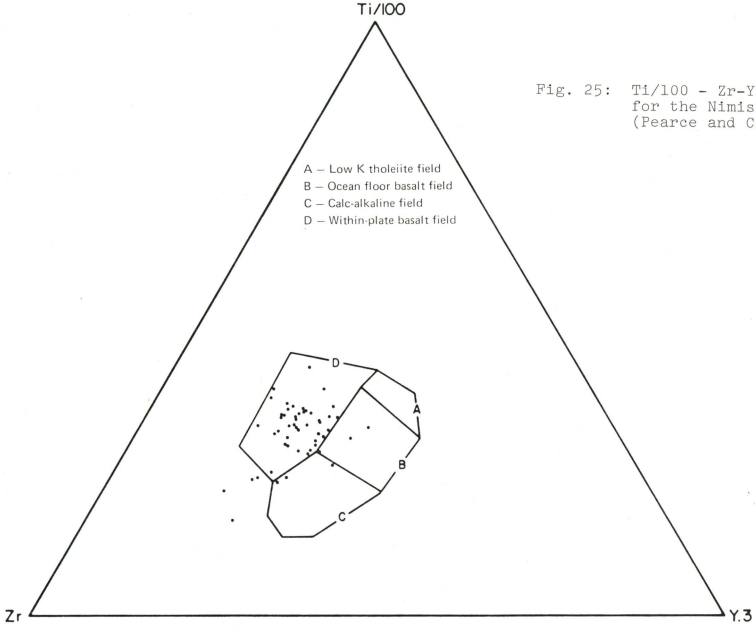

Fig. 25: Ti/100 - Zr-Y.3 diagram for the Nimish Subgroup (Pearce and Cann, 1973).

a very strong clustering in the "within plate basalt field", field D, with only minor scatter in the "ocean floor tholeiite" and "calc-alkaline basalt" fields. In relation to Cenozoic plate tectonics, within plate basalts are restricted to continental tholeiitic flood basalts, the alkalic shoshonitic magma series found on the continental side of subduction zones, alkalic oceanic island suites and ultra - alkalic to transitional basalt suites found in the major rift zones of the world. Although the Nimish volcanics are of Aphebian age and little is known of the nature of plate tectonics during the Proterozoic, the general geological, geophysical and geochemical features of the Nimish volcanics and surrounding areas most closely resemble the rift zone tectonic setting.

The average compositions of the mafic members of some possibly related volcanic rock series of the Labrador Trough and the averages of some well defined Cenozoic tectonic-volcanic associations are given in Table 12. The Hematite Lake and Doublet Group examples have been discussed previously while the data for the lamprophyres comes from near the Hematite Lake area also. The age of the lamprophyre suite, which consists of lamprophyres, carbonatites, kimberlites and melilite tuffs, is somewhat controversial as Dressler (1975) considered them to be possible Sokoman Formation equivalents while Dimroth (1970b) interpreted them to be post - Kaniapiskau in age.

Table 12

Comparison of trace element data for the Nimish Subgroup with other Proterozoic and modern basalt sequences.

	TiO_2	P_2O_5	Zr	Nb	Ga	Ni	Cr	V	Y	Nb/Y	Zr/Ti*
Petitsikapau Lake Fm.	2.35	0.38	197	29	23	37	50	269	32	0.906	0.124
Astray Lake Fm.	2.30	0.40	187	24	22	28	19	292	32	0.750	0.363
Intrusive rocks	1.41	0.25	147	25	18	97	172	197	23	1.09	–
Hematite Lake trachyandesite	1.50	0.14	–	–	–	–	–	–	–	–	–
Doublet Gp.	1.11	0.12	79	–	14	179	205	331	17	–	–
Lamprophyres (Dressler, 1975)	3.79	0.58	159	96	–	518	525	–	45	2.13	–
Little Aden suite	3.04	0.57	194	59	20	42	300	320	31	1.90	0.210
Mugford Gp.	1.73	0.22	–	–	17	169	283	–	–	–	–
Oceanic tholeiite	1.49	0.16	95	16	17	97	297	292	27	0.61	0.008
Oceanic island tholeiite	1.30	0.16	100	–	22	80	120	250	–	0.61	0.109
Oceanic alkali basalt	2.67	0.92	333	72	22	51	67	252	54	1.33	0.304
Calc-alkali basalt	1.05	0.21	100	6	17	25	40	255	19	0.22	0.109

– Data from Engel et al. (1967), Jakes and White (1972), Baragar (1960), Dimroth (1971), Cox et al. (1970), Barton (1975), Carmichael et al. (1974), Winchester and Floyd (1977) Dressler (1975). Averages from basic members only.

* Averages are taken for alkalic members only.

The Nimish volcanics, Hematite Lake lamphrophyre suite and trachyandesite volcanics are all within the "miogeosynclinal" facies of Dimroth et al. (1970), while the volcanics of the Doublet Group and Attikamagen Formation are the principle components of the complementary eugeosynclinal facies. The association of the three alkalic suiteswith the continental tectonic setting implied by the "miogeosynclinal" facies stratigraphy and the absence of any evidence of calc - alkaline volcanism is consistent with a time transgressive, tensional tectonic petrogenesis for these volcanic suites. The eugeosynclinal, tholeiitic character of the Doublet Group and Attikamagen Formation basalts might represent periods of more extensive rifting and dominantly tholeiitic volcanic activity. In relation to Cenozoic tectonics the Doublet Group and Attikamagen Formation basalts may possibly be the Aphebian age, ocean floor tholeiite complements to the rift facies alkaline volcanics of the Dyke Lake and Hematite Lake areas. The miogeosynclinal, alkaline suites could represent aborted rift zones, aulocogens to the main rift zone that produced the Doublet Group or the initial alkaline products of the tectonic/petrogenetic cycle that produced the Doublet Group.

The author realizes that the temporal and geological association of the Nimish and Doublet volcanic suites is only

consistent with some form of rift - induced petrogenesis if Cenozoic petrologic - tectonic associations hold in the most general sense for Aphebian volcanic suites. The author has no comment on the plausibility of the above assumption but notes that there is a tendency to treat Archean volcanic suites in a generalized "plate tectonic" model similar to Cenozoic models (see generally Windley, 1975) and that aulocogens containing alkalic volcanic rocks (Olade and Morton, 1972; Olade, 1975) have been identified within the Aphebian supracrustal sequence of the Coronation Geosyncline (Hoffmann, 1970).

Table 12 also compares the Nimish Subgroup with the Mugford volcanics of northeastern Labrador. The Mugford volcanics have been dated by Barton (1975) at 2369 ± 55 my. Smyth and Knight (1977) however have proposed that they are younger than this and are correlateable with the Ramah Group,(dated at 1893 my.; Wanless and Loveridge, 1978), and Snyder Group of northern Labrador. As such the Mugford volcanics represent the only suite of Aphebian volcanic rocks outside of the Labrador Trough for which chemical data are available.

The major and trace element data presented by Barton (1975) shows the Mugford Group to be a tholeiitic basalt suite. Stratigraphic evidence indicates that they were erupted as continental flood basalts in basins that were quickly filled

by continental clastic sediments. The group is low in the immobile refractory oxides TiO_2 and P_2O_5 and the element Ga relative to the Nimish Subgroup. Nevertheless, the continental tholeiite nature of the Mugford Group would seem to indicate that the Lower Proterozoic in Labrador was dominated by basaltic magmatism and probably was a time of widespread tensional tectonics and rifting.

CHAPTER VIII

ECONOMIC GEOLOGY

The Dyke Lake - Astray Lake area was surveyed for iron ore potential by Labrador Mining and Exploration and Iron Ore Company of Canada geologists during the years of 1949 to 1952. The work of 1952 included some detailed 1" to 200' mapping, trenching and assaying at promising localities of iron formation. None of the occurrences was considered to be of high enough grade to warrant any further exploration. Most of the iron formation in the Dyke Lake area was leached and enriched in iron, but no occurrences of the "soft ore" or "rubble ore" type, which constitutes ore in the main ore zone, have been found.

The Dyke Lake - Astray Lake area is generally poor in sulphide mineralization with only two occurrences noted. Small amounts of pyrite and chalcopyrite occur as vein and amygdaloidal minerals on the islands of Astray Lake while thin films of galena are found along fracture planes in intermediate volcanics west of Roger Lake. Neither of these occurrences warrants further work.

The petrogenetic interpretation of the Nimish Subgroup as a mildly alkaline volcanic suite associated with the initial stages of continental rifting implies metallogenic affinities with similar rock types and tectonic settings. During the Phanerozoic these environments usually show enrichments of rare earth elements, Nb, Ta, Hf, Li and other rare elements, in alkaline granitic or pegmatitic bodies associated with volcanic centres. As no acidic intrusives are exposed in association with the Nimish volcanics the economic potential of the Nimish Subgroup does not seem very great. Sawkins (1976) in a review of the metallogeny of intracontinental hotspot and rifting environments, suggests that the high heat flow and magmatic activity of these areas could also be responsible for some hydrothermal Pb - Zn and stratiform Cu deposits similar to the Zambian copper belt and the Mississippi Valley Pb - Zn deposits. In more advanced stages of rifting Ni - Cr and rare earth element deposits of layered basic intrusions and hydrothermal deposits of the Red Sea brine type may also be expected. No evidence for any of these types of mineralization was found except for the aforementioned sulphide showings.

In conclusion no further work appears warranted to assess the economic potential of the area. If further work on the accessible tonnages of iron formation is contemplated, the

most promising areas for assessment would be the south end of the large, canoe-shaped syncline north of Evans Lake and the long linear belt of iron formation that runs along the west shore of Astray Lake.

CHAPTER IX

CONCLUSIONS

(1) The general stratigraphy of the Knob Lake Group in the southern Labrador Trough is disrupted in the Dyke Lake - Astray Lake area by a submarine to subaerial, volcanic and sedimentary assemblage.

(2) This volcanic assemblage, which has been redefined as the Nimish Subgroup, consists of a lower Petitsikapau Lake Formation and an upper Astray Lake Formation along with associated intrusive rocks. The two volcanic formations are partially separated by the Sokoman Formation.

(3) Complex interbedding of the volcanics and an impure clastic facies of the iron formation occurs at the top and bottom of the Sokoman Formation, indicating contemporaneous volcanic, clastic and chemical sedimentary activity.

(4) The Sokoman Formation is divisible into lower, middle and upper members which are broadly correlative with similar divisions in the Knob Lake area.

(5) Detailed facies relationships of the Nimish volcanics and Sokoman iron formation imply a paleogeography dominated by a series of subaerially exposed volcanic islands and large, relatively flat sedimentary basins.

(6) The Sokoman Formation has numerous sections of leached and enriched material in the Dyke Lake area, but no deposits of economic grade iron ore were recognized.

(7) The Nimish Subgroup volcanics disrupted the style of folding during the Hudsonian orogenic event by producing close to open folds with closely spaced thrust faults, relative to the continuous, broad open folding found elsewhere in the Trough.

(8) The Nimish Subgroup lavas have been affected by lower greenschist facies metamorphism in which distinct additions of K_2O are suspected.

(9) The immobile trace element geochemistry implies that the Nimish lavas are a mildly alkaline volcanic suite which generally show an alkali basalt - trachyandesite - comendite differentiation scheme.

(10) The major element data is highly erratic but generally supports the petrologic classification based on the trace elements.

(11) Distinct subdivisions within the Petitsikapau Lake and Astray Lake Formations are recognized on the basis of petrographic, major element and "relatively immobile" trace element data.

(12) REE patterns of representative samples of the subdivisions are unique to those subdivisions and similar to

other Cenozoic alkali basalt, trachyandesite and comenditic rocks.

(13) The fractional crystallization petrogenetic relationships of the various subdivisions implied by the major and trace elements are for the most part supported by REE modelling calculations.

(14) The normal basic, normal intermediate and acidic lavas of the Astray Lake Formation consistently show anomalous results in REE modelling calculations primarily due to their distinct HREE patterns.

(15) The REE abundances of the intrusive rocks of the Nimish Subgroup are similar to the extrusive rocks, confirming that they are cogenetic with the Nimish lavas.

(16) The REE patterns of the intrusive rocks of the Nimish Subgroup are not compatible with their formation in crystal accumulation chambers of the fractional crystallization processes responsible for the formation of the Nimish lavas.

(17) The geological, geochemical and geophysical evidence indicates that the Nimish lavas represent a continental, alkaline volcanic suite possibly related to the initial tensional tectonic, rifting environment that preceeded the extrusion of the voluminous, tholeiitic lavas of the Doublet Group.

(18) The Nimish Subgroup lavas are barren of any significant sulphide mineralization.

BIBLIOGRAPHY

Abbey, S.
1974: Studies in standard samples of silicate rocks and minerals; Geol. Surv. Can. paper 74-41.

Albarede, F.
1976: Some trace element relationships among liquid and solid phases in the course of fractional crystallization of magmas; Geochim. Cosmochim. Acta, V. 40, p. 667.

Albarede, F. and Bottinga, Y.
1972: Kinetic disequilibrium in trace element partitioning between phenocrysts and host lavas; Geochim. Cosmochim. Acta, V. 36, p. 141.

Allegre, C.J.; Tremil, M. and Minster, J.F.
1977: Systematic use of trace elements in igneous processes: 1-fractional crystallization in volcanic suites; Contr. Miner. Petr., V. 60, p. 57.

Allegre, C.J. and Minster, J.F.
1978: Quantitative models of trace element behaviour in magmatic processes; Earth Planet. Sci. Lett., V. 38, p. 1.

American Commission on Stratagraphic Nomenclature
1970: Code of stratagraphic nomenclature, Amer. Assoc. Petr. Geol.

Arth, J.G.
1976: Behaviour of trace elements during magmatic processes - a summary of the theoretical models and their applications; Jour. Res. U.S.G.S., V. 4, No. 1, p. 41.

Bailey, D.K.
1974: Continental rifting and alkaline magmatism; In: The alkaline rocks, Ed. H. Sorenson, Garden City Press, Latchworth, England, p. 148.

1975: Experimental petrology relating to oversaturated peralkaline volcanics: a review; Bull. Volc., V. 38, p. 637.

Bailey, D.K. and Macdonald, R.
1969: Alkali feldspar fractionation trends and the derivation of peralkaline liquids; Amer. J. Sci., V. 267, p. 242.

Bailey, D.K. and Schairer, J.F.
1966: The system Na_2O-Al_2O_3-Fe_2O_3-SiO_2 at one atmosphere pressure and the petrogenesis of alkaline rocks; J. Petr., V. 7, p. 114.

Baker, I.
1968: Intermediate oceanic volcanic rocks and the "Daly Gap"; Earth Planet. Sci. Lett., V. 4, p. 103.

Baker, P.E.
1975: Peralkaline acidic volcanic rocks of oceanic islands; Bull. Volc., V. 38, p. 737.

Bandurkin, G.A.
1961: Behaviour of the rare earths in fluorine bearing media; Geochemistry USSR, p. 159.

Baragar, W.R.A.
1960: Petrology of basaltic rocks in the northern part of the Labrador Trough; Bull. Geol. Soc. Amer., V. 71, p. 1589.

1967: Wakuach Lake area, Quebec-Labrador, Geol. Surv. Can. Memoir 344.

Barberi, F.; Ferrara, G.; Santacroce, M.; Treuil, M. and Varet, J.
1975a: A transitional basalt - pantellerite sequence of fractional crystallization, the Boina Centre, (Afar Rift, Ethiopia); J. Petr., V. 16, p. 22.

Barberi, F.; Santacroce, R. and Varet, J.
1975b: Silicic peralkaline volcanic rocks of the Afar Depression, Ethiopia; Bull. Volc., V. 38, p. 755.

Barton, J.M.
1975: The Mugford Group volcanics of Labrador: age, geochemistry and tectonic setting; Can. Jour. Earth Sci., V. 12, p. 1196.

Bayley, R.W. and James, H.L.
1973: Precambrian iron formations of the United States; Econ. Geol., V. 68, p. 934.

Berlin, R. and Henderson, C.M.
1969: The distribution of Sr and Ba between alkali feldspar, plagioclase and groundmass phases in porphyritic trachytes and phonolites; Geochim. Cosmochim. Acta, V. 33, p. 247.

Beukes, N.J.
1973: Precambrian iron formations of southern Africa; Econ. Geol., V. 58, p. 960.

Beus, A.A.
1958: The role of complexes in the transfer and accumulation of rare earths in endogenic solutions; Geochemistry USSR, p. 388.

Bischoff, J.L. and Dickson, F.W.
1975: Hydrothermal processes along mid-ocean ridges; Earth Planet. Sci. Lett., V. 25, p. 385.

Bowden, J. and Whitley, D.
1974: Late stage alteration of some New England Granites; Contr. Miner. Petr., V. 34, p. 117.

Bryan, W.B.
1964: Relative abundance of intermediate members of the oceanic basalt - trachyte association: evidence from Clarion and Socorro Islands, Revillogigedo Islands, Mexico; J. Geophys. Res., V. 69, p. 3047.

Bultitude, R.J. and Green, D.H.
1971: Experimental studies on crystal-liquid relationships at high pressures in olivine nephelinite and basanite compositions; J. Petr., V. 12, p. 121.

Cann, J.R.
1969: Spilites from the Carlsberg Ridge, Indian Ocean; J. Petr., V. 10, p. 1.

1970: Rb, Sr, Y, Zr, and Nb in some ocean floor basaltic rocks, Earth Planet. Sci. Lett., V. 10, p. 7.

Carmichael, I.S.E.
1964: The petrology of Thingmuli, a Tertiary volcano in eastern Iceland; J. Petr., V. 5, p. 435.

Carmichael, I.S.E., Turner, F.J. and Verhoogen, J.
1974: Igneous Petrology; International Series in the Earth and Planetary Sciences; McGraw-Hill, Montreal, 739 p.

Chauvel, J.J. and Dimroth, E.
1974: Facies types and depositional environment of the Sokoman iron formation, Central Labrador Trough, Quebec, Canada; J. Sed. Petr., V. 44, p. 299.

Chayes, F.
1966: Relative abundance of intermediate members of the oceanic basalt - trachyte association; J. Geophys. Res., V. 68, p. 1519.

Cloud, P.E.
1973: Paleoecological significance of the banded iron formations; Econ. Geol., V. 68, p. 1135.

Cohen, L.H.; Ito, K. and Kennedy, G.C.
1967: Melting and phase relations in an anhydrous basalt to 40 kilobars; Amer. J. Sci., V. 265, p. 475.

Coish, R.A.
1977: Ocean floor metamorphism in the Betts Cove Ophiolite, Newfoundland; Contr. Miner. Petr., V. 60, p. 255.

Condie, K.C.; Viljoen, M.J. and Kable, E.J.D.
1977: Effect of alteration on element distribution in the Barberton greenstone belt, South Africa; Contr. Miner, Petro., V. 64, p. 75.

Coombs, D.S.
1963: Trends and affinities of basaltic magmas and pyroxenes as illustrated by the diopside-olivine-silica diagram; Miner. Soc. Amer. spec. paper #1.

Cox, K.C.; Gass, I.G. and Mallick, D.I.J.
1969: The evolution of the volcanoes of Aden and Little Aden, South Arabia, J. Geol. Soc. Lond., V. 124, p. 283.

1970: The peralkaline volcanic suite of Aden and Little Aden, South Arabia, J. Petr., V. 11, p. 433.

Cox, K.C.; Gurney, J.J. and Harte, B.
1973: Xenoliths from the Matsuko Pipe; In: Lesotho Kimberlites, Ed. P.H. Nixon, Cape and Transvaal Printers, Cape Town, South Africa, p. 76.

Delong, S.E.
1974: Distribution of Rb, Sr and Ni in igneous rocks, central and western islands, Alaska; Geochim. Cosmochim. Acta, V. 38, p. 1107.

DeGrace, J.R.; Kean, B.F.; Hsu, E. and Green, T.
1976: Geology of the Nippers Harbour area, (2E/13), Newfoundland; Newfoundland Dept. of Mines and Energy, Mineral development division report 76-4.

DeRoever, W.P.
1942: Olivine basalts and their alkaline differentiates in the Permian of Timor; In: Geological expeditions to the Lesser Sunda Islands, N.V. Noord-Hollandsche Vitgevers M.J., Amsterdam.

Dimroth, E.
1968: The evolution of the central segment of the Labrador geosyncline, Part 1: stratigraphy, facies and paleogeography; N. Jb. Palaont. Abh., V. 132, p. 22.

1970a: The evolution of the Labrador geosyncline; Bull. Geol. Soc. Amer., V. 81, p. 2717.

1970b: Meimechites and carbonatites of the Castignon Lake Complex; N. Jb. Miner. Abh., V. 112, p. 239.

1971: The evolution of the central segment of the Labrador geosyncline, Part 2: the ophiolitic suite, N. Jb. Palaont. Abh., V. 137, p. 209.

1977: Facies models 5: Models of physical sedimentation of iron formations; Geosci. Can., V. 4, p. 23.

Dimroth, E. and Chauvel, J.J.
1973: Petrography of the Sokoman Iron Formation in the central Labrador Trough, Quebec; Bull. Geol. Soc. Amer., V. 84, p. 111.

Dimroth, E.; Baragar, W.R.A.; Bergeron, R. and Jackson, G.D.
1970: The filling of the Circum-Ungava geosyncline; In: Symposium on basins and geosynclines of the Canadian Shield, Ed. A.J. Baer, Geol. Surv. Can. paper 70-40, p. 45.

Donaldson, J.A.
1966: Marian Lake map-area, Quebec-Newfoundland; Geol. Surv. Can. Memoir 338.

Drake, M.J. and Weill, D.F.
1972: The distribution of Sr, Ba, Eu^{+2}, Eu^{+3} and other REE between plagioclase feldspar and magmatic liquid: an experimental study; Trans. Amer. Geyphys. Union, V. 53, p. 553.

Dressler, B.
1975: Lamprophyres of the north-central Labrador Trough, Quebec, Canada, N. Jb. Miner. Monats., V. 6, p. 268.

Dudas, M.J.
1971: Trace element partitioning between volcanic plagioclase and dacitic plagioclase matrix; Earth Planet. Sci. Lett., V. 11, p. 440.

Dufresne, C.
1950: The Sawyer Lake-Snelgrove Lake map-area; Unpublished private report, Labrador Mining and Exploration Company Limited, Montreal.

1952: A study of the Kaniapiskau system in the Burnt Creek-Goodwood area, New Quebec and Labrador, Newfoundland; Unpublished Ph.D. thesis, McGill University, Montreal.

Duke, J.M.
1976: Experimental determination of partition coefficients of period 4 transition elements in olivine and clinopyroxene; J. Petr., V. 17, p. 420.

Eby, G.N.
1972: Determination of rare earth, scandium and yttrium abundances in rocks and minerals by an ion exchange-X-ray fluorescence procedure; Anal. Chem., V. 44, p. 2137.

Edgar, A.D.
1974: Experimental studies in the formation of alkaline rocks; In: The alkaline rocks, Ed. H. Sorenson, Garden City Press, Letchworth, England, p. 355.

Engel, A.E.J.; Engel, C.G. and Havens, R.G.
1965: Chemical characteristics of oceanic basalts and the upper mantle; Bull. Geol. Soc. Amer., V. 76, p. 719.

Eugster, H.P.
1969: Inorganic bedded cherts from the Mogadi area, Kenya; Contr. Miner. Petr., V. 22, p. 1.

Eugster, H.P. and Chou, I.M.
1973: The depositional environments of Precambrian banded iron formations; Econ. Geol., V. 68, p. 1144.

Eugster, H.P. and Jones, B.R.
1968: Gels composed of sodium aluminum silicate, Lake Mogadi, Kenya; Science, V. 161, p. 160.

Eugster, H.P. and Surdam, R.C.
1973: The depositional environment of the Green River Formation of Wyoming; Bull. Geol. Soc. Amer., V. 84, p. 1115.

Evans, J.L.
1977: Geology of the Dyke Lake - Astray Lake area; Newfoundland Dept. of Mines and Energy open file report 78-5.

Ewart, A. and Taylor, S.R.
1969: Trace element geochemistry of the rhyolitic volcanic rocks, central North Island, New Zealand: phenocryst data; Contr. Miner. Petr., V. 22, p. 127.

Ewart, A.; Taylor, S.R. and Capp, A.C.
1968a: Geochemistry of the pantellerites of Mayor Island, New Zealand; Contr. Miner. Petr., V. 17, p. 116.

1968b: Trace and minor element geochemistry of the rhyolitic volcanic rocks, central North Island, New Zealand; Contr. Miner., Petr., V. 18, p. 76.

Fahrig, W.F.
1949: The geology of the Astray to Birch Lake area of Labrador; Unpublished private report, Iron Ore Company of Canada, Montreal.

Ferrara, G. and Treuil, M.
1975: Petrologic implications of trace element and Sr isotope distributions in basalt - pantellerite suite; Bull. Volc., V. 38, p. 548.

Floyd, P.A.
1975: Geochemical variations in the greenstones of southwest England; J. Petr., V. 17, p. 335.

1977: Rare earth element mobility and geochemical characterization of spilitic rocks, Nature, V. 269, p. 134.

Floyd, P.A. and Winchester, J.A.
1977: Magma type and tectonic setting discrimination using immobile elements; Earth Planet. Sci. Lett., V. 27, p.211.

Foland, K.A.; Quinn, A.W. and Giletti, B.J.
1971: K-Ar and Rb-Sr Triassic and Cretaceous ages for intrusives of the White Mountain magma series, northern New England; Amer. J. Sci., V. 270, p. 321.

Frarey, M.J.
1961: Menihek Lakes, Newfoundland and Quebec; Geol. Surv. Can. map 10872.

Frarey, M.J. and Duffell, S.
1964: Revised stratagraphic nomenclature for the central part of the Labrador Trough; Geol. Surv. Can. paper 64-25.

French, B.M.
1973: Mineral assemblages in diagenetic and low grade metamorphic iron formations; Econ. Geol., V. 68, p. 1063.

Frey, F.A.; Bryan, W.B. and Thompsen, G.
1974: Atlantic ocean floor: geochemistry and petrology of basalts from legs 2 and 3 of the deep sea drilling project; J. Geophys. Res., V. 79, p. 5507.

Fryer, B.J.
1972: Age determinations on the Circum-Ungava geosyncline and the evolution of Precambrian banded iron formation; Can. J. Earth Sci., V.9, p. 652.

1977a: Trace element geochemistry of the Sokoman iron formation; Can. J. Earth Sci., V. 14, p. 1598.

1977b: Rare Earth evidence in iron formation for changing Precambrian oxidation states; Geochim. Cosmochim. Acta, V. 41, p. 361.

Fryer, B.J. and Edgar, A.D.
1977: Significance of rare earth distributions in coexisting minerals of peralkaline undersaturated rocks; Contr. Miner. Petr., V. 61, p. 35.

Fujiwara, Y. and Schwarz, E.J.
1975: Paleomagnetism of the Circum-Ungava Proterozoic foldbelt, 1: Cape Smith Komatiitic basalts; Can. J. Earth Sci., V. 12, p. 1785.

Gass, I.G.
1970: Tectonic and magmatic evolution of the Afro-Arabian dome; In: African magmatism and tectonics, Ed. T.N. Clifford and I.G. Gass, Oliver and Boyd, Edinburgh, Scotland, p. 285.

Gast, P.W.
1968: Trace element fractionation and the origin of the tholeiitic and alkaline magma types; Geochim. Cosmochim. Acta, V. 32, p. 1057.

1970: Dispersed elements in oceanic volcanic rocks; Phys. Earth Planet. Inter., V. 3, p. 246.

Green, D.H.
1969: The origin of basaltic and nephelinitic magmas in the earth's mantle; Tectonophysics, V.7, p. 409.

1973: Experimental melting studies on a model upper mantle composition at high pressures under water saturated and water understaturated conditions; Earth Planet. Sci. Lett., V. 19, p. 37.

Green, D.H. and Ringwood, A.E.
1967: The genesis of basaltic magmas; Contr. Miner. Petr., V. 15, p. 103.

Greenland, L.R.
1970: An equation for trace element distribution during magmatic crystallization; Amer. Miner., V. 55, p. 455.

Gross, G.A.
1961: Metamorphism of iron formations and its bearing on their benefication; Trans. Can. Inst. Min. Metall., V. 54, No. 585, p. 30.

1968: Geology of iron deposits in Canada; Geol. Surv. Can. Economic geology report 22.

Gunn, B.M. and Roobol, M.J.
1976: Metasomatic alteration of the predominantly island arc igneous suite of the Limestone Caribbees, (East Caribbean); Geol. Rundsch., V. 65, p. 1078.

Hajash, A.
1975: Hydrothermal processes along mid-ocean ridges: an experimental investigation; Contr. Miner. Petr., V. 53, p. 205.

Hajash, A. and Scott, R.B.
1976: Hydrothermal processes in the Atlantic Ocean Crust 26°N; Int. Assoc. Hydrol. Sci., Publ. No. 119, p. 35.

Hamilton, D.L. and MacKenzie, W.S.
1965: Phase equilibria studies in the system $NaAlSiO_4$-$KAlSiO_4$-SiO_2-H_2O; Miner. Mag., V. 34, p. 214.

Hanson, G.N.
1978: The application of trace elements to the petrogenesis of igneous rocks of granitic composition; Earth Planet. Sci. Lett., V. 38, p. 26.

Harrison, J.M.
1952: The Quebec-Labrador iron belt, Quebec and Newfoundland; Geol. Surv. Can. paper 52-20.

Harrison, J.M.; Howell, J.E. and Fahrig, W.F.
1972: A geological cross-section of the Labrador geosyncline near Schefferville, Quebec; Geol. Surv. Can. paper 70-57.

Hart, R.
1970: Chemical exchange between seawater and deep ocean basalts; Earth Planet. Sci. Lett., V. 9, p. 269.

Hart, S.R.
1969: K, Rb, Cs and K/Rb, K/Cs ratios of fresh and altered submarine basalts; Earth Planet. Sci. Lett., V. 6, p. 295.

Hart, S.R.; Erlank,A.J. and Kable, E.J.O.
1974: Seafloor basalt alteration; some chemical and Sr isotope effects; Contr. Miner. Petr., V. 44, p. 219.

Haskin, L.A.; Haskin, M.A.; Frey, F.A. and Wildeman, T.R.
1968: Relative and absolute terrestial abundances of the rare earths; In: Origin and distribution of the elements, Ed. L.H. Ahrens, Pergamon Press, New York, p. 889.

Helgeson, H.C.
1964: Complexing and hydrothermal ore deposits; Pergamon Press, New York.

1969: Handbook of theoretical activity diagrams; Freeman Press, San Francisco.

Hemley, J.J.
1959: Some mineralogical equilibria in the system K_2O-Al_2O_3-SiO_2-H_2O; Amer. J. Sci., V. 257, p. 241.

Henderson, P. and Dale, I.M.
1969: The partitioning of selected transition element ions between olivine and the groundmass of oceanic basalts; Chem. Geol., V. 5, p. 267.

Herrmann, A.G. and Wedepohl, K.H.
1970: Untersuchungen on spilitschen der variskischen geosynkline in Nord west deutschland; Contr. Miner. Petr., V. 29, p. 255.

Herrmann, A.G.; Potts, M.J. and Knake, D.
1974: Geochemistry of the rare earth elements in spilites from the oceanic and continental crust; Contr. Miner. Petr., V. 44, p. 1.

Hertogen, J. and Gijbels, R.
1976: Calculation of trace element fractionation during partial melting; Geochim. Cosmochim. Acta, V. 40, p. 313.

Higuchi, H. and Nagasawa, N.
1969: Partition of trace elements between rock forming minerals and the host volcanic rocks; Earth Planet. Sci. Lett., V. 7, p. 281.

Hoffmann, P.F.
1970: The Coronation geosyncline of Aphebian age, District of Mackenzie; Geol. Surv. Can. paper 70-40.

Hughes, C.J.
1973: Spilites, keratophyres and the igneous spectrum; Geol. Mag., V. 109, p. 513.

Irvine, T.N. and Baragar, W.R.A.
1972: A guide to the chemical classification of the common volcanic rocks; Can. J. Earth Sci., V.8, p. 523.

Jakes, P. and White, A.J.R.
1970: K/Rb ratios from rocks of island arcs; Geochim. Cosmochim. Acta, V. 34, p. 849.

1972: Major and trace element abundances in volcanic rocks of orogenic areas; Bull. Geol. Soc. Amer., V.83, p. 29.

James, H.L.
1954: Sedimentary facies of iron formations: Econ. Geol., V. 49, p. 235.

Jensen, B.B.
1973: Patterns of trace element partitioning; Geochim. Cosmochim. Acta, V.37, p. 2227.

Jolly, W.T. and Smith, R.E.
1972: Degradation and metamorphic differentiation of the Keweenawan tholeiitic lavas of northern Michigan; J. Petr., V. 13, p. 273.

Kavanagh, P.M.
1952: Geology of the Point Lake area, Labrador; Unpublished private report; Iron Ore Company of Canada, Montreal.

Kay, R.W. and Gast, P.W.
1973: The rare earth content and origin of alkali rich basalts; J. Geol., V. 81, p. 653.

Kearey, P.
1977: A regional structural model of the Labrador Trough, northern Quebec, from gravity studies, and its relevance to continental collision in the Precambrian; Earth Planet. Sci. Lett., V. 28, p.371.

Klien, C.
1973: Changes in mineral assemblage with metamorphism of some banded Precambrian iron formations; Econ. Geol., V. 71, p. 1075.

Klien, C. and Fink, R.P.
1976: Petrology of the Sokoman iron formation in the Howells River area, at the western edge of the Labrador Trough; Econ. Geol., V. 71, p. 453.

1977: Petrology of the Sokoman iron formation in the Howells River area, at the western edge of the Labrador Trough: a reply; Econ. Geol., V. 72, p. 319.

Krauskopf, K.
1967: Introduction to Geochemistry, McGraw Hill Press, San Francisco.

Kuno, H.
1966: Lateral variations in basaltic magma types across continental margins and island arcs; Bull. Volc., V. 29, p. 195.

Langmuir, C.H.; Bender, J.F. and Bence, A.E.
1977: Petrogenesis of basalts from the FAMOUS area: Mid-Atlantic ridge; Earth Planet. Scit. Lett., V. 36, p. 133.

Leeman, W.P.; Ma, M.S.; Murali, A.V. and Schmitt, R.A.
1978: Empirical estimation of magnetite-liquid distribution coefficients for some transition elements; Contr. Miner. Petr., V. 65, p. 269.

Macdonald, R.
1963: Relative abundance of intermediate members of the oceanic basalttrachyte association--a discussion; J. Geophys. Res., V. 68, p. 5100.

Macdonald, R.
1975a: Nomenclature and petrochemistry of the peralkaline oversaturated extrusive rocks; Bull. Volc., V. 38, p. 498.

1975b: Tectonic settings and magma associations; Bull. Volc., V. 38, p. 575.

Macdonald, R. and Bailey, D.K.
1973: The chemistry of the peralkaline oversaturated obsidians; U.S.G.S. prof. paper 440-N-1, p. N1-N37.

Macdonald, R.; Bailey, D.K. and Sutherland, D.S.
1970: Oversaturated peralkaline glassy trachytes from Kenya; J. Petr., V. 11, p. 507.

Martin, R.F.
1975: Role of water in pantellerite genesis; Bull. Volc., V. 38, p. 666.

Martin, R.F. and Piwinskii, A.J.
1972: Magmatism and tectonic settings; J. Geophys. Res., V. 77, p. 4966.

Martin, R.F.; Whittley, J.E. and Woolley, A.R.
1978: An investigation of rare earth mobility: fenitized quartzites, Borralon Complex, N.W. Scotland; Contr. Miner. Petr., V. 66, p. 69.

Masuada, A. and Kushiro, I.
1970: Experimental determination of partition coefficients of ten rare earth elements and barium between clinopyroxene and liquid in the synthetic silicate system at 20 Kabr pressure; Contr. Miner. Petr., V. 26, p. 42.

Masuada, A.; Nakamura, N. and Tanaka, T.
1973: Fine structures of mutually normalized rare earth patterns of chondrites; Geochim. Cosmochim. Acta, V. 37, p. 239.

Maxwell, S.J.
1952: Geology of the Gaisson Lake - Bray Lake area, Labrador; Unpublished private report, Iron Ore Company of Canada, Montreal.

Meliherscik, A.
1952: Geology of the Birch Lake area, Labrador; Unpublished private report, Iron Ore Company of Canada, Montreal.

Mercy, E. and O'Hara, M.J.
1967: Distribution of Mn, Cr, Ti and Ni in coexisting minerals of ultramafic rocks; Geochim. Cosmochim. Acta, V. 31, p. 2331.

Minster, J.F.; Minster, J.B.; Trevil, M. and Allegre, C.J.
1977: Systematic use of trace elements in igneous processes: II - inverse problem of fractional crystallization processes in volcanic suites; Contr. Miner. Petr., V. 61, p. 49.

Miyashiro, A.; Shido, F. and Ewing, M.
1969: Diversity and origin of abyssal tholeiite from the Mid-Atlantic ridge near 24° and 30°N latitude; Contr. Miner. Petr., V. 23, p. 38.

Mysen, B.O.
1978: Experimental determination of nickel partition coefficients between pargasite and garnet periodotite minerals and concentration limits of behaviour according to Henry's Law at high pressures and temperatures; Amer. J. Sci., V. 278, p. 217.

Nagasawa, H.
1970: Rare earth concentrations in zircons and apatites and their dacites and granites; Earth Planet. Sci. Lett., V. 34, p. 359.

Nagasawa, H. and Schnetzler, C.C.
1971: Partition of rare earth, alkali and alkaline earths between phenocrysts and an acidic igneous magma; Geochim. Cosmochim. Acta, V. 35, p. 1566.

Noble, D.C. and Parker, D.F.
1975: Peralkaline silicic volcanic rocks of the western United States; Bull. Volc., V. 38, p. 803.

O'Hara, M.J.
1965: Primary magmas and the origin of basalts; Scott. J. Geol., V.1, p. 19.

1968: The bearing of phase equilibria studies in synthetic and natural systems on the origin and evolution of basic and ultrabasic rocks; Earth Sci. Rev., V.4, p. 69.

1970: Upper mantle composition inferred from laboratory experiments and observation of volcanic products; Phys. Earth Planet. Inter., V. 3, p. 236.

1977: Geochemical evolution during fractional crystallization of a periodically refilled magma chamber; Nature, V. 266, p. 503.

O'Hara, M.J. and Mercey, E.L. P.
1963: Petrology and petrogenesis of some garnetiferous peridotites; Trans. Roy. Soc. Edinburgh, V. 65, p. 251.

O'Hara, M.J. and Yoder, H.S. Jr.
1967: Formation and fractionation of basic magams at high pressures; Scott, J. Geol., V. 3, p. 57.

Olade, M.A.D.
1975: Trace element and isotopic data and their bearing on the genesis of Precambrian spilites from the Authapuscow aulocogen, Great Slave Lake, Canada; Geol. Mag., V. 112, p. 283.

Olade, M.A.D. and Morton, R.D.
1972: Observations on the Proterozoic Seton Formation, East Arm of Great Slave Lake, Northwest Territories; Can. J. Earth Sci., V. 9, p. 1110.

Onuma, N.; Higuchi, H. and Wakita, H.
1968: Trace element partitioning between two pyroxenes and host lava; Earth Planet. Sci. Lett., V. 5, p. 47.

Pankhurst, R.J.
1977: Open system crystal fractionation and incompatible element variation in basalts; Nature, V. 268, p. 36.

Park, C.F.
1972: The iron ore deposits of the Pacific Basin; Econ. Geol., V. 62, p. 339.

Pearce, J.A.
1974: Basalt geochemistry used to investigate past tectonic environments on Cyprus: Tectonophysics, V. 25, p. 41.

Pearce, J.A. and Cann, J.R.
1971: Ophiolite origin investigated by discriminant analyses using Ti, Zr and Y; Earth Planet. Sci. Lett., V. 12, p. 339.

1973: Tectonic setting of basic volcanic rocks determined using trace element analyses; Earth Planet. Sci. Lett., V. 19, p. 290.

Pearce, T.H. and Donaldson, J.A.
1974: Proterozoic quench textured basalts from the Labrador geosyncline; Can. J. Earth Sci., V. 11, p. 1611.

Pearce, T.H., Gorman, B.E. and Birkett, T.C.
1975: TiO_2-P_2O_5-K_2O diagram: a method of discriminating between oceanic and non-oceanic basalts; Earth Planet. Sci. Lett., V. 23, p. 419.

Perrault, G.
1952: Geology of the Dyke Lake area, Labrador; Unpublished private report, Iron Ore Company of Canada, Montreal.

Philpotts, J.A.
1972: Redox estimations from a calculation of Eu^{+2} and Eu^{+3} concentrations in natural phases; Earth Planet. Sci. Lett., V. 9, p. 257.

Philpotts, J.A. and Schnetzler, C.C.
1970: Phenocryst-matrix partition coefficients for K, Rb, Sr and Ba with applications to anorthosite and basalt genesis; Geochim. Cosmochim. Act. V. 34, p. 307.

Philpotts, J.A.; Schnetzler, C.C. and Hart, S.R.
1969: Submarine basalts: some K, Rb, Sr, Ba, REE, H_2O and CO_2 data bearing on their alteration, modification of plagioclase and possible source materials; Earth Planet. Sci. Lett., V.7, p. 293.

Rodgers, J.
1970: The tectonics of the Appalachians; Wiley Interscience, N.Y.

Rose, H.J.; Adler, I. and Flanagan, F.J.
1962: Use of La_2O_3 as a heavy absorber in the X-ray fluorescence analysis of silicate rocks; U.S.G.S. Jour. of Res., 1962, p. B80-B82.

Sauvé, P.
1953: Clastic sedimentation during a period of volcanic activity, Astray Lake, Labrador; Unpublished M.Sc. thesis, Queen's University, Kingston, Ontario.

Sawkins, F.J.
1976: Metal deposits related to intracontinental hotspot and rifting environments; J. Geol., V. 84, p. 653.

Schnetzler, C.C. and Philpotts, J.A.
1968: Partition coefficients of rare earth elements and barium between igneous matrix material and rock forming mineral phenocrysts; In: Origin and distribution of the elements, Ed. L.H. Ahrens, Pergamon Press, Oxford.

Schwarzer, R.R. and Rodgers, J.J.W.
1974: A worldwide comparison of alkali olivine basalts and their differentiation trends; Earth Planet. Sci. Lett., V. 23, p. 286.

Schwellnus, J.F.G.
1957: Ore controls in deposits of the Knob Lake area, Labrador Trough; Unpublished Ph.D. thesis, Queen's University, Kingston, Ontario.

Scott, R.B. and Hajash, A.
1976: Initial submarine alteration of basaltic pillow lavas; a microprobe study; Amer. J. Sci., V. 276, p. 480.

Shaw, D.M.
1970: Trace element fractionation during anatexis; Geochim. Cosmochim. Acta, V. 34, p. 237.

Shimizu, N.
1974: An experimental study of the partitioning of K, Rb, Cs, Sr and Ba between clinopyroxene and liquid at high pressures; Geochim. Cosmochim. Acta, V. 38, p. 789.

Shimizu, N. and Kushiro, I.
1975: The partitioning of rare earths between garnet and liquid at high pressures: preliminary results; Geophys. Res. Lett., V. 2, p. 413.

Smith, R.E.
1968: Redistribution of major elements in the alteration of some basic lavas during burial metamorphism; J. Petr., V. 9, p. 191.

Smith, R.E. and Smith, S.E.
1976: Comments on the use of Ti, Zr, Y, Nb, Sr, K, P, and Nv in the classification of basaltic magmas; Earth Planet, Sci. Lett., V. 32, p. 114.

Spooner, E.T.C.
1977: Hydrodynamic model for the origin of the ophiolitic cupriferous pyrite ore deposits of Cyprus; In: Volcanic processes in ore genesis, Special publication No. 7, Geol. Soc. Lond.

Spooner, E.T.C. and Fyfe, W.S.
1973: Sub-sea metamorphism, heat and mass transfer; Contr. Miner. Petr., V. 42, p. 287.

Stevenson, I.M.
1952: Geological report of the Dyke Lake - Petitsikapau Lake area, Labrador; Unpublished private report, Iron Ore Company of Canada, Montreal.

Stockwell, C.H.
1964: Fourth report on structural provinces, orogenies and time classification of the Canadian Shield; In: Age determinations and geological studies, Geol. Surv. Can. paper 64-17, p. 1.

Taylor, S.R.
1965: The application of trace element data to problems in petrology; In: Physics and chemistry of the earth, Ed. L.H. Ahrens, Pergamon Press, Amsterdam, p. 133.

Taylor, S.R. and Gorton, M.P.
1977: Geochemical application of spark source mass spectrography-III: element sensitivity, precision and accuracy; Geochim. Cosmochim. Acta, V.41, p. 1375.

Thomas, M.D. and Gibb, R.A.
1977: Gravity anomalies and deep structures of the Cape Smith fold belt; Northern Ungava, Quebec; Geology, V. 5, p. 169.

Thompson, G.
1973: A geochemical study of low temperature interaction of seawater and oceanic igneous rocks; EOS Amer. Geophys. Union Trans., V. 54, p. 1015.

Thompson, G.; Shido, F. and Miyashiro, A.
1972: Trace elements in fractionated oceanic basalts; Chem. Geol., V. 9, p. 89.

Trendall, A.F.
1968: Three great basins of Precambrian iron formation deposition: a systematic comparison; Bull. Geol. Soc. Amer., V. 79, p. 1527.

1972: Revolution in earth history; Bull. Geol. Soc. Amer., V. 83, p. 287.

1973a: Precambrian iron formations of Australia; Econ. Geol., V. 68, p. 1023.

1973b: Varve cycles in the Willi Wolli Formation of the Precambrian Hammersely Group, Western Australia; Econ. Geol., V. 68, p. 1089.

Turekian, K.K.
1963: The chromium and nickel distribution in basaltic rocks and eclogites; Geochim. Cosmochim. Acta, V. 27, p. 835.

Upton, B.G.J.
1974: The alkaline province of southwest Greenland; In: The alkaline rocks, Ed. H. Sorenson, J. Wiley and Sons, N.Y., p. 622.

Usher, J.L.
1953: The geology of the Astray Lake area, Labrador; Unpublished private report, Iron Ore Company of Canada, Montreal.

Vallance, T.G.
1960: Spilites and the degradation of basic volcanic rocks; Presidential address to the Linnean society of New South Wales, V. 1, p. 1.

1969: Spilites again; Linnean Society Journal, V. 1, p. 29.

1974: Spilitic degradation of a tholeiitic basalt; J. Petr., V. 15, p. 84.

Van Dorr II, J.V.
1973: Iron formations in South America; Econ. Geol., V. 68, p. 1005.

Villari, L.
1975: The Island of Pantelleria; Bull. Volc., V. 38, p. 680.

Vogel, D.E.
1975: Precambrian weathering in acid metavolcanic rocks from the Superior Province, Villebon Township, south-central Quebec; Can. J. Earth Sci., V. 12, p. 2080.

Wanless, R.K. and Loveridge, W.D.
1978: Rubidium-strontium isotopic age studies, Geol. Surv. Can. report No. 2, (Canadian Shield), p. 56.

Wardle, R.J.
1976: Geology of the Snelgrove-Andre Lake area, Labrador; In: Report of activities for 1976, Newfoundland Dept. of Mines and Energy, Mineral development division, Ed. R.V. Gibbons, report 77-1, p. 71.

Wardle, R.J. and Doherty, A.
1977: Geology of the Wade-Timmins Lake area, Labrador; In: Report of activities, Newfoundland Dept. of Mines and Energy, Mineral development division, Ed. R.V. Gibbons, report 78-1, p. 65.

Wasson, J.T.
1974: Meteorites; Springer-Verlag Press, Berlin, 317 p.

Wedepohl, K.H. (ed.)
1974: Handbook of Geochemistry; Springer-Verlag Press, Berlin.

Whalen, J.B.
1976: Geology and geochemistry of the molybdenite showings of the Ackley City Batholith, Fortune Bay, Newfoundland; Unpubl. M.Sc. thesis, Memorial University, St. John's, Nfld., 267 p.

Whittaker, R.J. and Muntus, R.
1970: Ionic radius for use in geochemistry; Geochim. Cosmochim. Acta, V. 34, p. 945.

Williams, H.; Turner, E.J. and Gilbert, C.M.
1954: Petrography - an introduction to the study of rocks in thin sections; W.H. Freeman and Company, San Francisco, 406 p.

Wilson, A.D.
1955: A new method for the determination of ferrous iron in rocks and minerals; Geol. Surv. Gr. Brit. V. 9, p. 56.

Wilson, J.L.
1975: Carbonate facies in geological history; Springer-Verlag, Berlin, 471 p.

Winchester, J.A. and Floyd, P.A.
1976: Geochemical magma type discrimination: application to altered and metamorphosed basic igneous rocks; Earth Planet. Sci. Lett., V. 28, p. 459.

1977: Geochemical discrimination of different magma series and their differentiation products using immobile elements; Chem. Geol., V. 20, p. 325.

Windley, B.F. (Ed.)
1975: The Early History of the Earth; NATO Advanced Study Institute, University of Leicester, Leicester, England.

Wood, D.A.
1976: Element mobility during zeolite facies metamorphism in the Tertiary basalts of eastern Iceland; Contr. Miner. Petr., V. 55, p. 241.

Wright, J.B.
1966: Olivine nodules in a phonolite of the east Otaga alkaline province, New Zealand; Nature, V. 210, p. 519.

1969: Olivine nodules and related inclusions in trachyte from the Jos Plateau, Nigeria; Miner. Mag., V. 31, p. 370.

Zajac, I.S.
1974: The stratigraphy and mineralogy of the Sokoman Formation in the Knob Lake area, Quebec and Newfoundland; Geol. Surv. Can. Bulletin 220.

1977: Petrology of the Sokoman Formation in the Howells area, at the western edge of the Labrador Trough: a discussion; Econ. Geol., V. 72, p. 317.

Zeilinski, R.A. and Frey, F.A.
1974: An experimental study of the partitioning of a rare earth element in the system diopside-water; Geochim. Cosmochim. Acta, V. 38, p. 545.

APPENDIX A

Sampling and Analytical Procedures

A.1 - Sample Collection and Preparation:

Specimens were collected to obtain the least altered material available while retaining a good distribution of rock types and sample locations. No attempt was made to collect the different rock types in the proportions that they are exposed in outcrop. It is the author's opinion that the inferred percentages of mafic, intermediate and acidic samples are biased towards a silica rich distribution. The locations of the samples are indicated in fig. 1 (in pocket) while the analyses are presented in Appendix B.

Approximately 1.5 Kg samples were collected at each station and stored in plastic bags. Surface weathering was cleaned off with a five pound sledge hammer before shipping. Samples were washed with water prior to the following crushing procedure.

(1) Samples were crushed to 1-2 cm chips in a Brawn steel jaw crusher or by an eight pound sledge hammer and steel plate.

(2) A representative sample of these chips was crushed in a tungsten carbide, Brawn pulverizer for three minutes producing a rock powder of -100 mesh.

A total of eighty-four whole rock chemical analyses were made during the course of this thesis and are distributed as follows.

23 - Petitsikapau Lake Formation

18 - Astray Lake Formation

23 - Associated Intrusive Rocks

Twenty other analyses were rejected because of various petrographic and geochemical factors. Any samples showing 5% H_2O, Fe_2O_3 > FeO, Na_2O+K_2O > 12.0% or erratic variations in Zr, Nb, Y or Ga concentrations, when the samples were grouped by SiO_2 abundances, were not considered due to expected large scale metasomatism. All analyses were recalculated to 100 percent anhydrous before plotting.

It should be noted that the major and trace element data, excluding the REE analyses, were independently provided for the author by the geological laboratories of Memorial University under subcontract with the Newfoundland Department of Mines and Energy. The trace element data were obtained through the standard procedure of the laboratory and are considered reliable while the major element data were part of an on-going, in-lab experiment on a new method of XRF analyses for the major oxides (D. Press, pers. comm.). As is obvious from the analyses (Appendix B), the procedure has not been perfected by the time of this study. In consideration of the metamorphism involved, the general stress on trace element geochemistry in the thesis and the time and financial constraints of the Newfoundland Department of Mines and Energy and the author,

it was decided to use them with qualification. Considering the aforementioned points on the small significance placed on the major element chemistry in the thesis and the fact that all the analyses were recalculated to 100% anhydrous before plotting and any normative recalculations, the author believes that the geochemical inaccuracy inherent in these major element analyses do not seriously jeopardize the conclusions of the thesis.

A.2 - Analytical Procedures:

A.2.1 - Major Element Analysis:

Analysis of the major elements, SiO_2, Fe_2O_3 (total), TiO_2, CaO, K_2O, MgO, Al_2O_3, Na_2O, MnO and P_2O_5 of the igneous rocks were done using a Philips 1450 X-ray fluorescence spectrometer with an Ag tube.

Pressed powder pellets of the igneous rocks were prepared by mixing a 10 g sample with 1.3 g of a standard binding agent and pressing into a disc shape at 15 tons per sq. in. for one minute.

Due to time and instrument availability factors it was found impossible to obtain precision and accuracy data on the pressed powder method of major element analysis. As a means of estimating these parameters, six samples were analyzed for major elements by the fused pellet - XRF method described by

Rose et al. (1962). Precision and accuracy data of the fused pellet-XRF method is given in Table 14, while the analyzed abundances of the six representative samples, as determined by both XRF methods, is given in Table 15. The data for Table 14 comes from the unpublished work of R.G. Jamieson.

TABLE 13

PRECISION AND ACCURACY OF FUSED PELLET
XRF METHOD - MAJOR ELEMENTS*

ELEMENT	ACCEPTED VALUE BCR - 1	$\bar{X}$+	S	STANDARD ERROR OF MEAN	RANGE LOW	RANGE HIGH
SiO_2	54.85	54.23	.15	.06	54.05	54.42
TiO_2	2.22	2.14	.01	.004	2.13	2.15
Al_2O_3	13.68	13.46	.15	.06	13.21	13.68
Fe_2O_3	13.52	13.46	.05	.02	13.41	13.56
MnO	0.19	0.17	.004	.002	0.16	0.17
MgO	3.49	3.49	.05	.02	3.44	3.60
CaO	6.98	6.99	.03	.01	6.94	7.02
Na_2O	3.29	3.29	.09	.03	3.19	3.37
K_2O	1.68	1.65	.02	.008	1.64	1.68
P_2O_5	0.33	0.34	.02	.008	0.32	0.37
Total	100.23	99.23	.12	.05	99.07	99.39

* Accepted values according to Abbey, (1974).

+ Average of seven individually fused samples.

Table 14

RELATIVE ACCURACIES OF FUSED PELLET AND PRESSED PELLET XRF METHODS

	SiO_2	TiO_2	Al_2O_3	Fe_2O_3	MgO	CaO	Na_2O	K_2O	P_2O_5	MnO
JS - 111:										
METHOD #1	67.76	0.72	16.21	1.15	0.10	0.28	1.48	11.96	0.16	0.01
METHOD #2	69.17	0.88	16.11	1.22	0.0	0.19	1.51	11.52	0.15	0.01
% DIFFERENCE	+2.1%	+22.2%	-.6%	+6.1%	-	-32.1%	+2.0%	-3.7%	-6.3%	-
JS - 204:										
METHOD #1	59.17	0.91	15.83	8.56	1.54	3.07	3.06	5.67	0.20	0.18
METHOD #2	59.29	0.96	14.84	8.43	1.47	2.93	3.50	5.68	0.08	0.19
% DIFFERENCE	+.2%	+5.5%	-6.3%	-1.5%	-4.5%	-4.6%	+14.4%	+.2%	-60%	+5.6%
JS - 253:										
METHOD #1	44.23	1.02	12.62	12.69	16.89	7.28	1.92	0.80	0.11	0.18
METHOD #2	43.08	0.90	11.08	13.50	16.44	6.08	1.39	0.82	0.09	0.23
% DIFFERENCE	+1.9%	-11.8%	-12.2%	+6.4%	-2.6%	-16.5%	-27.6%	+2.5%	-20.7%	+27.8
JS - 133:										
METHOD #1	45.74	2.16	14.22	15.57	9.20	7.74	3.59	0.45	0.25	0.24
METHOD #2	42.49	1.70	13.24	18.74	9.42	6.80	2.92	0.48	0.19	0.29
% DIFFERENCE	-7.1%	-21.3%	-6.9%	+20.4%	+2.4%	-12.1%	-18.7%	+6.7%	-24%	+20.8%
JS - 500:										
METHOD #1	77.78	0.26	11.11	2.06	0.50	0.10	3.76	4.70	0.05	0.0
METHOD #2	78.24	0.29	10.64	2.07	0.39	0.03	3.35	4.31	0.04	0.01
% DIFFERENCE	+.6%	+11.5%	-4.2%	+.5%	-22.0%	-70%	-10.9%	-8.3%	-25.0%	-

METHOD #1 - FUSED PELLET METHOD

METHOD #2 - PRESSED PELLET METHOD

In general the analyses obtained by the rapid, pressed pellet method greatly exceeds the estimated composition based on the precision and accuracy in the standardized fused pellet method. All accuracies in the fused pellet method are within 5 percent, except for MnO, while the precisions are 1 percent or less. Estimated accuracies for the pressed pellet method range from about 5 percent for SiO_2, MgO and K_2O, 10 percent for Al_2O_3, Fe_2O_3 (total), and Na_2O, and 15-20 percent for TiO_2, CaO, P_2O_5 and MnO. The error in the accuracy of the pressed pellet method increases with decreasing concentration.

A.2.2 - Ferrous Iron Analysis:

Ferrous iron, FeO, was determined by the cold dissolution method of Wilson (1955) as described in Wilson (1968). Fe_2O_3 was recalculated by the following equation:

$$Fe_2O_3 = Fe_2O_3 \text{ (total)} - 1.11 \times FeO$$

A.2.3 - Loss on Ignition:

The loss on ignition was done by observing the weight loss after heating the sample for two hours in a furnace at 1050°C.

A.3 - Non-REE Trace Element Analysis:

A total of thirteen non-lanthanide trace element abundances were obtained for each sample. The trace elements determined are as follows: V, Cr, Ni, Cu, Zn, Ga, Rb, Sr, Y, Zr, Nb, Ba and Pb. The pellets prepared for the major element data on the igneous rocks were used in the trace element XRF runs also. The standard quoted precision and accuracies for this trace element analysis method is listed in Table 16. The data comes from a compilation of standard analyses prepared by Mr. D. Press. The accuracies are within 10 percent for all elements while the precisions are highly variable largely depending on the absolute abundances.

A.4 - Rare Earth Element Analysis:

The rare earth element abundances were determined by a modified version of the Ion exchange X-ray fluorescence procedure of Eby (1972). A generalized experimental method is listed below:

(1) 1.000 $\pm$ .0001 g of the sample was weighed into a 100 ml teflon beaker, wetted with demineralized water and treated with 10 ml of 2N HCl to dissolve any carbonate.

(2) 2 ml of a Tm spike containing $\sim$ 30 gm of Tm per ml was added and then the sample was treated with two

TABLE 15

PRECISION AND ACCURACY OF PRESSED PELLET
XRF METHOD - TRACE ELEMENTS

ELEMENT	ACCEPTED VALUE* G - 2	$\overline{X}$+	σ	STANDARD ERROR OF MEAN
V	34	43	3	.949
Cr	9	13	3	.949
Ni	6	2	2	.632
Cu	11	17	1	.316
Zn	85	85	2	.632
Ga	23	24	1	.316
Rb	170	166	2	.632
Sr	480	477	7	2.214
Y	12	11	2	.632
Zr	300	292	3	.949
Nb	14	10	1	.316
Ba	1850	1865	30	9.489
Pb	29	27	2	.632

* Accepted values according to Abbey, (1974).

\+ Average of 10 individually pressed pellets.

10 ml aliquots of concentrated HF until fully decomposed.

(3) Samples were taken to dryness and successively treated with 10 ml aliquots of 6N and 2N HCl. Finally the samples were redissolved 10 ml of .2N HCl.

(4) The solutions were then quantitatively transferred to previously cleaned and pH balanced ion exchange columns filled with -100 to -200 mesh, chromatographic grade, organic resin REXYN 101 (Na) (Fisher Scientific Company listing R-181).

(5) The columns were eluted with 110 ml of 2N HCl which removes all the elements except for the REE, Ba, Hf, Zr, Y and Sc.

(6) The REE, Y, Sc and Ba were collected in teflon beakers by eluting the columns with 100 ml of 6N HCl. This solution was evaporated to dryness and later dissolved in .2N HCl.

(7) A few drops of concentrated H_2SO_4 were added to precipitate out the Ba as $BaSO_4$ which was filtered off.

(8) Reeve Angel SA-2 ion exchange papers, previously cut to fit the sample holders, were added to the solution which was gradually brought down to dryness under a low intensity heat lamp.

(9) Both sides of the ion exchange paper were then run on the XRF with the raw count data reduced to ppm output by a modified version of the correction method outlined in Eby (1972).

Only samples having a yield greater than 80 percent were accepted. The yield is calculated by comparing the analyzed Tm abundance with the theoretical limit as determined by the amount of Tm spike added. Fryer (1977b) estimated the analytical error for all elements except Yb to be less than 10 percent, with Yb having an error less than 20 percent.

The analytical values listed in Tables 5, 6 and 7 are those obtained by this method for all samples except JS-098 which was scaled by a factor representing the difference in the Y values as determined by XRF and the Y value determined by the above wet chemical method. In this case the low yield of JS-098 caused an overcorrection in the data reduction, resulting in the Y value being 1.447x too high, and as a result all REE abundances were scaled down by a factor of .691. This data reduction produces a symmetric pattern relative to that implied by the raw data but La would have a value of 1809x chondrites rather than 1250x as plotted in fig. 16 and all the other REE would be scaled up by a similar factor.

APPENDIX B

Chemical Analyses and Norms

SAMPLE	JB77 057	JS77 181	JS77 57	JS77 133	
SIO2	45.78	43.55	43.14	42.49	
TIO2	1.43	1.44	1.87	1.70	
AL2O3	13.91	11.96	12.67	13.24	
FE2O3	5.18	4.44	6.13	7.30	
FEO	10.18	9.78	11.59	10.31	
MNO	.22	.19	.23	.29	
MGO	9.93	8.36	8.46	9.42	
CAO	7.65	8.29	7.57	6.80	
NA2O	2.56	1.48	1.99	2.92	
K2O	.80	2.27	1.24	.48	
P2O5	.23	.19	.20	.19	
LOI	4.00	4.16	4.78	4.72	
TOTAL	101.87	96.11	99.87	99.86	
ZR	121	138	123	109	
SR	0641	0548	0278	0226	
RB	015	053	030	017	
ZN	113	097	114	106	
CU	062	074	117	140	
BA	0429	0481	0947	0231	
NB	12	24	18	24	
GA	021	019	016	022	
PB	005	000	000	001	
NI	119	236	060	089	
CR	034	202	011	059	
V	253	184	199	358	
Y	0026	0019	0028	0027	
QTZ					
KSPAR	4.83	14.58	7.70	22.98	
ALB	22.12	13.61	17.70	25.96	
ANOR	24.61	20.96	23.10	22.70	
NEPH					
COR					
DIOP	10.46	18.46	12.49	9.35	
HYP	11.42	8.52	12.46	5.03	
OLIV	15.56	13.39	13.00	18.99	
MAG	7.67	6.99	9.34	11.12	
ILM	2.77	2.97	3.73	3.39	
APAT	.55	.48	.49	.46	

PETITSIKAPAU LAKE FORMATION NORMAL BASIC VOLCANICS

SAMPLE	JS77 90	JB77 34	JS77 41	JB77 27	JS77 238
SIO2	43.18	44.14	44.25	46.72	49.05
TIO2	2.30	2.52	2.10	2.25	2.30
AL2O3	14.15	13.39	14.34	13.92	14.43
FE2O3	9.07	8.43	6.57	7.26	7.80
FEO	9.34	10.38	11.01	8.33	7.44
MNO	.28	.27	.21	.21	.27
MGO	8.78	6.75	5.88	5.47	6.28
CAO	6.65	3.52	4.82	5.02	5.06
NA2O	1.89	3.45	2.72	3.40	3.07
K2O	1.29	2.62	2.75	2.54	2.49
P2O5	.43	.39	.22	.22	.46
LOI	4.87	4.08	4.45	3.94	3.55
TOTAL	102.23	99.94	99.32	99.28	102.20
ZR	198	189	179	183	200
SR	0651	0114	0829	0676	0498
RB	026	058	053	059	042
ZN	185	156	115	110	142
CU	040	064	032	032	049
BA	0524	1073	1228	1259	1387
NB	23	26	27	29	25
GA	022	024	019	021	023
PB	002	003	003	000	008
NI	038	039	026	049	034
CR	031	051	005	057	027
V	294	387	220	235	326
Y	0033	0033	0029	0030	0034
QTZ					1.73
KSPAR	7.82	19.16	17.11	15.23	14.90
ALB	16.47	20.68	24.26	30.14	26.31
ANOR	27.01	14.19	19.79	15.95	18.47
NEPH					
COR		1.36			
DIOP	3.45		3.63	7.38	3.49
HYP	23.65	18.69	3.00	9.00	18.14
OLIV	2.64	7.44	15.06	5.75	
MAG	13.50	12.40	10.03	11.03	11.45
ILM	4.48	5.02	4.20	4.48	4.42
APAT	1.03	1.06	.54	.54	1.08

PETITSIKAPAU LAKE FORMATION NORMAL BASIC VOLCANICS

SAMPLE	JB77 024	JB77 029	JS77 79	JB77 20	JS77 44
SIO2	47.29	46.98	47.02	46.40	46.96
TIO2	2.49	2.07	2.08	2.20	2.36
AL2O3	14.13	15.50	16.66	14.02	15.86
FE2O3	4.62	5.68	4.16	6.88	6.29
FEO	9.93	10.63	9.75	9.02	8.96
MNO	.21	.21	.16	.23	.18
MGO	4.87	2.99	3.82	5.32	8.45
CAO	5.41	2.09	4.41	5.04	3.88
NA2O	2.96	2.99	3.18	2.60	4.46
K2O	2.95	4.19	3.51	2.90	2.13
P2O5	.25	.24	.32	.28	.26
LOI	3.80	3.85	3.85	4.43	4.25
TOTAL	98.91	97.42	98.92	99.32	104.04
ZR	187	170	166	185	193
SR	0722	0223	0469	0905	0733
RB	046	072	064	061	047
ZN	097	128	109	107	105
CU	020	032	046	041	039
BA	1842	1818	1212	2682	1428
NB	28	30	21	28	32
GA	017	024	023	021	022
PB	000	000	001	001	005
NI	013	024	031	033	038
CR	012	006	030	018	032
V	219	220	274	215	271
Y	0029	0024	0027	0026	0028
QTZ					
KSPAR	18.30	26.44	21.80	18.03	12.60
ALB	26.30	27.01	28.23	23.14	31.49
ANOR	17.38	9.88	21.23	18.96	16.98
NEPH					3.40
COR		2.83	.24		
DIOP	8.02			5.13	.90
HYP	10.13	19.39	3.78	18.25	
OLIV	7.26	.86	13.40	.92	20.39
MAG	7.03	8.79	6.34	10.49	9.13
ILM	4.97	4.20	4.15	4.40	4.49
APAT	.61	.60	.78	.68	.60

PETITSIKAPAU LAKE FORMATION NORMAL BASIC VOLCANICS

SAMPLE	JS77 045	JS77 85	JB77 40	JS77 62	JS77 517
SIO2	47.16	48.31	50.26	47.84	48.35
TIO2	2.35	2.69	2.05	4.26	2.14
AL2O3	14.57	13.14	16.68	13.71	13.62
FE2O3	4.33	7.60	6.43	3.11	7.35
FEO	9.00	7.33	6.60	9.58	7.68
MNO	.20	.30	.22	.18	.22
MGO	3.44	6.88	3.35	8.63	3.66
CAO	4.40	7.37	4.60	5.84	5.00
NA2O	2.96	2.72	4.56	4.36	3.16
K2O	3.56	2.50	2.50	1.20	3.39
P2O5	.22	.39	.41	.34	.54
LOI	3.69	3.11	3.32	3.96	3.54
TOTAL	95.88	102.34	100.98	103.01	98.65
ZR	182	161	206	235	257
SR	0615	0487	0460	0271	0758
RB	065	062	058	020	064
ZN	095	124	113	087	136
CU	030	072	043	052	034
BA	1741	2564	1202	0000	2069
NB	30	32	23	34	36
GA	020	024	020	026	022
PB	006	008	000	000	003
NI	023	043	014	092	020
CR	007	042	020	138	006
V	228	418	245	444	190
Y	0027	0033	0032	0040	0041
QTZ		.16			2.01
KSPAR	22.79	14.87	15.11	7.16	20.97
ALB	27.13	23.16	39.47	35.73	27.98
ANOR	17.29	16.36	18.07	14.43	13.57
NEPH				.81	
COR					
DIOP	4.49	14.72	2.39	10.20	8.76
HYP	12.80	13.58	8.25		10.03
OLIV	3.30		2.21	18.14	
MAG	6.80	11.09	9.54	4.55	11.15
ILM	4.84	5.14	3.98	8.16	5.05
APAT	.55	.91	.97	.80	1.07

SAMPLE	JS77 46				
SIO2	50.68				
TIO2	2.05				
AL2O3	14.67				
FE2O3	6.26				
FEO	6.97				
MNO	.22				
MGO	2.91				
CAO	4.24				
NA2O	2.99				
K2O	4.58				
P2O5	.75				
LOI	3.39				
TOTAL	99.71				
ZR	291				
SR	0757				
RB	089				
ZN	125				
CU	029				
BA	1762				
NB	42				
GA	018				
PB	016				
NI	010				
CR	000				
V	117				
Y	0045				
QTZ	2.96				
KSPAR	28.06				
ALB	26.23				
ANOR	13.56				
NEPH					
COR					
DIOP	3.13				
HYP	10.81				
OLIV					
MAG	9.41				
ILM	4.04				
APAT	1.81				

PETITSIKAPAU LAKE FORMATION INTERMEDIATE VOLCANICS

SAMPLE	JS77 104				
SIO2	54.56				
TIO2	1.13				
AL2O3	15.34				
FE2O3	3.25				
FEO	6.70				
MNO	.16				
MGO	.50				
CAO	1.37				
NA2O	3.32				
K2O	7.14				
P2O5	.21				
LOI	2.99				
TOTAL	96.67				
ZR	0276				
SR	0076				
RB	0152				
ZN	0193				
CU	0021				
BA	0948				
NB	30				
GA	0030				
PB	0011				
NI	0007				
CR	0004				
V	0028				
Y	0053				
QTZ	1.14				
KSPAR	45.02				
ALB	29.97				
ANOR	6.03				
NEPH					
COR	.08				
DIOP					
HYP	9.92				
OLIV					
MAG	5.03				
ILM	2.29				
APAT	.52				

PETITSIKAPAU LAKE FORMATION ACIDIC VOLCANICS

SAMPLE	JS 111	JS77 98			
SIO2	69.17	67.90			
TIO2	.88	.51			
AL2O3	16.11	13.88			
FE2O3	.20	1.65			
FEO	.92	2.12			
MNO	.01	.03			
MGO		.70			
CAO	.19	.24			
NA2O	1.51	4.51			
K2O	11.52	5.12			
P2O5	.15	.05			
LOI	.72	1.05			
TOTAL	101.38	97.76			
ZR	502	927			
SR	0039	0788			
RB	205	135			
ZN	023	040			
CU	008	011			
BA	1133	0658			
NB	46	114			
GA	015	027			
PB	004	013			
NI	004	010			
CR	008	009			
V	021	020			
Y	0042	0127			
QTZ	16.05	20.35			
KSPAR	67.60	31.26			
ALB	12.69	39.43			
ANOR	.21	1.29			
NEPH					
COR	1.07	.48			
DIOP					
HYP	.09	3.60			
OLIV					
MAG	.29	2.47			
ILM	1.66	1.00			
APAT	.35	.12			

ASTRAY LAKE FORMATION DEPLETED BASIC VOLCANICS

SAMPLE	JB77 079	JS77 31			
SIO2	45.86	45.07			
TIO2	1.52	1.53			
AL2O3	13.87	14.06			
FE2O3	3.92	4.89			
FEO	9.72	10.06			
MNO	.20	.20			
MGO	6.65	5.48			
CAO	7.05	6.57			
NA2O	2.92	2.27			
K2O	1.44	2.42			
P2O5	.28	.23			
LOI	3.61	3.70			
TOTAL	97.04	96.48			
ZR	117	125			
SR	0619	0695			
RB	038	058			
ZN	104	114			
CU	048	042			
BA	0791	1920			
NB	13	17			
GA	023	025			
PB	000	000			
NI	066	059			
CR	044	041			
V	258	239			
Y	0024	0023			
QTZ					
KSPAR	9.10	15.39			
ALB	26.42	20.67			
ANOR	21.91	22.69			
NEPH					
COR					
DIOP	11.43	9.48			
HYP	9.94	12.89			
OLIV	11.34	2.59			
MAG	6.08	7.63			
ILM	3.09	3.13			
APAT	.70	.58			

ASTRAY LAKE FORMATION NORMAL BASIC VOLCANICS

SAMPLE	JS77 15	JB77 9	JS77 205	JS77 213	JS77 34
SIO2	48.20	47.71	47.18	46.19	43.97
TIO2	2.44	2.57	2.51	2.07	2.55
AL2O3	12.74	16.16	13.25	16.70	13.60
FE2O3	6.05	7.11	7.45	8.29	8.26
FEO	10.29	8.06	8.90	10.33	12.22
MNO	.27	.12	.22	.17	.23
MGO	5.55	2.09	5.67	4.09	6.44
CAO	6.42	4.55	6.02	2.74	3.26
NA2O	2.82	2.77	2.98	2.66	2.36
K2O	2.14	4.85	2.58	3.31	3.13
P2O5	.52	.28	.59	.36	.44
LOI	4.17	5.49	3.41	4.70	4.62
TOTAL	101.61	101.76	100.76	101.61	101.08
ZR	181	192	190	180	0198
SR	0412	0281	0396	0217	0249
RB	047	110	039	086	0046
ZN	137	080	126	120	0151
CU	025	036	033	025	0028
BA	0955	1148	1174	0970	1467
NB	22	34	23	33	24
GA	025	020	022	021	0022
PB	009	010	001	006	0001
NI	017	022	021	021	0017
CR	028	003	016	004	0019
V	313	241	329	226	0366
Y	0032	0028	0039	0028	0033
QTZ	1.01			2.95	
KSPAR	12.97	29.75	15.65	20.17	19.16
ALB	24.47	24.33	25.88	23.21	20.68
ANOR	16.19	18.00	15.56	11.89	14.19
NEPH					
COR				4.66	1.35
DIOP	10.95	3.21	9.33		
HYP	19.43	6.50	15.14	19.80	18.68
OLIV		1.77	1.06		7.44
MAG	8.99	10.70	11.09	12.39	12.40
ILM	4.75	5.07	4.89	4.05	5.02
APAT	1.24	.68	1.41	.86	1.06

ASTRAY LAKE FORMATION NORMAL BASIC VOLCANICS

SAMPLE	JS77 193				
SIO2	43.66				
TIO2	2.68				
AL2O3	13.93				
FE2O3	8.13				
FEO	13.19				
MNO	.21				
MGO	7.05				
CAO	3.17				
NA2O	2.85				
K2O	2.25				
P2O5	.45				
LOI	4.94				
TOTAL	102.51				
ZR	198				
SR	0180				
RB	034				
ZN	137				
CU	020				
BA	0860				
NB	24				
GA	025				
PB	007				
NI	020				
CR	022				
V	396				
Y	0037				
QTZ					
KSPAR	13.62				
ALB	24.70				
ANOR	13.36				
NEPH					
COR	2.01				
DIOP					
HYP	17.24				
OLIV	10.64				
MAG	12.07				
ILM	5.21				
APAT	1.07				

ASTRAY LAKE FORMATION DEPLETED INTERMEDIATE VOLCANICS

SAMPLE	JS77 032	JS77 33			
SIO2	56.86	57.73			
TIO2	.88	.97			
AL2O3	14.44	14.67			
FE2O3	3.27	2.97			
FEO	5.14	5.43			
MNO	.21	.21			
MGO	1.45	.91			
CAO	3.39	3.60			
NA2O	4.48	3.14			
K2O	4.83	6.05			
P2O5	.19	.18			
LOI	1.89	1.94			
TOTAL	97.03	97.80			
ZR	210	208			
SR	0225	0383			
RB	068	083			
ZN	091	099			
CU	023	021			
BA	1215	2196			
NB	25	25			
GA	021	023			
PB	005	005			
NI	012	012			
CR	014	007			
V	078	073			
Y	0030	0033			
QTZ	3.20	6.89			
KSPAR	29.98	37.25			
ALB	39.82	27.68			
ANOR	5.28	8.40			
NEPH					
COR					
DIOP	9.60	8.20			
HYP	4.92	4.74			
OLIV					
MAG	4.98	4.49			
ILM	1.76	1.92			
APAT	.46	.44			

ASTRAY LAKE FORMATION NORMAL INTERMEDIATE VOLCANICS

SAMPLE	JS 505	JS77 206	JS77 208		
SIO2	60.58	57.79	53.01		
TIO2	.80	1.03	1.12		
AL2O3	15.12	16.15	17.24		
FE2O3	1.89	2.29	3.27		
FEO	4.63	4.78	7.73		
MNO	.05	.12	.11		
MGO			.91		
CAO	.74	1.17	.06		
NA2O	1.79	2.33	4.98		
K2O	9.68	10.31	5.77		
P2O5	.19	.17	.16		
LOI	1.76	2.18	2.66		
TOTAL	97.23	98.32	97.02		
ZR	220	223	242		
SR	0045	0067	0106		
RB	141	136	070		
ZN	117	104	094		
CU	016	013	020		
BA	1173	1166	0831		
NB	31	31	35		
GA	025	026	029		
PB	002	003	000		
NI	013	008	006		
CR	007	013	010		
V	048	057	079		
Y	0040	0036	0031		
QTZ	9.79	.58			
KSPAR	59.89	63.34	36.17		
ALB	15.86	20.50	42.11		
ANOR	2.82	3.28	.39		
NEPH			1.41		
COR	.74		28.30		
DIOP		1.67			
HYP	5.98	4.73			
OLIV			9.75		
MAG	2.87	3.45	5.03		
ILM	1.59	2.03	2.26		
APAT	.46	.41	.05		

ASTRAY LAKE FORMATION ENRICHED INTERMEDIATE VOLCANICS

SAMPLE	JS77 204				
SIO2	59.29				
TIO2	.96				
AL2O3	14.84				
FE2O3	4.05				
FEO	3.95				
MNO	.19				
MGO	1.47				
CAO	2.93				
NA2O	3.50				
K2O	5.68				
P2O5	.08				
LOI	2.54				
TOTAL	99.48				
ZR	293				
SR	0241				
RB	068				
ZN	098				
CU	022				
BA	1713				
NB	37				
GA	022				
PB	007				
NI	007				
CR	014				
V	075				
Y	0034				
QTZ	9.34				
KSPAR	34.56				
ALB	30.49				
ANOR	8.24				
NEPH					
COR					
DIOP	4.88				
HYP	4.79				
OLIV					
MAG	6.05				
ILM	1.88				
APAT	.43				

ASTRAY LAKE FORMATION ACIDIC VOLCANICS

SAMPLE	JS77 500	JS77 501	JS77 502	JS77 503	
SIO2	78.24	77.53	74.87	78.21	
TIO2	.29	.28	.29	.29	
AL2O3	10.64	10.51	10.99	10.87	
FE2O3	1.06	1.51	1.09	1.53	
FEO	.91	.37	1.34	.65	
MNO	.01	.01	.01	.01	
MGO	.39	.43	.43	.41	
CAO	.03	.04	.09	.03	
NA2O	3.35	3.30	2.84	3.12	
K2O	4.31	4.37	5.23	4.81	
P2O5	.04	.05	.03	.03	
LOI	.40	.31	.60	.33	
TOTAL	99.67	98.71	97.81	100.29	
ZR	866	874	869	856	
SR	0015	0016	0033	0017	
RB	208	205	099	201	
ZN	027	070	032	031	
CU	006	010	013	008	
BA	0091	0056	0493	0120	
NB	97	95	94	96	
GA	031	029	027	031	
PB	005	006	012	005	
NI	013	014	010	015	
CR	003	003	007	003	
V	012	009	021	018	
Y	0137	0162	0136	0172	
QTZ	41.86	41.68	38.09	41.06	
KSPAR	25.66	26.24	31.13	28.44	
ALB	28.55	28.38	24.72	26.41	
ANOR			.37		
NEPH					
COR	.50	.40	.54	.54	
DIOP					
HYP	1.32	1.09	2.23	1.02	
OLIV					
MAG	1.55	.42	1.63	1.29	
ILM	.55	.54	.51	.55	
APAT	.09	.12	.07	.07	

SAMPLE	JS77 59	JS 048	JS77 095	JS77 464	
SIO2	42.63	44.72	45.37	61.26	
TIO2	1.28	2.14	1.76	1.02	
AL2O3	14.60	12.53	13.30	15.57	
FE2O3	6.22	6.89	7.09	2.01	
FEO	10.35	11.10	9.21	3.99	
MNO	.22	.32	.26	.04	
MGO	10.64	3.25	6.32	.48	
CAO	4.67	4.70	8.73	.89	
NA2O	3.01	3.91	3.09	3.59	
K2O	.80	4.22	1.10	6.95	
P2O5	.13	1.30	.24	.25	
LOI	5.27	2.25	3.53	1.77	
TOTAL	99.82	97.33	100.00	97.82	
ZR	130	375	163	510	
SR	0894	1734	0422	0072	
RB	027	149	027	163	
ZN	094	129	111	077	
CU	047	035	128	009	
BA	1526	1430	0326	0789	
NB	18	89	30	66	
GA	016	017	020	027	
PB	000	008	010	000	
NI	060	029	050	007	
CR	011	008	024	000	
V	199	107	368	040	
Y	0025	0036	0033	0051	
QTZ				10.33	
KSPAR	4.99	26.17	6.73	42.74	
ALB	26.90	23.67	27.09	31.61	
ANOR	24.21	4.38	19.86	3.10	
NEPH		5.99			
COR	.40			1.09	
DIOP		10.18	19.16		
HYP	5.58		3.21	5.47	
OLIV	25.50	11.68	9.25		
MAG	9.53	10.48	10.65	3.03	
ILM	2.57	4.27	3.46	2.02	
APAT	.32	3.17	.58	.60	

INTRUSIVE ROCKS EVANS LAKE PLUTON

SAMPLE	JS77 260	JS77 256	JS77 261	JS77 257	JS77 250
SIO2	43.52	44.37	44.68	43.84	44.16
TIO2	1.68	1.26	1.19	.94	.98
AL2O3	12.67	12.45	14.10	13.55	14.59
FE2O3	5.28	3.57	3.69	3.91	3.82
FEO	10.06	9.40	7.99	8.09	8.51
MNO	.22	.21	.19	.19	.19
MGO	10.75	8.52	6.24	8.66	7.44
CAO	9.05	8.45	10.67	8.20	8.24
NA2O	2.13	1.32	2.04	1.87	2.04
K2O	.48	1.71	.74	1.22	1.45
P2O5	.22	.13	.12	.10	.10
LOI	4.73	4.26	4.24	4.78	4.40
TOTAL	100.79	95.65	95.89	95.35	95.92
ZR	0160	093	094	096	094
SR	0424	0374	0408	0527	0608
RB	0023	032	023	031	030
ZN	0102	083	077	071	075
CU	0104	067	095	050	070
BA	0378	0969	0268	0498	0365
NB	32	15	15	15	14
GA	0021	021	019	016	018
PB	0001	003	001	000	000
NI	0201	198	097	182	139
CR	0199	512	220	422	298
V	0235	219	220	182	198
Y	0018	0016	0021	0017	0020
QTZ					
KSPAR	2.95	11.04	4.77	7.95	9.35
ALB	18.75	12.20	18.82	17.45	18.84
ANOR	24.54	25.12	29.58	27.54	28.77
NEPH					
COR					
DIOP	16.86	16.35	22.42	13.67	12.55
HYP	7.17	20.21	12.74	14.88	10.77
OLIV	17.87	6.35	3.02	9.94	11.30
MAG	7.96	5.65	5.83	6.25	6.05
ILM	3.32	2.61	2.46	1.97	2.03
APAT	3.53	.33	.30	.26	.25

INTRUSIVE ROCKS EVANS LAKE PLUTON

SAMPLE	JS77 253	JS77 221	JS77 219	JS77 255	
SIO2	43.08	46.08	45.74	47.26	
TIO2	.90	1.04	1.32	1.04	
AL2O3	11.08	14.40	12.76	14.47	
FE2O3	4.58	2.74	3.55	4.03	
FEO	8.72	8.48	9.02	6.59	
MNO	.23	.18	.30	.17	
MGO	16.44	6.47	6.27	7.36	
CAO	6.08	10.01	6.84	11.18	
NA2O	1.39	2.64	2.06	2.49	
K2O	.82	.59	2.47	.61	
P2O5	.09	.11	.13	.11	
LOI	5.61	4.30	3.83	4.14	
TOTAL	99.02	97.04	94.29	99.45	
ZR	070	0102	092	087	
SR	0204	0509	0511	0400	
RB	028	0016	067	014	
ZN	076	0073	076	063	
CU	049	0065	105	068	
BA	0213	0213	1274	0362	
NB	14	16	11	14	
GA	015	0018	016	017	
PB	000	0000	000	000	
NI	364	0081	085	107	
CR	912	0308	222	371	
V	179	0208	309	218	
Y	0019	0020	0022	0018	
QTZ					
KSPAR	5.18	3.76	16.11	3.78	
ALB	12.57	24.06	19.24	22.09	
ANOR	23.06	27.69	20.18	27.78	
NEPH					
COR					
DIOP	6.92	20.70	13.80	24.00	
HYP	19.34	8.96	16.76	9.86	
OLIV	23.58	8.08	5.07	3.95	
MAG	7.10	4.28	5.68	6.12	
ILM	1.83	2.13	2.27	2.07	
APAT	.22	.28	.33	.27	

INTRUSIVE ROCKS TYRA LAKE PLUTON

SAMPLE	JS77 166	JS77 171	JS77 170	JS77 162	
SIO2	43.08	43.58	47.38	50.32	
TIO2	2.57	2.53	2.39	1.57	
AL2O3	14.49	14.94	13.50	13.62	
FE2O3	5.01	4.95	4.31	4.74	
FEO	12.87	11.90	11.14	7.89	
MNO	.20	.20	.23	.19	
MGO	3.94	3.30	3.84	2.14	
CAO	4.65	5.03	5.58	7.75	
NA2O	2.63	2.76	3.82	4.37	
K2O	4.22	4.19	2.58	2.21	
P2O5	.25	.26	.51	.58	
LOI	3.35	4.73	3.56	2.83	
TOTAL	97.26	98.37	98.84	98.21	
ZR	183	192	340	369	
SR	0531	0650	0269	0478	
RB	130	135	042	022	
ZN	096	095	105	083	
CU	085	093	080	079	
BA	0646	0842	1361	0796	
NB	37	32	66	66	
GA	019	021	019	015	
PB	004	000	017	012	
NI	027	021	001	000	
CR	000	000	000	001	
V	259	257	092	059	
Y	0022	0023	0044	0042	
QTZ					
KSPAR	26.54	26.42	15.99	13.68	
ALB	15.42	16.68	33.89	38.74	
ANOR	16.25	17.07	12.66	11.55	
NEPH	4.48	4.46			
COR					
DIOP	5.80	6.87	11.12	21.11	
HYP			.23	1.71	
OLIV	17.98	15.06	13.55	1.48	
MAG	7.73	7.66	6.55	7.20	
ILM	5.19	5.13	4.76	3.12	
APAT	.68	.64	1.24	1.41	

INTRUSIVE ROCKS DYKE LAKE PLUTON

SAMPLE	JS 004	JS77 5			
SIO2	47.28	46.43			
TIO2	.97	1.07			
AL2O3	16.83	13.84			
FE2O3	2.81	4.62			
FEO	7.57	8.67			
MNO	.17	.19			
MGO	5.02	6.72			
CAO	7.28	8.98			
NA2O	3.12	1.88			
K2O	1.25	1.29			
P2O5	.25	.24			
LOI	3.41	3.25			
TOTAL	95.96	97.18			
ZR	101	0102			
SR	0637	0562			
RB	035	0022			
ZN	071	0103			
CU	059	0054			
BA	0652	0718			
NB	10	19			
GA	023	0022			
PB	000	0000			
NI	093	0081			
CR	042	0059			
V	183	0211			
Y	0024	0016			
QTZ		.86			
KSPAR	7.97	8.11			
ALB	28.50	16.92			
ANOR	30.47	27.14			
NEPH					
COR					
DIOP	5.86	15.45			
HYP	15.89	21.63			
OLIV	4.27				
MAG	4.40	7.13			
ILM	1.99	2.16			
APAT	.63	.59			

INTRUSIVE ROCKS EILLEEN LAKE PLUTON

SAMPLE	JS 292	JS77 20			
SIO2	44.99	44.65			
TIO2	1.60	1.43			
AL2O3	14.67	15.68			
FE2O3	5.57	5.91			
FEO	9.03	8.57			
MNO	.19	.20			
MGO	8.11	7.58			
CAO	4.68	5.93			
NA2O	4.09	3.85			
K2O	1.22	1.01			
P2O5	.25	.26			
LOI	4.30	4.38			
TOTAL	98.70	99.45			
ZR	149	211			
SR	0483	0670			
RB	014	019			
ZN	081	073			
CU	079	061			
BA	0686	0563			
NB	27	36			
GA	016	020			
PB	000	001			
NI	045	044			
CR	000	003			
V	118	121			
Y	0021	0026			
QTZ					
KSPAR	7.63	6.27			
ALB	34.87	32.40			
ANOR	19.13	23.67			
NEPH		1.00			
COR					
DIOP	3.27	4.71			
HYP					
OLIV	21.76	19.45			
MAG	8.55	9.01			
ILM	3.22	2.85			
APAT	.62	.64			

INTRUSIVE ROCKS ASTRAY LAKE PLUTON

SAMPLE	JS77 366				
SIO2	47.41				
TIO2	.94				
AL2O3	13.31				
FE2O3	3.21				
FEO	6.60				
MNO	.19				
MGO	5.67				
CAO	10.29				
NA2O	2.59				
K2O	.83				
P2O5	.14				
LOI	3.42				
TOTAL	94.60				
ZR	084				
SR	0420				
RB	015				
ZN	057				
CU	080				
BA	0390				
NB	10				
GA	016				
PB	002				
NI	106				
CR	299				
V	224				
Y	0017				
QTZ	1.41				
KSPAR	5.37				
ALB	24.01				
ANOR	24.37				
NEPH					
COR					
DIOP	25.05				
HYP	12.30				
OLIV					
MAG	5.10				
ILM	1.96				
APAT	.36				

INTRUSIVE ROCKS MARBLE LAKE PLUTON

SAMPLE	JS 382				
SIO2	48.98				
TIO2	1.77				
AL2O3	13.50				
FE2O3	3.82				
FEO	9.67				
MNO	.38				
MGO	6.17				
CAO	5.94				
NA2O	3.15				
K2O	2.33				
P2O5	.29				
LOI	3.64				
TOTAL	99.64				
ZR	126				
SR	0237				
RB	038				
ZN	072				
CU	047				
BA	0924				
NB	14				
GA	020				
PB	004				
NI	067				
CR	160				
V	332				
Y	0028				
QTZ					
KSPAR	14.33				
ALB	27.74				
ANOR	16.46				
NEPH					
COR					
DIOP	10.29				
HYP	13.99				
OLIV	7.19				
MAG	5.76				
ILM	3.50				
APAT	.70				

APPENDIX C

Commented Computer Program - STEM

```
C THIS PROGRAM IS DESIGNED TO MODEL TRACE ELEMENT BEHAVIOUR THROUGH MOST
C NORMAL IGNEOUS GEOLOGIC PROCESSES.  THE PROGRAM NAME IS 'STEM', OR SYS
C TEM FOR TRACE ELEMENT MODELLING.  PRESENTLY THE PROGRAM IS CAPABLE OF
C MODELLING A TOTAL OF 27 ELEMENTS AND 14 MINERALS THROUGH THE
C FOLLOWING PROCESSES: FRACTIONAL CRYSTALLISATION,(BOTH IN SURFACE
C AND TOTAL EQUILIBRIUM CONDITIONS), OHARA TYPE FRACTIONAL CRYSTALLISATI
C ON, BATCH PARTIAL MELTING, FRACTIONAL PARTIAL MELTING AND DYNAMIC
C PARTIAL MELTING.  THIS PROGRAM WAS PREPARED FOR THE COURSE GEOLOGY
C 6900 AND IS THE PROPERTY OF THE GEOLOGY DEPARTMENT OF
C MEMORIAL UNIVERSITY AND THE DEVELOPER, JIM EVANS.
C
C
C NOTE THAT ALL LINE NUMBERS REFERRED TO IN THE COMMENTS ARE RELATIVE
C TO THE SEQUENTIAL LINE NUMBERS ON THE PRINTOUT OF THE PROGRAM IN
C THE ACCOMPANYING REPORT.
C
C
C ALL ARRAY NAMES ARE ADEQUATELY EXPLAINED IN THE ACCOMPANYING TEXT.
      COMPLEX*16 KDGF(17)
      REAL  SORCE2(27),MODE(27,6),RESID(27),CHOND(27,2)
      REAL BKDX(27), KD(27,14,9),SORCE1(14),BKD(27),P(27)
      INTEGER ELEM(27),ELEMX(27),MINER(14),MINERX(14)
      INTEGER CONT1,CONT2,CONT3,CONT4,MF
      INTEGER CONT5,CONT6,CONT7,CONT8
      INTEGER CONT9,CONT10,CONT11,CONT12,CONT13
      DATA DATA1/06./,DATA2/09./,DATA3/11./,DATA4/12./
C
C LINES 30-39 READ IN THE ALPHABETIC HEADINGS, CHONDRITIC VALUES, ETC.
C
      READ(5,2)  (MINER(I),I=1,14)
    2 FORMAT(14(1X,A4))
      READ(5,3)  (ELEM(I),I=1,27)
    3 FORMAT(23(1X,A2),1X,2A2,2(1X,A2))
      READ(5,10)  (KDGP(I),I=1,17)
   10 FORMAT (2A8,64X)
      READ(5,1)  (CHOND(I,1),I=1,27)
    1 FORMAT  (8(1X,F8.3),8X)
      READ(5,4)  (((KD(I,J,K),I=1,27),J=1,14),K=1,9)
    4 FORMAT(17X,9F7.3)
C
C CONT 1-4 ARE CONTROL VARIABLES EXPLAINED IN THE TEXT.
C
      READ(5,5)CONT1,CONT2,CONT3,CONT4
    5 FORMAT  (5(1X,I2))
C
C LINES 48-54 READ IN THE SOURCE DATA FOR MODELLING.
C
      READ(5,6)  (MINERX(I),I=1,CONT1)
    6 FORMAT(26(I2,1X),I2)
      READ(5,6)  (ELEMX(I),I=1,CONT2)
      READ(5,9)  (SORCE1(I),I=1,CONT1)
```

```
    9  FORMAT( 7(1X,F5.2))
       READ(5,18) (SORCE2(J),J=1,CONT2)
   18  FORMAT (8(1X,F8.2),8X)
C
C LINE 59 IS THE MAIN BRANCH FOR FRACTIONAL CRYSTALLISATION OR PARTIAL
C MELTING. THE LATTER CONTINUES ON BELOW.
C
       IF (CONT4.EQ.13) GO TO 1000
C
C LINES 63-67 READ IN CONTROL VARIABLES FOR THE PARTIAL MELTING PROCESS.
C
       READ(5,5)CONT5,CONT6,CONT7,CONT8
       READ(5,8)  ((MODE(I,J),J=1,2),I=1,CONT8)
    8  FORMAT(7(F3.0,1X,F5.2,1X),10X)
       READ(5,7)  IBATCH,IDYNAM,DYNAMX
    7  FORMAT(2(I2,1X),F3.2,71X)
C
C LINES 72-83 INITIALIZE ALL VARIABLES AND CALCULATE THE BKD AND P TERMS
C SCREENING ALL KD TERMS FOR THE DUMMY 99.999 TERM.
C
       X=0.0
       RMFX=0.0
       DO 601 I=1,CONT2
       MODE(I,3)=0.0
       BKD(I)=0.0
       P(I)=0.0
       DO 602 J=1,CONT1
        IF ((KD(ELEMX(I),MINERX(J),CONT3)).EQ.99.999) GO TO 602
       BKD(I)=BKD(I)+ (SORCE1(J)/100.0*KD(ELEMX(I),MINERX(J),CONT3))
       P(I)=P(I)+(MODE(J,2)/100.0*KD(ELEMX(I),MINERX(J),CONT3))
  602  CONTINUE
  601  CONTINUE
C
C LINE 87 SETS UP THE MAJOR LOOP GOVERNING THE NUMBER OF REITERATIONS
C
       DO 200 MF=CONT5,CONT6,CONT7
       IF (X.EQ.1.0) GO TO 223
       CALL HEAD(MINER,MINERX,ELEM,ELEMX,KD,SORCE1,SORCE2,CONT1,
      $CONT2,CONT3 ,MODE,KDGP,BKD,CONT4,CHOND,P)
C
C SUBROUTINE HEAD ENABLES THE PRINTING OF THE KD, BKD AND SOURCE VALUES.
C THIS IS FOUND ON THE FIRST PAGE OF EACH PRINTOUT OF A SEPERATE CYCLE.
C
  223  RMF=MF/100.0
       IF(RMFX.EQ.RMF) GO TO 200
       IF (X.EQ.1.0)CALL HEAD(MINER,MINERX,ELEM,ELEMX,KD,SORCE1,
      $SORCE2,CONT1,CONT2,CONT3,MODE,KDGP,BKD,CONT4,CHOND,P)
       X=0.0
       RMP=RMF
C
C LINES 109-121 IS A SEQUENCE THAT CHECKS TO SEE IF THE MODEL
C CALL FOR A GREATER AMOUNT OF A CERTAIN MINERAL THAN IS IN THE SOURCE.
```

```
C IS SPECIFICALLY CHECKED IN LINE 55.  IF THAT EQUATION IS EQUAL TO OR
C GREATER THAN 0.0 THE TERM RMF WILL BE REDEFINED TO ITS MAXIMUM
C POSSIBLE VALUE.  EXECUTION WILL CONTINUE WITH THIS VALUE AND CONTROL
C WILL BE SENT OFF TO THE RECALC SUBROUTINE AT THE END OF THE CYCLE.
C
      DO 204 K=1,CONT1
      IF(MODE(K,2).EQ.0.0) GO TO 323
      IF (RMF-(SORCE1(K)/MODE(K,2)))323,220,220
  220 IF(RMP.LT.SORCE1(K)/MODE(K,2)) GO TO 323
      RMP=SORCE1(K)/MODE(K,2)
      K2=K
      X=1.0
  323 IF (K.LT.CONT1) GOTO 204
      IF(X.EQ.0.0) GO TO 204
      IF(RMFX-RMP) 31,32,33
   31 RMF=RMP
      RMFX=RMP
  204 CONTINUE
C
C LINES 128-141 ARE DESIGNED TO GIVE THE USER SOME IDEA OF
C HOW HIS/HER DATA INPUT EXCEEDED THE BOUNDS OF THE EQUATIONS AND HOW
C IT MIGHT BE CORRECTED.
C
      GO TO 36
   32 WRITE(6,34)
   34 FORMAT('1',/////////////,20X,' EQUATIONS ARE BOMBING OUT AFTER TH
     $E RECALCULATION EXERCIZE AS TWO PHASES ARE TOTALLY USED UP AT',/,2
     $0X,' THE SAME DEGREE OF PARTIAL MELTING.',/,20X,' SUGGEST SLIGHT A
     $LTERATION OF SOURCE OR MODE VALUES.')
      GO TO 3007
   33 WRITE(6,35)
   35 FORMAT('1',//////////,20X,' EQUATIONS ARE BOMBING OUT AFTER THE RE
     $CALCULATION EXERCIZE AS THE RECALCULATED  VALUES CALL FOR A SMALLE
     $R',/,20X,' DEGREE OF PARTIAL MELTING OR FRACTIONAL CRYSTALLIZATION
     $ THAN THE ORIGINAL VALUES.',/,20X,          ' SUGGEST ALTERATION SU
     $CH THAT NOT AS MANY MODE MINERAL VALUES ARE HIGHER THAN THE SOURCE
     $ VALUES.')
      GO TO 3007
C
C LINE 145 INITIATES THE LOOP THAT TREATS EACH ELEMENT SEPERATELY.
C
   36 DO 201 I=1,CONT2
      IF (MODE(I,3).LT.0.0) GO TO 201
      MODE(I,6)=MODE(I,3)
C
C LINES 152-153 CHECKS IF THE BOUNDARY VALUES HAVE BEEN RECALCULATED
C PREVIOUSLY AS THEY ARE TREATED BY DIFFERENT EQUATIONS IF THEY WERE.
C
      IF(RMFX.EQ.0.0) GO TO 231
      IF(RMFX-RMF) 206,231,231
C
C THE COMPLEX EQUATIONS FOR RECALCULATED DATA FOLLOWS.
```

```
C
 206  IF (IBATCH.EQ.14) GO TO 230
C
C LINE 161 TRANSFERS TO BATCH OR FRACTIONAL MELTING EQUATIONS.
C
      IF(RMFX.GT.RMF) GO TO 33
      MODE(I,3)=((SORCE2(I)*(1-(MODE(I,4)*RMFX/SORCE2(I))))/((1-RMFX)*
     $BKDX(I)))*((1-((P(I)*(RMF-RMFX))/(BKDX(I)*(1-RMFX))))**((1/P(I))-1
     $))
      MODE(I,5)=(SORCE2(I)/RMF)*((1-(1-MODE(I,4)*RMFX/SORCE2(I)))*((1-((
     $P(I)*(RMF-RMFX))/(BKD(I)*(1-RMFX))))**(1/P(I))))
      GO TO 232
 230  MODE(I,3)=SORCE2(I)/(BKDX(I)+(RMF*(1-P(I))+(RMFX*(P(I)-BKDX(I)))))
C
C LINES 173-198 IS THE PETROCHEMICAL SUBTRACTION SUBROUTINE DESIGNED FOR
C ELEMENTS K AND ZR.
C
 232  IF (ELEMX(I)-22)237,607,237
 237  IF (ELEMX(I)-12)207,607,207
 607  DO 605 II=1,CONT1
      IF(ELEMX(I).EQ.22) GO TO 606
      IF(MODE(II,1)-9)608,609,610
 608  IF(MODE(II,1).EQ.DATA1)MODE(I,3)=MODE(I,3)+(RMF*MODE(II,2)*1103.0)
      IF(MODE(I,3).GT.0.0) GO TO 605
      WRITE(6,122)ELEM(ELEMX(I))
      GO TO 605
 609  IF(MODE(II,1).EQ.DATA2)MODE(I,3)=MODE(I,3)+(RMF*MODE(II,2)*937.0)
      IF(MODE(I,3).GT.0.0) GO TO 605
      WRITE(6,122)ELEM(ELEMX(I))
      GO TO 605
 610  IF(MODE(II,1).EQ.DATA4)MODE(I,3)=MODE(I,3)+(RMF*MODE(II,2)*1119.0)
      IF(MODE(I,3).GT.0.0) GO TO 605
      WRITE(6,122)ELEM(ELEMX(I))
      GO TO 605
 606  IF(MODE(II,1).EQ.DATA3)MODE(I,3)=MODE(I,3)+(RMF*MODE(II,2)*4459.0)
      IF(MODE(I,3).GT.0.0) GO TO 605
      WRITE(6,122)ELEM(ELEMX(I))
      GO TO 605
 122  FORMAT('1',///////,10X,'THE ELEMENT',1X,A4,'HAS BEEN RECALCULATED
     $TO LESS THAN ZERO BY THE SUBTRACTION PROGRAM.  DISREGARD FURTHER U
     $SE OF THIS ELEMENT.')
 605  CONTINUE
      GO TO 207
C
C THIS IS WHERE THE EQUATIONS FOR UNRECALCULATED DATA BEGINS.
C
 231  IF (IBATCH.EQ.14) GO TO 234
      MODE(I,3)=(SORCE2(I)/BKD(I))*((1-(P(I)*RMF/BKD(I)))**((1/P(I))-1))
      MODE(I,5)=(SORCE2(I)/RMF)*(1-((1-(P(I)*RMF/BKD(I)))**(1/P(I))))
      GO TO 233
 234   MODE(I,3)=SORCE2(I)/(BKD(I)+RMF*(1-P(I)))
 233  IF (ELEMX(I)-22)227,607,227
```

```
 227  IF (ELEMX(I)-12) 207,607,207
C
C LINE 212 ACCESSES THE OPTIONAL DYNAMIC OPTION MODELLING EQUATION.
C
 207  IF (IDYNAM.EQ.16) GO TO 247
      IF (MF.EQ.CONT5) GO TO 247
      MODE(I,3)=MODE(I,3)*(1.0/(1.0+DYNAMX))+MODE(I,6)*(DYNAMX/(
     $1.0+DYNAMX))
 247  RESID(I)=(SORCE2(I)/(1-    RMF))*(1-(MODE(I,3)*    RMF/SORCE2(I)))
C
C LINE 220 RESETS THE SORCE1 ARRAY IF FRACTIONAL MELTING IS USED.
C
      IF (IBATCH.EQ.15) SORCE2(I)=RESID(I)
 201  CONTINUE
      RMFP=RMF*100.0
      WRITE(6,62) RMFP,KDGP(CONT3)
  62  FORMAT('1',      //,10X,                    'TRACE ELEMENT CONCENTRATION
     $S OF A ',1X,F5.2,1X,' % PARTIAL MELT OF THE FOLLOWING MODE USING',
     $1X,2A8,1X,'KD VALUES IS:')
      WRITE(6,63) KDGP(IBATCH),KDGP(IDYNAM),DYNAMX
  63  FORMAT(' ', 5X,2A8,'MELTING EQUATIONS WERE USED WITH THE',2A8,'OPT
     $ION WHICH INVOLVED',1X,F3.2,1X,       'WT. FRAC. OF LIQUID RETAINED
     $.')
      CALL RESULT (MINER,ELEM,MODE,CONT2,CONT8,RESID,ELEMX,CHOND,IBATCH)
C
C SUBROUTINE RESULT PRINTS THE RESULTS FOR MODE(I,3)
C MODE(I,5) AND RSEID(I).  THE PRINTOUT IS ON THE SECOND PAGE OF EACH
C PRINTOUT CYCLE.
C
      IF(RMFX-RMF) 202,208,202
C
C LINE 237 CHECKS TO SEE IF THE RECALC SUBROUTINE SHOULD BE CALLED.
C
  208 CALL RECALC (MINER,MINERX,ELEM,ELEMX,KD,SORCE1,SORCE2,
     $CONT1,CONT2,CONT3,MODE,RMF,K2,KDGP,BKD,P,CONT4,BKDX)
C
C SUBROUTINE RECALC WILL RECALCULATE THE MODE(I,2) AND SORCE1(I) TERMS
C WHEN ACCESSED FROM THIS POINT.
C
      IF (CONT3.EQ.30) GO TO 3007
C
C CONT3 =30 SIGNALS THAT THE SORCE1 HAS BEEN RECALCULATED TO A MONO -
C MINERALIC STATE.  EXECUTION WILL CEASE AT THIS POINT.
C
      GO TO 223
 202  IF (IBATCH.EQ.14) GO TO 200
      IF ((RMFX-RMF).EQ.0.0) GO TO 200
C
C CONTROL IS SENT OFF TO RECALC IF FRACTIONAL MELTING IS USED BUT IF IT
C ACCESSED FROM HERE THE MODE(I,2) TERM WILL NOT BE RESET.  K2 IS SET TO
C TO SIGNAL THAT IT IS COMING FROM THIS STATEMENT.
C
```

```
      K2=14
      CALL RECALC (MINER,MINERX,ELEM,ELEMX,KD,SORCE1,SORCE2,
     $CONT1,CONT2,CONT3,MODE,RMF,K2,KDGP,BKD,P,CONT4,BKDX)
 200  CONTINUE
      GO TO 3007
C
C THIS IS WHERE THE CALCULATIONS FOR FRACTIONAL CRYSTALLISATION START.
C
C LINES 271-277 READ IN THE CONTROL VARIABLES FOR THE FRACTIONAL CRYSTAL
C MODELLING AND INITIALIZE ALL VARIABLES.
C
 1000 XXXTAL=0.0
      IBATCH=14
      X=0.0
      READ(5,5)CONT9,CONT10,CONT11,CONT12,CONT13
      READ(5,8) ((MODE(I,J),J=1,2),I=1,CONT13)
      READ(5,1001)ICHARA,JOHARA,OHARAX,OHARAY
 1001 FORMAT(2(I2,1X),2(F3.2,1X),66X)
C
C LINES 282-286 GOVERN THE BRANCHING TO THE CHARA TYPE FRACTIONAL
C CRYSTALLISATION MODELLING SUBROUTINE.
C
      IF(IOHARA.EQ.0) GO TO 5005
      CALL OHARA (MINER,MINERX,ELEM,ELEMX,KD,SORCE1,SORCE2,CONT1,CONT2,
     $CONT3,CONT4,MODE,KDGP,BKD,CHOND,P,CONT20,RESID,IBATCH,
     $OHARAX,OHARAY,JOHARA )
      GO TO 3007
C
C LINES 290-299 INITIALIZE VARIABLES AND CALCULATE THE BKD TERMS.
C
 5005 DO 5003 I=1,CONT2
      MODE(I,3)=0.0
      MODE(I,4)=0.0
      BKD(I)=0.0
      P(I)=0.0
      DO 5004 J=1,CONT1
       IF ((KD(ELEMX(I),MINERX(J),CONT3)).EQ.99.999) GO TO 5004
      BKD(I)=BKD(I)+((MODE(J,2)/100.0)*KD(ELEMX(I),MINERX(J),CONT3))
 5004 CONTINUE
 5003 CONTINUE
C
C LINE 303 SETS UP THE LOOP GOVERNING THE NUMBER OF FRACTIONATION CYCLES
C
      DO 3002 IXTAL=CONT9,CONT10,CONT11
      IF (X.EQ.1.0) GO TO 3010
      CALL HEAD(MINER,MINERX,ELEM,ELEMX,KD,SORCE1,SORCE2,CONT1,
     $CONT2,CONT3,MODE,KDGP,BKD,CONT4,CHOND,P)
 3010 RIXTAL=IXTAL/100.0
      IF(XXXTAL.EQ.RIXTAL) GO TO 3002
      IF (X.EQ.1.0)CALL HEAD(MINER,MINERX,ELEM,ELEMX,KD,SORCE1,
     $SORCE2,CONT1,CONT2,CONT3,MODE,KDGP,BKD,CONT4,CHOND,P)
C
```

```
C LINES 312-329 CHECK IF THE EQUATIONS HAVE BEEN EXCEEDED, SIMILAR
C TO THAT DESCRIBED IN THE PARTIAL MELTING SECTION.
C
      X=0.0
      RIPTAL=RIXTAL
      DO 3004 K=1,CONT1
      IF(MODE(K,2).EQ.0.0) GO TO 3001
      IF(RIXTAL*MODE(K,2)-SORCE1(K))3001,3006,3006
 3006 IF((SORCE1(K)/MODE(K,2)).GT.RIPTAL) GO TO 3001
      RIPTAL=SORCE1(K)/MODE(K,2)
      K2=K
      X=1.0
 3001 IF(K.LT.CONT1) GO TO 3004
      IF(X.EQ.0.0) GO TO 3004
      IF(XXXTAL-RIPTAL)3011,32,33
 3011 RIXTAL=RIPTAL
      XXXTAL=RIXTAL
 3004 CONTINUE
C
C LINE 333 INITIATES THE LOOP TO TREAT EACH ELEMENT SEPERATELY.
C
      DO 1209 I=1,CONT2
      IF (MODE(I,3).LT.0.0) GO TO 1209
C
C LINE 339 DIRECTS THE CONTROL DEPENDING ON WHETHER SURFACE OR TOTAL
C EQUILIBRIUM IS DESIRED.  SUFACE EQUILIBRIUM EQUATIONS FOLLOW.
C
      IF(CONT12.EQ.10) GO TO 3008
      IBATCH=15
      MODE(I,3)=SORCE2(I)*((1.00-RIXTAL)**(BKD(I)-1.00))
C
C LINE 345 ACCESSES THE EQUATION GOVERNING RECALCULATED DATA PROBLEMS.
C
      IF(MODE(I,4).EQ.0.0) GO TO 3020
      MODE(I,3)=((RIXTAL-XXXTAL)/RIXTAL)*MODE(I,3)+MODE(I,4)*(XXXTAL/
     $RIXTAL)
C
C LINE 351-352 ACCESS THE PETROCHEMICAL SUBTRACTION SUBROUTINE.
C
 3020  IF (ELEMX(I)-22)1208,1607,1208
 1208 IF (ELEMX(I)-12)1207,1607,1207
 1207 RESID(I)=SORCE2(I)*(1-((1-RIXTAL)**(BKD(I))))/RIXTAL
      MODE(I,5)=BKD(I)*SORCE2(I)*((1-RIXTAL)**(BKD(I)-1))
      GO TO 1209
C
C LINES 357-384 ARE THE PETROCHEMICAL SUBTRACTION PROGRAM FOR FRACTIONAL
C CRYSTALLISATION PROBLEMS.
C
 1607 DO 1605 II=1,CONT1
      IF (ELEMX(I).EQ.22) GO TO 1606
      IF (MODE(II,1)-9)1601,1602,1603
 1601 IF(MODE(II,1).EQ.DATA1)MODE(I,3)=MODE(I,3)-(RIXTAL*MODE(II,2)*
```

```
     $1103.0)
      IF(MODE(I,3).GT.0.0) GO TO 1605
      WRITE(6,122) ELEM(ELEMX(I))
      GO TO 1605
 1602 IF(MODE(II,1).EQ.DATA2) MODE(I,3)=MODE(I,3)-(RIXTAL*MODE(II,2)*
     $937.0)
      IF(MODE(I,3).GT.0.0) GO TO 1605
      WRITE(6,122) ELEM(ELEMX(I))
      GO TO 1605
 1603 IF(MODE(II,1).EQ.DATA4) MODE(I,3)=MODE(I,3)-(RIXTAL*MODE(II,2)*
     $1119.0)
      IF(MODE(I,3).GT.0.0) GO TO 1605
      WRITE(6,122) ELEM(ELEMX(I))
      GO TO 1605
 1606 IF(MODE(II,1).EQ.DATA3) MODE(I,3)=MODE(I,3)-(RIXTAL*MODE(II,2)*
     $4459.0)
      IF(MODE(I,3).GT.0.0) GO TO 1605
      WRITE(6,122) ELEM(ELEMX(I))
 1605 CONTINUE
      IF (CONT12.EQ.11) GO TO 1207
      GO TO 1210
C
C EQUATIONS FOR TOTAL EQUILIBRIUM FRACTIONAL CRYSTALLISATION FOLLOW.
C
 3008 MODE(I,3)=SORCE2(I)/((1.00-RIXTAL)+(BKD(I)*RIXTAL))
      IF(MODE(I,4).EQ.0.0) GO TO 3021
      MODE(I,3)=((RIXTAL-XXXTAL)/RIXTAL)*MODE(I,3)+MODE(I,4)*(XXXTAL/
     $RIXTAL)
 3021 IF (ELEMX(I)-22) 1218,1607,1218
 1218 IF (ELEMX(I)-12) 1210,1607,1210
 1210 RESID(I)=BKD(I)*SORCE2(I)/(1-(1-BKD(I))*RIXTAL)
 1209 CONTINUE
      PIXTAL=RIXTAL*100.0
      WRITE(6,3009) PIXTAL,KDGP(CONT3),KDGP(CONT12)
 3009 FORMAT('1',     //,10X,'THE CALCULATED TRACE ELEMENT CONCENTRATIONS
     $ OF ',1X,F5.2,1X,'% FRACTIONATION OF THE FOLLOWING MODE WITH',1X,
     $2A8,1X,/,10X,' KD VALUES AND',1X,2A8,1X,'CONDITIONS ARE:')
      CALL RESULT (MINER,ELEM,MODE,CONT2,CONT1,RESID,ELEMX,CHOND,IBATCH)
      IF (X.EQ.0.0) GO TO 3002
      CALL RECALC (MINER,MINERX,ELEM,ELEMX,KD,SORCE1,SORCE2,
     $CONT1,CONT2,CONT3,MODE,RIXTAL,K2,KDGP,BKD,P,CONT4,BKDX)
      IF (CONT3.EQ.30) GO TO 3007
      GO TO 3010
 3002 CONTINUE
 3007 CONTINUE
      WRITE(6,3005)
 3005 FORMAT('1',/////////////,50X,' END OF EXECUTION.',/,10X' PROGRAM B
     $Y:',/,21X,' JAMES L. EVANS',/,21X,' DEPT. OF GEOLOGY',/,21X,' MEMO
     $RIAL UNIVERSITY',/,21X,' ST. JOHNS, NFLD.',/,21X,' FEB. 14, 1978')
      STOP
      END
      SUBROUTINE HEAD (MINER,MINERX,ELEM,ELEMX,KD,SORCE1,SORCE2,
```

```
     $CONT1,CONT2,CONT3,MODE,KDGP,BKD,CONT4,CHCND,P)
C
C SUBROUTINE HEAD IS ONLY A FORMATTED PRINTING EXERCIZE AND NEEDS NO EXP
C
      COMPLEX*16 KDGP(17)
      REAL KD(27,14,9),SORCE1(14),SORCE2(27),MODE(27,6),BKD(27)
      REAL CHOND(27,2),P(27)
      INTEGER ELEM(27),ELEMX(27),MINER(14),MINERX(14)
      INTEGER CONT1,CONT2,CONT3,CONT4
      DO 100 I=1,CONT2
 100  CHOND(I,2)=SORCE2(I)/CHOND(ELEMX(I),1)
      WRITE(6,50)KDGP(CONT4)
  50  FORMAT('1',/,20X,'CALCULATION OF TRACE ELEMENT',1X,2A8,1X,'MODEL',
     $/,35X,'***EVANS-1978***')
      WRITE(6,51)KDGP(CONT3)
  51  FORMAT(' ', //,10X,'INDIVIDUAL AND CALCULATED BULK KD VALUES USING
     $' ,1X,2A8,1X,'KD VALUES:',//)
      WRITE(6,52) (MINER(MINERX(I)),I=1,CONT1)
  52  FORMAT(' ',2X,'ELEM',5X,'P',6X,'BULK',2X,14(2X,A4,2X))
      DO 101 I=1,CONT2
      WRITE(6,53)ELEM(ELEMX(I)),P(I),BKD(I),(KD(ELEMX(I),MINERX(J),
     $CONT3),J=1,CONT1)
  53  FORMAT(' ',3X,A2,3X,16(F7.3,1X))
 101  CONTINUE
      WRITE(6,56)
  56  FORMAT(' ', //,10X,'SOURCE MODAL COMPOSITION:',//)
      WRITE(6,57) (MINER(MINERX(I)),I=1,CONT1)
  57  FORMAT(' ',10X,14(2X,A4,2X))
      WRITE(6,58) (SORCE1(I),I=1,CONT1)
  58  FORMAT(' ',/,10X,14(2X,F5.2,1X))
      WRITE(6,59)
  59  FORMAT(' ', //,10X,'SOURCE TRACE ELEMENT ABUNDANCES AND CHONDRITIC
     $ RATIOS:',//)
      IF(CONT2-10)90,90,91
  91  IXX=10
      WRITE(6,60) (ELEM(ELEMX(I)),I=1,IXX)
      WRITE (6,61) (SORCE2(I),I=1,IXX)
      WRITE (6,62) (CHOND(I,2),I=1,IXX)
      IF(CONT2-20)92,92,93
  93  IXX=20
      WRITE(6,60) (ELEM(ELEMX(I)),I=11,IXX)
      WRITE(6,61) (SORCE2(I),I=11,IXX)
      WRITE(6,62) (CHOND(I,2),I=11,IXX)
      WRITE(6,60) (ELEM(ELEMX(I)),I=21,CONT2)
      WRITE (6,61) (SORCE2(I),I=21,CONT2)
      WRITE (6,62) (CHOND(I,2),I=21,CONT2)
      GO TO 94
  92  WRITE(6,60) (ELEM(ELEMX(I)),I=11,CONT2)
      WRITE (6,61) (SORCE2(I),I=11,CONT2)
      WRITE (6,62) (CHOND(I,2),I=11,CONT2)
      GO TO 94
  90  WRITE(6,60) (ELEM(ELEMX(I)),I=1,CONT2)
```

```
      WRITE (6,61)  (SORCE2(I),I=1,CONT2)
      WRITE (6,62)  (CHOND(I,2),I=1,CONT2)
   94 CONTINUE
   60 FORMAT(' ',10X,10(4X,A2,4X))
   61 FORMAT(' ',1X,'ABUNDANCE',10(1X,F8.2,1X))
   62 FORMAT(' ',1X,'RATIO',4X,10(1X,F8.2,1X),/)
      RETURN
      END
      SUBROUTINE RESULT (MINER,ELEM,MODE,CONT2,CONT20,RESID,ELEMX,CHOND,
     $IBATCH)
C
C SUBROUTINE RESULT IS FORMATTED PRINTING ROUTINE
C
      REAL MODE(27,6),RESID(27),CHOND(27,2)
      INTEGER MINER(14),ELEM(27),CONT2,CONT20,ELEMX(27)
      DO 100 I=1,CONT2
  100 CHOND(I,2)=MODE(I,3)/CHOND(ELEMX(I),1)
      WRITE(6,63)(MINER(MODE(I,1)),I=1,CONT20)
   63 FORMAT(' ',/,10X,'MODE:',/,10X,14(2X,A4,2X))
      WRITE(6,64)(MODE(I,2),I=1,CONT20)
   64 FORMAT(' ',//,10X,14(1X,F6.2,1X))
      WRITE(6,65)
   65 FORMAT(' ',//,10X,'PARTIAL MELT OR FRACTIONATED LIQUID ELEMENT CON
     $CENTRATIONS AND CHONDRITIC RATIOS:',//)
      IF(CONT2-10)90,90,91
   91 IXX=10
      WRITE(6,60)(ELEM( ELEMX(I)),I=1,IXX)
      WRITE (6,61)  (MODE(I,3),I=1,IXX)
      WRITE (6,62)  (CHOND(I,2),I=1,IXX)
      IF(CONT2-20)92,92,93
   93 IXX=20
      WRITE(6,60)(ELEM( ELEMX(I)),I=11,IXX)
      WRITE(6,61)  (MODE(I,3),I=11,IXX)
      WRITE(6,62)  (CHOND(I,2),I=11,IXX)
      WRITE(6,60)(ELEM( ELEMX(I)),I=21,CONT2)
      WRITE (6,61)  (MODE(I,3),I=21,CONT2)
      WRITE (6,62)  (CHOND(I,2),I=21,CONT2)
      GO TO 94
   92 WRITE(6,60)(ELEM( ELEMX(I)),I=11,CONT2)
      WRITE (6,61)  (MODE(I,3),I=11,CONT2)
      WRITE (6,62)  (CHOND(I,2),I=11,CONT2)
      GO TO 94
   90 WRITE(6,60)(ELEM( ELEMX(I)),I=1,CONT2)
      WRITE (6,61)  (MODE(I,3),I=1,CONT2)
      WRITE (6,62)  (CHOND(I,2),I=1,CONT2)
   94 CONTINUE
   60 FORMAT(' ',10X,10(4X,A2,4X))
   61 FORMAT(' ',1X,'ABUNDANCE',10(1X,F8.2,1X))
   62 FORMAT(' ',1X,'RATIO',4X,10(1X,F8.2,1X),/)
      IF (IBATCH.EQ.14) GO TO 101
C
C THE VALUE OF IBATCH CHECKS TO SEE IF RESULTS ARE STORED IN MODE(I,5).
```

```
C
      DO 102 I=1,CONT2
 102  CHOND(I,2)=MODE(I,5)/CHOND(ELEMX(I),1)
      WRITE(6,103)
 103  FORMAT(' ', //,10X,'THE AGGREGRATE LIQUID OR INSTANTANEOUS CUMULAT
     $E CONCENTRATIONS AND CHONDRITIC RATIOS ARE:',/)
      IF(CONT2-10)80,80,81
  81  IXX=10
      WRITE(6,60)(ELEM( ELEMX(I)),I=1,IXX)
      WRITE (6,61) (MODE(I,5),I=1,IXX)
      WRITE (6,62) (CHOND(I,2),I=1,IXX)
      IF(CONT2-20)82,82,83
  83  IXX=20
      WRITE(6,60)(ELEM( ELEMX(I)),I=11,IXX)
      WRITE(6,61) (MODE(I,5),I=11,IXX)
      WRITE(6,62) (CHOND(I,2),I=11,IXX)
      WRITE(6,60)(ELEM( ELEMX(I)),I=21,CONT2)
      WRITE (6,61) (MODE(I,5),I=21,CONT2)
      WRITE (6,62) (CHOND(I,2),I=21,CONT2)
      GO TO 84
  82  WRITE(6,60)(ELEM( ELEMX(I)),I=11,CONT2)
      WRITE (6,61) (MODE(I,5),I=11,CONT2)
      WRITE (6,62) (CHOND(I,2),I=11,CONT2)
      GO TO 84
  80  WRITE(6,60)(ELEM( ELEMX(I)),I=1,CONT2)
      WRITE (6,61) (MODE(I,5),I=1,CONT2)
      WRITE (6,62) (CHOND(I,2),I=1,CONT2)
  84  CONTINUE
 101  WRITE(6,68)
  68  FORMAT(' ', //,10X,'THE RESIDUAL OR AGGREGRATE CUMULATE CONCENTRAT
     $IONS AND CHONDRITIC RATIOS ARE:',/)
      DO 110 I=1,CONT2
 110  CHOND(I,2)=RESID(I)/CHOND(ELEMX(I),1)
      IF(CONT2-10)95,95,96
  96  IXX=10
      WRITE(6,60)(ELEM( ELEMX(I)),I=1,IXX)
      WRITE (6,61) ( RESID(I),I=1,IXX)
      WRITE (6,62) (CHOND(I,2),I=1,IXX)
      IF(CONT2-20)97,97,98
  98  IXX=20
      WRITE(6,60)(ELEM( ELEMX(I)),I=11,IXX)
      WRITE(6,61) (RESID(I),I=11,IXX)
      WRITE(6,62) (CHOND(I,2),I=11,IXX)
      WRITE(6,60)(ELEM( ELEMX(I)),I=21,CONT2)
      WRITE (6,61) ( RESID(I),I=21,CONT2)
      WRITE (6,62) (CHOND(I,2),I=21,CONT2)
      GO TO 99
  97  WRITE(6,60)(ELEM( ELEMX(I)),I=11,CONT2)
      WRITE (6,61) ( RESID(I),I=11,CONT2)
      WRITE (6,62) (CHOND(I,2),I=11,CONT2)
      GO TO 99
  95  WRITE(6,60)(ELEM( ELEMX(I)),I=1,CONT2)
```

```
      WRITE (6,61)  ( RESID(I),I=1,CONT2)
      WRITE (6,62)  (CHOND(I,2),I=1,CONT2)
   99 CONTINUE
      RETURN
      END
      SUBROUTINE RECALC (MINER,MINERX,ELEM,ELEMX,KD,SORCE1,SORCE2,
     $CONT1,CONT2,CONT3,MODE,RMF,K,KDGP,BKD,P,CONT4,BKDX)
C
C SUBROUTINE RECALC IS A SUBROUTINE DESIGNED TO RECALCULATE MODE(I,2),
C SORCE1 AND BKD ARRAYS. THE LOGIC OF THE PROGRAM IS VERY SIMPLE AND THE
C EQUATIONS ARE GIVEN IN THE REPORT.
C
      COMPLEX*16 KDGP(17)
      REAL KD(27,14,9),SORCE1(14),SORCE2(27),MODE(27,6)
      REAL BKD(27),P(27),BKDX(27)
      INTEGER ELEM(27),ELEMX(27),MINER(14),MINERX(14)
      INTEGER CONT1,CONT2,CONT3,CONT4
      IF (K.EQ.14) GO TO 71
      IF(MODE(K,2).LT.100.00) GO TO 69
      WRITE(6,68)
   68 FORMAT('1',//////////,50X,' END OF EXECUTION',/,20X,  ' ALL MINERA
     $LS USED IN THE MODE HAVE BEEN USED UP IN THE SOURCE.')
      CONT3=30
      GO TO 94
   69 IF (CONT4.EQ.13) GO TO 70
      DO 603 I=1,CONT2
      BKDX(I)=BKD(I)
  603 MODE(I,4)=MODE(I,5)
   70 XI=0.0
      ABD=MODE(K,2)
      DO 205 L=1,CONT1
      SORCE1(L)=(SORCE1(L)-(RMF*MODE(L,2)))
      XI=XI+SORCE1(L)
      MODE(L,2)=MODE(L,2)*100.0/(100.0-ABD)
  205 CONTINUE
      MODE(K,2)=0.0
      SORCE1(K)=0.0
      DO 206 L=1,CONT1
      SORCE1(L)=((SORCE1(L)/XI)*100.0)
  206 CONTINUE
   74 DO 601 I=1,CONT2
      IF (CONT4.EQ.13) MODE(I,4)=MODE(I,3)
C
C MODE(I,4) IS TREATED DIFFERENTLY IN PARTIAL MELTING AND FRACTIONAL
C CRYSTALLISATION PROBLEMS BECAUSE OF THE DIFFERENT WAYS IT IS USED
C IN THE EQUATIONS.
C
      BKD(I)=0.0
      P(I)=0.0
      DO 602 J=1,CONT1
       IF ((KD(ELEMX(I),MINERX(J),CONT3)).EQ.99.999) GO TO 602
      BKD(I)=BKD(I)+ (SORCE1(J)/100.0*KD(ELEMX(I),MINERX(J),CONT3))
```

```
      IF (CONT4.EQ.12)P(I)=P(I)+(MODE(J,2)/100.0*KD(ELEMX(I),MINERX(J),
     $CONT3))
  602 CONTINUE
  601 CONTINUE
      IF (K.EQ.14) GO TO 94
      RMFP=RMF*100.0
      WRITE(6,67)MINER(MINERX(K)),RMFP,KDGP(CONT4)
   67 FORMAT('1',//////////,10X,'*****************************************
     $*************************************************************
     $',/,20X,'THE PHASE',1X,A4,1X,'HAS BEEN USED UP AT' ,1X,F5.2,1X    ,
     $'PERCENT ',1X,2A8,1X,'.  THE FOLLOWING ARE THE KD VALUES',/,20X   ,
     $' AND RECALCULATED SOURCE, MODE AND TRACE ELEMENT ABUNDANCES.'/,20
     $X,' EXECUTION WILL CONTINUE USING THESE COMPOSITIONS.')
      GOTO 94
   71 XI=0.0
      DO 72 L=1,CONT1
      SORCE1(L)=SORCE1(L)-(RMF*MODE(L,2))
      XI=XI+SORCE1(L)
   72 CONTINUE
      DO 73 L=1,CONT1
      SORCE1(L)=SORCE1(L)*100.0/XI
   73 CONTINUE
      GO TO 74
   94 CONTINUE
      RETURN
      END
      SUBROUTINE OHARA (MINER,MINERX,ELEM,ELEMX,KD,SORCE1,SORCE2,
     $CONT1,CONT2,CONT3,CONT4,MODE,KDGP,BKD,CHOND,P,CONT20,RESID,
     $IBATCH,OHARAX,OHARAY,JOHARA)
C
C THE SUBROUTINE OHARA IS SELF RUN AND DOESN'T RELATE TO THE MAIN
C PROGRAM.  A DESCRIPTION OF THE GENERAL LOGIC IS GIVEN IN THE REPORT.
C
      COMPLEX*16 KDGP(17)
      INTEGER CONT1,CONT2,CONT3,CONT4,CONT20
      INTEGER MINER(14),MINERX(14),ELEM(27),ELEMX(27)
      REAL KD(27,14,9),SORCE1(14),SORCE2(27),MODE(27,6),BKD(27)
      REAL CHOND(27,2),P(27),RESID(27),SORCEX(14),SORCEY(27)
      DATA DATA1/06./,DATA2/09./,DATA3/11./,DATA4/12./
      IBATCH=15
C
C IBATCH IS SET TO 15 FOR PRINTING PURPOSES.  SEE RESULT SUBPROGRAM.
C
      DO 120 I=1,CONT1
      SORCEX(I)=SORCE1(I)
C
C SORCEX AND SORCEY STORE THE ORIGINAL SORCE1 AND SORCE2 COMPOSITIONS
C WHICH ARE USED IN THE LATER MAGMATIC MIXING EQUATIONS.
C
  120 CONTINUE
      DO 130 I=1,CONT2
      RESID(I)=0.0
```

```
      MODE(I,3)=0.0
      SORCEY(I)=SORCE2(I)
 130  CONTINUE
      DO 100 J=1,JOHARA
C
C LINE 683 SETS UP THE MAIN LOOP FOR THE NUMBER OF CYCLES TO RUN.
C
      DO 104 K=1,CONT1
      IF ((OHARAX*MODE(K,2))-SORCE1(K)) 104,104,116
C
C LINES 686-696 CHECK TO SEE THAT THE EQUATIONS WILL NOT BE EXCEEDED.
C
 116  WRITE(6,107) MINER(MINERX(K))
 107  FORMAT('1',///////,'EQUATIONS ARE BOMBING OUT BECAUSE YOU ARE CALL
     $ING FOR A GREATER AMOUNT OF',1X,A4,1X,'THAN IS IN THE SOURCE')
      OHARAX=SORCE1(K)/MODE(K,2)
      WRITE(6,124)OHARAX
 124  FORMAT(' ',10X,'THE VALUE OHARAX HAS BEEN RECALCULATED TO ',1X,
     $F3.2,1X,'OR THE MAXIMUM ALLOWABLE VALUE AND EXECUTION WILL CONTINU
     $E.')
 104  CONTINUE
C
C LINES 700-709 CALCULATE THE BKD TERM.
C
      DO 121 K=1,CONT2
      P(K)=0.0
      BKD(K)=0.0
      DO 123 I=1,CONT1
      IF ((KD(ELEMX(K),MINERX(I),CONT3)).EQ.99.999) GO TO 123
      BKD(K)=BKD(K)+((MODE(I,2)/100.0)*(KD(ELEMX(K),MINERX(I),CONT3)))
 123  CONTINUE
 121  CONTINUE
      CALL HEAD(MINER,MINERX,ELEM,ELEMX,KD,SORCE1,SORCE2,CONT1,
     $CONT2,CONT3,MODE,KDGP,BKD,CONT4,CHOND,P)
C
C LINE 713 SETS UP THE LOOP TO TREAT EACH ELEMENT SEPERATELY.
C
      DO 101 I=1,CONT2
      IF (MODE(I,3).LT.0.0) GO TO 101
C
C IF AN ELEMENT IS RECALCULATED TO LESS THAN ZERO IT IS DISREGARDED.
C
      MODE(I,3)=SORCE2(I)*(OHARAX+OHARAY)*((1-OHARAX)**(BKD(I)-1))/
     $(1-((1-OHARAX-OHARAY)*((1-OHARAX)**(BKD(I)-1))))
C
C LINES 723-754 IS THE PETROCHEMICAL SUBTRACTION SUBROUTINE FOR K AND ZR
C
      IF(ELEMX(I)-22) 102,103,102
 102  IF(ELEMX(I)-12) 108,103,108
 103  DO 105  II=1,CONT1
      IF(ELEMX(I).EQ.22) GO TO 106
      IF (MODE(II,1)-9) 131,132,133
```

```
 131 IF(MODE(II,1).EQ.DATA1)MODE(I,3)=MODE(I,3)-(OHARAX*MODE(II,2)*
    $1103.0)
     IF(MODE(I,3).GT.0.0) GO TO 105
     WRITE(6,122)ELEM(ELEMX(I))
     GO TO 101
 132 IF(MODE(II,1).EQ.DATA2)MODE(I,3)=MODE(I,3)-(OHARAX*MODE(II,2)*
    $937.0)
     IF(MODE(I,3).GT.0.0) GO TO 105
     WRITE(6,122)ELEM(ELEMX(I))
     GO TO 101
 133 IF(MODE(II,1).EQ.DATA4)MODE(I,3)=MODE(I,3)-(OHARAX*MODE(II,2)*
    $1119.0)
     IF(MODE(I,3).GT.0.0) GO TO 105
     WRITE(6,122)ELEM(ELEMX(I))
     GO TO 101
 106 IF(MODE(II,1).EQ.DATA3)MODE(I,3)=MODE(I,3)-(OHARAX*MODE(II,2)*
    $4459.0)
     IF(MODE(I,3).GT.0.0) GO TO 105
     WRITE(6,122)ELEM(ELEMX(I))
     GO TO 101
 122 FORMAT('1',///////,05X,'THE ELEMENT',2X,A4,'HAS BEEN RECALCULATED
    $TO LESS THAN ZERO BY THE SUBTRACTION PROGRAM.  DISREGARD FURTHER U
    $SE OF THIS ELEMENT.')
 105 CONTINUE
 108 MODE(I,5)=BKD(I)*SORCE2(I)*((1-OHARAX)**(BKD(I)-1))
     RESID(I)=(RESID(I)*(J-1)/J)+(MODE(I,5)*1/J)
 101 CONTINUE
C
C LINES 759-767 DO THE MAGMATIC MIXING MODELLING THE REINTRUSION
C OF THE PARENTAL MAGMA.  THE LOGIC IS DESCRIBED IN THE TEXT.
C
     DO 109 K=1,CONT1
     SORCE1(K)=(SORCE1(K)-(MODE(K,2)*OHARAX))*  (1.0/(1.0-OHARAX))
     SORCE1(K)=(SORCE1(K)*(1.0-OHARAX-OHARAY))+(SORCEX(K)*(OHARAX+
    $OHARAY))
 109 CONTINUE
     DO 110 K=1,CONT2
     SORCE2(K)=(MODE(K,3)*(1.0-OHARAX-OHARAY))+(SORCEY(K)*(OHARAX+
    $OHARAY))
 110 CONTINUE
     WRITE(6,114)
 114 FORMAT('1',//,20X,'TRACE ELEMENT CONCENTRATIONS USING OHARA TYPE M
    $ODELLING .')
      WRITE(6,117)OHARAX,OHARAY
 117 FORMAT(' ',10X,'PROCESS INVOLVES',1X,F3.2,1X,'WT. FRACTION OF CRYS
    $TAL FRACTIONATION AND',1X,F3.2,1X,'WT. FRACTION OF EXTRUSIVE IN EA
    $CH CYCLE.')
     WRITE(6,115)
 115 FORMAT(' ',10X,'ALL EQUATIONS ARE CALCULATED WITHOUT THE ZONE REFI
    $NING TERM OUTLINED IN OHARA, 1977.')
     CALL RESULT (MINER,ELEM,MODE,CONT2,CONT1,RESID,ELEMX,CHOND,IBATCH)
 100 CONTINUE
```

```
111  CONTINUE
     RETURN
     END
```

APPENDIX D

Operating Manual to the Computer

Program - STEM

Discussion of Computer Program for Trace Element Modelling:

This section is designed to give a general review of the theoretical modelling of trace element behaviour during the major igneous processes that are treated in the computer program, Appendix C. No attempt will be made to criticize any of the applied methods as this is just a statement of the equations used and their sources. Both partial melting and fractional crystallization processes will be reviewed.

This appendix supplements the commented computer program STEM, or "System for Trace Element Modelling", Appendix C, and is only meant to provide a brief background to the logic of the program and the user oriented features. The program will be discussed systematically, process by process, to lay out the system design to facilitate any future changes.

At its present state the program is capable of modelling up to 27 elements and 14 minerals through batch melting, fractional melting, "dynamic" partial melting, fractional crystallization, (both in surface and total equilibrium conditions, and O'Hara-type fractional crystallization which calls for periodic rejuvenation of the magma chamber. The program is totally self-sufficient and will print out appropriate error messages when the limits of the program or equations are exceeded. Error messages are printed to give some idea of the nature of the problem and how the user might adjust his data input.

Discussion will follow by first defining the variable and array names, and then treat each modelling process separately, thereby enabling integration with the comments on the logic design in the program.

Variable and Array Definitions:

Real Arrays:

SORCE1(13)- array containing coded mineral types to be used in the modelling. Coding as follows:

01- olivine 02- orthopyroxene 03- diopside
04- augite 05- hornblende 06- phlogopite
07- plagioclase 08- garnet 09- biotite
10- apatite 11- zircon 12- K- feldspar
13- magnetite 14- quartz

SORCE2(27)- array containing coded element types to be used in the modelling. Coding as follows:

01= La 02= Ce 03= Pr 04= Nd 05= Sm
06= Eu 07= Gd 08= Dy 09= Er 10= Yb
11= Lu 12= K 13= Rb 14= Sr 15= Ba
16= Cr 17= Ni 18= Ti 19= Sc 20= Y
21= Nb 22= Zr 23= Mn 24= V 25= U
26= Th 27= Ga

KD(27, 13, 9)- three dimensional array containing nine full sets of individual mineral/liquid distribution coefficients for all 27 elements and 14 minerals. The element and mineral code numbers were defined previously, while the Kd sets are defined as follows:

01- average basaltic 02- high basaltic
03- low basaltic 04- average dacitic
05- high dacitic 06- low dacitic

07- average rhyolitic 08- high rhyolitic

09- low rhyolitic

*Note that some KD values are more accurate than others and the user should use his own discretion. Discussion of the sources and methods of compilation are given later in this section.

BKD(27)- array containing bulk Kd values for each element.

P(27)- array containing bulk P values for each element, used in partial melting equations only.

BKDX(27)- array containing bulk Kd values for each element at the critical point of melting or crystal fractionation when a component mineral is totally used up in the source.

CHOND(27, 2)- array containing the chondritic abundances of the 27 elements in (I,1). Values of the REE were taken from Taylor and Gorton, (1977), while those for the other elements are from Wasson, (1975). CHOND(I,2) is used to store the chondritic ratios for printing.

RESID(27)- array containing element concentrations in the residue of partial melting processes or aggregrate cumulate concentrations in fractional crystallization processes.

MODE(27, 6)- multi-purpose array:

MODE(I,1)- coded number of mineral in the crystal cumulates or in the composition to be partially melted.

MODE(I,2)- percentage of each mineral as defined in MODE(I,1).

MODE(I,3)- the calculated trace element concentrations in the liquid as modelled by fractional crystallization or partial melting processes.

MODE(I,4)- trace element concentration of the liquid at the critical point of phase exhaustion in the source, similar to BKDX(I).

MODE(I,5)- aggregrate liquid composition used in compiling various fractional melting steps, or the instantaneous composition of a phenocryst assemblage in fractional crystallization modelling.

MODE(I,6)- composition of the liquid from the previous partial melting step; used only in "dynamic" type partial melting.

Integer Arrays:

ELEM(27)- used for storing alphabetic symbols of elements for printing.

ELEMX(27)- contains the numbers of the elements used in modelling. This is used for printing and accessing a specific Kd file in cases where elements aren't chosen sequentially.

MINER(13)- array containing the alphabetic characters of the minerals for printing.

MINERX(13)- similar to ELEMX relating to minerals.

Complex Arrays:

KDGP(17)- an alphabetic array stored in 2A8 that is used for printing processes in defining the options used.

Real Variables:

DYNAMX- a term that defines the weight fraction of melt that is left behind in "dynamic" partial melting.

OHARAX-	the mass fraction of the cumulate formed from the magma in each cycle of OHARA type fractionation.
OHARAY-	mass fraction of the liquid which is extracted as a lava in each cycle of OHARA type fractionation.
RMF-	weight fraction of material that is partially melted in any one cycle.
RMFX-	critical weight fraction in partial melting equations at which point a phase is used up in the source.
RMFP-	the same as RMF but increased 100x for printing.
X-	coded variable used to signal the calling of the recalculation exercize.
RIXTAL-	weight fraction of material to be fractionated in any one fractional crystallization cycle.
XXXTAL-	the same as RMFX for fractional crystallization processes.
PIXTAL-	the same as RMFP but for fractional crystallization processes.
ABD-	a dummy variable in the recalculation subroutine used to store the number of the phase that has been used up in the source.

Integer Variables:

CONT1-	total number of minerals used.
CONT2-	total number of elements used.
CONT3-	Kd vector set used.
CONT4-	coded control number: 12- Partial melting 13- Fractional Crystallization
CONT5-	beginning percentage of partial melting.

CONT6-	end percentage of partial melting.
CONT7-	increment value for cycles between CONT5 and CONT6.
CONT8-	number of minerals in mode of partially melting material. Should be the same as CONT1.
CONT9-	same as CONT5 for fractional crystallization.
CONT10-	same as CONT6 for fractional crystallization.
CONT11-	same as CONT7 for fractional crystallization.
CONT12-	coded variable to determine the type of fractional crystallization equations desired: 10- Nernst or Total Equilibrium 11- Rayleigh or Surface Equilibrium
CONT13-	number of minerals fractionating. Should be the same as CONT1.
IBATCH-	option control variable: 14- Batch melting 15- Fractional melting
IDYNAM-	option control variable: 16- "Normal" fractional or batch partial melting. 17- "Dynamic" fractional or batch partial melting.
IOHARA-	option control variable: 0- Normal fractional crystallization. 1- OHARA type fractional crystallization.
JOHARA-	number of fractional crystallization cycles desired in OHARA type modelling.
MF-	counting variable in loops of partial melting modelling.
K2-	stores mineral code number of exhausted phase for recalculation exercize.

Partial Melting:

There are basically three theoretical mechanisms by which partial melting may occur: 1.) continuous removal of the melt from the residual solid, or fractional melting, 2.) continuous removal of the melt from the residual solid and collection of this melt in a single, completely mixed chamber, and 3.) continuous equilibrium of the liquid phase with the residual solid until removal of the liquid from the solid, or batch melting. A special option, termed the "dynamic" option, can be used with either batch or fractional melting. This option, which was discussed non-mathematically by Langmuir et al., (1977), provides the user with the option of leaving a certain proportion of the partially melted liquid behind to mix with partial melts of a following melting cycle. In some cases, such as those which involve a large degree of partial melting, this sort of situation might be more realistic as it is hard to envisage a perfect separation of a liquid and its residual solid. These various processes cover the major methods envisaged for magma segregation during partial melting processes. No geological data can be applied to the choice of one or the other of the processes and hence it is left to the user's discretion.

In this program, partial melting methods 1 and 2 are grouped together with the answers for both types printed when fractional melting is called for. Batch melting is the alternate to this combined form of fractional melting while

the "dynamic" option may be applied to either case in a secondary fashion. In this, and all following examples, the method of accessing any one of the specific options will be left to the section on control cards and data input at the end of the appendix. For a discussion of the relative efficiency of the various methods in changing trace element abundances and ratios the reader is referred to Shaw, (1970), and Langmuir et al., (1977).

Note that in all the printouts the formatted titles are made up of two phrases connected by an "or". In all cases the first phrase refers to partial melting calculations while the second is for fractional crystallization.

Batch Melting:

From Shaw, (1970), the basic equation for modelling batch partial melting is derived, eqn. 1:

$$(1)\quad MODE(I,3) = \frac{SORCE2(I)}{BKD(I) + RMF \times (1 - P(I))}$$

.....where the bulk distribution coefficient and P terms are defined by the following equations:

$$(2)\quad BKD(I) = X_o^i \times KD^{I/i} + X_o^j \times KD^{I/j} \ .....$$

$$(3)\quad P(I) = p_1^i \times KD^{I/i} + p_1^j \times KD^{I/j} \ .....$$

.....where: X_o^i = weight fraction of phase i in the starting assemblage.

p_1^i = weight fraction of phase i in the melting assemblage.

$KD^{I/i}$ = the distribution coefficient of element I between phase i and the coexisting silicate liquid.

The distribution coefficient is defined as the ratio of the concentration of an element in a crystalline mineral phase to the concentration of that element in the coexisting liquid.

In all calculations of BKD(I) and P(I) the equations are screened for any dummy Kd values marked 99.999. This number is reserved for cases in which an element used is a structural component of a certain mineral, and hence doesn't follow the quantitative models for trace element behaviour. The possible cases are K in potash feldspar, biotite and phlogobite and Zr in zircon. In models where these combinations are called upon the results are recalculated by petrochemical subtraction equations after the normal trace element modelling, so the results printed are a good approximation to the expected composition. The equation used for the petrochemical subtraction is:

$$(4) \quad \mathrm{MODE}(I,3) = \mathrm{MODE}(I,3) + (\mathrm{RMF} \times \mathrm{MODE}(J,2) \times \text{weight fraction of element, I in mineral J})$$

A similar equation which subtracts the amount from the residual liquid is used in the modelling of fractional crystallization.

In cases where modal melting occurs, ie. where the melting mineral proportions are the same as those in the source rock, P(I)=KD(I) and hence equation 1 reduces to the form:

$$(5)\quad MODE(I,3) = \frac{SORCE2(I)}{BKD(I) + RMF \times (1 - BKD(I))}$$

In the case where, extensive partial melting occurs and one of the phases in the source has been used up, equation 1 is rewritten in the form derived by Hertogen and Gijbels, (1976), for a multi-step process:

$$(6)\quad MODE(I,3) = \frac{SORCE2(I)}{BKDX(I) + RMF \times (1 - P(I)) + RMFX \times (P(I) - BKDX(I))}$$

This sort of calculation will work for any number of phase depletions and source recalculations with the terms BKD(I) and RMFX recalculated for each critical point. The logic of the recalculation exercize will be explained later.

In this model, as in all others, the concentration of the residual solid is always printed out. The concentration, RESID(I), is obtained through the mass balance equation from Hertogen and Gijbels, (1976), eqn. 20:

$$(7)\quad RESID(I) = \frac{SORCE2(I)}{1 - RMF} \times \left(1 - \frac{MODE(I,3)}{SORCE2\ (I)} \times RMF\right)$$

Fractional Melting:

Fractional melting is by far the more potent method of increasing incompatible trace element concentrations in liquids derived by partial melting, but puts more constraints on the conceptualized geological process. Equations for the single stage process were originally derived by Gast,

(1968), and modified by Shaw, (1970). Equations for the multistage problem were derived by Hertogen and Gijbels, (1976).

From eqn. 13+14 of Shaw, (1970), we get the standard equations for the instantaneous and aggregrate liquid compositions:

$$(8)\quad MODE(I,3) = \frac{SORCE2(I)}{BKD(I)} \times \left(1 - \frac{P(I) \times RMF}{BKD(I)}\right)^{1/P(I) - 1}$$

$$(9)\quad MODE(I,5) = \frac{SORCE2(I)}{RMF} \times \left(1 - \left(1 - \frac{P(I) \times RMF}{BKD(I)}\right)^{1/P(I)}\right)$$

.....with all terms defined in preceeding sections. If it is desired to continue the melting after the period in which one or more of the phases in the source has been used up, the equations become much more complex. Equations 10+11, taken from Hertogen and Gijbels, (1976), (their equations 18+19), are analogous to equations 8+9 for systems that have been recalculated, and would reduce down to equation 8+9 if BKDX(I)=0.0, RMFX=0.0 and if the P(I) terms were equal.

$$(10)\quad MODE(I,3) = \left(\frac{SORCE2(I) \times \left(1 - \left(\frac{MODE(I,4) \times RMRX}{SORCE2(I)}\right)\right)}{(1 - RMFX) \times BKDX(I)}\right) \times \left(1 - \frac{P(I) \times (RMF - RMFX)}{BKDX(I) \times (1 - RMFX)}\right)^{1/P(I) - 1}$$

$$(11)\ \mathrm{MODE}(I,5) = \frac{\mathrm{SORCE2}(I)}{\mathrm{RMF}} \times \left(1 - \left(1 - \frac{\mathrm{MODE}(I,4)}{\mathrm{SORCE2}(I)} \times \mathrm{RMFX}\right)\right) \times \left(1 - \frac{P(I) \times (\mathrm{RMF} - \mathrm{RMFX})}{\mathrm{BKDX}(I) \times (1 - \mathrm{RMFX})}\right)^{1/P(I)}$$

Residual solid concentrations are calculated by the same mass-balance equation as for batch melting, eqn. 7.

The arrays SORCE1 and SORCE2 are recalculated at the end of each fractional melting cycle. SORCE2(I) is set equal to RESID(I) while SORCE1(I) is treated in the recalculation subprogram as discussed later.

Dynamic Melting Option:

The "dynamic" partial melting option models a certain degree of inefficiency in the separation of the partially melted liquid from the residual solid. No modelling equations were given in the original discussion by Langmuir et al., (1977), but it can be treated by inputting a control variable to govern the mass fraction of the liquid that is to be left behind in any one cycle, and mass balancing the concentrations of the individual elements from cycle 1 and 2 to give a weighted average composition.

This option is available with both batch and fractional melting but is most applicable to fractional melting as it calls for instantaneous removal of the liquid, which is the somewhat unrealistic process that this option is designed to compensate for. The equation for this recalculation is:

$$(12)\ \mathrm{MODE(I,3)=MODE(I,3)}\times\frac{1.0}{1.0+\mathrm{DYNAMX}}+\mathrm{MODE(I,6)}\times\frac{\mathrm{DYNAMX}}{1.0+\mathrm{DYNAMX}}$$

This calculation is done before the residual concentrations are calculated so the RESID(I) values will be those present as if the mixing occurred before the liquid separated from the residual solid.

Fractional Crystallization:

The program essentially offers three methods of modelling fractional crystallization: (1) Nernst, or total equilibrium modelling, (2) Rayleigh, or surface equilibrium modelling and (3) O'Hara-type modelling. The first of these calls for total equilibrium between the fractionating crystals and its host melt, the second implies only surface equilibrium and is more appropriate where zoned phenocrysts are present while the third model invokes periodic intrusion of parental magma into the partially fractionated, cumulate-liquid chamber. The first option is best used in intrusive complexes where the slow cooling rates will promote diffusion controlled equilibrium while the second is more appropriate in high level fractionation chambers where the phenocrysts are effectively removed from the system. O'Hara-type modelling best fits areas where parental magma generation, through partial melting, is not a singular process, such that there is possibility of reintrusion and magmatic mixing. This is best visualized in areas such as the

Mid-Atlantic ridge where adiabatic partial melting could be occurring simultaneously at a number of areas under the ridge.

Equations governing trace element behaviour during fractional crystallization are based on a quantitative description of the distillation process as applied to the theory of crystal growth from solution. The development of the equations has largely been the work of Greenland (1970), and Alberede and Bottinga (1972), and has lately been reviewed by Arth (1976), and Allegre and Minster (1978). Alberede and Bottinga (1972), and Allegre and Minster (1978) have developed equations for disequilibrium diffusion kinetics modelling which have been left out of this program.

Total Equilibrium Fractional Crystallization:

Total equilibrium, or Nernst type fractional crystallization equations are very similar to those of batch partial melting and just involve a slight revision of terms. Equation 13, modified from Arth (1976), eqn. 11, gives the general form for this type of modelling:

$$(13) \quad \text{MODE}(I,3) = \frac{\text{SORCE2}(I)}{(1.0 - \text{RIXTAL}) + \text{BKD}(I) \times \text{RIXTAL}}$$

This equation expands to the following form when RIXTAL is defined as in Arth (1976):

$$(13a) \quad \text{MODE}(I,3) = \frac{\text{SORCE2}(I)}{\text{RIXTAL} + \text{BDK}(I) \times (1 - \text{RIXTAL}}$$

.....which is exactly the same format as eqn. 5 with the BKD(I) and RIXTAL terms reversed. As the RIXTAL values are entered in this program as numbers reflecting the weight fraction of cumulates formed rather than the weight fraction of liquid remaining, the modified equation 13 is used.

The BKD(I) terms are calculated for fractionating cumulate phase as in eqn. 2, and are derived without the dummy 99.999 KD(I,J,K) value. A petrochemical subtraction subroutine is added to compensate for this.

The aggregrate concentration in the residual cumulate fraction is given by eqn. 14 from Alberede and Bottinga, (1972), eqn. 10.

$$(14) \quad \text{RESID(I)} = \frac{\text{BKD(I)} \times \text{SORCE2(I)}}{1 - (1 - \text{BKD(I)} \times \text{RIXTAL})}$$

This value is printed as the aggregrate cumulate composition in the results.

Surface Equilibrium Fractional Crystallization:

Surface equilibrium, or Rayleigh type fractional crystallization is analagous to fractional melting in that it is an exponential equation in contrast to the linear equations of batch melting and Nernst-type fractional crystallization. Although it is an exponential equation it is not symmetric with the fractional melting equations. Equation 15, taken from Alberede and Bottinga, (1972), eqn. 11, gives the liquid composition in this Rayleigh type modelling:

(15) MODE(I,3) = SORCE2(I) x $(1 - \text{RIXTAL})^{\text{BKD(I)} - 1}$

The printout for Rayleigh type modelling offers two compositions for each element in the cumulate fraction. The first set of data is that for the instantaneous composition of the settling crystals and would be appropriate for modelling compositions in porphyritic sub-volcanic intrusives or extrusives that look like they have carried up phenocrysts in situ. The second set of data gives the aggregrate composition which approximates the cumulate section of any layered intrusive. The variations in instantaneous cumulate compositions through time and/or phase exhaustion/recalculation cycles would approximate variations in layering components, while the aggregrate composition models the situation of extensive post-settling diffusion and re-equilibration.

Equation 16 from Alberede and Bottinga, (1972), eqn. 12, gives the instantaneous composition of the fractionating component:

(16) MODE(I,5) = BKD(I) x SORCE2(I) x $(1 - \text{RIXTAL})^{\text{BKD(I)} - 1}$

By integration eqn. 16 over variations in RIXTAL the aggregrate composition in the cumulate solid is obtained, eqn. 17, which is derived from eqn. 13 of Alberede and Bottinga, (1972).

(17) RESID(I) = SORCE2(I) x $\left(\frac{1 - (1 - \text{RIXTAL})^{\text{BKD(I)}}}{\text{RIXTAL}}\right)$

Similar to the partial melting equations, the fractional crystallization option is compatible with a limited number of phase depletions and recalculations. Obviously the limit is the point where all of the source, and hence all the crystallizing fraction, is recalculated to a single mineral. In cases of fractionating after the recalculation exercise has been accessed the liquid composition, MODE(I,3), is modified by the following equation:

$$(18)\ \mathrm{MODE(I,3)}=\mathrm{MODE(I,3)}\times\left(\frac{\mathrm{RIXTAL-XXXTAL}}{\mathrm{RIXTAL}}\right)+\mathrm{MODE(I,4)}\times\frac{\mathrm{XXXTAL}}{\mathrm{RIXTAL}}$$

... which takes the percentage of the fractionation above the critical point, XXXTAL, multiplies it by the concentration derived for the present amount of fractionation, MODE(I,3), and adds the complementary percentages of the concentrations that were found at the critical point, MODE(I,4).

O'Hara-Type Fractional Crystallization:

O'Hara-type fractional crystallization is modelled around the situation of an individual magma chamber undergoing normal, surface equilibrium fractional crystallization that is periodically interrupted by the intrusion of a batch of fresh parental magma that mixes with the liquid residue and commences the fractionation cycle again. The amount of fresh parental magma added in each cycle is equal to the amount that is lost through crystal settling and lava extrusion processes, so the

volume of the magma chamber remains constant. This sort of modelling would be applicable to cases where there is a gradual incompatible element buildup with no complementary depletion in compatible elements, as the periodic reintrusion will tend to increase the incompatible elements such as Zr and Rb while keeping a fairly constant Ni and Cr value.

The logic of the equations for this type of modelling are incompatible with the main flow of the program, and as a result it is treated in a separate subprogram, OHARA, which is interfaced with the HEAD and RESULT subprograms for printing purposes.

The general equation that governs the trace element concentrations of the residual liquid in O'Hara-type fractional crystallization is as follows:

$$(19)\quad \mathrm{MODE(I,3)} - \frac{\mathrm{SORCE2(I)} \times (\mathrm{OHARAX}+\mathrm{OHARAY}) \times (1-\mathrm{OHARAX})^{\mathrm{BKD(I)}-1}}{1-(1-\mathrm{OHARAX}-\mathrm{OHARAY}) \times (1-\mathrm{OHARAX})^{\mathrm{BKD(I)}-1}}$$

This equation is a slightly modified version of O'Hara's eqn.1 (1977), in which the zone refining term, 1(Cq/Co), is left out.

Equations for the concentration in the cumulate fraction in this sort of modelling were not given by O'Hara (1977), but the instantaneous composition of the cumulates would approximate that for normal surface equilibrium fractional crystallization, eqn. 15, while the aggregate cumulate concentrations would be a mass balanced average of the instantaneous concentrations of the preceding cycles, eqn. 20:

$$(20)\ \mathrm{RESID(I)} = (\mathrm{RESID(I)} \times \frac{J - I}{J}) \times (\mathrm{MODE(I,5)} \times \frac{1}{J})$$

.....in which the RESID(I) term is always retained from the previous cycle.

In this sort of modelling the arrays SORCE1 and SORCE2 have to be recalculated at the end of each cycle to accommodate the influx of primitive parental magma. SORCE1(K) is recalculated in a two step process: 1.) subtracting the crystal cumulate fraction and normalizing to 100 percent, 2.) mass balancing the residual liquid and the parental magma through the combined loss of the crystal cumulates and the extruded lavas, as shown in eqn. 21+22.

$$(21)\ \mathrm{SORCE1(K)} = (\mathrm{SORCE1(K)} - \mathrm{MODE(K,2)} \times \mathrm{OHARAX}) \times (\frac{1.0}{1.0 - \mathrm{OHARAX}})$$

$$(22)\ \mathrm{SORCE1(K)} = \mathrm{SORCE1(K)} \times (1 - \mathrm{OHARAX} - \mathrm{OHARAY}) + \mathrm{SORCEX(K)} \times (\mathrm{OHARAX} + \mathrm{OHARAY})$$

SORCE2(K) is recalculated in a one step equation similar to eqn. 22 using MODE(I,3) and SORCEY(I).

$$(23)\ \mathrm{SORCE2(K)} = \mathrm{MODE(K,3)} \times (1 - \mathrm{OHARAX} - \mathrm{OHARAY}) + \mathrm{SORCE2(K)} \times (\mathrm{OHARAX} + \mathrm{OHARAY})$$

The BKD(I) values are recalculated and printed out after each cycle of magmatic mixing. The "99.999" chemical subtraction feature is included in this subprogram also.

This subprogram does not have a continuous recalculation exercise because of the complications in the

recalculations of the source composition during each cycle. When the limits to the equations are exceeded in this subprogram, the term OHARAX will be assigned its maximum possible value and execution will continue using this value. The periodic reintrusion of the parental magma into the system is designed to prohibit the depletion of any one mineral phase in the source, as the lack of the continuous recalculation exercize in this process is not too significant.

The RECALC Subroutine:

The recalculation subprogram, RECALC, is designed to recalculate the SORCE1 and MODE(I,2) arrays when the degree of partial melting or fractional crystallization calls for more of one mineral than there is in the source. It is also called during fractional melting equations to recalculate the SORCE1 array. It doesn't recalculate the MODE(I,2) array in this case.

This subprogram is in a very general state now but could be easily changed to recalculate the mineral component values by a specific function rather than their original abundances. This could be especially useful in modelling the "step-like" fashion of phase exhaustion in the partial melting of synthetic mantle compositions. In this case the mineral recalculation functions could be derived from the coordinates of the residual source material as projected in the CMAS system diagrams through progressive partial melting.

The recalculation exercise is called at the point when:

(24) (SORCE2(I) - (RMF "or" RIXTAL) x MODE(I,2)) $<$ 0.0

.....which indicates the exhaustion of phase I in SORCE1. At this point RMF or RIXTAL are set to the maximum possible value without exceeding the bounds of eqn. 24 and execution continues with the recalculation occurring at the end of the cycle.

The recalculation is done in two steps: 1.) the amount of the critical phase is stored in ABD and the remaining amounts of all the other source minerals are calculated and totalled, 2.) the source minerals then are treated as a percentage of the total and normalized to 100 percent for further execution. The recalculation of SORCE1(I) is done in two equations:

(25) SORCE1(I) = SORCE1(I) - RMF x MODE(I,2)

(26) $\text{SORCE1(I)} = \left(\frac{\text{SORCE1(I)}}{\text{XI}}\right) \times 100.0$

.....where XI is the sum of all the SORCE1 terms from eqn. 25. In recalculating MODE(I,2) this can be combined into one equation:

(27) $\text{MODE(I,2)} = \frac{\text{MODE(I,2)} \times 100.0}{100.0 - \text{ABD}}$

The BKD(I) and P(I) terms are recalculated after each exercise and appropriate messages will be printed.

If the RECALC subprogram is called after a previous RECALC exercise had set both the MODE(I,2) and SORCE1(I) arrays to a monomineralic situation in which MODE(I,2)= SORCE1(I)= 100.0, an error message will be printed and execution will cease.

KD Values:

Appendix E contains two tabulated set of KD values that have been compiled by the author. The first set used all the experimentally and geologically determined KD values available while the second set is based upon extrapolation of the ONUMA diagrams presented in Jensen, (1973), to estimate unknown mineral-liquid KD values. A copy of both data sets is supplied with the submitted program and the user can use his own discretion. In general it seems that the main differences of the two sets are in the compatible element/ ferromagnesian mineral KD values where the "Jensen" data set tends to be more systematic and less extreme, while the experimentally calculated data is often much more variable.

A brief review will be given of the major sources of data and the methods of extrapolation and estimation.

The REE, K, Rb, Sr and Ba data for all minerals except magnetite were taken directly from the compilation of Arth, (1976). His major sources of data are listed in the

bibliography. In places where no "low" or "high" data are present, the "average" value is carried over with no changes. For completeness and ease of formatting, such alkali minerals as K-feldspar, zircon and apatite, which are usually only found in acidic rocks, are repeated in the intermediate and mafic members. The mafic olivine/REE, Rb, K, Sr and Ba data were transferred directly to the intermediate and acidic members with no changes. La and Pr KD values were obtained by extrapolation of Ce and Nd data as no experimental work was available.

Control on the transition element data are much poorer than the REE data and are somewhat contradictory within the literature. For an example of the range of internal inconsistencies see Ewart and Taylor, (1969). As was mentioned the two data sets were calculated with different priorities and should be consulted before beginning any modelling.

The available geologically determined data for the transition elements comes from Ewart and Taylor,(1969), Ewart et al., (1968), Henderson and Dale, (1969), and Delong, (1974). The only experimental study in this field is Duke, (1976).

Generally, in data set 1, TI, V, Cr, Mn and Ni data for olivine and augite/diopside are taken from Duke, (1976), while Sc, Ga, and Y data for orthopyroxene, augite, diopside and hornblende were taken from Ewart and Taylor, (1969). All other data is derived from extrapolations from Jensen, (1973).

For plagioclase, the study of Dudas et al., (1971), was used for Cr, Sc and Mn while Ga was obtained from Ewart et al., (1968), with all other data from Jensen, (1973).

The REE data for magnetite was compiled from a number of studies of lunar rocks, while the transition elements were obtained from Ewart et al., (1968).

All unmentioned data was taken from the study of Jensen, (1973), which along with Arth, (1976) were the only sources for data set 2.

The following are a few notes on the methods of extrapolation and estimation used in this compilation:

1.) In the case of unavailable dacitic KD values the "average", "high" and "low" KD values from the available mafic and acidic data was averaged and assumed to approximate the real dacitic value. This averaging method was found to be consistent with the dacitic KD data available.

2.) Where separate data on diopside and augite don't exist they were arbitrarily made equal or given slight, mineralogically reasonable, variations, ie. Cr(diop.) > Cr (aug.), Ti(aug) > Ti(diop.).

3.) Phlogopite and biotite were treated in the same way as diopside and augite.

4.) Y was made equal to Dy when no available Y data existed. Similarly Nb was made equal to Y following the findings of Winchester and Floyd, (1977), who showed that this ratio varied very little during the differentiation of most

magma series.

5.) U and Th were carried over from the augite data of Jensen, (1973), and varied slightly in more compatible minerals such as hornblende. They were arbitrarily set at 50.000 for both apatite and zircon.

6.) If only mafic transition element data was available they were carried over to the dacitic and rhyolitic classes by estimating a coefficient of variation from comparison of similar mineral diagrams calculated for different host rocks, as presented by Jensen, (1973). All KD values were increased by this standard amount. This method was found to be fairly consistent and usually resulted in a 5x increase from mafic to dacitic sets with a further 2x increase from dacitic to acidic tables.

7.) All the KD values are stored on cards with three cards to a mineral and are properly titled so they can be easily accessed for future changes. The elements are listed in the order that they appear on the printout in the appendix.

Ordering of Data Input for Trace Element Modelling Data

1.) Control cards are entered after the last Kd value cards at the end of the deck- (Last one will be marked "Mag. Low Rhyol.")

2.) First card contains 4 numbers entered in 1x, I2 fashion, ie. skip a space and then use a 2 digit integer. Numbers represent variables as follows.....

Cont 1= # of minerals used
Cont 2= # of elements used
Cont 3= Code of set of Kd values
Cont 4= Coded modelling type.

Cont 3:
1= Average basaltic Kds
2= High " "
3= Low " "
4= Average dacitic Kds
5= High " "
6= Low " "
7= Average rhyolitic Kds
8= High " "
9= Low " "

Cont 4:
12= Partial melting
13= Fractional Crystallization.

3.) Second card contains the codes for the individual minerals: Enter then in I2, 1x fashion ie. same as above but in opposite order.

01= olivine	02= orthopyroxene	03= diopside
04= augite	05= hornblende	06= phlogobite
07= plagioclase	08= garnet	09= biotite
10= apatite	11= zircon	12= K-feldspar
13= magnetite	14= quartz	

4.) The third card contains the coded elements to be used

01= La,	02= Ce,	03= Pr,	04= Nd,	05= Sm,	06= Eu,
07= Gd,	08= Dy,	09= Er,	10= Yb,	11= Lu,	12= K,
13= Rb,	14= Sr,	15= Ba,	16= Cr,	17= Ni,	18= Ti,
19= Sc,	20= Y,	21= Nb,	22= Zr,	23= Mn,	24= V,
25= U,	26= Th,	27= Ga.			

Note: All numbers entered in the same manner as 3.), and should be listed in numeric order.

5.) The fourth card contains the modal mineralogy of the source material. This data is entered in 1x, F5.2 fashion, ie. skip a space and then enter the modes in xx.xx fashion. Only 7 values per card are possible.

6.) The fifth card or cards will contain the source trace element abundances. These are entered in 1x, F8.2 fashion, ie. skip a space then enter the number in xxxxx.xx fashion.

Note: For both 5.) and 6.) the data has to be entered in the same order as it is listed in 3.) and 4.).

Note: In 6.) only 8 trace elements will fit on one card. As many cards as necessary should be used here in order to satisfy 4.). To check the format you should print your last value on line 72 of the computer card, for every eighth value entered.

7.) The format of the sixth card depends on whether partial melting or fractional crystallization is chosen. If a 12 is entered in Cont 4 the format is as follows:

Partial Melting: The card will contain 4 values entered in 1x, I2 fashion.

Cont 5- beginning value of partial melting Entered as a number between 0-99.

Cont 6- End value of partial melting.

Cont 7- Increment value between Cont 5 and Cont 6.

Cont 8- Number of minerals in the melting mineralogy. Enter the same number as Cont 1.

If Cont 4 equals 13 then the card contains 5 values:

Fractional Crystallization:

Cont 9- beginning value for fractional crystallization. Entered as Cont 5.

Cont 10- End value for above.

Cont 11- Increment value for above.

Cont 12- 10= total equilibrium
11= surface equilibrium

Cont 13- Number of minerals in the fractionating mineralogy. Enter the same number as Cont 1.

8.) The seventh card or cards contains the coded values for the fractionating or partially melting material. This data is entered in (F3.0, 1x, F5.2, 1x) fashion as described previously. A total of seven groups of two numbers will be taken on any one card. To check format the last digit should be typed in column 70.

Note: The same number of minerals should be used in the source and fractionating mineral data. If it is desired not to involve a certain mineral in the fractionating mineralogy it should be entered as a zero, ie. 00.000.

9.) Similar to 7.) the nature of the final control card depends upon what was entered in Cont 4.

Partial Melting: Three coded values entered in 2(I2, 1x), F3.2 representing the following:

IBATCH - control variable to choose batch or fractional melting.
14- Batch Melting
15- Fractional Melting

IDYNAM - control variable to choose normal or "dynamic" melting
16- Normal Melting
17- "Dynamic" Melting

DYNAMX - variable for the weight fraction of material to leave behind in "dynamic" melting. Leave blank if IDYNAM = 16.

Fractional Crystallization:

Four coded values entered in 2(I2, 1x), 2(F3.2, 1x).

IOHARA - option control variable:
0- Normal fractional crystallization
1- Ohara type fractional crystallization.
Leave rest of card blank if IOHARA = 0.

JOHARA - number of cycles desired in Ohara type modelling.

OHARAX - weight fraction of cumulates in each Ohara type modelling cycle.

OHARAY - weight fraction of material that is extruding as a lava in each Ohara type modelling cycle.

10.) The control cards are followed by 2 JCL cards to signal the end of the job. The first has /* in the first 2 columns while the second has //.

11.) A set of sequentially numbered JCL cards is given with the data sets.

APPENDIX E

Tabulated Kd Data

AVERAGE BASALTIC KD VALUES - KD SET #1

ELEM	OLIV	OPX	DIOP	AUG	HORN	PHLG	PLAG
LA	00.006	00.020	00.045	00.010	00.145	00.035	00.140
CE	00.006	00.024	00.070	00.025	00.200	00.034	00.120
PR	00.006	00.028	00.095	00.155	00.265	00.033	00.100
NO	00.006	00.033	00.120	00.310	00.330	00.032	00.081
SM	00.006	00.054	00.180	00.500	00.520	00.031	00.067
EU	00.006	00.054	00.180	00.510	00.590	00.030	00.340
GD	00.007	00.091	00.190	00.610	00.630	00.030	00.063
DY	00.009	00.150	00.210	00.680	00.640	00.030	00.055
ER	00.011	00.230	00.170	00.650	00.550	00.034	00.063
YB	00.014	00.340	00.160	00.620	00.490	00.042	00.067
LU	00.016	00.420	00.130	00.560	00.430	00.046	00.060
K	00.005	00.014	00.011	00.038	00.960	99.999	00.170
RB	00.007	00.022	00.015	00.031	00.290	03.080	00.071
SR	00.014	00.017	00.120	00.120	00.460	00.081	01.830
BA	00.009	00.013	00.013	00.026	00.420	01.090	00.230
CR	02.700	00.600	20.000	10.000	03.000	12.600	00.100
NI	23.800	06.000	04.500	04.500	07.000	20.000	00.008
TI	00.070	00.500	00.340	00.900	00.800	01.000	00.010
SC	00.100	01.230	02.000	02.920	02.180	05.300	00.020
Y	00.010	00.150	00.210	00.680	00.640	00.030	00.055
NB	00.010	00.150	00.210	00.680	00.640	00.030	00.055
ZR	00.010	00.150	00.200	00.400	01.000	00.030	00.005
MN	01.250	01.440	00.630	00.630	00.940	06.000	00.060
V	00.050	00.800	01.300	01.300	04.000	12.000	00.080
U	00.017	00.017	00.017	00.017	00.540	00.450	00.090
TH	00.013	00.013	00.013	00.013	00.540	00.310	00.090
GA	00.600	00.600	00.505	00.505	00.800	04.000	01.000

AVERAGE BASALTIC KD VALUES - KD SET #1

ELEM	GARN	BIOT	APAT	ZIRC	KFLD	MAG	QTZ
LA	00.008	00.033	26.500	02.400	00.053	00.098	00.000
CE	00.028	00.037	34.700	02.640	00.044	00.110	00.000
PR	00.048	00.040	42.055	02.800	00.035	00.125	00.000
NO	00.068	00.044	57.100	02.200	00.025	00.130	00.000
SM	00.290	00.058	62.000	03.140	00.010	00.150	00.000
EU	00.490	00.145	30.400	03.140	01.130	00.100	00.000
GD	00.970	00.082	56.300	12.000	00.011	00.120	00.000
DY	03.170	00.097	50.700	45.700	00.006	00.140	00.000
ER	06.560	00.162	37.200	135.00	00.006	00.155	00.000
YB	11.500	00.179	23.900	270.00	00.012	00.170	00.000
LU	11.900	00.185	20.200	323.00	00.006	00.190	00.000
K	00.015	99.999	00.000	00.000	99.999	00.000	00.000
RB	00.042	03.260	00.000	00.000	00.340	00.000	00.000
SR	00.012	00.120	01.000	00.000	03.870	00.000	00.000
BA	00.023	06.360	00.000	00.000	06.120	00.000	00.000
CR	03.280	12.600	00.000	00.000	00.670	96.500	00.000
NI	02.000	20.000	00.000	00.000	00.020	23.333	00.000
TI	00.500	02.000	00.000	00.000	00.040	34.000	00.000
SC	01.000	11.300	00.000	01.000	00.197	02.250	00.000
Y	03.170	00.097	50.700	45.700	00.006	00.000	00.000
NB	03.170	00.097	50.700	45.700	00.006	00.000	00.000
ZR	00.500	01.000	00.000	99.999	00.100	00.000	00.000
MN	05.000	06.000	00.000	00.000	00.310	03.225	00.000
V	01.280	12.000	00.000	00.000	00.200	79.950	00.000
U	00.100	00.450	50.000	50.000	00.100	00.000	00.000
TH	00.100	00.310	50.000	50.000	00.088	00.000	00.000
GA	01.000	04.000	01.000	00.000	00.950	00.000	00.000

LOW BASALTIC KD VALUES - KD SET #1

ELEM	OLIV	OPX	DIOP	AUG	HORN	PHLG	PLAG
LA	00.008	00.028	00.050	00.100	00.230	00.035	00.320
CE	00.009	00.038	00.096	00.210	00.340	00.034	00.280
PR	00.010	00.048	00.140	00.320	00.440	00.033	00.240
NO	00.010	00.058	00.180	00.430	00.560	00.032	00.200
SM	00.011	00.100	00.260	00.740	00.930	00.031	00.170
EU	00.010	00.079	00.260	00.750	01.100	00.030	00.730
GD	00.012	00.171	00.270	00.870	01.150	00.030	00.210
DY	00.014	00.293	00.310	01.000	01.050	00.030	00.190
ER	00.017	00.460	00.230	01.100	01.000	00.034	00.240
YB	00.023	00.670	00.230	01.000	00.980	00.042	00.300
LU	00.026	00.840	00.190	00.950	00.820	00.046	00.240
K	00.008	00.019	00.014	00.078	01.400	99.999	00.360
RB	00.011	00.029	00.015	00.039	00.430	03.006	00.140
SR	00.019	00.024	00.150	00.150	00.640	00.081	02.870
BA	00.011	00.014	00.013	00.046	00.730	01.090	00.590
CR	04.200	00.700	30.000	20.000	04.000	17.400	00.200
NI	49.200	07.000	07.900	07.900	08.000	25.000	00.010
TI	00.120	00.600	00.430	00.430	01.000	01.500	00.020
SC	00.300	01.330	02.040	03.040	02.220	05.800	00.030
Y	00.014	00.290	00.310	01.000	01.000	00.030	00.240
NB	00.014	00.290	00.310	01.000	01.000	00.030	00.240
ZR	00.010	00.300	00.310	00.600	01.200	00.030	00.010
MN	01.430	01.530	00.710	00.710	00.970	06.130	00.060
V	00.080	00.900	02.150	01.150	07.000	18.000	00.150
U	00.020	00.020	00.017	00.020	00.800	00.500	01.000
TH	00.015	00.015	00.013	00.015	00.700	00.430	00.100
GA	00.700	00.700	00.650	00.650	00.800	04.500	01.200

LOW BASALTIC KD VALUES - KD SET #1

ELEM	GARN	BIOT	APAT	ZIRC	KFLD	MAG	QTZ
LA	00.008	00.033	37.000	03.300	00.053	00.098	00.000
CE	00.028	00.037	52.500	03.000	00.044	00.110	00.000
PR	00.048	00.040	67.000	02.700	00.033	00.125	00.000
NO	00.068	00.044	81.100	02.430	00.025	00.130	00.000
SM	00.290	00.058	89.800	03.700	00.018	00.150	00.000
EU	00.490	00.145	50.200	05.220	01.130	00.100	00.000
GD	00.970	00.082	78.000	14.000	00.011	00.120	00.000
DY	03.170	00.097	69.200	53.500	00.006	00.140	00.000
ER	06.560	00.162	51.200	152.00	00.006	00.155	00.000
YB	11.500	00.179	37.000	299.00	00.012	00.170	00.000
LU	11.900	00.185	30.200	366.00	00.006	00.190	00.000
K	00.015	99.999	00.000	00.000	99.999	00.000	00.000
RB	00.042	03.260	00.000	00.000	00.340	00.000	00.000
SR	00.012	00.120	01.000	00.000	03.870	00.000	00.000
BA	00.023	06.360	00.000	00.000	06.120	00.000	00.000
CR	03.280	17.400	00.000	00.000	00. 70	150.00	00.000
NI	03.000	25.000	00.000	00.000	00.020	30.000	00.000
TI	00.500	01.500	00.000	00.000	00.040	40.000	00.000
SC	01.000	05.800	00.000	01.000	00.197	03.000	00.000
Y	03.170	00.030	50.700	45.700	00.006	00.000	00.000
NB	03.170	00.030	50.700	45.700	00.006	00.000	00.000
ZR	00.500	00.300	00.000	99.999	00.100	00.000	00.000
MN	05.000	06.130	00.000	00.000	00.310	04.000	00.000
V	01.280	18.000	00.000	00.000	00.200	100.00	00.000
U	00.100	00.500	50.000	50.000	00.100	00.000	00.000
TH	00.100	00.430	50.000	50.000	00.088	00.000	00.000
GA	01.000	04.500	01.000	00.000	00.950	00.000	00.000

HIGH BASALTIC KD VALUES - KD SET #1

ELEM	OLIV	OPX	DIOP	AUG	HORN	PHLG	PLAG
LA	00.002	00.001	00.032	00.027	00.060	00.035	00.022
CE	00.002	00.002	00.043	00.077	00.094	00.034	00.023
PR	00.002	00.005	00.054	00.127	00.130	00.033	00.023
NO	00.003	00.008	00.065	00.170	00.160	00.032	00.023
SM	00.003	00.014	00.090	00.260	00.240	00.031	00.024
EU	00.005	00.023	00.091	00.270	00.260	00.030	00.055
GD	00.004	00.032	00.095	00.320	00.280	00.030	00.017
DY	00.006	00.054	00.105	00.500	00.310	00.030	00.010
ER	00.008	00.076	00.107	00.460	00.240	00.034	00.010
YB	00.009	00.110	00.092	00.430	00.230	00.042	00.006
LU	00.009	00.110	00.071	00.270	00.220	00.046	00.004
K	00.005	00.009	00.008	00.004	00.330	99.999	00.019
RB	00.008	00.015	00.014	00.015	00.045	03.080	00.016
SR	00.009	00.010	00.078	00.093	00.190	00.081	01.290
BA	00.009	00.012	00.013	00.004	00.100	01.090	00.050
CR	01.200	00.500	10.000	08.000	02.000	07.800	00.080
NI	08.400	05.000	01.100	01.100	06.000	15.000	00.006
TI	00.020	00.400	00.250	00.150	00.800	00.500	00.005
SC	00.050	01.130	01.800	02.800	02.140	05.000	00.010
Y	00.006	00.054	00.105	00.500	00.310	00.030	00.010
NB	00.006	00.054	00.105	00.500	00.310	00.030	00.010
ZR	00.007	00.100	00.100	00.200	00.600	00.030	00.003
MN	01.070	01.350	00.550	00.450	00.910	05.870	00.040
V	00.020	00.700	00.550	00.450	03.000	06.000	00.060
U	00.015	00.015	00.017	00.017	00.150	00.200	00.070
TH	00.010	00.010	00.013	00.013	00.100	00.190	00.070
GA	00.500	00.500	00.360	00.360	00.800	03.500	00.800

HIGH BASALTIC KD VALUES - KD SET #1

ELEM	GARN	BIOT	APAT	ZIRC	KFLD	MAG	QTZ
LA	00.008	00.033	13.500	02.450	00.055	00.098	00.000
CE	00.028	00.037	18.000	02.290	00.044	00.110	00.000
PR	00.048	00.040	22.500	02.150	00.035	00.125	00.000
NO	00.068	00.044	27.400	01.970	00.025	00.130	00.000
SM	00.290	00.058	29.300	02.580	00.018	00.150	00.000
EU	00.490	00.145	20.500	01.070	01.130	00.100	00.000
GD	00.970	00.082	27.200	10.000	00.011	00.120	00.000
DY	03.170	00.097	25.600	37.800	00.006	00.140	00.000
ER	06.560	00.162	20.000	119.00	00.006	00.155	00.000
YB	11.500	00.179	13.100	242.00	00.012	00.170	00.000
LU	11.900	00.185	11.200	281.00	00.006	00.190	00.000
K	00.015	99.999	00.000	00.000	99.999	00.000	00.000
RB	00.042	03.2 0	00.000	00.000	00.340	00.000	00.000
SR	00.012	00.120	01.000	00.000	03.870	00.000	00.000
BA	00.023	0 .3 0	00.000	00.000	06.120	00.000	00.000
CR	03.280	07.800	00.000	00.000	00. 70	50.000	00.000
NI	01.000	15.000	00.000	00.000	00.020	15.000	00.000
TI	00.500	01.000	00.000	00.000	00.040	28.000	00.000
SC	01.000	05.000	00.000	01.000	00.197	01.500	00.000
Y	03.170	00.030	50.700	45.700	00.006	00.000	00.000
NB	03.170	00.030	50.700	45.700	00.006	00.000	00.000
ZR	00.500	00.030	00.000	99.999	00.100	00.000	00.000
MN	05.000	05.870	00.000	00.000	00.310	02.500	00.000
V	01.280	06.000	00.000	00.000	00.200	57.000	00.000
U	00.100	00.200	50.000	50.000	00.100	00.000	00.000
TH	00.100	00.190	50.000	50.000	00.088	00.000	00.000
GA	01.000	03.500	01.000	00.000	00.950	00.000	00.000

AVERAGE DACITIC KD VALUES - KD SET #1

ELEM	OLIV	OPX	DIOP	AUG	HORN	PHLG	PLAG
LA	00.005	00.067	00.120	00.350	00.100	00.107	00.275
CE	00.006	00.087	00.285	00.475	00.899	00.132	00.240
PR	00.006	00.107	00.440	00.590	01.850	00.157	00.205
ND	00.006	00.123	00.612	00.710	02.800	00.186	00.170
SM	00.006	00.162	00.925	01.085	03.990	00.211	00.130
EU	00.006	00.112	00.870	01.035	03.440	00.265	02.110
GD	00.007	00.216	01.020	01.230	05.480	00.190	00.090
DY	00.009	00.305	01.070	01.305	06.200	00.115	00.086
ER	00.011	00.440	00.985	01.225	05.940	00.102	00.084
YB	00.014	00.600	00.870	01.100	04.890	00.106	00.077
LU	00.016	00.660	00.835	01.050	04.530	00.028	00.062
K	00.005	00.019	00.024	00.038	00.521	99.999	00.263
RB	00.010	00.012	00.024	00.032	00.152	12.010	00.048
SR	00.014	00.011	00.318	00.283	00.241	00.377	02.840
BA	00.009	00.006	00.072	00.079	00.232	18.195	00.360
CR	13.000	03.000	100.00	50.000	15.000	12.600	00.245
NI	150.00	30.000	25.000	20.000	35.000	20.000	00.016
TI	00.350	01.000	01.800	01.800	01.500	02.000	00.020
SC	00.100	00.900	06.500	13.140	06.000	11.306	00.101
Y	00.010	00.305	00.945	00.945	06.200	00.030	00.086
NB	00.010	00.305	00.945	00.945	06.200	00.030	00.086
ZR	00.010	00.305	00.945	00.945	05.000	00.030	00.086
MN	07.000	09.000	03.500	03.000	05.000	06.000	00.178
V	00.250	04.000	07.500	07.000	20.000	12.000	00.160
U	00.017	00.077	00.077	00.077	05.000	00.450	00.070
TH	00.013	00.060	00.060	00.060	05.000	00.300	00.059
GA	00.600	00.800	01.010	01.010	00.900	04.000	01.000

AVERAGE DACITIC KD VALUES - KD SET #1

ELEM	GARN	BIOT	APAT	ZIRC	KFLD	MAG	QTZ
LA	00.260	00.034	23.700	02.800	00.054	00.098	00.000
CE	00.350	00.037	34.700	02.640	00.044	00.110	00.000
PR	00.440	00.040	45.700	02.400	00.034	00.125	00.000
NO	00.530	00.044	57.100	02.200	00.025	00.130	00.000
SM	02.660	00.058	62.000	03.140	00.010	00.150	00.000
EU	01.500	00.145	30.400	03.040	01.130	00.100	00.000
GD	10.500	00.082	56.300	12.000	00.011	00.120	00.000
DY	28.600	00.097	50.700	45.700	00.006	00.140	00.000
ER	42.800	00.162	37.200	135.00	00.006	00.155	00.000
YB	39.900	00.179	23.900	270.00	00.012	00.170	00.000
LU	29.600	00.185	20.200	323.00	00.006	00.190	00.000
K	00.020	99.999	00.000	00.000	99.999	00.000	00.000
RB	00.009	03.2 0	00.000	00.000	00.340	00.000	00.000
SR	00.015	00.120	01.000	00.000	03.870	00.000	00.000
BA	00.017	06.360	00.000	00.000	06.120	00.000	00.000
CR	03.280	12.600	00.000	00.000	00.670	96.500	00.000
NI	04.500	20.000	00.000	00.000	00.020	23.333	00.000
TI	00.500	02.000	00.000	00.000	00.040	34.000	00.000
SC	01.000	11.300	00.000	01.000	00.197	02.250	00.000
Y	03.170	00.097	50.700	45.700	00.006	00.000	00.000
NB	03.170	00.097	50.700	45.700	00.006	00.000	00.000
ZR	00.500	01.000	00.000	99.999	00.100	00.000	00.000
MN	05.000	06.000	00.000	00.000	00.310	03.225	00.000
V	01.280	12.000	00.000	00.000	00.200	79.950	00.000
U	00.100	00.450	50.000	50.000	00.100	00.000	00.000
TH	00.100	00.310	50.000	50.000	00.088	00.000	00.000
GA	01.000	04.000	01.000	00.000	00.950	00.000	00.000

LOW DACITIC KD VALUES - KD SET #1

ELEM	OLIV	OPX	DIOP	AUG	HORN	PHLG	PLAG
LA	00.008	00.125	00.200	00.440	00.350	00.102	00.350
CE	00.009	00.149	00.373	00.575	01.055	00.132	00.315
PR	00.010	00.175	00.540	00.710	01.750	00.162	00.280
NO	00.010	00.204	00.730	00.855	02.525	00.186	00.245
SM	00.011	00.240	01.040	01.275	04.515	00.211	00.160
EU	00.010	00.147	01.135	01.380	03.500	00.265	02.470
GD	00.012	00.312	01.235	01.535	05.800	00.190	00.170
DY	00.014	00.422	01.470	01.815	07.250	00.115	00.135
ER	00.017	00.595	01.240	01.625	07.500	00.102	00.156
YB	00.023	00.200	01.125	01.505	04.990	00.106	00.165
LU	00.026	00.990	01.000	02.503	03.560	00.128	00.135
K	00.008	00.011	00.026	00.058	00.741	99.999	00.290
RB	00.011	00.016	00.015	00.036	00.222	02.010	00.091
SR	00.019	00.016	00.341	00.333	00.331	00.377	03.635
BA	00.011	00.008	00.072	00.089	00.387	08.195	00.449
CR	21.600	02.800	150.00	100.00	20.000	17.400	00.670
NI	250.00	35.000	40.000	40.000	40.000	25.000	00.020
TI	00.600	01.200	02.500	02.400	02.000	03.000	00.040
SC	00.300	01.000	07.000	13.680	07.000	11.600	00.197
Y	00.014	00.122	01.395	01.395	07.000	00.030	00.135
NB	00.014	00.122	01.395	01.395	07.000	00.030	00.135
ZR	00.010	00.400	01.395	01.395	06.000	05.000	00.100
MN	07.000	07.500	03.500	03.500	35.000	06.130	00.310
V	00.400	04.500	10.000	06.000	04.000	18.000	00.200
U	00.020	00.090	00.090	00.090	06.000	00.500	00.100
TH	00.015	00.070	00.080	00.080	06.000	00.430	00.088
GA	00.700	00.900	01.300	01.300	01.000	04.500	01.200

LOW DACITIC KD VALUES - KD SET #1

ELEM	GARN	BIOT	APAT	ZIRC	KFLD	MAG	QTZ
LA	00.260	00.034	37.000	03.300	00.054	00.098	00.000
CE	00.350	00.037	52.500	03.000	00.044	00.110	00.000
PR	00.440	00.040	67.000	02.700	00.034	00.125	00.000
NO	00.530	00.044	81.100	02.430	00.025	00.130	00.000
SM	02.660	00.058	89.800	03.700	00.010	00.150	00.000
EU	01.500	00.145	50.200	05.220	01.130	00.100	00.000
GD	10.500	00.082	78.000	14.000	00.011	00.120	00.000
DY	28.600	00.097	69.200	53.500	00.006	00.140	00.000
ER	42.800	00.162	51.200	152.00	00.006	00.155	00.000
YB	39.900	00.179	37.000	299.00	00.012	00.170	00.000
LU	29.600	00.185	30.200	366.00	00.006	00.190	00.000
K	00.020	99.999	00.000	00.000	99.999	00.000	00.000
RB	00.009	03.260	00.000	00.000	00.034	00.000	00.000
SR	00.015	00.120	01.000	00.000	03.870	00.000	00.000
BA	00.017	06.360	00.000	00.000	06.120	00.000	00.000
CR	03.280	17.400	00.000	00.000	00.670	150.00	00.000
NI	06.000	25.000	00.000	00.000	00.020	30.000	00.000
TI	00.500	03.000	00.000	00.000	00.040	40.000	00.000
SC	01.000	11.600	00.000	01.000	00.197	03.000	00.000
Y	03.170	00.030	50.700	45.700	00.006	00.000	00.000
NB	03.170	00.030	50.700	45.700	00.006	00.000	00.000
ZR	00.500	05.000	00.000	99.999	00.100	00.000	00.000
MN	05.000	06.130	00.000	00.000	00.310	04.000	00.000
V	01.280	18.000	00.000	00.000	00.200	100.00	00.000
U	00.100	00.500	50.000	50.000	00.100	00.000	00.000
TH	00.100	00.430	50.000	50.000	00.088	00.000	00.000
GA	01.000	04.500	01.000	00.000	00.950	00.000	00.000

HIGH DACITIC KD VALUES - KD SET #1

ELEM	OLIV	OPX	DIOP	AUG	HORN	PHLG	PLAG
LA	00.001	00.031	00.050	00.050	00.100	00.100	00.109
CE	00.002	00.042	00.202	00.219	00.737	00.132	00.097
PR	00.003	00.043	00.350	00.370	01.300	00.160	00.085
NO	00.003	00.063	00.503	00.555	02.095	00.186	00.072
SM	00.003	00.087	00.805	00.890	04.170	00.211	00.054
EU	00.005	00.058	00.601	00.690	02.380	00.265	00.508
GD	00.004	00.131	00.798	00.910	04.790	00.190	00.039
DY	00.006	00.192	00.663	01.135	06.405	00.115	00.025
ER	00.008	00.303	00.589	00.765	05.520	00.102	00.024
YB	00.009	00.420	00.616	00.785	03.840	00.106	00.018
LU	00.009	00.435	00.676	00.775	02.310	00.128	00.017
K	00.005	00.006	00.023	00.021	00.181	99.999	00.060
RB	00.010	00.009	00.023	00.024	00.030	02.010	00.029
SR	00.009	00.009	00.297	00.305	00.106	00.377	02.845
BA	00.010	00.007	00.072	00.068	00.072	08.195	00.179
CR	07.000	02.500	50.000	40.000	10.000	07.800	00.060
NI	40.000	25.000	05.500	05.500	30.000	15.000	00.010
TI	00.100	00.800	01.250	00.750	01.000	01.000	00.010
SC	00.050	00.800	06.000	12.000	05.000	11.000	00.030
Y	00.006	00.192	00.473	00.473	05.000	00.030	00.025
NB	00.006	00.492	00.473	00.473	05.000	00.030	00.025
ZR	00.007	00.200	00.800	00.800	04.000	03.000	00.060
MN	05.400	02.500	02.700	02.500	04.500	05.870	00.033
V	00.100	03.500	02.700	02.500	15.000	06.000	00.100
U	00.015	00.077	00.077	00.077	04.000	00.200	00.040
TH	00.010	00.059	00.059	00.059	04.000	00.190	00.032
GA	00.500	00.700	00.720	00.720	00.800	03.500	00.800

HIGH DACITIC KD VALUES - KD SET #1

ELEM	GARN	BIOT	APAT	ZIRC	KFLD	MAG	QTZ
LA	00.260	00.029	13.500	02.450	00.054	00.098	00.000
CE	00.350	00.034	18.000	02.290	00.044	00.110	00.000
PR	00.440	00.039	22.500	02.150	00.034	00.125	00.000
NO	00.530	00.044	27.400	01.970	00.025	00.130	00.000
SM	02.660	00.058	29.300	02.580	00.018	00.150	00.000
EU	01.500	00.145	20.500	01.070	01.130	00.100	00.000
GD	10.500	00.082	27.200	10.000	00.011	00.120	00.000
DY	28.600	00.097	25. 00	37.800	00.006	00.140	00.000
ER	42.800	00.162	20.000	119.00	00.006	00.155	00.000
YB	39.900	00.179	13.100	242.00	00.012	00.170	00.000
LU	29.600	00.185	11.200	281.00	00.006	00.190	00.000
K	00.020	99.999	00.000	00.000	99.999	00.000	00.000
RB	00.009	03.2 0	00.000	00.000	00.340	00.000	00.000
SR	00.015	00.120	01.000	00.000	03.870	00.000	00.000
BA	00.017	0 .3 0	00.000	00.000	06.120	00.000	00.000
CR	03.280	07.800	00.000	00.000	00. 70	50.000	00.000
NI	03.000	15.000	00.000	00.000	00.020	15.000	00.000
TI	00.500	01.000	00.000	00.000	00.040	28.000	00.000
SC	01.000	11.000	00.000	01.000	00.197	01.500	00.000
Y	03.170	00.030	50.700	45.700	00.006	00.000	00.000
NB	03.170	00.030	50.700	45.700	00.006	00.000	00.000
ZR	00.500	03.000	00.000	99.999	00.100	00.000	00.000
MN	05.000	05.870	00.000	00.000	00.310	02.500	00.000
V	01.280	06.000	00.000	00.000	00.200	57.000	00.000
U	00.100	00.200	50.000	50.000	00.100	00.000	00.000
TH	00.100	00.190	50.000	50.000	00.088	00.000	00.000
GA	01.000	03.500	01.000	00.000	00.950	00.000	00.000

AVERAGE RHYOLITIC KD VALUES - KD SET #1

ELEM	OLIV	OPX	DIOP	AUG	HORN	PHLG	PLAG
LA	00.006	00.115	00.215	00.215	00.200	00.175	00.300
CE	00.006	00.150	00.260	00.260	01.520	00.230	00.270
PR	00.006	00.185	00.305	00.305	02.900	00.285	00.240
ND	00.006	00.220	00.350	00.350	04.260	00.340	00.210
SM	00.006	00.270	00.380	00.380	07.770	00.390	00.130
EU	00.006	00.170	00.270	00.270	05.140	00.500	02.150
GD	00.007	00.340	00.460	00.460	10.000	00.350	00.097
DY	00.009	00.460	00.550	00.550	13.000	00.200	00.064
ER	00.011	00.005	00.730	00.730	12.000	00.170	00.055
YB	00.014	00.880	00.990	00.990	08.380	00.170	00.049
LU	00.016	00.900	01.140	01.114	05.500	00.210	00.016
K	00.005	00.002	00.002	00.002	00.031	99.999	00.100
RB	00.007	00.002	00.002	00.002	00.014	00.940	00.041
SR	00.014	00.008	00.008	00.008	00.022	00. 72	04.400
BA	00.009	00.002	00.002	00.002	00.044	15.300	00.308
CR	20.000	06.000	200.00	100.00	30.000	12. 00	00.245
NI	300.00	60.000	50.000	40.000	70.000	20.000	00.016
TI	00.700	02.000	03.600	03.600	03.000	02.000	00.020
SC	00.100	01.800	16.280	26.280	12.000	11.300	00.101
Y	00.010	00.900	01.890	01.890	09.175	00.030	00.086
NB	00.010	00.900	01.890	01.890	09.175	00.030	00.086
ZR	00.010	00.630	01.900	01.900	10.000	00.030	00.086
MN	14.000	18.000	07.000	06.000	10.000	06.000	00.178
V	00.500	08.000	15.000	14.000	40.000	12.000	00.160
U	00.017	00.153	00.153	00.153	07.000	00.450	00.070
TH	00.013	00.117	00.117	00.117	07.000	00.310	00.059
GA	00.600	00.900	02.778	02.778	00.900	04.000	01.000

AVERAGE RHYOLITIC KD VALUES - KD SET #1

ELEM	GARN	BIOT	APAT	ZIRC	KFLD	MAG	QTZ
LA	00.260	00.335	26.000	02.800	00.054	00.098	00.000
CE	00.350	00.320	34.700	02.640	00.044	00.110	00.000
PR	00.440	00.305	42.000	02.400	00.034	00.125	00.000
NO	00.530	00.290	57.100	02.200	00.025	00.130	00.000
SM	02.660	00.260	62.000	03.140	00.010	00.150	00.000
EU	01.500	00.240	30.400	03.140	01.130	00.100	00.000
GD	10.500	00.280	56.300	12.000	00.011	00.120	00.000
DY	28.600	00.290	50.700	45.700	00.006	00.140	00.000
ER	42.800	00.350	37.200	135.00	00.006	00.155	00.000
YB	39.900	00.440	23.900	270.00	00.012	00.170	00.000
LU	29.600	00.330	20.200	323.00	00.006	00.190	00.000
K	00.020	99.999	00.000	00.000	99.999	00.000	00.000
RB	00.009	02.240	00.000	00.000	00.340	00.000	00.000
SR	00.015	00.120	01.000	00.000	03.870	00.000	00.000
BA	00.017	09.700	00.000	00.000	06.120	00.000	00.000
CR	07.000	12.600	00.000	00.000	00. 70	96.500	00.000
NI	09.000	20.000	00.000	00.000	00.020	23.333	00.000
TI	00.500	02.000	00.000	00.000	00.040	34.000	00.000
SC	01.000	11.300	00.000	01.000	00.197	02.250	00.000
Y	03.170	00.097	50.700	45.700	00.006	00.000	00.000
NB	03.170	00.097	50.700	45.700	00.006	00.000	00.000
ZR	00.500	04.000	00.000	99.999	00.100	00.000	00.000
MN	05.000	06.000	00.000	00.000	00.310	03.225	00.000
V	01.280	12.000	00.000	00.000	00.200	79.950	00.000
U	00.100	00.450	50.000	50.000	00.100	00.000	00.000
TH	00.100	00.310	50.000	50.000	00.088	00.000	00.000
GA	01.000	04.000	01.000	00.000	00.950	00.000	00.000

LOW RHYOLITIC KD VALUES - KD SET #1

ELEM	OLIV	OPX	DIOP	AUG	HORN	PHLG	PLAG
LA	00.008	00.215	00.350	00.350	00.400	00.175	00.380
CE	00.009	00.260	00.650	00.650	01.770	00.230	00.350
PR	00.009	00.305	00.950	00.950	03.100	00.285	00.320
ND	00.010	00.350	01.280	01.280	04.490	00.340	00.290
SM	00.011	00.380	01.810	01.810	08.100	00.390	00.150
EU	00.010	00.270	02.010	02.010	05.900	00.500	02.810
GD	00.012	00.460	02.200	02.200	10.500	00.350	00.130
DY	00.014	00.550	02.630	02.630	13.500	00.200	00.080
ER	00.017	00.730	02.250	02.250	14.000	00.170	00.072
YB	00.023	00.990	02.010	02.010	09.000	00.170	00.070
LU	00.026	01.140	01.810	01.810	06.300	00.210	00.008
K	00.008	00.002	00.037	00.037	00.081	99.999	00.100
RB	00.011	00.002	00.032	00.032	00.014	00.940	00.041
SR	00.019	00.008	00.516	00.516	00.022	00.672	04.400
BA	00.011	00.002	00.131	00.131	00.044	15.300	00.308
CR	42.000	05.600	300.00	200.00	40.000	17.400	00.670
NI	500.00	70.000	80.000	80.000	80.000	25.000	00.020
TI	00.840	01.900	04.000	04.000	08.000	03.000	00.040
SC	00.300	02.000	20.500	27.500	12.000	11.600	00.197
Y	00.014	00.900	02.790	02.790	10.000	00.030	00.135
NB	00.014	00.900	02.790	02.790	10.000	00.030	00.135
ZR	00.010	00.800	02.800	02.800	10.000	05.000	00.100
MN	14.000	15.000	07.000	07.000	10.000	06.130	00.310
V	00.800	09.000	20.000	12.000	40.000	18.000	00.200
U	00.020	00.180	00.153	00.153	08.000	00.500	00.100
TH	00.015	00.127	00.117	00.117	08.000	00.430	00.088
GA	00.700	01.000	03.575	03.575	01.000	04.500	01.200

LOW RHYOLITIC KD VALUES - KD SET #1

ELEM	GARN	BIOT	APAT	ZIRC	KFLD	MAG	QTZ
LA	00.260	00.335	37.000	03.300	00.054	00.098	00.000
CE	00.350	00.320	52.500	03.000	00.044	00.110	00.000
PR	00.440	00.305	67.000	02.700	00.034	00.125	00.000
ND	00.530	00.290	81.100	02.430	00.025	00.130	00.000
SM	02.660	00.260	89.800	03.700	00.018	00.150	00.000
EU	01.500	00.240	50.200	05.220	01.130	00.100	00.000
GD	10.500	00.280	78.000	14.000	00.011	00.120	00.000
DY	28.600	00.290	69.200	53.500	00.006	00.140	00.000
ER	42.800	00.350	51.200	152.00	00.006	00.155	00.000
YB	39.900	00.440	37.000	299.00	00.012	00.170	00.000
LU	29.600	00.330	30.200	366.00	00.006	00.190	00.000
K	00.020	99.999	00.000	00.000	99.999	00.000	00.000
RB	00.008	02.240	00.000	00.000	00.340	00.000	00.000
SR	00.015	00.120	01.000	00.000	03.870	00.000	00.000
BA	00.017	09.700	00.000	00.000	06.120	00.000	00.000
CR	10.000	17.400	00.000	00.000	00. 70	150.00	00.000
NI	15.000	25.000	00.000	00.000	00.020	30.000	00.000
TI	00.500	03.000	00.000	00.000	00.040	40.000	00.000
SC	01.000	11.600	00.000	01.000	00.197	03.000	00.000
Y	03.170	00.030	50.700	45.700	00.006	00.000	00.000
NB	03.170	00.030	50.700	45.700	00.006	00.000	00.000
ZR	00.500	05.000	00.000	99.999	00.100	00.000	00.000
MN	05.000	06.130	00.000	00.000	00.310	04.000	00.000
V	01.280	18.000	00.000	00.000	00.200	100.00	00.000
U	00.100	00.500	50.000	50.000	00.100	00.000	00.000
TH	00.100	00.430	50.000	50.000	00.800	00.000	00.000
GA	01.000	04.500	01.000	00.000	00.950	00.000	00.000

HIGH RHYOLITIC KD VALUES - KD SET #1

ELEM	OLIV	OPX	DIOP	AUG	HORN	PHLG	PLAG
LA	00.001	00.060	00.070	00.070	00.100	00.180	00.195
CE	00.002	00.082	00.360	00.360	01.380	00.230	00.170
PR	00.002	00.100	00.650	00.650	02.700	00.280	00.145
ND	00.003	00.120	00.940	00.940	04.030	00.340	00.120
SM	00.003	00.160	01.520	01.520	07.100	00.390	00.084
EU	00.005	00.093	01.110	01.110	04.500	00.500	00.960
GD	00.004	00.230	01.500	01.500	09.300	00.350	00.060
DY	00.006	00.330	01.220	01.220	12.500	00.200	00.040
ER	00.008	00.530	01.070	01.070	10.800	00.170	00.038
YB	00.009	00.730	01.114	01.114	07.450	00.170	00.030
LU	00.009	00.760	01.280	01.280	04.400	00.210	00.030
K	00.005	00.002	00.037	00.037	00.081	99.999	00.100
RB	00.008	00.002	00.032	00.032	00.014	00.940	00.041
SR	00.009	00.008	00.516	05.000	00.022	00. 72	04.400
BA	00.008	00.002	00.131	05.000	00.044	15.300	00.308
CR	14.000	05.000	100.00	80.000	20.000	07.800	00.060
NI	80.000	50.000	11.000	11.000	60.000	15.000	00.010
TI	00.420	01.500	03.200	03.200	04.000	01.000	00.010
SC	00.050	01.600	15.200	25.200	10.000	11.000	00.030
Y	00.006	00.900	00.945	00.945	08.400	00.030	00.025
NB	00.006	00.900	00.945	00.945	08.400	00.030	00.025
ZR	00.007	00.400	01.600	01.600	08.000	03.000	00.060
MN	09.000	15.000	05.500	05.000	09.000	05.870	00.033
V	00.200	07.000	05.500	05.000	30.000	06.000	00.100
U	00.015	00.140	00.153	00.153	00.140	00.200	00.040
TH	00.010	00.118	00.117	00.117	00.110	00.190	00.032
GA	00.500	00.800	01.980	01.980	00.800	03.500	00.800

HIGH RHYOLITIC KD VALUES - KD SET #1

ELEM	GARN	BIOT	APAT	ZIRC	KFLD	MAG	QTZ
LA	00.260	00.335	13.500	02.350	00.054	00.098	00.000
CE	00.350	00.320	18.000	02.290	00.044	00.110	00.000
PR	00.440	00.305	22.500	02.150	00.034	00.125	00.000
ND	00.530	00.290	27.400	01.970	00.025	00.130	00.000
SM	02.660	00.260	29.300	02.580	00.018	00.150	00.000
EU	01.500	00.240	20.500	01.070	01.130	00.100	00.000
GD	10.500	00.280	27.200	10.000	00.011	00.120	00.000
DY	28.600	00.290	25.600	37.800	00.006	00.140	00.000
ER	42.800	00.350	20.000	119.00	00.006	00.155	00.000
YB	39.900	00.440	13.100	242.00	00.012	00.170	00.000
LU	29.600	00.330	11.200	281.00	00.006	00.190	00.000
K	00.020	99.999	00.000	00.000	99.999	00.000	00.000
RB	00.008	02.240	00.000	00.000	00.340	00.000	00.000
SR	00.015	00.120	01.000	00.000	03.870	00.000	00.000
BA	00.017	09.700	00.000	00.000	06.120	00.000	00.000
CR	05.000	07.800	00.000	00.000	00.670	50.000	00.000
NI	07.000	1 .000	00.000	00.000	00.020	15.000	00.000
TI	00.500	01.000	00.000	00.000	00.040	28.000	00.000
SC	01.000	11.000	00.000	01.000	00.197	01.500	00.000
Y	03.170	00.030	50.700	45.700	00.006	00.000	00.000
NB	03.170	00.030	50.700	45.700	00.006	00.000	00.000
ZR	00.500	03.000	00.000	99.999	00.100	00.000	00.000
MN	05.000	05.870	00.000	00.000	00.310	02.500	00.000
V	01.280	06.000	00.000	00.000	00.200	57.000	00.000
U	00.100	00.200	50.000	50.000	00.100	00.000	00.000
TH	00.100	00.190	50.000	50.000	00.088	00.000	00.000
GA	01.000	03.500	01.000	00.000	00.950	00.000	00.000

AVERAGE BASALTIC KD VALUES - KD SET #2

ELEM	OLIV	OPX	DIOP	AUG	HORN	PHIG	PLAG
LA	00.006	00.020	00.045	00.010	00.145	00.035	00.140
CE	00.006	00.024	00.070	00.025	00.200	00.034	00.120
PR	00.006	00.028	00.095	00.155	00.265	00.033	00.100
ND	00.006	00.033	00.120	00.310	00.330	00.032	00.081
SM	00.006	00.054	00.180	00.500	00.520	00.031	00.067
EU	00.006	00.054	00.180	00.510	00.590	00.030	00.340
GD	00.007	00.091	00.190	00.610	00.630	00.030	00.063
DY	00.009	00.150	00.210	00.680	00.640	00.030	00.055
ER	00.011	00.230	00.170	00.650	00.550	00.034	00.063
YB	00.014	00.340	00.160	00.620	00.490	00.042	00.067
LU	00.016	00.420	00.130	00.560	00.430	00.046	00.060
K	00.005	00.014	00.011	00.038	00.960	99.999	00.170
RB	00.007	00.022	00.015	00.031	00.290	03.080	00.071
SR	00.014	00.017	00.120	00.120	00.460	00.081	01.830
BA	00.009	00.013	00.013	00.026	00.420	01.090	00.230
CR	02.700	00.600	20.000	10.000	03.000	12.600	00.100
NI	23.800	06.000	04.500	04.500	07.000	20.000	00.008
TI	00.070	00.500	00.340	00.900	00.800	01.000	00.010
SC	00.100	01.230	02.000	02.920	02.180	05.300	00.020
Y	00.010	00.150	00.210	00.680	00.640	00.030	00.055
NB	00.010	00.150	00.210	00.680	00.640	00.030	00.055
ZR	00.010	00.150	00.200	00.400	01.000	00.030	00.005
MN	01.250	01.440	00.630	00.630	00.940	06.000	00.060
V	00.050	00.800	01.300	01.300	04.000	12.000	00.080
U	00.017	00.017	00.017	00.017	00.540	00.450	00.090
TH	00.013	00.013	00.013	00.013	00.540	00.310	00.090
GA	00.600	00.600	00.505	00.505	00.800	04.000	00.090

AVERAGE BASALTIC KD VALUES - KD SET #2

ELEM	GARN	BIOT	APAT	ZIRC	KFLD	MAG	QTZ
LA	00.008	00.033	26.500	02.400	00.053	00.098	00.000
CE	00.028	00.037	34.700	02.640	00.044	00.110	00.000
PR	00.048	00.040	42.055	02.800	00.035	00.125	00.000
ND	00.068	00.044	57.100	02.200	00.025	00.130	00.000
SM	00.290	00.058	62.000	03.140	00.010	00.150	00.000
EU	00.490	00.145	30.400	03.140	01.130	00.100	00.000
GD	00.970	00.082	56.300	12.000	00.011	00.120	00.000
DY	03.170	00.097	50.700	45.700	00.006	00.140	00.000
ER	06.560	00.162	37.200	135.00	00.006	00.155	00.000
YB	11.500	00.179	23.900	270.00	00.012	00.170	00.000
LU	11.900	00.185	20.200	323.00	00.006	00.190	00.000
K	00.015	99.999	00.000	00.000	99.999	00.000	00.000
RB	00.042	03.260	00.000	00.000	00.340	00.000	00.000
SR	00.012	00.120	01.000	00.000	03.870	00.000	00.000
BA	00.023	06.360	00.000	00.000	06.120	00.000	00.000
CR	03.280	12.600	00.000	00.000	00.670	96.500	00.000
NI	02.000	20.000	00.000	00.000	00.020	23.333	00.000
TI	00.500	02.000	00.000	00.000	00.040	34.000	00.000
SC	01.000	11.300	00.000	01.000	00.197	02.250	00.000
Y	03.170	00.097	50.700	45.700	00.006	00.000	00.000
NB	03.170	00.097	50.700	45.700	00.006	00.000	00.000
ZR	00.500	01.000	00.000	99.999	00.100	00.000	00.000
MN	05.000	06.000	00.000	00.000	00.310	03.225	00.000
V	01.280	12.000	00.000	00.000	00.200	79.950	00.000
U	00.100	00.450	50.000	50.000	00.100	00.000	00.000
TH	00.100	00.310	50.000	50.000	00.088	00.000	00.000
GA	01.000	04.000	01.000	00.000	00.950	00.000	00.000

LOW BASALTIC KD VALUES - KD SET #2

ELEM	OLIV	OPX	DIOP	AUG	HORN	PHLG	PLAG
LA	00.008	00.028	00.050	00.100	00.230	00.035	00.320
CE	00.009	00.038	00.096	00.210	00.340	00.034	00.280
PR	00.010	00.048	00.140	00.320	00.440	00.033	00.240
ND	00.010	00.058	00.180	00.430	00.560	00.032	00.200
SM	00.011	00.100	00.260	00.740	00.930	00.031	00.170
EU	00.010	00.079	00.260	00.750	01.100	00.030	00.730
GD	00.012	00.171	00.270	00.870	01.150	00.030	00.210
DY	00.014	00.293	00.310	01.000	01.050	00.030	00.190
ER	00.017	00.460	00.230	01.100	01.000	00.034	00.240
YB	00.023	00.670	00.230	01.000	00.980	00.042	00.300
LU	00.026	00.840	00.190	00.950	00.820	00.046	00.240
K	00.008	00.019	00.014	00.078	01.400	99.999	00.360
RB	00.011	00.029	00.015	00.039	00.430	03.006	00.140
SR	00.019	00.024	00.150	00.150	00.640	00.081	02.870
BA	00.011	00.014	00.013	00.046	00.730	01.090	00.590
CR	04.200	00.700	30.000	20.000	04.000	17.400	00.200
NI	49.200	07.000	07.900	07.900	08.000	25.000	00.010
TI	00.120	00.600	00.430	00.430	01.000	01.500	00.020
SC	00.300	01.330	02.040	03.040	02.220	05.800	00.030
Y	00.014	00.290	00.310	01.000	01.000	00.030	00.240
NB	00.014	00.290	00.310	01.000	01.000	00.030	00.240
ZR	00.010	00.300	00.310	00.600	01.200	00.030	00.010
MN	01.430	01.530	00.710	00.710	00.970	06.130	00.060
V	00.080	00.900	02.150	01.150	07.000	18.000	00.150
U	00.020	00.020	00.017	00.020	00.800	00.500	01.000
TH	00.015	00.015	00.013	00.015	00.700	00.430	00.100
GA	00.700	00.700	00.650	00.650	00.800	04.500	00.100

LOW BASALTIC KD VALUES - KD SET #2

ELEM	GARN	BIOT	APAT	ZIRC	KFLD	MAG	QTZ
LA	00.008	00.033	37.000	03.300	00.053	00.098	00.000
CE	00.028	00.037	52.500	03.000	00.044	00.110	00.000
PR	00.048	00.040	67.000	02.700	00.033	00.125	00.000
ND	00.068	00.044	81.100	02.430	00.025	00.130	00.000
SM	00.290	00.058	89.800	03.700	00.018	00.150	00.000
EU	00.490	00.145	50.200	05.220	01.130	00.100	00.000
GD	00.970	00.082	78.000	14.000	00.011	00.120	00.000
DY	03.170	00.097	69.200	53.500	00.006	00.140	00.000
ER	06.560	00.162	51.200	152.00	00.006	00.155	00.000
YB	11.500	00.179	37.000	299.00	00.012	00.170	00.000
LU	11.900	00.185	30.200	366.00	00.006	00.190	00.000
K	00.015	99.999	00.000	00.000	99.999	00.000	00.000
RB	00.042	03.260	00.000	00.000	00.340	00.000	00.000
SR	00.012	00.120	01.000	00.000	03.870	00.000	00.000
BA	00.023	06.360	00.000	00.000	06.120	00.000	00.000
CR	03.280	17.400	00.000	00.000	00. 70	150.00	00.000
NI	03.000	25.000	00.000	00.000	00.020	30.000	00.000
TI	00.500	01.500	00.000	00.000	00.040	40.000	00.000
SC	01.000	05.800	00.000	01.000	00.197	03.000	00.000
Y	03.170	00.030	50.700	45.700	00.006	00.000	00.000
NB	03.170	00.030	50.700	45.700	00.006	00.000	00.000
ZR	00.500	00.300	00.000	99.999	00.100	00.000	00.000
MN	05.000	06.130	00.000	00.000	00.310	04.000	00.000
V	01.280	18.000	00.000	00.000	00.200	100.00	00.000
U	00.100	00.500	50.000	50.000	00.100	00.000	00.000
TH	00.100	00.430	50.000	50.000	00.088	00.000	00.000
GA	01.000	04.500	01.000	00.000	00.950	00.000	00.000

HIGH BASALTIC KD VALUES - KD SET #2

ELEM	OLIV	OPX	DIOP	AUG	HORN	PHLG	PLAG
LA	00.002	00.001	00.032	00.027	00.060	00.035	00.022
CE	00.002	00.002	00.043	00.077	00.094	00.034	00.023
PR	00.002	00.005	00.054	00.127	00.130	00.033	00.023
ND	00.003	00.008	00.065	00.170	00.160	00.032	00.023
SM	00.003	00.014	00.090	00.260	00.240	00.031	00.024
EU	00.005	00.023	00.091	00.270	00.260	00.030	00.055
GD	00.004	00.032	00.095	00.320	00.280	00.030	00.017
DY	00.006	00.054	00.105	00.500	00.310	00.030	00.010
ER	00.008	00.076	00.107	00.460	00.240	00.034	00.010
YB	00.009	00.110	00.092	00.430	00.230	00.042	00.006
LU	00.009	00.110	00.071	00.270	00.220	00.046	00.004
K	00.005	00.009	00.008	00.004	00.330	99.999	00.019
RB	00.008	00.015	00.014	00.015	00.045	03.080	00.016
SR	00.009	00.010	00.078	00.093	00.190	00.081	01.290
BA	00.009	00.012	00.013	00.004	00.100	01.090	00.050
CR	01.200	00.500	10.000	08.000	02.000	07.800	00.080
NI	08.400	05.000	01.100	01.100	06.000	15.000	00.006
TI	00.020	00.400	00.250	00.150	00.800	00.500	00.005
SC	00.050	01.130	01.800	02.800	02.140	05.000	00.010
Y	00.006	00.054	00.105	00.500	00.310	00.030	00.010
NB	00.006	00.054	00.105	00.500	00.310	00.030	00.010
ZR	00.007	00.100	00.100	00.200	00.600	00.030	00.003
MN	01.070	01.350	00.550	00.450	00.910	05.870	00.040
V	00.020	00.700	00.550	00.450	03.000	06.000	00.060
U	00.015	00.015	00.017	00.017	00.150	00.200	00.070
TH	00.010	00.010	00.013	00.013	00.100	00.190	00.070
GA	00.500	00.500	00.360	00.360	00.800	03.500	00.080

HIGH BASALTIC KD VALUES - KD SET #2

ELEM	GARN	BIOT	APAT	ZIRC	KFLD	MAG	QTZ
LA	00.008	00.033	13.500	02.450	00.055	00.098	00.000
CE	00.028	00.037	18.000	02.290	00.044	00.110	00.000
PR	00.048	00.040	22.500	02.150	00.035	00.125	00.000
ND	00.068	00.044	27.400	01.970	00.025	00.130	00.000
SM	00.290	00.058	29.300	02.580	00.018	00.150	00.000
EU	00.490	00.145	20.500	01.070	01.130	00.100	00.000
GD	00.970	00.082	27.200	10.000	00.011	00.120	00.000
DY	03.170	00.097	25.600	37.800	00.006	00.140	00.000
ER	06.560	00.162	20.000	119.00	00.006	00.155	00.000
YB	11.500	00.179	13.100	242.00	00.012	00.170	00.000
LU	11.900	00.185	11.200	281.00	00.006	00.190	00.000
K	00.015	99.999	00.000	00.000	99.999	00.000	00.000
RB	00.042	03.2 0	00.000	00.000	00.340	00.000	00.000
SR	00.012	00.120	01.000	00.000	03.870	00.000	00.000
BA	00.023	0 .3 0	00.000	00.000	06.120	00.000	00.000
CR	03.280	07.800	00.000	00.000	00. 70	50.000	00.000
NI	01.000	15.000	00.000	00.000	00.020	15.000	00.000
TI	00.500	01.000	00.000	00.000	00.040	28.000	00.000
SC	01.000	05.000	00.000	01.000	00.197	01.500	00.000
Y	03.170	00.030	50.700	45.700	00.006	00.000	00.000
NB	03.170	00.030	50.700	45.700	00.006	00.000	00.000
ZR	00.500	00.030	00.000	99.999	00.100	00.000	00.000
MN	05.000	05.870	00.000	00.000	00.310	02.500	00.000
V	01.280	06.000	00.000	00.000	00.200	57.000	00.000
U	00.100	00.200	50.000	50.000	00.100	00.000	00.000
TH	00.100	00.190	50.000	50.000	00.088	00.000	00.000
GA	01.000	03.500	01.000	00.000	00.950	00.000	00.000

AVERAGE DACITIC KD VALUES - KD SET #2

ELEM	OLIV	OPX	DIOP	AUG	HORN	PHLG	PLAG
LA	00.005	00.067	00.120	00.350	00.100	00.107	00.275
CE	00.006	00.087	00.285	00.475	00.899	00.132	00.240
PR	00.006	00.107	00.440	00.590	01.850	00.157	00.205
ND	00.006	00.123	00.612	00.710	02.800	00.186	00.170
SM	00.006	00.162	00.925	01.085	03.990	00.211	00.130
EU	00.006	00.112	00.870	01.035	03.440	00.265	02.110
GD	00.007	00.216	01.020	01.230	05.480	00.190	00.090
DY	00.009	00.305	01.070	01.305	06.200	00.115	00.086
ER	00.011	00.440	00.985	01.225	05.940	00.102	00.084
YB	00.014	00.600	00.870	01.100	04.890	00.106	00.077
LU	00.016	00.660	00.835	01.050	04.530	00.028	00.062
K	00.005	00.019	00.024	00.038	00.521	99.999	00.263
RB	00.010	00.012	00.024	00.032	00.152	12.010	00.048
SR	00.014	00.011	00.318	00.283	00.241	00.377	02.840
BA	00.009	00.006	00.072	00.079	00.232	18.195	00.360
CR	13.000	03.000	100.00	50.000	15.000	12.600	00.245
NI	150.00	30.000	25.000	20.000	35.000	20.000	00.016
TI	00.350	01.000	01.800	01.800	01.500	02.000	00.020
SC	00.100	00.900	06.500	13.140	06.000	11.306	00.101
Y	00.010	00.305	00.945	00.945	06.200	00.030	00.086
NB	00.010	00.305	00.945	00.945	06.200	00.030	00.086
ZR	00.010	00.305	00.945	00.945	05.000	00.030	00.086
MN	07.000	09.000	03.500	03.000	05.000	06.000	00.178
V	00.250	04.000	07.500	07.000	20.000	12.000	00.160
U	00.017	00.077	00.077	00.077	05.000	00.450	00.070
TH	00.013	00.060	00.060	00.060	05.000	00.300	00.059
GA	00.600	00.800	01.010	01.010	00.900	04.000	00.800

AVERAGE DACITIC KD VALUES - KD SET #2

ELEM	GARN	BIOT	APAT	ZIRC	KFLD	MAG	QTZ
LA	00.260	00.034	23.700	02.800	00.054	00.098	00.000
CE	00.350	00.037	34.700	02.640	00.044	00.110	00.000
PR	00.440	00.040	45.700	02.400	00.034	00.125	00.000
ND	00.530	00.044	57.100	02.200	00.025	00.130	00.000
SM	02.660	00.058	62.000	03.140	00.010	00.150	00.000
EU	01.500	00.145	30.400	03.040	01.130	00.100	00.000
GD	10.500	00.082	56.300	12.000	00.011	00.120	00.000
DY	28.600	00.097	50.700	45.700	00.006	00.140	00.000
ER	42.800	00.162	37.200	135.00	00.006	00.155	00.000
YB	39.900	00.179	23.900	270.00	00.012	00.170	00.000
LU	29.600	00.185	20.200	323.00	00.006	00.190	00.000
K	00.020	99.999	00.000	00.000	99.999	00.000	00.000
RB	00.009	03.2 0	00.000	00.000	00.340	00.000	00.000
SR	00.015	00.120	01.000	00.000	03.870	00.000	00.000
BA	00.017	06.360	00.000	00.000	06.120	00.000	00.000
CR	03.280	12.600	00.000	00.000	00.670	96.500	00.000
NI	04.500	20.000	00.000	00.000	00.020	23.333	00.000
TI	00.500	02.000	00.000	00.000	00.040	34.000	00.000
SC	01.000	11.300	00.000	01.000	00.197	02.250	00.000
Y	03.170	00.097	50.700	45.700	00.006	00.000	00.000
NB	03.170	00.097	50.700	45.700	00.006	00.000	00.000
ZR	00.500	01.000	00.000	99.999	00.100	00.000	00.000
MN	05.000	06.000	00.000	00.000	00.310	03.225	00.000
V	01.280	12.000	00.000	00.000	00.200	79.950	00.000
U	00.100	00.450	50.000	50.000	00.100	00.000	00.000
TH	00.100	00.310	50.000	50.000	00.088	00.000	00.000
GA	01.000	04.000	01.000	00.000	00.950	00.000	00.000

LOW DACITIC KD VALUES - KD SET #2

ELEM	OLIV	OPX	DIOP	AUG	HORN	PHLG	PLAG
LA	00.008	00.125	00.200	00.440	00.350	00.102	00.350
CE	00.009	00.149	00.373	00.575	01.055	00.132	00.315
PR	00.010	00.175	00.540	00.710	01.750	00.162	00.280
ND	00.010	00.204	00.730	00.855	02.525	00.186	00.245
SM	00.011	00.240	01.040	01.275	04.515	00.211	00.160
EU	00.010	00.147	01.135	01.380	03.500	00.265	02.470
GD	00.012	00.312	01.235	01.535	05.800	00.190	00.170
DY	00.014	00.422	01.470	01.815	07.250	00.115	00.135
ER	00.017	00.595	01.240	01.625	07.500	00.102	00.156
YB	00.023	00.200	01.125	01.505	04.990	00.106	00.165
LU	00.026	00.990	01.000	02.503	03.560	00.128	00.135
K	00.008	00.011	00.026	00.058	00.741	99.999	00.290
RB	00.011	00.016	00.015	00.036	00.222	02.010	00.091
SR	00.019	00.016	00.341	00.333	00.331	00.377	03.635
BA	00.011	00.008	00.072	00.089	00.387	08.195	00.449
CR	21.600	02.800	150.00	100.00	20.000	17.400	00.670
NI	250.00	35.000	40.000	40.000	40.000	25.000	00.020
TI	00.600	01.200	02.500	02.400	02.000	03.000	00.040
SC	00.300	01.000	07.000	13.680	07.000	11.600	00.197
Y	00.014	00.122	01.395	01.395	07.000	00.030	00.135
NB	00.014	00.122	01.395	01.395	07.000	00.030	00.135
ZR	00.010	00.400	01.395	01.395	06.000	05.000	00.100
MN	07.000	07.500	03.500	03.500	35.000	06.130	00.310
V	00.400	04.500	10.000	06.000	04.000	18.000	00.200
U	00.020	00.090	00.090	00.090	06.000	00.500	00.100
TH	00.015	00.070	00.080	00.080	06.000	00.430	00.088
GA	00.700	00.900	01.300	01.300	01.000	04.500	00.900

LOW DACITIC KD VALUES - KD SET #2

ELEM	GARN	BIOT	APAT	ZIRC	KFLD	MAG	QTZ
LA	00.260	00.034	37.000	03.300	00.054	00.098	00.000
CE	00.350	00.037	52.500	03.000	00.044	00.110	00.000
PR	00.440	00.040	67.000	02.700	00.034	00.125	00.000
ND	00.530	00.044	81.100	02.430	00.025	00.130	00.000
SM	02.660	00.058	89.800	03.700	00.010	00.150	00.000
EU	01.500	00.145	50.200	05.220	01.130	00.100	00.000
GD	10.500	00.082	78.000	14.000	00.011	00.120	00.000
DY	28.600	00.097	69.200	53.500	00.006	00.140	00.000
ER	42.800	00.162	51.200	152.00	00.006	00.155	00.000
YB	39.900	00.179	37.000	299.00	00.012	00.170	00.000
LU	29.600	00.185	30.200	366.00	00.006	00.190	00.000
K	00.020	99.999	00.000	00.000	99.999	00.000	00.000
RB	00.009	03.260	00.000	00.000	00.034	00.000	00.000
SR	00.015	00.120	01.000	00.000	03.870	00.000	00.000
BA	00.017	06.360	00.000	00.000	06.120	00.000	00.000
CR	03.280	17.400	00.000	00.000	00.670	150.00	00.000
NI	06.000	25.000	00.000	00.000	00.020	30.000	00.000
TI	00.500	03.000	00.000	00.000	00.040	40.000	00.000
SC	01.000	11.600	00.000	01.000	00.197	03.000	00.000
Y	03.170	00.030	50.700	45.700	00.006	00.000	00.000
NB	03.170	00.030	50.700	45.700	00.006	00.000	00.000
ZR	00.500	05.000	00.000	99.999	00.100	00.000	00.000
MN	05.000	06.130	00.000	00.000	00.310	04.000	00.000
V	01.280	18.000	00.000	00.000	00.200	100.00	00.000
U	00.100	00.500	50.000	50.000	00.100	00.000	00.000
TH	00.100	00.430	50.000	50.000	00.088	00.000	00.000
GA	01.000	04.500	01.000	00.000	00.950	00.000	00.000

HIGH DACITIC KD VALUES - KD SET #2

ELEM	OLIV	OPX	DICP	AUG	HCHN	PHLG	PLAG
LA	00.001	00.031	00.050	00.050	00.100	00.100	00.109
CE	00.002	00.042	00.202	00.219	00.737	00.132	00.097
PR	00.003	00.043	00.350	00.370	01.300	00.160	00.085
ND	00.003	00.063	00.503	00.555	02.095	00.186	00.072
SM	00.003	00.087	00.805	00.890	04.170	00.211	00.054
EU	00.005	00.058	00.601	00.690	02.380	00.265	00.508
GD	00.004	00.131	00.798	00.910	04.790	00.190	00.039
DY	00.006	00.192	00.663	01.135	06.405	00.115	00.025
ER	00.008	00.303	00.589	00.765	05.520	00.102	00.024
YB	00.009	00.420	00.616	00.785	03.840	00.106	00.018
LU	00.009	00.435	00.676	00.775	02.310	00.128	00.017
K	00.005	00.006	00.023	00.021	00.181	99.999	00.060
RB	00.010	00.009	00.023	00.024	00.030	02.010	00.029
SR	00.009	00.009	00.297	00.305	00.106	00.377	02.845
BA	00.010	00.007	00.072	00.068	00.072	08.195	00.179
CR	07.000	02.500	50.000	40.000	10.000	07.800	00.060
NI	40.000	25.000	05.500	05.500	30.000	15.000	00.010
TI	00.100	00.800	01.250	00.750	01.000	01.000	00.010
SC	00.050	00.800	06.000	12.000	05.000	11.000	00.030
Y	00.006	00.192	00.473	00.473	05.000	00.030	00.025
NB	00.006	00.492	00.473	00.473	05.000	00.030	00.025
ZR	00.007	00.200	00.800	00.800	04.000	03.000	00.060
MN	05.400	02.500	02.700	02.500	04.500	05.870	00.033
V	00.100	03.500	02.700	02.500	15.000	06.000	00.100
U	00.015	00.077	00.077	00.077	04.000	00.200	00.040
TH	00.010	00.059	00.059	00.059	04.000	00.190	00.032
GA	00.500	00.700	00.720	00.720	00.800	03.500	00.700

HIGH DACITIC KD VALUES - KD SET #2

ELEM	GARN	BIOT	APAT	ZIRC	KFLD	MAG	QTZ
LA	00.260	00.029	13.500	02.450	00.054	00.098	00.000
CE	00.350	00.034	18.000	02.290	00.044	00.110	00.000
PR	00.440	00.039	22.500	02.150	00.034	00.125	00.000
NO	00.530	00.044	27.400	01.970	00.025	00.130	00.000
SM	02.660	00.058	29.300	02.580	00.018	00.150	00.000
EU	01.500	00.145	20.500	01.070	01.130	00.100	00.000
GD	10.500	00.082	27.200	10.000	00.011	00.120	00.000
DY	28.600	00.097	25. 00	37.800	00.006	00.140	00.000
ER	42.800	00.162	20.000	119.00	00.006	00.155	00.000
YB	39.900	00.179	13.100	242.00	00.012	00.170	00.000
LU	29.600	00.185	11.200	281.00	00.006	00.190	00.000
K	00.020	99.999	00.000	00.000	99.999	00.000	00.000
RB	00.009	03.2 0	00.000	00.000	00.340	00.000	00.000
SR	00.015	00.120	01.000	00.000	03.870	00.000	00.000
BA	00.017	0 .3 0	00.000	00.000	06.120	00.000	00.000
CR	03.280	07.800	00.000	00.000	00. 70	50.000	00.000
NI	03.000	15.000	00.000	00.000	00.020	15.000	00.000
TI	00.500	01.000	00.000	00.000	00.040	28.000	00.000
SC	01.000	11.000	00.000	01.000	00.197	01.500	00.000
Y	03.170	00.030	50.700	45.700	00.006	00.000	00.000
NB	03.170	00.030	50.700	45.700	00.006	00.000	00.000
ZR	00.500	03.000	00.000	99.999	00.100	00.000	00.000
MN	05.000	05.870	00.000	00.000	00.310	02.500	00.000
V	01.280	06.000	00.000	00.000	00.200	57.000	00.000
U	00.100	00.200	50.000	50.000	00.100	00.000	00.000
TH	00.100	00.190	50.000	50.000	00.088	00.000	00.000
GA	01.000	03.500	01.000	00.000	00.950	00.000	00.000

AVERAGE RHYOLITIC KD VALUES - KD SET #2

ELEM	OLIV	OPX	DICP	AUG	HORN	PHLG	PLAG
LA	00.006	00.115	00.215	00.215	00.200	00.175	00.300
CE	00.006	00.150	00.260	00.260	01.520	00.230	00.270
PR	00.006	00.185	00.305	00.305	02.900	00.285	00.240
ND	00.006	00.220	00.350	00.350	04.260	00.340	00.210
SM	00.006	00.270	00.380	00.380	07.770	00.390	00.130
EU	00.006	00.170	00.270	00.270	05.140	00.500	02.150
GD	00.007	00.340	00.460	00.460	10.000	00.350	00.097
DY	00.009	00.460	00.550	00.550	13.000	00.200	00.064
ER	00.011	00.005	00.730	00.730	12.000	00.170	00.055
YB	00.014	00.880	00.990	00.990	08.380	00.170	00.049
LU	00.016	00.900	01.140	01.114	05.500	00.210	00.016
K	00.005	00.002	00.002	00.002	00.031	99.999	00.100
RB	00.007	00.002	00.002	00.002	00.014	00.940	00.041
SR	00.014	00.008	00.008	00.008	00.022	00. 72	04.400
BA	00.009	00.002	00.002	00.002	00.044	15.300	00.308
CR	09.000	00.670	04.500	02.500	04.080	12. 00	00.245
NI	41.750	38.500	16.000	16.000	63.000	20.000	00.016
TI	00.600	01.700	03.600	03.600	06.000	02.000	00.020
SC	00.100	01.800	16.280	26.280	12.000	11.300	00.101
Y	00.010	00.900	01.890	01.890	09.175	00.030	00.086
NB	00.010	00.900	01.890	01.890	09.175	00.030	00.086
ZR	00.010	00.630	01.900	01.900	10.000	00.030	00.086
MN	23.000	12.960	11.430	11.430	12.000	06.000	00.178
V	12.000	04.700	05.400	05.400	25.000	12.000	00.160
U	00.017	00.153	00.153	00.153	07.000	00.450	00.070
TH	00.013	00.117	00.117	00.117	07.000	00.310	00.059
GA	00.600	00.900	02.778	02.778	00.900	08.000	00.800

AVERAGE RHYOLITIC KD VALUES - KD SET #2

ELEM	GARN	BIOT	APAT	ZIRC	KFLD	MAG	QTZ
LA	00.260	00.335	26.000	02.800	00.054	00.098	00.000
CE	00.350	00.320	34.700	02.640	00.044	00.110	00.000
PR	00.440	00.305	42.000	02.400	00.034	00.125	00.000
ND	00.530	00.290	57.100	02.200	00.025	00.130	00.000
SM	02.660	00.260	62.000	03.140	00.010	00.150	00.000
EU	01.500	00.240	30.400	03.140	01.130	00.100	00.000
GD	10.500	00.280	56.300	12.000	00.011	00.120	00.000
DY	28.600	00.290	50.700	45.700	00.006	00.140	00.000
ER	42.800	00.350	37.200	135.00	00.006	00.155	00.000
YB	39.900	00.440	23.900	270.00	00.012	00.170	00.000
LU	29.600	00.330	20.200	323.00	00.006	00.190	00.000
K	00.020	99.999	00.000	00.000	99.999	00.000	00.000
RB	00.009	02.240	00.000	00.000	00.340	00.000	00.000
SR	00.015	00.120	01.000	00.000	03.870	00.000	00.000
BA	00.017	09.700	00.000	00.000	06.120	00.000	00.000
CR	03.280	12.600	00.000	00.000	00. 70	96.500	00.000
NI	15.000	20.000	00.000	00.000	00.020	23.333	00.000
TI	00.500	02.000	00.000	00.000	00.040	34.000	00.000
SC	01.000	11.300	00.000	01.000	00.197	02.250	00.000
Y	03.170	00.097	50.700	45.700	00.006	00.000	00.000
NB	03.170	00.097	50.700	45.700	00.006	00.000	00.000
ZR	00.500	04.000	00.000	99.999	00.100	00.000	00.000
MN	05.000	06.000	00.000	00.000	00.310	03.225	00.000
V	01.280	12.000	00.000	00.000	00.200	79.950	00.000
U	00.100	00.450	50.000	50.000	00.100	00.000	00.000
TH	00.100	00.310	50.000	50.000	00.088	00.000	00.000
GA	01.000	08.000	00.000	01.000	00.950	00.000	00.000

LOW RHYOLITIC KD VALUES - KD SET #2

ELEM	OLIV	OPX	DIOP	AUG	HORN	PHIG	PLAG
LA	00.008	00.215	00.350	00.350	00.400	00.175	00.380
CE	00.009	00.260	00.650	00.650	01.770	00.230	00.350
PR	00.009	00.305	00.950	00.950	03.100	00.285	00.320
ND	00.010	00.350	01.280	01.280	04.490	00.340	00.290
SM	00.011	00.380	01.810	01.810	08.100	00.390	00.150
EU	00.010	00.270	02.010	02.010	05.900	00.500	02.810
GD	00.012	00.460	02.200	02.200	10.500	00.350	00.130
DY	00.014	00.550	02.630	02.630	13.500	00.200	00.080
ER	00.017	00.730	02.250	02.250	14.000	00.170	00.072
YB	00.023	00.990	02.010	02.010	09.000	00.170	00.070
LU	00.026	01.140	01.810	01.810	06.300	00.210	00.008
K	00.008	00.002	00.037	00.037	00.081	99.999	00.100
RB	00.011	00.002	00.032	00.032	00.014	00.940	00.041
SR	00.019	00.008	00.516	00.516	00.022	00.672	04.400
BA	00.011	00.002	00.131	00.131	00.044	15.300	00.308
CR	11.200	00.710	04.950	02.950	11.000	17.400	00.670
NI	78.600	54.000	55.000	55.000	44.000	25.000	00.020
TI	00.840	01.900	04.000	04.000	08.000	03.000	00.040
SC	00.300	02.000	20.500	27.500	12.000	11.600	00.197
Y	00.014	00.900	02.790	02.790	10.000	00.030	00.135
NB	00.014	00.900	02.790	02.790	10.000	00.030	00.135
ZR	00.010	00.800	02.800	02.800	10.000	05.000	00.100
MN	24.000	36.000	12.150	12.150	14.730	06.130	00.310
V	14.500	10.000	07.000	07.000	06.000	18.000	00.200
U	00.020	00.180	00.153	00.153	08.000	00.500	00.100
TH	00.015	00.127	00.117	00.117	08.000	00.430	00.088
GA	00.700	01.000	03.575	03.575	01.000	09.000	01.000

LOW RHYOLITIC KD VALUES - KD SET #2

ELEM	GARN	BIOT	APAT	ZIRC	KFLD	MAG	QTZ
LA	00.260	00.335	37.000	03.300	00.054	00.098	00.000
CE	00.350	00.320	52.500	03.000	00.044	00.110	00.000
PR	00.440	00.305	67.000	02.700	00.034	00.125	00.000
ND	00.530	00.290	81.100	02.430	00.025	00.130	00.000
SM	02.660	00.260	89.800	03.700	00.018	00.150	00.000
EU	01.500	00.240	50.200	05.220	01.130	00.100	00.000
GD	10.500	00.280	78.000	14.000	00.011	00.120	00.000
DY	28.600	00.290	69.200	53.500	00.006	00.140	00.000
ER	42.800	00.350	51.200	152.00	00.006	00.155	00.000
YB	39.900	00.440	37.000	299.00	00.012	00.170	00.000
LU	29.600	00.330	30.200	366.00	00.006	00.190	00.000
K	00.020	99.999	00.000	00.000	99.999	00.000	00.000
RB	00.008	02.240	00.000	00.000	00.340	00.000	00.000
SR	00.015	00.120	01.000	00.000	03.870	00.000	00.000
BA	00.017	09.700	00.000	00.000	06.120	00.000	00.000
CR	03.280	17.400	00.000	00.000	00. 70	150.00	00.000
NI	15.000	25.000	00.000	00.000	00.020	30.000	00.000
TI	00.500	03.000	00.000	00.000	00.040	40.000	00.000
SC	01.000	11.600	00.000	01.000	00.197	03.000	00.000
Y	03.170	00.030	50.700	45.700	00.006	00.000	00.000
NB	03.170	00.030	50.700	45.700	00.006	00.000	00.000
ZR	00.500	05.000	00.000	99.999	00.100	00.000	00.000
MN	05.000	06.130	00.000	00.000	00.310	04.000	00.000
V	01.280	18.000	00.000	00.000	00.200	100.00	00.000
U	00.100	00.500	50.000	50.000	00.100	00.000	00.000
TH	00.100	00.430	50.000	50.000	00.800	00.000	00.000
GA	01.000	09.000	00.000	01.000	00.950	00.000	00.000

HIGH RHYOLITIC KD VALUES - KD SET #2

ELEM	OLIV	OPX	DIOP	AUG	HORN	PHLG	PLAG
LA	00.001	00.060	00.070	00.070	00.100	00.180	00.195
CE	00.002	00.082	00.360	00.360	01.380	00.230	00.170
PR	00.002	00.100	00.650	00.650	02.700	00.280	00.145
ND	00.003	00.120	00.940	00.940	04.030	00.340	00.120
SM	00.003	00.160	01.520	01.520	07.100	00.390	00.084
EU	00.005	00.093	01.110	01.110	04.500	00.500	00.960
GD	00.004	00.230	01.500	01.500	09.300	00.350	00.060
DY	00.006	00.330	01.220	01.220	12.500	00.200	00.040
ER	00.008	00.530	01.070	01.070	10.800	00.170	00.038
YB	00.009	00.730	01.114	01.114	07.450	00.170	00.030
LU	00.009	00.760	01.280	01.280	04.400	00.210	00.030
K	00.005	00.002	00.037	00.037	00.081	99.999	00.100
RB	00.008	00.002	00.032	00.032	00.014	00.940	00.041
SR	00.009	00.008	00.516	00.516	00.022	00. 72	04.400
BA	00.008	00.002	00.131	00.131	00.044	15.300	00.308
CR	07.800	00.620	03.850	02.000	00.520	07.800	00.060
NI	38.000	22.500	33.000	33.000	33.000	15.000	00.010
TI	00.420	01.500	03.200	03.200	04.000	01.000	00.010
SC	00.050	01.600	15.200	25.200	10.000	11.000	00.030
Y	00.006	00.900	00.945	00.945	08.400	00.030	00.025
NB	00.006	00.900	00.945	00.945	08.400	00.030	00.025
ZR	00.007	00.400	01.600	01.600	08.000	03.000	00.060
MN	02.000	08.505	10.710	10.710	10.000	05.870	00.033
V	01.000	04.400	05.500	05.500	04.000	06.000	00.100
U	00.015	00.140	00.153	00.153	00.140	00.200	00.040
TH	00.010	00.118	00.117	00.117	00.110	00.190	00.032
GA	00.500	00.800	01.980	01.980	00.800	07.000	0.6000

HIGH RHYOLITIC KD VALUES - KD SET #2

ELEM	GARN	BIOT	APAT	ZIRC	KFLD	MAG	QTZ
LA	00.260	00.335	13.500	02.350	00.054	00.098	00.000
CE	00.350	00.320	18.000	02.290	00.044	00.110	00.000
PR	00.440	00.305	22.500	02.150	00.034	00.125	00.000
ND	00.530	00.290	27.400	01.970	00.025	00.130	00.000
SM	02.660	00.260	29.300	02.580	00.018	00.150	00.000
EU	01.500	00.240	20.500	01.070	01.130	00.100	00.000
GD	10.500	00.280	27.200	10.000	00.011	00.120	00.000
DY	28.600	00.290	25.600	37.800	00.006	00.140	00.000
ER	42.800	00.350	20.000	119.00	00.006	00.155	00.000
YB	39.900	00.440	13.100	242.00	00.012	00.170	00.000
LU	29.600	00.330	11.200	281.00	00.006	00.190	00.000
K	00.020	99.999	00.000	00.000	99.999	00.000	00.000
RB	00.008	02.240	00.000	00.000	00.340	00.000	00.000
SR	00.015	00.120	01.000	00.000	03.870	00.000	00.000
BA	00.017	09.700	00.000	00.000	06.120	00.000	00.000
CR	03.280	07.800	00.000	00.000	00.670	50.000	00.000
NI	15.000	1 .000	00.000	00.000	00.020	15.000	00.000
TI	00.500	01.000	00.000	00.000	00.040	28.000	00.000
SC	01.000	11.000	00.000	01.000	00.197	01.500	00.000
Y	03.170	00.030	50.700	45.700	00.006	00.000	00.000
NB	03.170	00.030	50.700	45.700	00.006	00.000	00.000
ZR	00.500	03.000	00.000	99.999	00.100	00.000	00.000
MN	05.000	05.870	00.000	00.000	00.310	02.500	00.000
V	01.280	06.000	00.000	00.000	00.200	57.000	00.000
U	00.100	00.200	50.000	50.000	00.100	00.000	00.000
TH	00.100	00.190	50.000	50.000	00.088	00.000	00.000
GA	01.000	07.000	00.000	01.000	00.950	00.000	00.000

APPENDIX F

General Petrographic Descriptions

INTRODUCTION:

This appendix is included as a general reference for the petrology and geochemistry of the volcanic rocks discussed in Chapter V and VI. The descriptions are not meant to provide a comprehensive overview of all the thin section work undertaken by the author in the course of this thesis, but merely as a generalized compilation of the data designed to supplement the descriptions presented in Chapter II. No petrographic data are presented for any sedimentary or metamorphic rock type other than the Nimish Subgroup volcanic rocks. This was considered unnecessary because of the general lack of these samples that were collected, the lack of emphasis on those geological features of the area, both by the Newfoundland Department of Mines and Energy and my thesis supervisory committee, and the previously presented descriptions in Chapter II, IV and Evans (1978).

As an introduction one should say that the volcanics of the Nimish Subgroup are petrographically, not a very interesting suite of rocks. The rocks are generally structureless in outcrop and aside from occasional plagioclase phenocrysts there is little or no textural data to report. As a result only a brief petrographic summary of the subdivisions of the Nimish Subgroup as recognized in Chapter VI will be presented to supplement the geochemical discussion.

The rather monotonous, nondescript character of the Nimish Subgroup volcanics also reflects their photogenic qualities. Due to financial and time considerations of the Newfoundland Department of Mines and Energy, the technical staff of the Department of Geology and the author, and the relatively small amount of information that would be gained from the inclusion of field photographs and photomicrographs into this appendix, it was decided to leave them out.

The reader who wishes more petrographic and field data is referred to Evans (1978) and the files of the Newfoundland Department of Mines and Energy which contain full petrographic descriptions for all samples listed in Fig. 1 as well as a large number of photographs. This information is available upon request (R.J. Wardle, pers. comm.).

Petitsikapau Lake Formation:

Depleted Basic Lavas:

These lavas are predominantly fine to medium grained, aphyric, structureless mafic volcanic rocks. Mineralogically they include relict primary augite, plagioclase feldspar and magnetite along with a general secondary assemblage of chlorite, albite, epidote, adularia and opaques. No porphyritic varieties were recognized and a general intersertal texture is preserved.

Normal Basic Lavas:

These lavas are often vesicular and/or amygdaloidal with varying assemblages of chlorite, hematite, quartz, epidote and calcite filling the vesicles. Pillow lava formation is common with cholritic rims up to 10 cm noted. Highly vesicular pillow rims are preserved in some localities.

In thin section these lavas are fine to medium grained, commonly plagioclase porphyritic mafic volcanic rocks. The plagioclase phenocrysts are often complex crystal aggregates forming coarse glomerophenocrysts up to 5 cm in length. These crystals are usually partially replaced by alkali feldspar, muscovite and carbonate. Euhedral to subhedral microphenocrysts of magnetite are always present while relict augite phenocrysts are occasionally found. Porphyritic intersertal to pilotaxitic volcanic textures predominant within the secondary mesostasis assemblage of chlorite, epidote, alkali feldspar and opaques.

Sample JS - 104:

This sample has a general porphyritic texture with roughly equal amounts of subhedral phenocrysts of albite and potash feldspar up to 2 cm in length. The phenocrysts are relatively fresh and show minimal clouding effects of corrosion and clay mineral and muscovite alteration along grain boundaries. The feldspar crystals are flow-banded and set in a matrix of quartz,

alkali feldspar and small subhedral opaque crystals with minor amounts of secondary chlorite, epidote and muscovite. A hyalopilitic to trachytic texture predominates.

Sample JS - 111:

This sample is slightly amygdaloidal with quartz, hematite and chlorite filling the small vesicles. Euhedral to subhedral potash feldspar phenocrysts up to 2 cm in length that are crudely aligned in a flowbanded texture comprise 25 - 35% of this rock. Fine grained intergrowths of quartz, alkali feldspar and opaques comprise the mesostasis. The phenocryst and groundmass phases are relatively fresh with a small degree of clay mineral and/or muscovite alteration.

Sample JS - 098:

This sample is best classified as a rhyodacite porphyry with roughly equal amounts of orthoclase and albite which comprise roughly 30% of the rock. The phenocrysts are euhedral to subhedral, up to 2 cm in length and are coarsely flowbanded. The matrix for this sample is a grey, very fine grained to aphanitic assemblage of quartz, alkali feldspar and minor opaques. Alteration effects are similar to those described for JS - 111.

Astray Lake Formation:

Depleted Basic Lavas:

A general description for the depleted basic category of the Astray Lake Formation would not significrntly differ from the equivalent description of the Petitsikapau Lake Formation depleted basic lavas and need not be repeated here.

Normal Basic Lavas:

The normal basic lavas of the Astray Lake Formation are similar in all respects to the normal basic lavas of the Petitsikapau Lake Formation. The only significant difference lies in the percentage of exposed plagioclase porphyritic lavas and well preserved pillow lava localities. Aside from these quantitative differences the general description of the normal basic lavas given previously would apply.

Depleted Intermediate Lavas:

In outcrop this rock type is generally a massive, grey to black, plagioclase porphyritic andesite or trachyandesite. The phenocrysts are euhedral to subhedral, up to 1 cm in length, and show a poorly developed flow alignment texture. The phenocrysts locally show partial replacement by alkali feldspar and muscovite while the mesostasis consists of a secondary assemblage of chlorite, alkali feldspar and opaques with minor epidote and quartz. A porphyritic intersertal texture predominates.

Normal Intermediate Lavas:

This rock type is unique within the Astray Lake Formation in having randomly arranged, euhedral phenocrysts of potash feldspar comprising 10 - 15% of the rock. These phenocrysts are very fresh with minor clay mineral alteration along grain boundaries and are set in a grey, very fine grained intergrowth of alkali feldspar, chlorite, opaques and minor quartz.

Enriched Intermediate Lavas:

These rocks are slightly porphyritic andesites/trachyandesites with subhedral phenocrysts of plagioclase feldspar up to 1 cm in length. Phenocrysts are partially corroded and replaced by variable assemblages of muscovite, alkali feldspar and clay minerals. The phenocrysts are randomly oriented within a grey matrix of alkali feldspar, quartz, chlorite and opaques.

Acidic Lavas:

This highly homogeneous group of samples are very fine grained, aphyric, red to maroon rhyolitic flows. Relict devitrification textures are partially preserved in the quartz and alkali feldspar mineralogy. Specks of hematite dust are dispersed throughout the samples. Sample JS - 502 contains about 15 percent modal euhedral sanidine phenocrysts.